UNIVERSITY OF SOUTHAMPTON

FACULTY OF ENGINEERING AND PHYSICAL SCIENCES
School of Physics and Astronomy

Flavour from the grand unification scale to the electroweak scale

by

Elena Perdomo Méndez

Thesis for the degree of Doctor of Philosophy

September 2019

UNIVERSITY OF SOUTHAMPTON

ABSTRACT

FACULTY OF ENGINEERING AND PHYSICAL SCIENCES
School of Physics and Astronomy

Doctor of Philosophy

FLAVOUR FROM THE GRAND UNIFICATION SCALE TO THE ELECTROWEAK SCALE

by Elena Perdomo Méndez

The flavour puzzle, the origin of the three families of quarks and leptons, with their observed pattern of masses and mixing, persist as one of the deepest enigmas unanswered by the Standard Model. The discovery of neutrino masses makes the flavour puzzle even more acute, but also provides new features like small neutrino masses and large lepton mixing. The smallness of neutrino masses may be explained with a type-I seesaw mechanism, which introduces at least two right-handed neutrinos, while a large lepton mixing may be an indication of an underlying non-Abelian family symmetry.

We extend these ideas into unified models of flavour based on $S_4 \times SO(10)$ and $A_4 \times SU(5)$, which are spontaneously broken to the minimal supersymmetric Standard Model. We give a dynamical origin to Yukawa couplings, leading to predictive mass matrix structures for both quarks and leptons and giving a natural understanding for the hierarchies between fermion masses. We also address the doublet-triplet splitting and the μ problem, proton decay and GUT breaking. We perform a χ^2 fit to available data in each of the models and we also find that in one of the $S_4 \times SO(10)$ models, the correct baryon asymmetry of the Universe can be reproduced through N_2 thermal leptogenesis. In the case of the $A_4 \times SU(5)$ model, we include extra dimensions whose orbifold geometry leads to the discrete symmetry. We also introduce the modular symmetry, which is used as a family symmetry, meaning that the Yukawa couplings in this model become modular forms.

Lastly, we present an extension of the Standard Model with a $U(1)'$ symmetry and an additional fourth family of vector-like fermions to give a possible explanation for the recent R_K and R_{K^*} anomalies. The Z' gets induced couplings to the second family of left-handed lepton doublets and to the third family of left-handed quark doublets, accounting for the measured B-meson decay ratios while consistent with existing experimental constraints.

Contents

List of Figures

List of Tables

Declaration of Authorship

I, Elena Perdomo Méndez, declare that this thesis entitled "Flavour from the grand unification scale to the electroweak scale" and the work presented in it are my own and has been generated by me as the result of my own original research. I confirm that:

1. This work was done wholly or mainly while in candidature for a research degree at this University;
2. Where any part of this thesis has previously been submitted for a degree or any other qualification at this University or any other institution, this has been clearly stated;
3. Where I have consulted the published work of others, this is always clearly attributed;
4. Where I have quoted from the work of others, the source is always given. With the exception of such quotations, this thesis is entirely my own work;
5. I have acknowledged all main sources of help;
6. Where the thesis is based on work done by myself jointly with others, I have made clear exactly what was done by others and what I have contributed myself;
7. Parts of this work have been published as: [1], [2], [3] and [4].

Signed: .....

Date: .....

Acknowledgements

I would like to thank all the people that has encouraged me during this time and who have made possible the completion of this thesis. In first place, an special thank you to my supervisor Steve King, for your endless support. You have guided me always with fruitful discussions in the last three years and your time has been invaluable to me. I am also very grateful to all my collaborators: Francisco de Anda, Fredrik Björkeroth, Adam Falkowski, Mathias Pierre and Patrick Vaudrevange.

During this time in Southampton, there has been many people next to me and I thank them all. Hynek, thank you for the countless times having a chat and a beer together. Lauri, for reminding me the wonderful world we live in. Eirini, thank you for welcoming me in your house and making it our house. Thanks to all the people in my office, to Adam, Jack, Matt, Michele, Sam, Simon and Will for each Friday evening at the Stags. Thank you to the Greek team: Angelis, Thanasis and Nikos and to Gerardo, Joan and Roberto for making this a familiar place.

I am very grateful to all the Elusiνes family. Specially, thanks to Álvaro, Gonzalo, Nuno and Rupert, for making the best possible time at any school or conference. I keep all the adventures in my heart. Thank you to all the people that made my time unforgettable during my secondments in Paris, Geneva and Japan.

Thanks to my oldest friends and the best ones that one could ask for: Álvaro, Ancor, Carlota, Edu, Gara, Lilly, Marta, Muza, Noe and Pablo. Even in the farthest distance, you have always been there and you will always be. Thank you to Maria, for sitting next to me once we started the journey of Physics and for continuing being by my side.

A very special thank you to my parents, Rosa and Berto, who have been the great pillars of my life. Thank you for being next to me in every aspect of my life, for teaching me to keep pushing forward, for encouraging me to enjoy the only life we have, for holding me anytime I needed and for letting me being myself. Thank you to the other two parts of me, my brothers Alberto, for always making me laugh, and Javier, for being an example to follow.

Finally, to my love Felipe, for showing me that dreaming bigger is possible. Thank you for so many wonderful moments and for making me smile. Thank you, for always having time to listen to me, for your patience and support in my darkest moments. You are my sunshine.

To my parents, Rosa and Berto,
for making this possible.

Nomenclature

SM	Standard Model
EW	Electroweak
QCD	Quantum chromodynamics
SSB	Spontaneous symmetry breaking
VEV	Vacuum expectation value
CKM	Cabibbo-Kobayashi-Maskawa
CP	Charge-parity
GIM	Glashow-Iliopoulus-Maiani
PMNS	Pontecorvo-Maki-Nakagawa-Sakata
LHC	Large Hadron Collider
SUSY	Supersymmetry
MSSM	Minimal supersymmetric Standard Model
LSP	Lightest supersymmetric particle
DM	Dark Matter
B	Baryon number
L	Lepton number
GUT	Grand unified theory
BSM	Beyond the Standard Model
BAU	Baryon asymmetry of the Universe
4D	4-dimensional
5D	5-dimensional
6D	6-dimensional
CSD	Constrained sequential dominance
CG	Clebsch-Gordan
TB	Tri-bimaximal
DW	Dimopoulos-Wilczek
FCNC	Flavour-changing neutral-current
CL	Confidence level

Chapter 1

Introduction

In this chapter, we give a brief introduction to the Standard Model and to some of the main theoretical and experimental open questions still unresolved in particle physics. In particular, we tackle the problem of neutrino masses within a type-I seesaw mechanism. We continue summarizing the idea of supersymmetry, originally motivated by the hierarchy problem and we show the unification of gauge couplings within the minimal supersymmetric Standard Model. This leads to a discussion of grand unified theories, in which we focus on $SU(5)$ and $SO(10)$. Subsequently, we present the flavour puzzle and the use of non-Abelian discrete symmetries to address it. The next section is devoted to the baryon asymmetry of the Universe and we introduce the leptogenesis mechanism. Finally, we establish the advantages of the inclusion of extra dimensions. These open questions and possible solutions motivate us to propose new models which are presented in the following chapters.

1.1 The Standard Model

The Standard Model (SM) is a gauge theory based on the gauge symmetry group $SU(3)_C \times SU(2)_L \times U(1)_Y$, which describes the strong and electroweak (EW) interactions. The gauge group of quantum chromodynamics (QCD) is $SU(3)_C$ [5–7], with subscript C for color. The gauge group of electroweak interactions is $SU(2)_L \times U(1)_Y$ [8–11], where the subscript L refers to the fact that only left-handed fields transform non-trivially under $SU(2)_L$ and Y refers to the weak hypercharge.

The field content of the SM and its corresponding transformation properties under the gauge group $SU(3)_C \times SU(2)_L \times U(1)_Y$ are given in table 1.1. There are three families of chiral fermion fields,[1] encoded in the subscript $i = 1, 2, 3$ in table 1.1a. The left-handed fields are $SU(2)_L$ doublets, while their right-handed partners transform as

[1] Chiral fields are defined in appendix C.

Field	Representation		
	$SU(3)_C$	$SU(2)_L$	$U(1)_Y$
Q_{Li}	3	2	1/6
u_{Ri}	3	1	2/3
d_{Ri}	3	1	$-1/3$
L_{Li}	1	2	$-1/2$
e_{Ri}	1	1	-1

(a) Chiral fermionic fields. The subscript $i = 1, 2, 3$ runs over the three families of the Standard Model.

Field	Representation		
	$SU(3)_C$	$SU(2)_L$	$U(1)_Y$
G^a	8	1	0
W^b	1	3	0
B	1	1	0
H	1	2	1/2

(b) Gauge bosonic fields and Higgs field ($a = 1, ..., 8$, $b = 1, 2, 3$).

Table 1.1: Standard Model field content.

$SU(2)_L$ singlets.[2] For the leptons, the doublet $L_{Li} = (\nu_{Li}, e_{Li})^T$ contains the left-handed charged lepton and its corresponding left-handed neutrino, where the family index refers to the electron, muon and tau. The SM does not include the right-handed partner of the neutrino field and we only have right-handed charged leptons e_{Ri}. The quark field $Q_{Li} = (u_{Li}, d_{Li})^T$ includes the up and down quarks $Q_{L1} = (u_L, d_L)^T$, the charm and strange quarks $Q_{L2} = (c_L, s_L)^T$, and the top and bottom quarks $Q_{L3} = (t_L, b_L)^T$. Their corresponding right-handed partners are given by u_{Ri} and d_{Ri}. The quarks also transform as triplets under $SU(3)_C$ and we are suppressing the color index. Therefore, the SM contains a total of 15 chiral fields within each family. Additionally, we have the spin-1 gauge boson fields in table 1.1b: eight massless gluons G^a ($a = 1, ..., 8$) for the strong interaction $SU(3)_C$ and the gauge fields W^b ($b = 1, 2, 3$) and B of the $SU(2)_L \times U(1)$ gauge theory. Finally, the SM also contains the $SU(2)_L$-doublet scalar field $H = (H^+, H^0)^T$ (Higgs doublet), which causes the spontaneous symmetry breaking (SSB) of the electroweak group to the electromagnetic subgroup:

$$SU(3)_C \times SU(2)_L \times U(1)_Y \xrightarrow{\text{SSB}} SU(3)_C \times U(1)_{\text{QED}} \tag{1.1}$$

The SSB mechanism [12–17] generates the masses of the weak gauge bosons and the masses and mixing of the fermions. It also gives rise to the appearance of a physical scalar particle in the model, the Higgs particle.

The Standard Model does not incorporate the right-handed neutrino field, ν_{Ri}, meaning that the SM predicts massless neutrinos and we will address this problem in section 1.2.

The gauge transformations under the SM gauge group, with the infinitesimal form for

[2] Although the charge conjugate of right-handed fields ψ_R^c transform as left-handed fields, they remain singlets under $SU(2)_L$. Similarly for the left-handed fields, whose charge conjugated fields transform as right-handed fields but they behave as doublets under $SU(2)_L$.

the gauge field transformations, are the following:

$$\begin{aligned}
U(1)_Y: &\quad \psi \to \exp(i\lambda_Y(x)Y_\psi)\psi, \quad H \to \exp(i\lambda_Y(x)Y_H)H, \\
&\quad B_\mu \to B_\mu + \frac{1}{g'}\partial_\mu\lambda_Y(x) \\
SU(2)_L: &\quad \psi \to \exp(i\lambda_L^a(x)T^a)\psi, \quad H \to \exp(i\lambda_L^a(x)T^a)H, \\
&\quad W_\mu^a \to W_\mu^a + \frac{1}{g}\partial_\mu\lambda_L^a(x) + \epsilon^{abc}W_\mu^b\lambda_L^c(x) \\
SU(3)_C: &\quad \psi \to \exp(i\lambda_C^a(x)t^a)\psi, \quad G_\mu^a \to G_\mu^a + \frac{1}{g_s}\partial_\mu\lambda_C^a(x) + f^{abc}G_\mu^b\lambda_C^c(x),
\end{aligned} \tag{1.2}$$

where ψ is a generic fermion field and repeated indices are always taken as summed. The coupling strength of the hypercharge, weak and strong interactions are given by g', g and g_s, respectively. Y is the hypercharge operator and T^a and t^a are the $SU(2)_L$ and $SU(3)_C$ generators, respectively. When acting upon a doublet representation of $SU(2)_L$, $T^a = \sigma^a/2$ where σ^a are the Pauli matrices, while when acting upon singlets $T^a = 0$. For the case of $SU(3)_C$, the triplet representations transform with $t^a = \lambda^a/2$, where λ^a are the Gell-Mann matrices, while singlet representations transforms as $t^a = 0$. The antisymmetric structure constants of $SU(3)_C$, f^{abc}, are defined in terms of the group generators $[t^a, t^b] = if^{abc}t^c$, where a, b, c run from 1 to 8. For $SU(2)_L$, a, b, c run from 1 to 3 and $f^{abc} = \epsilon^{abc}$, the totally antisymmetric three-index tensor defined so that $\epsilon^{123} = 1$.

The most general renormalizable Lagrangian invariant under the $SU(3)_C \times SU(2)_L \times U(1)_Y$ gauge transformations in equation (1.2) is given by

$$\mathcal{L} = \mathcal{L}_{\text{kinetic}} + \mathcal{L}_{\text{Yukawa}} + \mathcal{L}_H. \tag{1.3}$$

The kinetic term contains

$$\mathcal{L}_{\text{kinetic}} = \sum_\psi i\bar{\psi}\gamma^\mu D_\mu\psi - \frac{1}{4}G_{\mu\nu}^a G^{a\mu\nu} - \frac{1}{4}W_{\mu\nu}^a W^{a\mu\nu} - \frac{1}{4}B_{\mu\nu}B^{\mu\nu}, \tag{1.4}$$

where the field strength tensors for the $U(1)_Y$, $SU(2)_L$ and $SU(3)_C$ interactions are

$$\begin{aligned}
B_{\mu\nu} &= \partial_\mu B_\nu - \partial_\nu B_\mu \\
W_{\mu\nu}^a &= \partial_\mu W_\nu^a - \partial_\nu W_\mu^a + g\epsilon^{abc}W_\mu^b W_\nu^c \\
G_{\mu\nu}^a &= \partial_\mu G_\nu^a - \partial_\nu G_\mu^a + g_s f^{abc}G_\mu^b G_\nu^c.
\end{aligned} \tag{1.5}$$

The covariant derivative encodes the kinetic and the gauge interactions and it is given by

$$D_\mu = \partial_\mu - ig'B_\mu Y - igW_\mu^a T^a - ig_s G_\mu^a t^a. \tag{1.6}$$

The terms involved in the Lagrangian term $\mathcal{L}_H$ in equation 1.3 are

$$\mathcal{L}_H = (D_\mu H)^\dagger (D^\mu H) - V(H), \tag{1.7}$$

where the scalar potential is given by

$$V(H) = \mu^2 H^\dagger H + \lambda (H^\dagger H)^2 \qquad (\mu^2 < 0,\ \lambda > 0). \tag{1.8}$$

The minimum of this potential is away from $|H|$=0 and the vacuum expectation value (VEV), or minimum energy state, is not invariant under $SU(2)_L \times U(1)_Y$ transformations. The gauge symmetry $SU(2)_L \times U(1)_Y$ is spontaneously broken [12–17] to the gauge group $U(1)_{\text{QED}}$ of electromagnetic interactions. We can find a gauge (the so-called *unitary gauge*) in which the doublet scalar field takes the form

$$H(x) = \frac{1}{\sqrt{2}} \begin{pmatrix} 0 \\ v + h(x) \end{pmatrix}, \tag{1.9}$$

where h is a real scalar field, the Higgs boson field. From equations. 1.8 and 1.9, we find that a minimum of the potential is given by

$$\langle 0|H|0\rangle = \frac{1}{\sqrt{2}} \begin{pmatrix} 0 \\ v \end{pmatrix}, \qquad v = \sqrt{\frac{-\mu^2}{\lambda}}. \tag{1.10}$$

The vacuum is invariant under the unbroken gauge group $U(1)_{\text{QED}}$ with generator Q

$$e^{i\lambda_Q(x)Q} \langle 0|H|0\rangle = \langle 0|H|0\rangle, \tag{1.11}$$

leading to well-known expression for the electric charge

$$Q = T^3 + Y. \tag{1.12}$$

After diagonalizing the gauge kinetic term $(D_\mu H)^\dagger (D^\mu H)$ in the unitary gauge, we can deduce that the masses for the $W^\pm$ and Z bosons are

$$M_W = \frac{gv}{2}, \quad M_Z = \sqrt{\frac{g^2 + g'^2}{4}} v. \tag{1.13}$$

The relation between the gauge and the mass eigenstates is given by

$$\begin{aligned} W^+_\mu &= \frac{W^1_\mu - iW^2_\mu}{\sqrt{2}}, \\ W^-_\mu &= \frac{W^1_\mu + iW^2_\mu}{\sqrt{2}} \\ Z_\mu &= c_W W^3_\mu - s_W B_\mu, \\ A_\mu &= s_W W^3_\mu + c_W B_\mu, \end{aligned} \tag{1.14}$$

where $s_W = \sin\theta_W$, $c_W = \cos\theta_W$ and θ_W is the weak mixing angle or Weinberg angle satisfying the relation $\cos\theta_W = M_W/M_Z$. The state A_μ does not couple to the Higgs field and thus does not acquire a mass after gauge symmetry breaking. This state is identified as the photon.

The covariant derivative in terms of the gauge boson mass basis is

$$D_\mu = \partial_\mu - ig_s G^a_\mu t^a - \frac{g}{\sqrt{2}}(W^+_\mu T^+ + W^-_\mu T^-) - i\frac{e}{s_W c_W} Z_\mu (T^3 - s^2_W Q) - ieA_\mu Q, \quad (1.15)$$

where $T^\pm$ are the raising and lowering operators of $SU(2)_L$, with $T^\pm = \sigma^\pm = \frac{1}{2}(\sigma^1 \pm i\sigma^2)$ and e is the electromagnetic coupling such that $e = g' c_W$.

1.1.1 Fermion masses and quark mixing

The Yukawa couplings in equation 1.3 are given by

$$\mathcal{L}_{\text{Yukawa}} = -\left(Y^d_{ij}\overline{Q_{Li}} H d_{Rj} + Y^u_{ij}\overline{Q_{Li}}\tilde{H} u_{Rj} + Y^e_{ij}\overline{L_{Li}} H e_{Rj} + \text{H.c.}\right), \quad (1.16)$$

where $\tilde{H} = i\sigma^2 H^*$, $i, j = 1, 2, 3$ are family indices and the matrices Y^d, Y^u and Y^e are complex 3×3 matrices of Yukawa coupling constants. After gauge symmetry breaking, the terms in equation 1.16 give rise to fermion masses

$$\mathcal{L}_M = -\left(\overline{d_L} M_d d_R + \overline{u_L} M_u u_R + \overline{e_L} M_e e_R + \text{H.c.}\right), \quad (1.17)$$

where

$$M_d = \frac{v}{\sqrt{2}} Y^d, \quad M_u = \frac{v}{\sqrt{2}} Y^u, \quad M_e = \frac{v}{\sqrt{2}} Y^e \quad (1.18)$$

are the mass matrices. We have arranged the members of a fermion family into a single vector, i.e. $d = (d_1, d_2, d_3)^T$, where d_i for $i = 1, 2, 3$ are the down-type quark flavour interaction eigenstates and similarly for the up-type quarks and charged leptons. Since the Standard Model does not contain right-handed neutrinos, ν_{Ri}, there is no Yukawa coupling and neutrinos are predicted to be massless within the SM.

The physical massive fermion fields can be found by diagonalizing the mass matrices. We diagonalize M^d and M^u using appropriate unitary transformation matrices

$$V^d_L M_d V^{d\dagger}_R = \begin{pmatrix} m_d & 0 & 0 \\ 0 & m_s & 0 \\ 0 & 0 & m_b \end{pmatrix}, \quad V^u_L M_u V^{u\dagger}_R = \begin{pmatrix} m_u & 0 & 0 \\ 0 & m_c & 0 \\ 0 & 0 & m_t \end{pmatrix}. \quad (1.19)$$

Thus we can write the quark mass eigenstates as

$$\begin{pmatrix} d \\ s \\ b \end{pmatrix}_{L,R} = V^d_{L,R} \begin{pmatrix} d_1 \\ d_2 \\ d_3 \end{pmatrix}_{L,R} \quad \text{and} \quad \begin{pmatrix} u \\ c \\ t \end{pmatrix}_{L,R} = V^u_{L,R} \begin{pmatrix} u_1 \\ u_2 \\ u_3 \end{pmatrix}_{L,R} . \tag{1.20}$$

Since the up-type and the down-type quarks are rotated into the mass eigenstates with different unitary matrices, there is a mismatch between the flavour basis and the mass eigenstate basis in the charged-current $W^\pm$ interactions, where the couplings to the physical left-handed quarks are given by

$$\frac{-g}{\sqrt{2}}(\overline{u_L}, \overline{c_L}, \overline{t_L})\gamma^\mu W^+_\mu V_{\text{CKM}} \begin{pmatrix} d_L \\ s_L \\ b_L \end{pmatrix} + \text{H.c.}, \quad V_{\text{CKM}} = V^u_L V^{d\dagger}_L. \tag{1.21}$$

The Cabibbo-Kobayashi-Maskawa (CKM) matrix V_{CKM} [18, 19] is a 3×3 unitary matrix, which can be parametrized in terms of three mixing angles and a charged-parity (CP)-violating KM phase δ^q [19]. One common choice is given by [20]

$$V_{\text{CKM}} = \begin{pmatrix} 1 & 0 & 0 \\ 0 & c_{23} & s_{23} \\ 0 & -s_{23} & c_{23} \end{pmatrix} \begin{pmatrix} c_{13} & 0 & s_{13}e^{-i\delta^q} \\ 0 & 1 & 0 \\ -s_{23}e^{i\delta^q} & 0 & c_{13} \end{pmatrix} \begin{pmatrix} c_{12} & s_{12} & 0 \\ -s_{12} & c_{12} & 0 \\ 0 & 0 & 1 \end{pmatrix}, \tag{1.22}$$

where $s_{ij} = \sin\theta_{ij}$, $c_{ij} = \cos\theta_{ij}$. These are fundamental parameters of the SM, describing flavour-changing interactions.

Since the photon couplings Q and the Z boson couplings $(T^3 - \sin^2\theta_W Q)$ are universal to all three families, the neutral currents are flavour diagonal. This is a manifestation of the GIM mechanism introduced by Glashow, Iliopoulus and Maiani [21].

The charged-lepton mass term can be also diagonalized through unitary transformations

$$U^e_L M_e U^{e\dagger}_R = \begin{pmatrix} m_e & 0 & 0 \\ 0 & m_\mu & 0 \\ 0 & 0 & m_\tau \end{pmatrix}. \tag{1.23}$$

The charged-lepton mass eigenstates become

$$\begin{pmatrix} e \\ \mu \\ \tau \end{pmatrix}_{L,R} = U^e_{L,R} \begin{pmatrix} e_1 \\ e_2 \\ e_3 \end{pmatrix}_{L,R} \tag{1.24}$$

The mass eigenfields e, μ and τ are said to be the flavour eigenfields of the charged leptons, i.e. the flavour of a charged lepton is defined by its mass. Since neutrinos are predicted to be massless in the SM, a neutrino ν_α is said to be of flavour α (where $\alpha =$

e, μ, τ), if it is produced or detected in a charged current interaction process involving the charged lepton flavour α.

1.2 Neutrino masses and the seesaw mechanism

The discovery of neutrino masses is a clear hint that new physics beyond the Standard Model is needed. In 2015, the Nobel Prize of Physics was awarded to Takaaki Kajita and Arthur B. McDonald "for the discovery of neutrino oscillations, which shows that neutrinos have mass" and "for their key contributions to the experiments which demonstrated that neutrinos change identities".

The most common choice to accommodate neutrino masses is to extend the Standard Model field content in table 1.1 and include N_R right-handed neutrinos, $\nu_{Ri} = (\nu_{R1}, ..., \nu_{RN_R})$, which are singlets under the SM gauge group. The right-handed neutrino fields do not couple to the gauge fields but new Yukawa couplings arise

$$\mathcal{L}_{\text{Yukawa},D} = -Y^{\nu}_{ij}\overline{L_{Li}}\tilde{H}\nu_{Rj} + \text{H.c.}, \tag{1.25}$$

which, after spontaneous symmetry breaking, give rise to the neutrino mass term

$$\mathcal{L}_D = -\overline{\nu_L} M_D \nu_R + \text{H.c.} \tag{1.26}$$

The subscript D refers to Dirac mass term and $M_D = vY^{\nu}/\sqrt{2}$ is a complex $3 \times N_R$ matrix. Additionally, if we allow lepton number violation, there is another neutrino mass term (Majorana mass term) compatible with gauge invariance given by

$$\mathcal{L}_R = -\frac{1}{2}\overline{\nu^c_R} M_R \nu_R + \text{H.c.}, \tag{1.27}$$

where $\psi^c \equiv C\overline{\psi}^T$ denotes the charge conjugate field, where C is known as the charge conjugation matrix, see appendix C. A Majorana mass term for the left-handed neutrino fields is possible below the electroweak symmetry breaking scale since the neutrino has zero electric charge. However, before SSB a renormalizable Majorana mass term for the left-handed neutrino fields is not gauge invariant under $SU(2)_L \times U(1)_Y$. The type-I seesaw mechanism [22–26] assumes this term to be zero to begin with, but is generated effectively by right-handed neutrinos.

Collecting together the Dirac mass term 1.26 and the Majorana mass term 1.27, we can write the seesaw mass matrix as

$$\begin{pmatrix} \overline{\nu_L} & \overline{\nu^c_R} \end{pmatrix} \begin{pmatrix} 0 & M_D \\ (M_D)^T & M_R \end{pmatrix} \begin{pmatrix} \nu^c_L \\ \nu_R \end{pmatrix}, \tag{1.28}$$

which, after diagonalization, effectively generates a Majorana mass term for the left-

handed fields. The Majorana masses M_R are not an effect of gauge symmetry breaking and therefore the scale can be orders of magnitude larger than the electroweak scale, $M_{EW} \sim \mathcal{O}(10^2)$ GeV. In the approximation where $M_R \gg M_D$, the Majorana mass term for left-handed fields, after diagonalization, is given by

$$\mathcal{L}_L = -\frac{1}{2}\overline{\nu_L} m^\nu \nu_L^c + \text{H.c.}, \tag{1.29}$$

where m_ν, in terms of the seesaw formula, is

$$m_\nu = -M_D M_R^{-1} (M_D)^T. \tag{1.30}$$

The smallness of neutrino masses is understood in the seesaw mechanism through the suppression by the heavy scale M_R. For example, if we take M_D to be 1 GeV (roughly equal to the charm quark mass), then a neutrino mass of 0.1 eV requires a right-handed neutrino mass of 10^{10} GeV.

1.2.1 Lepton mixing

From the antisymmetry of the charge conjugation matrix C and the anticommutativity of fermion fields, one can deduce that a Majorana mass matrix must be symmetric. A complex symmetric matrix can be diagonalized by an unitary matrix such that

$$U_L^\nu m^\nu (U_L^\nu)^\dagger = \begin{pmatrix} m_1 & 0 & 0 \\ 0 & m_2 & 0 \\ 0 & 0 & m_3 \end{pmatrix}. \tag{1.31}$$

The charged-current interactions, involving charged-leptons and neutrinos, in the mass basis is

$$\frac{-g}{\sqrt{2}}(\overline{e_L}, \overline{\mu_L}, \overline{\tau_L})\gamma^\mu W_\mu^+ U_{\text{PMNS}} \begin{pmatrix} \nu_{1L} \\ \nu_{2L} \\ \nu_{3L} \end{pmatrix} + \text{H.c.}, \quad U_{\text{PMNS}} = U_L^e (U_L^\nu)^\dagger, \tag{1.32}$$

where U_L^e is the unitary matrix diagonalizing the charged-lepton mass term in equation 1.23 and U_{PMNS} is the lepton mixing matrix or Pontecorvo-Maki-Nakagawa-Sakata (PMNS) matrix [27–30]. The neutrino flavour eigenstates are defined through their charged current interactions with charged-leptons, therefore

$$\begin{pmatrix} \nu_{eL} \\ \nu_{\mu L} \\ \nu_{\tau L} \end{pmatrix} = U_{\text{PMNS}} \begin{pmatrix} \nu_{1L} \\ \nu_{2L} \\ \nu_{3L} \end{pmatrix}. \tag{1.33}$$

If neutrinos are massive, the neutrino flavour eigenfields are rotated against the neutrino mass eigenfields by the unitary matrix U_{PMNS}. In the standard PDG parametriza-

tion [31], the unitary matrix U_{PMNS} is given by three mixing angles θ^l_{ij}, the Dirac CP phase δ^l and two Majorana phases α_{21} and α_{31} such that

$$U_{\text{PMNS}} = \begin{pmatrix} 1 & 0 & 0 \\ 0 & c_{23} & s_{23} \\ 0 & -s_{23} & c_{23} \end{pmatrix} \begin{pmatrix} c_{13} & 0 & s_{13}e^{-i\delta^l} \\ 0 & 1 & 0 \\ -s_{23}e^{i\delta^l} & 0 & c_{13} \end{pmatrix} \begin{pmatrix} c_{12} & s_{12} & 0 \\ -s_{12} & c_{12} & 0 \\ 0 & 0 & 1 \end{pmatrix} \begin{pmatrix} 1 & 0 & 0 \\ 0 & e^{i\frac{\alpha_{21}}{2}} & 0 \\ 0 & 0 & e^{i\frac{\alpha_{31}}{2}} \end{pmatrix}, \tag{1.34}$$

where in this case $c_{ij} = \cos\theta^l_{ij}$ and $s_{ij} = \sin\theta^l_{ij}$. The Majorana phases are unphysical for Dirac neutrinos since a phase field redefinition leaves the Dirac mass term invariant while the Majorana mass term would not be invariant.

Observable	Data	
	Best fit	1σ range
θ^ℓ_{12} /°	33.82	$33.06 \to 34.60$
θ^ℓ_{13} /°	8.610	$8.480 \to 8.740$
θ^ℓ_{23} /°	48.30	$46.40 \to 49.40$
δ^ℓ /°	222.0	$194.0 \to 260.0$
$\Delta m^2_{21}/(10^{-5}\,\text{eV}^2)$	7.390	$7.190 \to 7.600$
$\Delta m^2_{32}/(10^{-3}\,\text{eV}^2)$	2.523	$2.493 \to 2.555$

Table 1.2: Neutrino oscillation parameters, for the normal ordered case (without Super-Kamiokande atmospheric data), from the fit to global data done by NuFit collaboration, version 4.1 [32]. The data included by NuFit come from solar experiments [33–45], atmospheric experiments [46–48], reactor experiments [49–53] and accelerator experiments [54–58].

The transition probability of producing a neutrino of flavour α and detecting a neutrino of flavour β depends on the mass squared differences $\Delta m^2_{21} \equiv m^2_2 - m^2_1$, $\Delta m^2_{3j} \equiv m^2_3 - m^2_j$, the mixing angles, θ^l_{ij} and the CP violating phase δ^l but it does not depend on the Majorana phases nor the masses themselves. Thus, there are six observables which can be determined by neutrino oscillations. These are known as the solar mixing angle θ^l_{12} and solar mass splitting Δm^2_{21}, atmospheric mixing angle θ^l_{23} and atmospheric mass splitting Δm^2_{3i}, the reactor mixing angle θ^l_{13} and the CP violating phase δ^l. Furthermore, current experimental data cannot yet determine the mass ordering of neutrinos, defined as normal ($\Delta m^2_{32} > 0$) or inverted ordering ($\Delta m^2_{31} < 0$), although there is a preference for normal mass ordering [32]. There is a cosmological limit on the total sum of the three neutrino masses $\sum m_i = m_1 + m_2 + m_3 < 0.23$ eV [59]. If neutrinos are Majorana particles, neutrinoless double beta decay $0\nu\beta\beta$ (which violates lepton number by two units) can give us information about neutrino masses as well. The rate of $0\nu\beta\beta$ is proportional to the effective Majorana mass $m_{\beta\beta} = \sum_i m_i U^2_{ei}$, where we have suppressed the PMNS subindex in the unitary mass matrix U_{PMNS}. Recent searches set a limit on the neutrino mass of $m_{\beta\beta} \lesssim 0.06 - 0.200$ eV [60, 61]. Furthermore, neutrinoless double beta decay is sensitive to normal and inverted mass ordering and future experiments will be able to confirm or set stronger constraints in the ordering of neutrino masses. We show the oscillation parameters for normal mass ordering, without Super-Kamiokande atmospheric data, given by the NuFit-4.1 collaboration [32] in table 1.2.

1.3 Supersymmetry

Supersymmetry (SUSY) [62–66] is an extension of space-time symmetry beyond the Poincaré group which transforms a fermionic field into a bosonic field and vice versa. In a supersymmetric theory the irreducible representations are known as "supermultiplets", containing both fermion and boson states, each being a "superpartner" of the other. Each supermultiplet contains an equal number of fermion and boson degrees of freedom and particles within the same supermultiplet must also be in the same representation of the gauge group. Therefore, in SUSY the content of the SM is duplicated as shown in tables 1.3 and 1.4. The superpartners of quarks and leptons are scalars called "squarks" and "sleptons". Each fermion and its scalar superpartner are accommodated in a "chiral supermultiplet", which is the simplest possible combination for a supermultiplet consisting of a single Weyl fermion and a complex scalar field. The gauge bosons together with their superpartners "gauginos" are combined in a "gauge" or "vector" supermultiplet. The Higgs field is accommodated in a chiral multiplet, together with a spin-1/2 superpartner, the Higgsino.

Supersymmetry was intended to address the "hierarchy problem" [67–70] or the fact that the Higgs mass receives quantum corrections quadratically divergent with the energy cutoff Λ_{UV}, i.e. $\Delta m_H^2 \propto \Lambda_{\text{UV}}^2$. The ultraviolet momentum cutoff is interpreted as the scale at which new physics enters. If we consider this scale to be the Planck scale $M_P \sim \mathcal{O}(10^{19})$ GeV, where gravity effects need to be included, we would require a large fine tuning between the tree level mass and the radiative corrections given that there are 17 orders of magnitude between the energy cutoff and the Higgs mass, $m_H \sim 125$ GeV. In the Standard Model, these quantum corrections come from loop diagrams involving fermions, however, if we include supersymmetry, the scalar superpartners will contribute to the quantum corrections with a relative minus sign leading to a cancellation of the SM contributions. This cancellation occurs to all orders by the supersymmetric non-renormalisation theorem [71, 72].

Since we have not yet observed any scalar particle with the same mass as the known fermions, supersymmetry must be broken a low energies. If we still want supersymmetry to provide an explanation for the hierarchy problem, we can only consider "soft" supersymmetry breaking terms (containing only mass terms and coupling parameters with positive mass dimension). In this case, the relationships between dimensionless couplings that hold in an unbroken supersymmetric theory are maintained, and the cancellation between scalar and fermion loop diagrams still occur. However, there will be contributions from associated soft terms with scale m_{soft}, i.e. $\Delta m_H^2 \propto m_{\text{soft}}^2$. Since the Large Hadron Collider (LHC) has set some limits on the mass of the sparticles of about 2 TeV, the hierarchy problem is reintroduced, where some degree of fine tuning has to be accepted.

The hierarchy problem is not the only motivation to consider supersymmetry. SUSY

also provides a dark matter (DM) candidate when assuming "R-parity" [73]. A consequence of this symmetry is that it provides a stable supersymmetry particle, the so called lightest supersymmetric particle (LSP), which can be considered as a dark matter candidate. Furthermore, SUSY leads to the unification of gauge couplings in the Minimal Supersymmetric Standard Model (MSSM) [74–78], as we will see in section 1.3.2. Supersymmetry can also be used to unify gravity with the strong and electroweak interactions [79–81].

1.3.1 How to build supersymmetric models

Supersymmetry relates fermionic and bosonic states. Both states are described in terms of a supermultiplet, which is an irreducible representation of the supersymmetry algebra. Additionally, we need an extra ingredient to close the supersymmetry algebra, the auxiliary fields. In the case of chiral multiplets, the auxiliary field is given by a new complex scalar field F, which does not have a kinetic term and with equations of motion given by $F = F^* = 0$. Similarly, for a vector multiplet, we need a new real bosonic auxiliary field D with no kinetic term. They are really just tools that allow the supersymmetry algebra to close off-shell. In summary, a chiral supermultiplet contains a Weyl fermion ψ, a complex scalar ϕ and auxiliary field F, while a vector supermultiplet consists of a gauge field A_μ, gaugino λ and auxiliary field D.

The most general Lagrangian density of masses and non-gauge interactions for particles that live in a chiral multiplet, consistent with supersymmetry, is given by

$$\mathcal{L}_{\text{int}} = \left(-\frac{1}{2}W^{ij}\psi_i\psi_j + W^i F_i\right) + \text{H.c.}, \tag{1.35}$$

where W^{ij} and W^i are the functional derivatives

$$W^i = \frac{\delta W}{\delta \phi_i}, \quad W^{ij} = \frac{\delta^2 W}{\delta\phi_i \delta\phi_j}. \tag{1.36}$$

The function W is called the superpotential and it is an holomorphic function of the scalar fields ϕ_i treated as complex variables,

$$W = L^i\phi_i + \frac{1}{2}M^{ij}\phi_i\phi_j + \frac{1}{6}y^{ijk}\phi_i\phi_j\phi_k. \tag{1.37}$$

The most general non-gauge interactions for chiral supermultiplets are determined by the superpotential W, where the terms in equation 1.37 are constrained to be gauge invariant terms. For example, L^i parameters will only appear if ϕ_i is a gauge singlet.

The scalar potential of the theory is given in terms of the superpotential by

$$V(\phi, \phi^*) = W^i W_i^* = F^{*i}F_i, \tag{1.38}$$

where in the last equality we used the equations of motion for the auxiliary fields $F_i = -W_i^*$ and $F^{*i} = -W^i$. In fact, once one studies the Lagrangian for gauge supermultiplets and the gauge interactions, the complete scalar potential contains terms also proportional to the auxiliary fields D, i.e. $V(\phi, \phi^*) = F^{*i}F_i + \frac{1}{2}\sum_a D^a D^a$. These two types of terms are known as "F-term" and "D-term", respectively. The F-terms are fixed by Yukawa couplings and fermion mass terms while the D-terms are fixed by gauge interactions. Since in this thesis we are interested in the flavour sector, concerning about Yukawa couplings and mass terms, we will not explicitly show the form of Lagrangian for the gauge interactions and we will not mention again the D-terms.

Equivalently, we can use the superfield [82, 83] language. A superfield contains as components all the bosonic, fermionic and auxiliary fields within the corresponding supermultiplet, for example $\Phi_i \supset (\phi_i, \psi_i, F_i)$ and it is a function of the "superspace" coordinates, containing not only the usual bosonic space-time coordinates but also fermionic anticommuting coordinates. The gauge quantum numbers and the mass dimension of a chiral superfield are the same as of its scalar component. The superpotential would be the same as in equation 1.37, substituting ϕ_i by Φ_i.

1.3.2 The Minimal Supersymmetric Standard Model

The Minimal Supersymmetric Standard Model (MSSM) contains the SM fields and its superpartners, see tables 1.3 and 1.4. We duplicated the number of Higgs fields to cancel gauge anomalies. The condition that one has to satisfy to avoid gauge anomalies is $\mathrm{Tr}[T_3^2 Y] = \mathrm{Tr}[Y^3] = 0$, where the traces run over all of the left-handed Weyl fermions. If we only had one Higgs field, its superpartner, the Higgsino, would have weak hypercharge $Y = 1/2$, spoiling the cancellation that was automatically done in the SM. This is not the only reason to add another Higgs field, since the superpotential is an holomorphic function of the chiral superfields, it would not be possible to write the up-type quark Yukawa coupling as in equation 1.16, using the complex conjugate of a single Higgs field.

The most general superpotential in the MSSM is given by

$$W_{\mathrm{MSSM}} = Y^u_{ij}\hat{Q}_i\hat{\bar{u}}_j\hat{H}_u + Y^d_{ij}Q_i\hat{\bar{d}}_j\hat{H}_d + Y^e_{ij}\hat{L}_i\hat{\bar{e}}_j\hat{H}_d + \mu\hat{H}_u\hat{H}_d, \tag{1.39}$$

where $\hat{H}_u$, $\hat{H}_d$, $\hat{Q}$, $\hat{L}$, $\hat{\bar{u}}$, $\hat{\bar{d}}$, $\hat{\bar{e}}$ are the chiral superfields appearing in table 1.3. The subindex $i, j = 1, 2, 3$ corresponds to the family index while the $SU(3)_C$ color and $SU(2)_L$ weak isospin indices are suppressed. The "μ term" is the supersymmetric version of the Higgs boson mass in the SM, leading to

$$-\mathcal{L}_{\text{supersymmetric Higgs mass}} = |\mu|^2(|H_u^+|^2 + |H_d^0|^2 + |H_u^0|^2 + |H_d^-|^2). \tag{1.40}$$

The soft supersymmetry breaking terms, compatible with gauge invariance within the

Names		spin 0	spin 1/2	$SU(3)_c, SU(2)_L, U(1)_Y$
squarks, quarks	$\hat{Q}$	$(\tilde{u}_L \quad \tilde{d}_L)$	$(u_L \quad d_L)$	$(3,\ 2,\ \frac{1}{6})$
	$\hat{\bar{u}}$	$\tilde{u}_R^*$	$u_R^\dagger$	$(\bar{3},\ 1,\ -\frac{2}{3})$
	$\hat{\bar{d}}$	$\tilde{d}_R^*$	$d_R^\dagger$	$(\bar{3},\ 1,\ \frac{1}{3})$
sleptons, leptons	$\hat{L}$	$(\tilde{\nu}_L \quad \tilde{e}_L)$	$(\nu_L \quad e_L)$	$(1,\ 2,\ -\frac{1}{2})$
	$\hat{\bar{e}}$	$\tilde{e}_R^*$	$e_R^\dagger$	$(1,\ 1,\ 1)$
Higgs, higgsinos	$\hat{H}_u$	$(H_u^+ \quad H_u^0)$	$(\tilde{H}_u^+ \quad \tilde{H}_u^0)$	$(1,\ 2,\ \frac{1}{2})$
	$\hat{H}_d$	$(H_d^0 \quad H_d^-)$	$(\tilde{H}_d^0 \quad \tilde{H}_d^-)$	$(1,\ 2,\ -\frac{1}{2})$

Table 1.3: Chiral supermultiplets in the MSSM. The spin 1/2 are left-handed two component Weyl fermions. The spin 0 are complex scalar fields.

Names	spin 1/2	spin 1
gluino, gluon	$\tilde{g}$	g
winos, W bosons	$\tilde{W}^\pm \ \tilde{W}^0$	$W^\pm \ W^0$
bino, B boson	$\tilde{B}^0$	B^0

Table 1.4: Gauge supermultiplets in the MSSM.

MSSM field content, are given by

$$\begin{aligned}\mathcal{L}_{\text{soft}}^{\text{MSSM}} = &-\frac{1}{2}\left(M_3\tilde{g}\tilde{g} + M_2\tilde{W}\tilde{W} + M_1\tilde{B}\tilde{B} + \text{H.c.}\right) \\ &-\left(\tilde{\bar{u}}a_u\tilde{Q}H_u - \tilde{\bar{d}}a_d\tilde{Q}H_d - \tilde{\bar{e}}a_e\tilde{L}H_d + \text{H.c.}\right) \\ &-\tilde{Q}^\dagger m_Q^2\tilde{Q} - \tilde{L}^\dagger m_L^2\tilde{L} - \tilde{\bar{u}}m_{\bar{u}}^2\tilde{\bar{u}}^\dagger - \tilde{\bar{d}}m_{\bar{d}}^2\tilde{\bar{d}}^\dagger - \tilde{\bar{e}}m_{\bar{e}}^2\tilde{\bar{e}}^\dagger \\ &-m_{H_u}^2H_u^*H_u - m_{H_d}^2H_d^*H_d - (bH_uH_d + \text{H.c.}).\end{aligned} \tag{1.41}$$

We need negative soft supersymmetry-breaking squared-mass terms for the Higgs scalars in equation 1.41 ($m_{H_u}^2 < 0$ and $m_{H_d}^2 < 0$) to get electroweak symmetry breaking (otherwise the minimum of the potential in equation 1.40 is found for $H_u^0 = H_d^0 = 0$). Then μ should be of order 10^2 or 10^3 GeV to get a Higgs VEV at the EW scale without too much miraculous cancellation between the $|\mu|^2$ and the negative soft mass terms. A new problem arises known as the "μ problem", since there is not any symmetry protecting the $|\mu|^2$ term, it could be of order of the Planck mass scale, so in particular why should it be roughly of the same order as the soft mass terms? After including the F-terms, D-terms and soft supersymmetry-breaking terms, the minimum of the Higgs potential is found for $H_u^+ = H_d^- = 0$, while the neutral components have non-zero VEVs, $v_u = \langle H_u^0 \rangle$ and $v_d = \langle H_d^0 \rangle$, satisfying

$$v_u^2 + v_d^2 = v^2 \simeq 174 \text{ GeV}, \tag{1.42}$$

where v is the SM electroweak VEV. The ratio of the VEVs is usually written in terms

of a new free parameter β as

$$\tan\beta \equiv \frac{v_u}{v_d}. \tag{1.43}$$

1.3.3 *R*-parity

An extra ingredient is usually added to supersymmetry. There are processes in SUSY which violate baryon number (B) and lepton number (L) leading to proton decay and other B- and L-violating processes which have not been seen experimentally. In order to avoid these processes, a new symmetry is added known as "R-parity" [73], with a conserved quantum number defined as

$$P_R = (-1)^{3(B-L)+2s}, \tag{1.44}$$

where s refers to the spin of the particle. When we drop the part depending on the spin in equation 1.44, we are left with "matter parity" [84–87]

$$P_M = (-1)^{3(B-L)}. \tag{1.45}$$

Under matter parity, all the quarks and leptons supermultiplets have charge $P_M = -1$, while the Higgs and the gauge supermultiplets have matter parity $P_M = +1$. When enforcing matter parity, the MSSM does not have any renormalizable interactions that violate B or L. Matter parity commutes with supersymmetry, since all members of a given supermultiplet have the same matter parity.

In the case of R-parity, the particles within the same supermultiplet do not share the same charge. All SM particles have even R-parity ($P_R = +1$) while the supersymmetric partners, the sparticles, have odd R-parity ($P_R = -1$). Matter parity and R-parity conservation are equivalent in the sense that any interaction vector will satisfy $(-1)^{2s} = +1$ to conserve angular momentum. If R-parity is exactly conserved, every interaction vertex has to contain an even number of $P_R = -1$ sparticles. This leaves us with a stable particle given by the lightest supersymmetric particle (LSP), which can be a good dark matter (DM) candidate [88, 89] if it is electrically neutral and it interacts weakly with ordinary matter.

In general, symmetries that when acting on different fields within the same supermultiplet have different transformation properties are called R symmetries and do not commute with supersymmetry. Sometimes, in model building one uses continuous $U(1)$ R symmetries or discrete $\mathbb{Z}_N$ which are then broken to R-parity, a discrete $\mathbb{Z}_2$ symmetry. The superpotential must carry charge $+2$ under R symmetries to conserve R symmetry.

1.4 Grand Unified Theories

A grand unified theory (GUT) accommodates gauge coupling unification at a scale M_{GUT}, much larger than the electroweak scale but below the Planck scale M_P. The Standard Model would be the limit of this new theory at low energies. It was first proposed by [90, 91] as a theory for quarks and leptons beyond the Standard Model (BSM). Originally, the first models of GUTs did not include supersymmetry but most of them have been ruled out and we will focus on supersymmetric grand unification.

In the Standard Model, the three gauge couplings at the electroweak scale are very different, however they evolve and change with energy according to their renormalisation group equations and they may converge at some higher scale. Once the MSSM is considered, the new extra particles provide additional contributions leading to apparent unification of gauge couplings at a scale $M_{\text{GUT}} \sim 10^{16}$ GeV, which we call the grand unification scale, motivating SUSY GUT models. Figure 1.1 shows the renormalisation evolution of the inverse gauge couplings α_i^{-1}, where $\alpha_i = g_i^2/4\pi$, for both cases the Standard Model and the MSSM.[3]

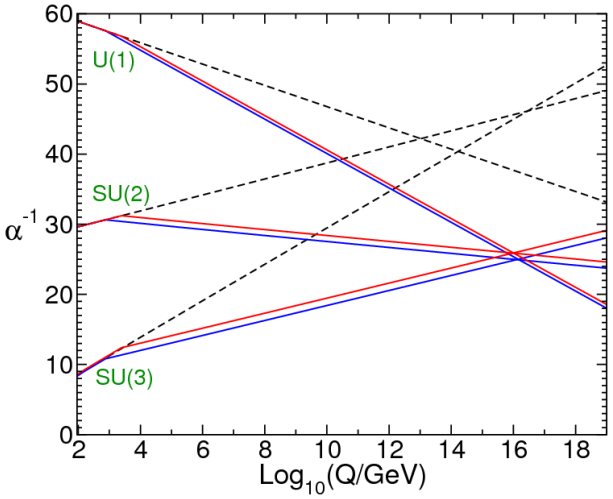

Figure 1.1: Inverse gauge couplings α^{-1} two-loop renormalization group evolution in the Standard Model (dashed lines) and the MSSM (solid lines). Figure from [92].

Additionally, a grand unified theory gives an explanation of why the charge of the proton is equal but opposite to the charge of the electron. This is known as the charge quantization problem in the Standard Model, namely why the quark charges are quantized into multiples of $e/3$, where e is the electron charge. In a grand unified theory, quarks and leptons are assigned to an unique multiplet therefore their charges must be related since the trace of any generator has to be zero.

A grand unified theory is described by a larger symmetry group G containing the SM,

[3] In this normalisation, $g_1 = \sqrt{5/3}g'$, $g_2 = g$ and $g_3 = g_s$.

i.e.

$$G \supset SU(3)_C \times SU(2)_L \times U(1)_Y. \tag{1.46}$$

Since the SM is rank four the group G has to be of rank four or greater. The first model proposed was the Pati-Salam group $SU(4)_C \times SU(2)_L \times SU(2)_R$ [91]. Even though it can not be considered as true unification, because it still has three different couplings, it was the first model whose quarks and leptons were unified into single multiplets, where the leptons are the fourth colour and the charge assignment is left-right symmetric. The choice of a GUT group can be quite large, but in the following we will focus on $SU(5)$ [90] and $SO(10)$ [93, 94]. Other choices are larger $SU(N)$ groups or the exceptional group E_6, but we will not consider them in this thesis.

1.4.1 SU(5)

The minimal choice towards a GUT is based on the $SU(5)$ group which is rank four (the other simple rank 4 algebras could not work since they do not have complex representations). To embed the Standard Model gauge group in $SU(5)$, one can take the $SU(3)_C$ and $SU(2)_L$ generators on the upper-left 3×3 and lower-right 2×2 blocks, respectively, in traceless 5×5 matrices for $SU(5)$ generators of the fundamental representation **5**. The $U(1)_Y$ generator is then given by the commutation relation with $SU(3)_C \times SU(2)_L$, i.e. $\mathrm{diag}(-1/3,-1/3,-1/3,1/2,1/2)$.

A left-handed family of leptons and quarks transform like $\overline{\mathbf{5}} \oplus \mathbf{10}$ in the $SU(5)$ model

$$\overline{\mathbf{5}} = \begin{pmatrix} d_r^c \\ d_b^c \\ d_g^c \\ e^- \\ -\nu_e \end{pmatrix}_L , \quad \mathbf{10} = \begin{pmatrix} 0 & u_g^c & -u_b^c & -u_r & -d_r \\ -u_g^c & 0 & u_r^c & -u_b & -d_b \\ u_b^c & -u_r^c & 0 & -u_g & -d_g \\ u_r & u_b & u_g & 0 & -e^+ \\ d_r & d_b & d_g & e^+ & 0 \end{pmatrix}_L , \tag{1.47}$$

where r, b, g are quark colours and c denotes the charge conjugated fermions.[4] Note that there is no space for the right-handed neutrinos within this multiplet and they have to be added as singlets of $SU(5)$ if desired. Furthermore, with this multiplet structure the sum of the quantum numbers Q, T_3 and Y are zero within one multiplet, as it should, since the trace of any of these generators must be equal to zero. The trace of the charge operator Q on the $\overline{\mathbf{5}}$ representation being equal to zero forces the charge of the down quark to be 1/3 of the charge of an electron. Similarly, one finds that the charge of the up quark to be 2/3 of the positron charge, giving a solution to the charge quantization problem of the Standard Model.

To preserve local gauge invariance under $SU(5)$ the gauge bosons in the **24** adjoint representation are introduced. The Standard Model gauge fields (gluons and electroweak

[4] The bar in $\overline{\mathbf{5}}$ refers to the complex conjugate of the fundamental representation **5**.

bosons) are unified in a single **24** adjoint. In addition to the SM gauge bosons, new X and Y gauge bosons appear from the 12 remaining degrees of freedom in the **24** representation. These new gauge fields produce new interactions in which quarks are transformed into leptons and vice-versa, thus violating lepton and baryon number.[5] These new transitions lead to nucleon decays.

The Higgs field, necessary to break the electroweak symmetry at the weak scale, is accommodated in a **5** multiplet of $SU(5)$.[6] This representation not only has the Higgs doublet under $SU(2)$ but it has three additional states known as colour-triplet Higgs scalars. The Higgs triplet also violates lepton and baryon number, inducing nucleon decay. Due to the strong constraints on nucleon decays, the mass of the Higgs triplet has to be very high, close to $M_{\rm GUT}$. This leads to a problem known as the doublet-triplet splitting problem since we need the Higgs doublet to be at the electroweak scale while having GUT-scale Higgs triplets, however we would expect fields from the same multiplet to have equal-scale masses. This problem also arises in other models based in different GUT groups than $SU(5)$ and we will address it in the models presented in this thesis.

The breaking of $SU(5)$ down to $SU(3)_C \times SU(2)_L \times U(1)_Y$ can be done by a Higgs multiplet in the **24** representation developing a VEV $\propto \mathrm{diag}(1, 1, 1, -3/2, -3/2)$, which commutes with $SU(3)_C \times SU(2)_L \times U(1)_Y$. Therefore, this VEV gives masses to the X, Y gauge bosons of the $SU(5)$ group but not to the electroweak gauge bosons, which remains massless until the **5** Higgs multiplet acquires a VEV.

We mentioned before that the new gauge bosons X and Y as well as the Higgs triplets lead to nucleon decays. These processes induces effective four fermion interactions of the form $qqql/\Lambda^2$, where q and l refers to a quark or a lepton, respectively. The scale Λ is associated with the mass scale of the mediating particle. There are heavy constraints from the non-observation of nucleon decay, for example, the null result on search for the dominant decay mode of a proton decaying into a positron plus a neutral pion constrains Λ to be larger than $\mathcal{O}(10^{15})$ GeV [31]. In a non-SUSY $SU(5)$ model, gauge coupling unification is expected to be reached well below 10^{15} GeV, therefore non-SUSY $SU(5)$ is heavily constrained by the non-observation of nucleon decay. In SUSY GUTs the grand unification scale is $M_{\rm GUT} \sim 2 \times 10^{16}$ GeV predicting a lifetime of the proton about $\tau \sim 10^{36}$ years, larger than the current constraints 10^{31-34} years (depending on the model). In SUSY GUTs, there are additional dimension four and dimension five operators. Operators of dimension four can be eliminated requiring R-parity within the model. In SUSY $SU(5)$ GUTs, dimension-five operators are generically generated via the triplet Higgs exchange and they must necessarily obtain masses of order the GUT scale.

[5] The difference between baryon and lepton number $B - L$ is conserved in these transitions.

[6] In the MSSM the two Higgs multiplets H_u and H_d are contained in a **5** and a $\overline{\mathbf{5}}$ representation, respectively.

Additionally, one must be careful with the mass scale of the new particles. The gauge coupling unification in the MSSM assumes that there is no additional field content between the supersymmetry scale, usually of the order $\mathcal{O}$(TeV) and the GUT scale $M_{\rm GUT}$. New particles will contribute to the running of gauge couplings (when the new particles are non-singlets), mainly at their mass scales. This is another reason to have the colour-triplet Higgs at high scale, no to spoil gauge coupling unification. This is also valid for any GUT group chosen.

1.4.2 SO(10)

The next simple unification is based on the gauge group $SO(10)$ which is rank 5. All matter fields are unified into a single representation, the **16** fundamental representation. It includes all quark and lepton fields and also accommodates a singlet under the SM, which can be associated with the right-handed neutrino. The gauge fields are in the **45** adjoint representation. The product of two matter representations gives $\mathbf{16} \otimes \mathbf{16} = \mathbf{10} \oplus \mathbf{126} \oplus \mathbf{120}$. We can construct Yukawa couplings if the Higgs field is in the **10** representation since the product $\mathbf{10} \otimes \mathbf{10}$ contains the singlet representation (although other possibilities include Higgs fields in the **120** or **126** representations). Since all fermions are unified into a single representation, there is only one Yukawa coupling predicting equal fermion masses at the GUT scale which is phenomenologically ruled out. Therefore, it is necessary to add additional Higgs fields to build a viable theory.

The breaking of $SO(10)$ into the SM model can be done through different directions since it contains as subgroups both the Pati-Salam group $SU(4)_C \times SU(2)_L \times SU(2)_R$ as well as $SU(5) \times U(1)$. The breaking path depends on the Higgs field representation which acquires a VEV, see e.g. [95] for an extended overview of the possible breaking schemes. In general, if $SO(10)$ is broken to the Pati-Salam group $SU(4)_C \times SU(2)_L \times SU(2)_R$, the fundamental representation is decomposed as $\mathbf{16} \to (\mathbf{4},\mathbf{2},\mathbf{1}) \oplus (\bar{\mathbf{4}},\mathbf{1},\mathbf{2})$, $\mathbf{10} \to (\mathbf{6},\mathbf{1},\mathbf{1}) \oplus (\mathbf{1},\mathbf{2},\mathbf{2})$ and $\mathbf{45} \to (\mathbf{1},\mathbf{3},\mathbf{1}) \oplus (\mathbf{1},\mathbf{1},\mathbf{3}) \oplus (\mathbf{15},\mathbf{1},\mathbf{1}) \oplus (\mathbf{6},\mathbf{2},\mathbf{2})$. When $SO(10)$ is broken in the direction of $SU(5) \times U(1)$, then $\mathbf{16} \to \bar{\mathbf{5}}_3 \oplus \mathbf{10}_{-1} \oplus \mathbf{1}_{-5}$, $\mathbf{10} \to \mathbf{5}_2 \oplus \bar{\mathbf{5}}_{-2}$ and $\mathbf{45} \to \mathbf{1}_0 \oplus \mathbf{10}_4 \oplus \overline{\mathbf{10}}_{-4} \oplus \mathbf{24}_0$.

The right-handed Majorana masses M_R can be generated from the non-renormalisable operators

$$\frac{\lambda_{ij}}{\Lambda} \bar{H}\bar{H}\psi_i\psi_j \to \frac{\lambda_{ij}}{\Lambda} \langle v_{\bar{H}} \rangle^2 \nu_i^c \nu_j^c \equiv M_R^{ij} \nu_i^c \nu_j^c, \tag{1.48}$$

where Λ may be of order the Plank scale, ψ is in the **16** representation, and $\bar{H}$ are Higgs in the $\overline{\mathbf{16}}$ representation whose right-handed neutrino component gets a VEV $\langle v_{\bar{H}} \rangle$, breaking $SO(10)$ down to $SU(5)$ at the GUT scale. The right-handed neutrino is denoted as ν^c.

Gauge coupling unification as well as charge quantization are also achieved in $SO(10)$. The doublet-triplet splitting problem is also appearing in models based on $SO(10)$ and

we will discuss how to solve it in each of the models presented in this thesis. Proton decay discussion follows as in the case of $SU(5)$.

1.5 The flavour puzzle

The flavour puzzle in the Standard Model can be summarized by the lack of understanding of the following questions:

- Why are there 3 families of quarks and leptons?
- Why is there such a large hierarchy between the different fermion masses, ranging from the lightest neutrino, on the order of meV, to the top quark, with mass $m_t \approx 173$ GeV?
- Why is the mixing pattern in the quark sector, given by the CKM matrix, so small while the lepton mixing, characterized by the PMNS matrix, is so large?
- What is the origin of CP violation?

The Standard Model does not account for the three different families of fermions that transform in the same gauge representation under the SM gauge group but differ by their mass. Most of the free parameters of the SM are related to the questions above. The Yukawa couplings of fermions to the Higgs field are not predicted by the theory and have to be measured experimentally. If we assume an extension of the SM, with three right-handed neutrinos, there are 22 (20 if $B - L$ is conserved) independent low-energy parameters in the flavour sector, the Yukawa couplings of quarks and charged leptons, the mixing parameters and CP-phase in the CKM and PMNS matrices, the neutrino masses and two Majorana phases (only if neutrinos are Majorana particles).

There is no justification for the large range between fermion masses, from few MeV to over 100 GeV in the quark sector. One can go one step further and ask why the hierarchy between different fermion types is not conserved through the families, e.g. why does the ratio between up quark and down quark masses $m_u/m_d \lesssim 1$ differ from that of the charm and strange quarks $m_c/ms \sim 10$, or top and bottom quarks $m_t/m_b \sim 50$?[7] Furthermore, the range between masses is enlarged when considering neutrino masses which are no larger than $\mathcal{O}(100)$ meV, many orders of magnitude below the lightest charged fermion, the electron, with mass $m_e \sim 0.5$ MeV. We have seen that one possible solution to have so tiny neutrino masses is given by the seesaw mechanism in section 1.2.

The third question is concerned about the fact that the CKM mixing matrix is small compared with the PMNS mixing matrix. The largest mixing angle in the quark sector is

[7] These numbers change with the scale due to the renormalization group equations and are merely indicative.

given by the Cabbibo angle with $\theta_{12}^q \approx 13^\circ$ and the rest being almost negligible, however in the leptonic sector all mixing angles are sizeable. This is analogous to understand the evidence that the hierarchy in the neutrino sector is much milder than the one in the charged fermions.

One possible argument for considering three families instead of two relates to CP violation, as discovered by Kobayashi and Maskawa [19]. Once one includes three weakly interacting families, a new complex phase is automatically introduced in the mixing matrix leading to CP violation, which is not appearing in the case of a two-family system. CP violation was experimentally discovered in neutral kaon decays in 1964 [96], and observed in recent years in B meson decays. There are also experimental hints [32] that CP is violated in the lepton sector. In fact, CP violation is necessary to understand the baryon asymmetry of the universe (BAU), as discussed in section 1.6. However, this is not enough to understand why there are three families in the SM since the CP violation in the CKM matrix is not sufficient to explain the observed baryon asymmetry.

1.5.1 Discrete flavour symmetries

We are interested in following a guide principle, comparable to the gauge principle, to tackle the flavour puzzle such that the Yukawa couplings are deducted from first principles. In the absence of fermion masses, the Standard Model contains an accidental global symmetry $[U(3)]^5$, which is the maximal symmetry preserved by the kinetic terms. Each $U(3)$ corresponds to a family symmetry for each fermion-type, i.e. Q_L, u_R, d_R, L_L, e_R. If we add right-handed neutrinos, there would be an extra $U(3)$ symmetry. Clearly, this symmetry is broken once one considers the observed fermion masses, however we can imagine a situation where a global family symmetry is imposed at high energies and which is then broken by the VEV of some scalar field. Such fields are usually called "flavons" and they can give a dynamical origin to the Yukawa parameters of the Standard Model. The flavon field, denoted by ϕ, is a gauge singlet under the SM and it couples to the fermions ψ and Higgs field H giving rise to Yukawa terms after the symmetry is broken, e.g.

$$\mathcal{L} \supset \frac{1}{\Lambda}\phi\overline{\psi}H\psi \rightarrow \frac{\langle\phi\rangle}{\Lambda}\overline{\psi}H\psi \rightarrow Y\overline{\psi}H\psi, \tag{1.49}$$

where Λ is the mass scale of the high energy theory.

Family symmetries restrict the Yukawa couplings such that one can possibly explain some of the features of masses and mixing. There are models based in global continuous flavour symmetries, however they lead to massless Goldstone bosons [97–99] after spontaneous symmetry breaking. A more common choice in the literature is the use of discrete flavour symmetries, more specifically, non-Abelian discrete symmetries (for reviews, see e.g. [100–103]). The main interest of these groups from a physics point of

view is that, because of the non-Abelian aspect, it is necessary that at least some of the representations must be matrices. Therefore, some non-Abelian discrete symmetries may include non-trivial triplet representations, providing a posteriori justification for the observation of three families of fermions. Some of the simplest such groups are A_4 and S_4 which are subgroups of $SU(3)$. Their irreducible representations and their Kronecker product rules are listed in appendix A. GUT models together with either A_4 or S_4 symmetries are described in chapters 2, 3 and 4.

Although we will focus in non-Abelian discrete symmetries, it is worth mentioning one of the most popular Abelian family symmetries, proposed by Froggatt and Nielsen [104]. It is based on a flavour $U(1)$ symmetry under which the fermions are distinguished. Each family has a different $U(1)$ charge such that the usual Yukawa terms have positive integer charges. Additionally, one includes a flavon field ξ which typically has a $U(1)$ charge assignment of -1. Therefore, you can construct Yukawa interactions using different powers n_{ij} of the flavon field to compensate the charges of the fermion fields, i.e.

$$c_{ij}\left(\frac{\xi}{\Lambda}\right)^{n_{ij}}\overline{\psi}_{iL}\psi_{jR}H, \tag{1.50}$$

where H is the Higgs doublet, ψ is a fermion field, i and j are family indices and c_{ij} are undetermined order one coefficients. After the flavon field acquires a VEV, the hierarchies between the different fermion masses are determined solely by the $U(1)$ charge assignments, since the effective Yukawa couplings become $Y_{ij} = c_{ij}(\langle\xi\rangle/\Lambda)^{n_{ij}}$. This idea can also be implemented using $\mathbb{Z}_N$ discrete symmetries if preferred. In chapter 4, this mechanism is used in combination with A_4 family symmetry, meaning that Abelian and non-Abelian symmetries can be combined to explain flavour structures.

Coming back to discrete non-Abelian family symmetry models, there are two different approaches one can follow. The first is based on "direct" models, in which the discrete symmetry is partially broken and a residual symmetry remains after flavour breaking, while in the second approach, the so-called "indirect" models, no part of the original symmetry is present at low scale. The symmetry is broken by the flavon VEVs. Depending on the alignments of these flavons and how they are broken, we will have different flavour structures.

The motivation for direct models is given by the leptonic sector. In the basis of (approximately) diagonal charged leptons and assuming neutrinos to be Majorana, the neutrino mass matrix is always symmetric under a Klein symmetry $\mathbb{Z}_2 \times \mathbb{Z}_2$ while the charged lepton mass matrix is $\mathbb{Z}_3$ symmetric. In the case that the Klein symmetry is generated by the generators S and U of S_4, given in appendix A.1, then the PMNS mixing matrix is associated with tri-bimaximal (TB) mixing [105, 106], which predicts $\sin\theta_{23} = 1/\sqrt{2}$, $\sin\theta_{12} = 1/\sqrt{3}$, $\theta_{13} = 0$ and no CP violation. Although TB is already excluded, the good agreement of data at that time motivated the use of non-Abelian discrete symmetries in flavour models. In direct models the full Klein-symmetry in the

neutrino sector and the $\mathbb{Z}_3$ symmetry in the charged lepton sector arise as a subgroup of the initial family symmetry since the flavons fields which break the symmetry preserve these subgroups.

In the indirect approach, we do not demand these accidental symmetries to arise as a subgroup of the original family symmetry after it has been broken. The possible vacuum alignments of the flavon fields are not restricted to preserve any subgroup of the original family symmetry and therefore the options to construct a phenomenologically successful flavour model are enlarged. The possible alignments will depend on the allowed couplings and field content of the model. Chapter 2 is based on a semidirect model in which only part of the accidental symmetry can be identified with a generator of the family symmetry (in this case only one of the two $\mathbb{Z}_2$ symmetries of the Klein symmetry is generated by the SU generator of S_4) while chapters 3 and 4 are indirect models.

1.6 The baryon asymmetry of the Universe

The ΛCDM model [107] is known as the "standard model" for Big Bang cosmology. The name Λ refers to the positive cosmological constant which is responsible for the accelerated expansion of the Universe [108]. The term "CDM" alludes to cold dark matter. It is the minimal model able to reproduce most cosmological observations, such us the existence and anisotropies of the CMB, the large-scale galaxy structure, the abundances of light elements and the accelerating expansion of the Universe. Together with the ΛCDM model, it is believed that at very early stages the Universe went through a period of superluminal expansion known as inflation [109–111], which explains why the Universe is spatially-flat, homogeneous and isotropic.

However, the ΛCDM model does not address the fact that we have only observed primordial matter but not antimatter, i.e. it does not give an explanation for the baryon asymmetry of the Universe (BAU). It cannot be explained using very specific initial conditions within the framework of an inflationary model, since any asymmetry at the beginning of the Universe would be wash-out during the inflationary period. Therefore, the baryon asymmetry of the Universe must be generated after inflation and before Big Bang nucleosynthesis (BBN), when the first light elements were formed. It is necessary to find a mechanism which explains the observed baryon-to-photon ratio

$$\eta_B = \frac{n_B - n_{\overline{B}}}{n_\gamma} = (6.10 \pm 0.04) \times 10^{-10}, \tag{1.51}$$

where $n_B - n_{\overline{B}}$ is the difference between the baryons and antibaryons density and n_γ is the number photon density. Since primordial antimatter has not been observed, $n_B \gg n_{\overline{B}}$, one uses the baryon-to-photon ratio η_B to understand the baryon asymmetry of the Universe.

In 1967, Sakharov [112] realised that three conditions must be satisfied for baryogenesis to occur in a particle physics theory, i.e.

- Baryon number (B) violation.
- Charge (C) and charge-parity (CP) violation.
- The process must occur out of thermal equilibrium.

The first condition is not satisfied at tree level in the Standard Model. If we think in terms of grand unified theories, we already mentioned that the new gauge bosons X and Y can mediate baryon number violating interactions, however present bounds suggest that inflation reheated well below GUT energies (the reheating temperature T_{RH} cannot be higher than $\sim 10^{15}$ GeV from CMB observations [59]), and thus thermal GUT baryogenesis is not viable.

Focusing again in the Standard Model, baryon number (B) and lepton number (L) are accidental symmetries of the Lagrangian, however $B+L$ is violated by the $SU(2)$-chiral anomaly, while $B-L$ is conserved also at the quantum level. Sphalerons [113] are non-perturbative field configurations which violate B and L number but conserve $B-L$. The sphaleron transitions are efficient for temperatures above the electroweak symmetry breaking. Therefore, if baryon asymmetry has been produced above the EW scale, sphalerons will wash out any primordial baryon asymmetry. On the other hand, the sphaleron processes open up a new possibility of producing a net lepton asymmetry at high scales and use sphalerons to convert the initial lepton asymmetry into a baryon asymmetry. This solution is known as leptogenesis and it was first proposed by Fukugita and Yanagida [114].

The second condition presented by Sakharov has to do with charge (C) and charge-parity (CP) violation. This is easily understood if we consider a decay $X \to Y + B$ and the C-conjugate process $\overline{X} \to \overline{Y} + \overline{B}$, where X and Y are $B = 0$ states. If charge is conserved, the decay rates of these two processes are equal $\Gamma(X \to Y + B) = \Gamma(\overline{X} \to \overline{Y} + \overline{B})$. If there are equal number of states X and C-conjugate states $\overline{X}$, then the net baryon production vanishes in the case of C-conserving interactions. Additionally, one also needs CP-violating interactions. Consider, for example, the chiral decays $X \to q_L + q_L$ and $X \to q_R + q_R$, where q is a quark state with $B \neq 0$. Even though, C-violation means $\Gamma(X \to q_L + q_L) \neq \Gamma(\overline{X} \to \overline{q}_L + \overline{q}_L)$, CP-conservation implies $\Gamma(X \to q_L + q_L) = \Gamma(\overline{X} \to \overline{q}_R + \overline{q}_R)$ and $\Gamma(X \to q_R + q_R) = \Gamma(\overline{X} \to \overline{q}_L + \overline{q}_L)$ and therefore, the total decay rates of X and $\overline{X}$ into baryons and antibaryons are again equal:

$$\Gamma(X \to q_L + q_L) + \Gamma(X \to q_R + q_R) = \Gamma(\overline{X} \to \overline{q}_R + \overline{q}_R) + \Gamma(\overline{X} \to \overline{q}_L + \overline{q}_L). \quad (1.52)$$

Thus, as long as the initial state has equal numbers of X and $\overline{X}$, we end up with no net baryon asymmetry if C or CP are conserved.

Finally the process must occur out of thermal equilibrium, since otherwise any baryon asymmetry initially produced would be washed-out by the inverse process. Suppose again the decay $X \to Y + B$. If the process occurs in thermal equilibrium, then the rate in one direction is identical to the rate in the opposite direction, i.e. $\Gamma(X \to Y + B) = \Gamma(Y + B \to X)$, such that no net baryon asymmetry is produced.

We can conclude that, in principle, it is possible to satisfy all the Sakharov conditions within the Standard Model. However, the amount of CP violation in the SM is not enough to generate the observed baryon asymmetry and baryogenesis within the SM has already been ruled out. Therefore, the baryon asymmetry of the Universe requires some extension of the SM. In the following, we will focus in the leptogenesis procedure presented by Fukugita and Yanagida [114], which is a natural solution once we add right-handed neutrinos to the SM. In fact, the seesaw mechanism, which is the most common choice to explain neutrino masses, makes a perfect scenario to address the baryon asymmetry of the Universe through leptogenesis.

1.6.1 Leptogenesis

The original leptogenesis mechanism [114] relies on the type-I seesaw mechanism. The lepton asymmetry is generated through the out of equilibrium decay of heavy right-handed neutrinos into leptons (or anti-leptons) and Higgs bosons via Yukawa couplings. CP violation occurs in the decay due to interference effects at one loop, which can lead to a net lepton asymmetry. In most models, the lightest right-handed neutrino mass $M_1 \ll 10^{15}$ GeV is compatible with the upper bound in the reheating temperature after inflation $T_{RH} \lesssim 10^{15}$ GeV, meaning that the asymmetry generated is not washed-out by the inflationary epoch.

The right-handed neutrinos do not carry lepton number and therefore the decay of a right-handed neutrino into lepton-Higgs and the inverse process violate lepton number ($|\Delta L| = 1$). At temperatures $T \gg 100$ GeV, the sphaleron transitions violate $B + L$ but conserve $B - L$. If we start with a lepton asymmetry, we could end up with about 1/3 of the $B - L$ asymmetry in the form of a baryon asymmetry while the other -2/3 of the $B - L$ asymmetry would be in the form of a lepton number.

The type-I seesaw mechanism provides the necessary ingredients to satisfy the three Sakharov conditions: baryon asymmetry after sphaleron transitions, C and CP violation of the process and out-of-equilibrium decays for which one requires $T \ll M_R$, where T is the temperature of the Universe at the time of the decay and M_R is the mass of the right-handed neutrino. Now, one needs to check quantitative if it is possible to reproduce the observed baryon-to-photon ratio. The amount of CP-violation will depend on δ^l, the CP phase of the PMNS matrix (experimentally there is a preference for non-zero δ^l given by global fits [32]). Additionally, one has to take into account the wash-out due

to inverse decays and scattering. Let us give a simple example of the mechanism in a toy model of thermal leptogenesis.

Thermal leptogenesis is based on the thermal production of the right-handed neutrinos. In this example we assume very hierarchical right-handed neutrinos $M_1 \ll M_2, M_3$ so that the right-handed neutrino N_1 is the last heavy neutrino to decay out of equilibrium and generates the lepton asymmetry. The evolution of the right-handed neutrino abundance, N_{N_1}, is given by the Boltzmann equation

$$\frac{dN_{N_1}}{dz} = -D_1(N_{N_1} - N_{N_1}^{\rm eq}), \tag{1.53}$$

where $z \equiv M_1/T$ and $N_{N_1}^{\rm eq}$ is the abundance at thermal equilibrium. The decay factor D_1 is proportional to the ratio of the total decay width Γ_{D_1} to the expansion rate of the Universe. For a more detailed explanation of the decay factor we refer to [115].

The lepton asymmetry is converted into a baryon asymmetry through sphalerons. These processes conserve the $B-L$ asymmetry and the final baryon asymmetry is approximately 1/3 of the $B-L$ asymmetry. The evolution of the $B-L$ asymmetry is described by

$$\frac{dN_{B-L}}{dz} = \varepsilon_1 D_1(N_{N_1} - N_{N_1}^{\rm eq}) - W N_{B-L}. \tag{1.54}$$

The first term on the right-hand side corresponds to the $B-L$ asymmetry produced. The parameter ε_1 is proportional to the CP asymmetry and it is given by

$$\varepsilon_1 = \frac{\Gamma(N_1 \to lH) - \Gamma(\overline{N}_1 \to \overline{lH})}{\Gamma(N_1 \to lH) + \Gamma(\overline{N}_1 \to \overline{lH})}, \tag{1.55}$$

where the lepton l is by definition the lepton produced by the decay of the N_1 right-handed neutrino and, in general, it will be a combination of the flavour eigenstates. It is computed from the interference of the tree level with one loop self-energy and vertex diagrams in figure 1.2. The parameter ε_1 will be proportional to the neutrino Yukawa matrix and the specific value is model dependant.

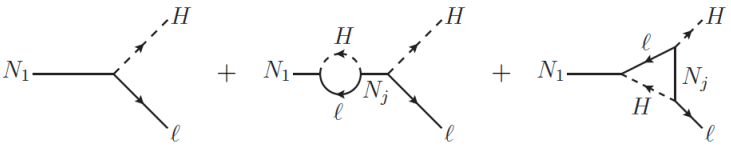

Figure 1.2: Diagrams contributing to the CP asymmetry in right-handed neutrino decays.

The second term in the right-hand side of equation 1.54 takes into account the wash-out meaning that this term is not a source of $B-L$ asymmetry but instead it tries to re-equilibrate the number of leptons and anti-leptons. It contains information about inverse decays and scattering processes, we refer again to [115] for details.

The set of Boltzmann equations 1.53 and 1.54 may be solved for thermal initial conditions

at $z = 0$ to give the final asymmetry N^f_{B-L} at $z \gg 1$. The solution can be written as $N^f_{B-L} = \varepsilon_1 \kappa_1$, where κ_1 is known as the efficiency factor.

Finally, one needs to compare the $B-L$ asymmetry with the observed baryon-to-photon ratio η_B, using the relation

$$\eta_B = a_{\rm sph} \frac{N^f_{B-L}}{N^{\rm rec}_\gamma}, \tag{1.56}$$

where $N^{\rm rec}_\gamma \simeq 37$ and $a_{\rm sph} = 28/79 \simeq 1/3$ [116, 117].[8] The factor $a_{\rm sph}$ takes into account the number of $B-L$ asymmetry converted into a baryon asymmetry by the sphalerons while $N^{\rm rec}_\gamma$ accounts for the production of photons after leptogenesis until recombination, when nuclei and electrons combined to form atoms.

In chapter 3, we present a model in which the correct BAU is obtained through N_2-leptogenesis, meaning that the second right-handed neutrino decays are the ones responsible for the asymmetry. The reason is that the lightest right-handed neutrino is too light to produce the observed BAU. We take into account the wash-out due to inverse decays into N_1 as well as flavour effects.

1.7 Extra dimensions

The idea of extra dimensions was introduced in the 1920s by Kaluza-Klein [118, 119] in an attempt to unify gravity with electromagnetism. The new concept of this theory was to extend general relativity in the presence of a fifth dimension. The 5-dimensional (5D) gravity would manifest in our observable 4-dimensional (4D) space-time as gravitational, electromagnetic and a new scalar field. More recently, during the late 1970s and the 1980s, higher dimensional theories gained renewed interests seeking for the unification of gravity with electroweak and strong interactions in a consistent quantum theory. This idea led to superstring and supergravity theories, which are described in ten and eleven space-time dimensions respectively.

To overcome the fact that we do not observe extra dimensions, these are assumed to be compactified and finite in size. The energies necessary to experimentally observe the extra dimensions are of the order of the length scale at which the compact dimensions live. This compactification can break the higher-dimensional Lorentz invariance or the higher-dimensional Poincaré invariance as in orbifolds where translational invariance is explicitly broken. Furthermore, the compactification of extra dimensions can also introduce non-trivial boundary conditions, a mechanism that can be used for symmetry breaking.

In this thesis, the motivation to consider extra dimensions is that they offer a simple

[8] This expression is valid for the Standard Model plus three right-handed neutrinos. In the case of the MSSM, for example, there will be another factor of 2 due to the decay of the right-handed sneutrinos.

and elegant way to break GUT symmetries by appropriate boundary conditions, as first proposed by Kawamura [120–122]. The basic idea is that the GUT symmetry is realised in 5 or more space-time dimensions and it is broken to the Standard Model by using GUT-symmetry violating boundary conditions on an orbifold compactification. Within this approach, the doublet-triplet splitting problem is easily solved by leaving only the light Higgs doublets after orbifolding, as we will see in chapter 4. Additionally, discrete symmetries may arise from orbifold compactifications [123], which might be used as the flavour symmetry.

1.7.1 A compactified 5-dimensional toy model

We introduce a 5D toy model to illustrate the appearance of Kaluza-Klein modes after compactification of the extra dimension. The usual four space-time dimensions are parametrized by x^μ, where $\mu = 0, 1, 2, 3$, while the extra dimension is specified by y. In general, these coordinates can be combined into $z^M = (x^\mu, y)$, where M now runs over all the space-time indices. In this case, we compactify the extra dimension on a circle of radius R, i.e. we make the identification

$$y \sim y + 2\pi R. \tag{1.57}$$

We are now able to expand the field ϕ as a Fourier series on the extra dimensional space

$$\phi(x^\mu, y) = \sum_n \phi^{(n)}(x^\mu) e^{inky}, \tag{1.58}$$

where $k = 1/R$ is given by the condition $\phi(x^\mu, y) = \phi(x^\mu, y + 2\pi R)$ (known as ordinary compactification). We can apply the Klein-Gordon equation for a massless particle $\partial^M \partial_M \phi = (\partial^\mu \partial_\mu - \partial^y \partial_y)\phi = 0$ to the field Fourier expansion in equation 1.58, such that

$$\sum_n (\partial^\mu \partial_\mu - \partial^y \partial_y)\phi^{(n)}(x^\mu) e^{iny/R} = 0. \tag{1.59}$$

When we further simplify this equation, we end up with an equation of motion given by

$$\sum_n (\partial^\mu \partial_\mu + {m^{(n)}}^2)\phi^{(n)}(x^\mu) e^{iny/R} = 0, \tag{1.60}$$

which corresponds to the equation of motion for a set of fields $\phi^{(n)}(x^\mu)$, with a mass $m^{(n)} = n/R$. To recap, we started with a 5-dimensional massless particle, which, after applying the compactification conditions, has been split in an infinite set of 4-dimensional particles with ever increasing mass. Klein assumed R to be extremely small such that all the Kaluza-Klein modes with $n > 0$ would have stayed out of reach for experiments. For energies $E \ll R^{-1}$, heavy fields can be integrated out and the effective four dimensional theory will only depend on the zero mode $n = 0$, which is independent of y.

1.7.2 Orbifold compactification

In the following, we will be interested in orbifold compactifications. In chapter 4 we construct a model based on $SU(5)$ gauge symmetry and 6-dimensional (6D) supersymmetry (corresponding to $\mathcal{N}=2$ SUSY in 4D, where $\mathcal{N}$ refers to the number of supersymmetries, i.e. the number of distinct copies of supersymmetry generators). Orbifold compactifications have the advantage of breaking the extended $\mathcal{N}=2$ SUSY to $\mathcal{N}=1$ SUSY in 4D, in addition to the breaking of the GUT symmetry to the SM gauge group.

In general, the model is constructed based on a gauge group G on a manifold $M = \mathcal{M}_4 \times C$, where $\mathcal{M}_4$ is the 4D Minkowski space-time and the manifold C (with coordinate y) is supposed to have a symmetry under a discrete group K, i.e.

$$K: \ (x^\mu, y) \to (x^\mu, k[y]). \tag{1.61}$$

In the previous toy model, C is taken to be the set of real numbers which we then mod out by the equivalence $y \sim y + 2\pi R$ generated by the discrete translation group $K = \mathbb{Z}$, leading to the smooth space $R/\mathbb{Z} = S^1$, the circle of radius R. After compactification, the gauge symmetry of the theory is still G but now defined on the smaller physical space $\mathcal{M}_4 \times S^1$. In this example, K acts freely, i.e.

$$k[y] \neq y, \ \forall y \in C, \ \forall k \neq 1 \in K. \tag{1.62}$$

However, there are cases when the action of K has fixed points ($k[y] = y$ for some $y \in C, \ k \neq 1$). In such a case, the space C/K is known as an orbifold compactification. To understand the advantage of orbifold compactification, we have to consider the action of K in field space

$$K: \ \phi(x^\mu, y) \to R_k \ \phi(x^\mu, k^{-1}[y]), \tag{1.63}$$

where R_k is a matrix representation of K and K is now to be thought of as a subgroup of the gauge group G. In an orbifold with fixed points, the gauge symmetry of the theory, G, remains the same away from these fixed points, while at the fixed points, the gauge symmetry is reduced to a subgroup $H_y \subset G$. The subgroup H_y can be found as follows, first consider, at each y, the subgroup $F_y \subset K$ which leaves y fixed, i.e. $F_y \equiv \{k \in K: \ k[y] = y\}$. Then, the unbroken gauge group H_y at y is the centralizer of F_y in G, i.e. the elements of G that commute with the elements of F_y and it is given by

$$H_y = \{g \in G: \ gk = kg, \forall k \in F_y\}. \tag{1.64}$$

Therefore, in general, the gauge group of the theory can be broken to a subgroup at the fixed points after orbifold compactification. Furthermore, to have a consistent theory the action of the discrete group K on field space must be an automorphism of the Lie-algebra of the original gauge group G. This means that the action of K will map the Lie-algebra of the group G into itself preserving the multiplication law, in this way the

discrete group K is assured to be a symmetry of the gauge action, for more details see [124, 125].

1.7.2.1 An example: the $S^1/(\mathbb{Z}_2 \times \mathbb{Z}_2')$ orbifold

Consider the $S^1/(\mathbb{Z}_2 \times \mathbb{Z}_2')$ orbifold, where in this case $C = S^1$, the circle with radius R and $\mathbb{Z}_2 \times \mathbb{Z}_2'$ is the discrete group acting on the extra coordinate y. The action of the $S^1/\mathbb{Z}_2$ orbifold is to identify the points $y \sim -y$, i.e. identify points of the circle opposite with respect to a given diameter. Additionally, one imposes an extra constraint to obtain the orbifold $S^1/(\mathbb{Z}_2 \times \mathbb{Z}_2')$, which is $y' \sim -y'$, where $y' \equiv y + \pi R/2$. The orbifold action can be written as

$$P:\ y \to -y \quad \text{and} \quad P':\ y' \to -y'. \tag{1.65}$$

There are two inequivalent fixed points (also known as 4-dimensional walls) at $y = 0$ and $y = \pi R/2$. The orbifold $S^1/(\mathbb{Z}_2 \times \mathbb{Z}_2')$ has a fundamental domain of $0 \leq y \leq \frac{\pi R}{2}$, since any other point of the circle S^1 can be mapped from that region using the action of $\mathbb{Z}_2 \times \mathbb{Z}_2'$.

Assume now a field $\Phi(x^\mu, y)$ which is a N-multiplet under some symmetry group G. The action of the $\mathbb{Z}_2 \times \mathbb{Z}_2'$ parity on field space is defined by

$$P:\ \Phi(x^\mu, y) \to P_\Phi \Phi(x^\mu, -y) \quad \text{and} \quad P':\ \Phi(x^\mu, y') \to P'_\Phi \Phi(x^\mu, -y'). \tag{1.66}$$

The matrices P_Φ and P'_Φ are $N \times N$ matrix representations of the two $\mathbb{Z}_2$ actions, meaning that they satisfy $(P_\Phi)^2 = (P'_\Phi)^2 = 1$, where 1 refers to the $N \times N$ identity matrix. We can classify the fields by their (P, P') eigenvalues $(\pm 1, \pm 1)$, with Kaluza-Klein modes

$$\begin{aligned}
\Phi_{++}(x^\mu, y) &= \sqrt{\frac{2}{\pi R}} \sum_n \Phi_{++}^{(2n)}(x^\mu) \cos \frac{2ny}{R}, \\
\Phi_{+-}(x^\mu, y) &= \sqrt{\frac{2}{\pi R}} \sum_n \Phi_{+-}^{(2n+1)}(x^\mu) \cos \frac{(2n+1)y}{R}, \\
\Phi_{-+}(x^\mu, y) &= \sqrt{\frac{2}{\pi R}} \sum_n \Phi_{-+}^{(2n+1)}(x^\mu) \sin \frac{(2n+1)y}{R}, \\
\Phi_{--}(x^\mu, y) &= \sqrt{\frac{2}{\pi R}} \sum_n \Phi_{--}^{(2n+2)}(x^\mu) \sin \frac{(2n+2)y}{R},
\end{aligned} \tag{1.67}$$

where n is an integer and each field $\Phi_{++}^{(2n)}(x^\mu)$, $\Phi_{+-}^{(2n+1)}(x^\mu)$, $\Phi_{-+}^{(2n+1)}(x^\mu)$ and $\Phi_{--}^{(2n+2)}(x^\mu)$ acquires a mass $\frac{2n}{R}$, $\frac{2n+1}{R}$, $\frac{2n+1}{R}$ and $\frac{2n+2}{R}$ upon compactification, respectively. Therefore, 4-dimensional massless fields appear only in $\Phi_{++}^{(2n)}(x^\mu)$. Additionally, some fields vanish at the fixed points, for example, $\Phi_{-+}(x^\mu, 0) = \Phi_{--}(x^\mu, 0) = 0$ at $y = 0$ and $\Phi_{+-}(x^\mu, \pi R/2) = \Phi_{--}(x^\mu, \pi R/2) = 0$ at $y = \pi R/2$.

We now study an $SU(5)$ gauge theory with minimal SUSY in 5D (with 8 real super-

charges, corresponding to $\mathcal{N}=2$ SUSY in 4D). We assume that, at minimum, the bulk must have the 5D vector superfield, corresponding to a vector supermultiplet, V, and a chiral multiplet, Σ, in terms of 4d $\mathcal{N}=1$ SUSY such that both of them transform in the adjoint representation **24** of $SU(5)$.

We assume that the $\mathbb{Z}_2$ orbifold action on field space is given by

$$\begin{aligned} V^A(x^\mu, y)T^A &\to V^A(x^\mu, -y)PT^AP^{-1} \\ \Sigma^A(x^\mu, y)T^A &\to -\Sigma^A(x^\mu, -y)PT^AP^{-1}, \end{aligned} \tag{1.68}$$

and similarly for the $\mathbb{Z}_2'$ transformation, obtained by replacing y and P by y' and P'. The matrices T^A are the 5×5 generators of $SU(5)$ with $A=1,...,24$. The parity assignments are chosen to be $P=\text{diag}(1,1,1,1,1)$ and $P'=\text{diag}(-1,-1,-1,1,1)$. With this assignment and the first transformation given in equation 1.68, the $SU(5)$ gauge symmetry group is broken down to $SU(3)\times SU(2)\times U(1)$ at the fixed point $y=\pi R/2$ but it is unbroken in the bulk and on $y=0$. This is because

$$P'T^aP'^{-1}=T^a, \quad P'T^{\hat{a}}P'^{-1}=-T^{\hat{a}}, \tag{1.69}$$

where T^a are the gauge generators of $SU(3)\times SU(2)\times U(1)$ and $T^{\hat{a}}$ are the rest of the gauge generators.

Additionally, the overall sign in the second line of equation 1.68 breaks the 4D $\mathcal{N}=2$ SUSY to 4D $\mathcal{N}=1$ SUSY on both fixed points at $y=0$ and $y=\pi R/2$. Since only the $(+,+)$ fields contain massless zero modes, we end up with the gauge and gaugino content of the 4D $\mathcal{N}=1$ MSSM at low energies.

With this example, we have illustrated that when K acts non-freely on the extra dimensional manifold C, i.e. there exist fixed points and additionally, the action of K does not commute with the symmetry of the theory G, then this symmetry is broken to a subgroup of G at the 4-dimensional fixed points.

We have also seen that only the fields with positive parity assignments have zero-massless modes. We can make use of this parity choice to achieve the doublet-triplet splitting of Higgs multiplets in GUTs. We will select the parities in such a way that the doublets contain zero massless modes while the triplets are heavy. This mechanism is used in chapter 4.

1.7.3 Family symmetry from extra dimensions

Discrete symmetries may naturally arise as the remnant symmetry of the space-time symmetry after it is broken down to the 4-dimensional Poincaré symmetry through orbifold compactification. As an example, we show the original proposal by Altarelli,

Feruglio and Lin [123] in which the tetrahedral symmetry of A_4 arises after compactification of the two extra dimensions in a $T_2/\mathbb{Z}_2$ orbifold, where T_2 refers to a torus.

We start with a model in 6 dimensions whose two extra dimensions are compactified into an orbifold $T_2/\mathbb{Z}_2$. The two extra dimensions, x_5 and x_6 are combined into a complex coordinate $z = x_5 + ix_6$. The torus T_2 is defined then by the following identifications

$$\begin{aligned} &z \sim z + 1 \\ &z \sim z + \gamma, \quad \text{where} \quad \gamma = e^{i\frac{\pi}{3}}. \end{aligned} \tag{1.70}$$

The action of the $\mathbb{Z}_2$ parity is defined as

$$z \sim -z. \tag{1.71}$$

The set of equations 1.70 and 1.71 define the orbifold $T_2/\mathbb{Z}_2$ and the fundamental domain is shown in figure 1.3. This orbifold contains four fixed points given by $(z_1, z_2, z_3, z_4) = (1/2, (1+\gamma)/2, \gamma/2, 0)$, i.e. these points remain unchanged under the orbifold action. Furthermore, the segments labelled by a in figure 1.3 are identified, and similarly for those labelled by b and c. Once we identify these segments, we find that the orbifold is a regular tetrahedron with vertices at the four fixed points. If one assumes that the space-time symmetry, before compactification, consisted of the 6D translations and 6D proper Lorentz transformations, then the orbifold has broken it to the 4D space-time symmetry times the discrete group of rotations and translations A_4. This group can be generated by two transformations

$$\begin{aligned} &\mathcal{S} : z \to z + \frac{1}{2}, \\ &\mathcal{T} : z \to \omega z, \quad \text{where} \quad \omega \equiv \gamma^2. \end{aligned} \tag{1.72}$$

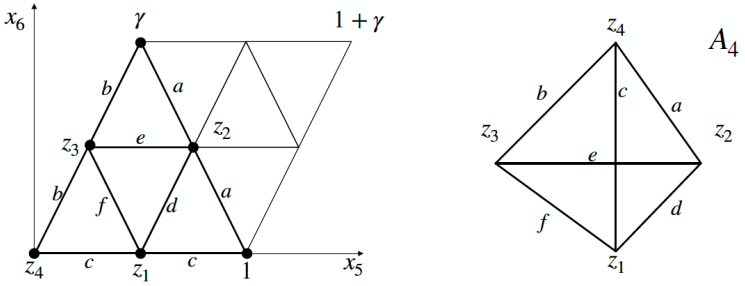

Figure 1.3: Orbifold $T_2/\mathbb{Z}_2$ with fixed points (z_1, z_2, z_3, z_4) and fundamental domain outlined in bold. The segments with same label are identified one with each other such that the orbifold is exactly a regular tetrahedron with edges a, b, c, d, e, f and vertices given by the four fixed points of the orbifold.

These two transformations induce even permutations of the four fixed points, such that

$$\begin{aligned} \mathcal{S} &: (z_1, z_2, z_3, z_4) \to (z_4, z_3, z_2, z_1) \\ \mathcal{T} &: (z_1, z_2, z_3, z_4) \to (z_2, z_3, z_1, z_4). \end{aligned} \tag{1.73}$$

These two generators satisfy the presentation of A_4[9], i.e. $\mathcal{S}^2 = \mathcal{T}^3 = (\mathcal{S}\mathcal{T})^3 = 1$. Other discrete symmetry groups can arise from different orbifold compactifications. For a list of $T_2/\mathbb{Z}_N$ orbifolds with their associated discrete symmetry, we refer to [126].

It is possible to build a model in the 6D space-time $\mathcal{M}_4 \times T_2/\mathbb{Z}_2$, with fields either living at the fixed points, known as 4D "brane" fields, or "bulk" fields, depending on both the uncompactified coordinates x^μ and the complex coordinate z. In chapter 4, a 6-dimensional supersymmetric $SU(5)$ GUT model has been constructed along these lines, in which the family symmetry arises from the orbifold of the extra dimensions.

1.7.4 Modular symmetry and modular forms

Toroidal compactification is one of the most common and simple compactifications. In general, a torus can be defined by giving two periods in the complex plane

$$z \sim z + \omega_1, \quad z \sim z + \omega_2, \tag{1.74}$$

where ω_1 and ω_2 are assumed to be finite, non-zero and their ratio is not real. Here, the variable z refers again to the complex coordinate $z = x_5 + ix_6$, where x_5 and x_6 are the two extra dimension coordinates. The torus is then characterized by the complex plane $\mathbb{C}$ modulo a two-dimensional lattice $\Lambda_{(\omega_1,\omega_2)}$, where $\Lambda_{(\omega_1,\omega_2)} = \{m\omega_1 + n\omega_2, m, n \in \mathbb{Z}\}$,

$$T_2 = \mathbb{C}/\Lambda_{(\omega_1,\omega_2)}. \tag{1.75}$$

Without loss of generality, we can apply the transformation $z \to z/\omega_2$, such that the torus is equivalent to one whose periods are 1 and $\tau = \omega_1/\omega_2$ and we can restrict τ to the upper half-plane $\mathcal{H} = \text{Im } \tau > 0$. There exists alternative periods

$$\omega_1' = a\omega_1 + b\omega_2 \quad \text{and} \quad \omega_2' = c\omega_1 + d\omega_2, \tag{1.76}$$

which define the same lattice, if $a, b, c, d \in \mathbb{Z}$ and $ad - bc = 1$, or equivalently

$$\begin{pmatrix} \omega_1' \\ \omega_2' \end{pmatrix} = \begin{pmatrix} a & b \\ c & d \end{pmatrix} \begin{pmatrix} \omega_1 \\ \omega_2 \end{pmatrix}, \quad \text{where} \quad \begin{pmatrix} a & b \\ c & d \end{pmatrix} \in SL(2, \mathbb{Z}). \tag{1.77}$$

[9] An additional transformation $z \to z^*$ also permutes the fixed points. This transformation belongs to the full 6D Poincaré group, which includes not only 6D translations and proper Lorentz transformations, but also discrete symmetries. In this case, if one assumes the 6D Poincaré symmetry before compactification, the orbifold leads to the product of 4D Poincaré times the discrete group S_4 (instead of A_4).

Therefore, the torus defined by the modulus τ is equivalent to one with modulus parameter given by

$$\tau' = \frac{\omega_1'}{\omega_2'} = \frac{a\tau + b}{c\tau + d}. \tag{1.78}$$

An $SL(2,\mathbb{Z})$ transformation on the modulus parameter τ and its negative are equivalent, as can be seen from equations 1.77 and 1.78. Therefore, we can use the infinite discrete group $PSL(2,\mathbb{Z}) = SL(2,\mathbb{Z})/\mathbb{Z}_2$, generated by

$$S : \tau \to -1/\tau \quad \text{and} \quad T : \tau \to \tau + 1, \tag{1.79}$$

to describe the transformations that relate equivalent tori. This group is also known as the modular group $\Gamma \equiv PSL(2,\mathbb{Z})$[10] and its generators satisfy

$$S^2 = (ST)^3 = 1. \tag{1.80}$$

If one imposes an extra constraint given by $T^N = 1$, the finite modular groups Γ_N are realized. Depending on the value of N, the finite modular group Γ_N is isomorphic to different permutation groups, for example, $\Gamma_2 \simeq S_3$, $\Gamma_3 \simeq A_4$, $\Gamma_4 \simeq S_4$ and $\Gamma_4 \simeq A_5$.

In theories where the extra dimensions are compactified on a $T_2/\mathbb{Z}_N$ orbifold, the superpotential has to be invariant under the modular symmetry [127, 128]. In general, a set of chiral supermultiplets, $\varphi^{(I)}$, are assumed to transform in a representation $\rho^{(I)}$ of the finite modular group Γ_N with weight $k^{(I)}$, i.e.

$$\begin{aligned} &\tau \to \frac{a\tau + b}{c\tau + d}, \\ &\varphi^{(I)} \to (c\tau + d)^{-k_I} \rho^{(I)} \varphi^{(I)}. \end{aligned} \tag{1.81}$$

The invariance of the superpotential under the modular group provides a strong restriction on the theory since the couplings have to become modular forms whose weight cancel the sum of the weights of the supermultiplets. For example, consider a term in the superpotential given by

$$W \supset Y(\tau)\varphi^{(1)} \dots \varphi^{(n)}. \tag{1.82}$$

To build an invariant term, $Y(\tau)$ should be a modular form with weight k_Y, where $k_Y \geq 0$ is an integer, transforming in the representation ρ of Γ_N:

$$Y(\tau') \to (c\tau + d)^{k_Y} \rho Y(\tau), \tag{1.83}$$

with k_Y and ρ such that the weight k_Y compensates the overall weight of the product $\varphi^{(1)} \dots \varphi^{(n)}$, i.e. $k_Y = k_1 + \dots + k_n$ and the product of representations $\rho \times \rho^{(1)} \dots \rho^{(n)}$ contains an invariant singlet under Γ_N. Therefore, the couplings in equation 1.82 are constrained to the possible modular forms that satisfy these conditions. We refer to

[10] Some authors define the modular group to be $PSL(2,\mathbb{Z})$, while others define it to be the larger group $SL(2,\mathbb{Z})$.

appendix A.2.2 for a basis of modular forms for $\Gamma_3 \simeq A_4$ with different weights k_Y.

In chapter 4, we build a supersymmetric $SU(5)$ model in 6D where the two extra dimensions are compactified on a $T_2/\mathbb{Z}_2$ orbifold. Some of the Yukawa couplings become modular forms giving rise to mass matrix structure and therefore providing a possible interpretation of the flavour puzzle.

Chapter 2

A natural $S_4 \times SO(10)$ model of flavour

In chapter 1, we introduced some of the questions left unanswered by the Standard Model such as neutrino masses and mixing, the hierarchy problem, the charge quantisation and the apparent unification of gauge forces at high energies, and the flavour puzzle among others. In this chapter we present a natural $S_4 \times SO(10)$ supersymmetric grand unified theory of flavour which aims to explain the observed masses and mixing patterns of quarks and leptons and which is capable to address the questions above. It is mainly based on the work published in [1].

2.1 Introduction

From a theoretical point of view, the choice of an $SO(10)$ grand unified theory is preferred, since it predicts three right-handed neutrinos and makes neutrino mass inevitable. We combine it with an S_4 symmetry since it is one of the simplest and smallest family symmetry groups that admit triplet representations. Furthermore, if one assumes that the Klein symmetry of the neutrino mass matrix is generated by the S, U and T generators of S_4 (shown in appendix A.1), then the PMNS matrix is equal to the tri-bimaximal (TB) mixing matrix, such that one can associate TB mixing with the discrete symmetry group S_4 [129]. Even though TB mixing is already ruled-out due to the observation of a non-zero reactor angle, we follow a semi-direct approach in which the flavon vacuum alignments only preserve a generator of the symmetry (specifically, the SU generator). Then, S_4 naturally leads to constrained sequential dominance-3 (CSD3), meaning that the flavons are aligned in the following directions $(0, 1, -1)^T$, $(1, 3, -1)^T$ and $(0, 1, 0)^T$, which gives successful predictions in the neutrino sector as we explain below.

To generate neutrino masses we apply the type-I seesaw mechanism with three right-

handed neutrinos. Furthermore, we consider sequential dominance (SD) of right-handed neutrinos [130–133], which is a natural framework to realize large lepton mixing and normal neutrino hierarchy within the type-I seesaw. SD postulates three right-handed neutrinos, where one of them, usually the heaviest one, is almost decoupled from the seesaw mechanism, and is responsible for the lightest physical neutrino mass m_1. Of the remaining two, one gives the dominant seesaw contribution and is mainly responsible for the (heaviest) atmospheric neutrino mass m_3 and mixing, while the other gives a subdominant contribution, responsible for the (second-heaviest) solar neutrino mass m_2 and mixing. SD therefore predicts $m_1 \ll m_2 \ll m_3 \sim 50$ meV. The amount of atmospheric and solar mixing is governed by ratios of Yukawa couplings, which can easily be large, while the reactor mixing is typically $U_{e3} \lesssim \mathcal{O}(m_2/m_3) \approx 0.17$. This successful prediction was made over a decade before the reactor angle was measured [134–136].

One may go further and impose constraints on the Yukawa couplings in order to achieve predictions for mixing, as in constrained sequential dominance (CSD) [137–141]. A particularly successful scheme is known as CSD3 [142, 143] where the neutrino Yukawa matrix is controlled by particular vacuum expectation values (VEVs) of three triplet flavon fields $\langle \phi_i \rangle$, as discussed later. The particular flavon vacuum alignments may be enforced by an S_4 symmetry and are fixed by a superpotential which we do not specify here but was shown in [142]. After implementing the seesaw mechanism, the above flavons yield a light effective left-handed Majorana neutrino mass matrix,

$$m_\nu = \mu_1 Y_{11} + \mu_2 Y_{22} + \mu_3 Y_{33}, \tag{2.1}$$

where $Y_{ij} \sim \langle \phi_i \rangle \langle \phi_j \rangle^T$, up to S_4 Clebsch-Gordan (CG) factors. Each of the matrices Y_{ii} is quadratic in $\langle \phi_i \rangle$ and therefore has rank 1. The SD condition implies that $\mu_2 > \mu_1$ and hence maximal atmospheric mixing is controlled by Y_{22}, solar mixing is controlled by Y_{11}, while Y_{33} plays no important role in neutrino physics due to the smallness of μ_3, which implies that m_1 is similarly small.

In the present chapter we propose a natural $S_4 \times SO(10)$ Grand Unified Theory of flavour in which the CSD3 model of neutrinos is embedded. Our guiding principles are firstly simplicity, involving the fewest number of low-dimensional fields, secondly naturalness, and thirdly completeness, in particular addressing the doublet-triplet splitting problem. What does natural mean? For us it means that we have a qualitative explanation of charged fermion mass and mixing hierarchies, as for neutrino mass and mixing, with all dimensionless parameters $\mathcal{O}(1)$, and in particular that the Yukawa matrices are obtained from sums of low-rank matrices, as in equation 2.1, where each matrix in the sum naturally accounts for the mass of a particular family, analogous to SD in the neutrino sector. This qualitative picture of "universal sequential dominance" is underpinned by a detailed quantitative fit of the fermion spectrum.

To accomplish these goals, we need to add two Higgs **10**s, H^u_{10} and H^d_{10}, which will

give rise, at low energy, to the minimal supersymmetric Standard Model (MSSM) Higgs doublets, H_u and H_d, respectively, with no appreciable Higgs mixing effects. After GUT breaking, the Higgs H_{10}^u couples to up-type quarks and neutrinos, with Yukawa matrices given by an universal CSD3 structure as in equation 2.1. The Yukawa matrices for the charged leptons and down-type quarks, which couple to H_{10}^d, have a different universal structure where Y_{11} is replaced by $Y_{12} \sim \langle\phi_1\rangle \langle\phi_2\rangle^T$. Then quark mixing is mostly originated in the down-type quark sector, with the down and strange quark masses successfully realised by having a zero entry in the (1,1) element of the down-type quark Yukawa matrix Y^d, as in the Gatto-Sartori-Tonin (GST) approach [144], with a milder hierarchy among down-type quarks as compared to up-type quarks.

The model accurately fits all available quark and lepton data. We give analytical estimations for quark mixing angles and we recognize some tension in the predicted observables. This tension is alleviated by assuming rather large SUSY threshold corrections. All dimensionless couplings in the renormalisable theory are naturally assumed $\mathcal{O}(1)$ and the hierarchy in the flavon VEVs fixes the scales of all but one parameter. The model reduces to the MSSM at lower energies, a μ term of $\mathcal{O}$(TeV) is achieved as well as doublet-triplet splitting and proton decay operators are Planck scale suppressed. The model requires an auxiliary $\mathbb{Z}_4^2$ and $\mathbb{Z}_4^R$ symmetry and a spectrum of messenger fields to achieve all the features above.

The model introduced here differs from previous models based on $S_4 \times SO(10)$ [145–148], (see also [149–151]).[1] Firstly, the full symmetry is different, since we use an extra $\mathbb{Z}_4^2 \times \mathbb{Z}_4^R$ symmetry, while earlier works use a $\mathbb{Z}_n$ [146–148]. Furthermore, we only include small Higgs representations **10** (fundamental), **16** (spinor) and **45** (adjoint) and do not allow the large Higgs representations such as the $\overline{\mathbf{126}}$ and **120** which are used in the other approaches. As a consequence our neutrino masses follow from a type-I seesaw mechanism, rather than a type-II seesaw employed in other papers. In further contrast, we do not allow Higgs mixing: the MSSM Higgs doublets H_u and H_d emerge directly from H_{10}^u and H_{10}^d, respectively, whereas in [145–148] they arise as unconstrained linear combinations of doublets contained in 10- and 126-dimensional Higgs fields. In addition we consider doublet-triplet splitting. These features are largely absent from earlier works. Another important difference is that we have used the CSD3 vacuum alignments in [142], whereas the vacuum alignments used in most previous works were geared towards TB mixing, and do not naturally provide a large reactor angle. Indeed our model is motivated by the success of CSD3 in the neutrino sector.

[1] Previous works on $SO(10)$ models with non-Abelian discrete flavour symmetries are found in [152–161], and further flavoured GUTs can be found in [162–187]. More recently, a generalised approach to flavour symmetries in $SO(10)$ is considered in [188].

2.2 The model

2.2.1 Overview of the model

All the fermions of the Standard Model are unified in a single superfield ψ which transforms as a $(3', 16)$ representation of $S_4 \times SO(10)$. We also include two Higgs fields $H_{10}^{u,d}$ in $(1, 10)$ representation and three flavon fields ϕ_i, with $i = 1, 2, 3$ in $(3', 1)$ representation. The flavons are assumed to have CSD3 vacuum alignments [142]

$$\langle \phi_1 \rangle = v_1 \begin{pmatrix} 1 \\ 3 \\ -1 \end{pmatrix}, \quad \langle \phi_2 \rangle = v_2 \begin{pmatrix} 0 \\ 1 \\ -1 \end{pmatrix}, \quad \langle \phi_3 \rangle = v_3 \begin{pmatrix} 0 \\ 1 \\ 0 \end{pmatrix}, \tag{2.2}$$

with VEVs driven to scales with the hierarchy[2]

$$v_1 \ll v_2 \ll v_3 \sim M_{\text{GUT}}. \tag{2.3}$$

The idea is that the up-type quark Yukawa matrix Y^u and neutrino Yukawa matrix Y^ν arise from effective terms like

$$H_{10}^u(\psi\phi_1)(\psi\phi_1) + H_{10}^u(\psi\phi_2)(\psi\phi_2) + H_{10}^u(\psi\phi_3)(\psi\phi_3), \tag{2.4}$$

where the bracket means that the fields inside are contracted into a singlet representation of S_4. Due to the hierarchy of the flavon VEVs in equation 2.3, each rank-1 matrix in the sum in equation 2.4 contributes dominantly to a particular family, giving a rather natural understanding of the hierarchical Yukawa couplings $y_u \sim v_1^2/M_{\text{GUT}}^2$, $y_c \sim v_2^2/M_{\text{GUT}}^2$, $y_t \sim v_3^2/M_{\text{GUT}}^2$, and similarly for the neutrino Yukawa couplings.

The operators in equation 2.4 are nonrenormalisable and they will have denominator scales of order M_{GUT}, determined by the VEVs of additional Higgs adjoint **45**s, leading to various CG factors. Consequently, the Yukawa matrices Y^u and Y^ν are a sum of rank-1 matrices as in equation 2.1, with independent coefficients multiplying each rank-1 matrix, where $Y_{ij} \sim \langle \phi_i \rangle \langle \phi_j \rangle^T$, up to S_4 CG factors. Since the expansion breaks down for the third family, in section 2.2.4 we shall find a renormalisable explanation of the third-family Yukawa couplings. The right-handed neutrino Majorana mass matrix will also have the same universal form, leading to the seesaw mass matrix as in equation 2.1.

The down-type quark Yukawa matrix Y^d and charged lepton Yukawa matrix Y^e are slightly different

$$H_{10}^d(\psi\phi_1)(\psi\phi_2) + H_{10}^d(\psi\phi_2)(\psi\phi_2) + H_{10}^d(\psi\phi_3)(\psi\phi_3). \tag{2.5}$$

[2] In the full model we shall not provide an explanation for this hierarchy of VEVs, nor shall we repeat the vacuum alignment superpotential responsible for the alignments in equation 2.2, which is discussed in [142]. We note that the alignments $\langle \phi_1 \rangle$ and $\langle \phi_2 \rangle$ preserve the SU generator of S_4.

In equation 2.5, there is a mixed term involving ϕ_1 and ϕ_2, leading to a new rank-2 Yukawa structure $Y_{12} \sim \langle\phi_1\rangle \langle\phi_2\rangle^T$. This new term gives rise to two new features which are welcome: firstly, it enforces a zero in the (1,1) element of Y^d, giving the GST relation for the Cabibbo angle, i.e. $\theta_{12}^q \approx \sqrt{y_d/y_s}$, and it also leads to a milder hierarchy in the down and charged lepton sectors.

To guarantee all the above features of the model, it is necessary to introduce additional symmetries and fields.

2.2.2 Field content and Yukawa superpotential

We now present the full superfield content of the model in table 2.1. All known SM fermions are contained in a "matter" superfield ψ. Additionally, we include three triplet flavons ϕ_a $(a = 1, 2, 3)$ which acquire CSD3 vacuum alignments, two Higgs **10**s containing one each of the electroweak-scale Higgs $SU(2)$ doublets,[3] a spinor $H_{\overline{16}}$ which breaks $SO(10)$ (and gives masses to the right-handed neutrinos along with the singlet field ρ), as well as several Higgs adjoints. The χ superfields are messengers that are integrated out below the GUT scale, and are given GUT-scale masses by the VEV of H_{45}^Z.

Field	Representation				
	S_4	$SO(10)$	$\mathbb{Z}_4$	$\mathbb{Z}_4$	$\mathbb{Z}_4^R$
ψ	$3'$	16	1	1	1
H_{10}^u	1	10	0	2	0
H_{10}^d	1	10	2	0	0
$H_{\overline{16}}$	1	$\overline{16}$	2	1	0
H_{16}	1	16	1	2	0
$H_{45}^{X,Y}$	1	45	2	1	0
H_{45}^Z	1	45	1	2	0
H_{45}^{B-L}	1	45	2	2	2
ϕ_1	$3'$	1	0	0	0
ϕ_2	$3'$	1	2	0	0
ϕ_3	$3'$	1	0	2	0

(a) Matter, Higgs and flavon superfields.

Field	Representation				
	S_4	$SO(10)$	$\mathbb{Z}_4$	$\mathbb{Z}_4$	$\mathbb{Z}_4^R$
$\overline{\chi}_1$	1	$\overline{16}$	3	3	1
χ_1	1	16	0	3	1
$\overline{\chi}_2$	1	$\overline{16}$	1	3	1
χ_2	1	16	2	3	1
$\overline{\chi}_3$	1	$\overline{16}$	3	1	1
χ_3	1	16	0	1	1
χ_3'	1	16	3	2	1
χ_2'	1	16	1	0	1
ρ	1	1	2	2	1

(b) Messenger superfields.

Table 2.1: Field content giving the Yukawa superpotential in equation 2.6.

We also include two $\mathbb{Z}_4$ symmetries that forbid any mixed flavon Yukawa terms and a R symmetry, $\mathbb{Z}_4^R$, under which the superpotential has total charge two, and which is broken at the GUT scale by the H_{45}^{B-L} VEV to $\mathbb{Z}_2^R$, the usual R (or matter) parity in the MSSM, ensuring a stable lightest supersymmetric particle (LSP). This symmetry also helps achieving the doublet-triplet splitting problem, ensuring that only two light Higgs doublets (and no Higgs triplets) are present in the effective MSSM and it also

[3] We assume that the MSSM Higgs doublets H_u, H_d lie completely inside the $SO(10)$ multiplets H_{10}^u, H_{10}^d, respectively. This is justified in section 2.2.5.

controls the μ term. $\mathbb{Z}_4^R$ is the smallest R symmetry that can achieve the above, and is specially motivated within $SO(10)$ [189]. We shall also assume a spontaneously broken canonical CP symmetry at the high scale.

With this superfield content and symmetries, the most general renormalisable Yukawa superpotential that can be written at the GUT scale is

$$\begin{aligned} W_Y^{(\mathrm{GUT})} = {} & \psi\phi_a\overline{\chi}_a + \overline{\chi}_a\chi_a H_{45}^Z + \chi_a\chi_a H_{10}^u + \rho\chi_3 H_{\overline{16}} + M_\rho\rho\rho \\ & + \overline{\chi}_b\chi'_b\left(H_{45}^X + H_{45}^Y\right) + \chi'_b\chi'_b H_{10}^d + \chi_1\chi_2 H_{10}^d, \end{aligned} \tag{2.6}$$

where we sum over indices $a = 1, 2, 3$ and $b = 2, 3$, and have suppressed $\mathcal{O}(1)$ coefficients λ that multiply each term. Furthermore, there are two essential terms that appear suppressed by one Planck mass M_P and they are given by

$$W_Y^{(\mathrm{Planck})} = \frac{\chi_a\chi_a H_{\overline{16}} H_{\overline{16}}}{M_P} + \frac{\psi\psi\phi_3 H_{10}^d}{M_P}, \tag{2.7}$$

where $a = 1, 2, 3$. The first term couples $H_{\overline{16}}$ to fermions via the messengers χ_a. The second term is allowed by the symmetries and cannot be ignored since it contributes to the fermion Yukawa matrices at the same order of the smallest GUT-scale terms.

The adjoint Higgs superfields acquire VEVs, in general complex, at the GUT scale, i.e. $\langle H_{45}^k\rangle \sim M_{\mathrm{GUT}}$ with $k = X, Y, Z, B-L$. $H_{45}^{X,Y,Z}$ gain arbitrary (SM-preserving) VEVs, providing CG factors which separate the quark and lepton masses. We elaborate on this feature in section 2.2.3. H_{45}^{B-L} gains a VEV in the direction that preserves $B-L$, generating GUT-scale masses for Higgs triplets via the Dimopoulos-Wilczek (DW) mechanism [190–192]. Our implementation of the DW mechanism is described in section 2.2.5.

The VEVs of ϕ_1 and ϕ_2 are assumed to get VEVs well below the GUT scale, i.e. $\langle\phi_{1,2}\rangle \ll M_{\mathrm{GUT}}$, while $\langle\phi_3\rangle \sim M_{\mathrm{GUT}}$. Therefore, the scale at which the flavour symmetry is broken, along with CP, is the GUT scale. At low scales no residual CP symmetry survives, however CP does play a role in fixing phases in the mass matrices. As $\langle\phi_3\rangle$ is near the messenger scale, the process of integrating out messengers $\chi_3, \overline{\chi}_3$ is not trivial. The correct procedure and the consequences of having a flavon VEV near M_{GUT} are discussed in detail in section 2.2.4, where we verify also that the third family of Yukawa couplings are renormalisable at the electroweak scale.

The mass and Yukawa matrices arise from the diagrams in figures 2.1-2.3.[4] The three diagrams in figure 2.1 correspond to the ultraviolet completion of the three terms in equation 2.4, while those in figure 2.2 are the completion of the terms in equation 2.5. The diagrams ensure correct S_4 group theory contractions and introduce CG coefficients due to the $H_{45}^{X,Y,Z}$ VEVs. These diagrams are analogous to how the seesaw mechanism replaces the Weinberg operator for neutrino mass. Of course neutrino mass itself in this

[4] The diagrams were drawn with `JaxoDraw` [193].

model is more subtle, since both the Dirac and right-handed Majorana masses arise from these diagrams.

Each diagram leads to a 3×3 matrix, whose internal structure is dictated by the vacuum alignment of the relevant flavon VEV in equation 2.2. The Yukawa and mass matrices are consequently given as a sum over these matrices. A prominent feature is a texture zero in the (1,1) element of Y^d and Y^e, which realises the GST relation for the Cabibbo angle. The full derivation and the exact matrices that we fit to data are given in section 2.3.

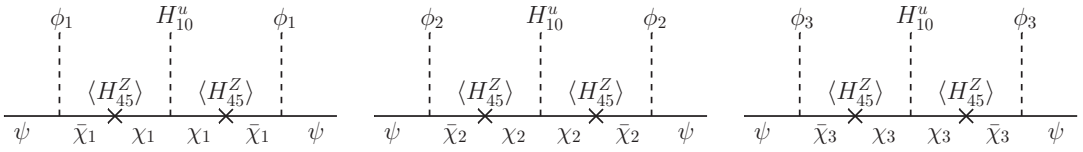

Figure 2.1: Diagrams coupling ψ to H^u_{10}. When flavons acquire VEVs, these give the up-type quark and Dirac neutrino Yukawa matrices.

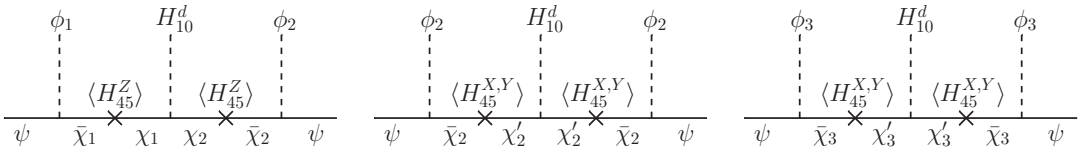

Figure 2.2: Diagrams coupling ψ to H^d_{10}. When flavons acquire VEVs, these give the down-type quark and charged lepton Yukawa matrices.

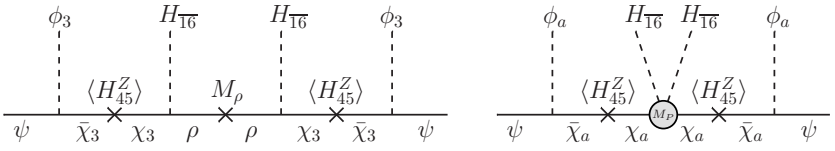

Figure 2.3: Diagrams coupling ψ to $H_{\overline{16}}$. One copy of the right diagram may be drawn for each of $a = 1, 2, 3$, although for $a = 3$, its contribution is negligible compared to the left diagram. When flavons acquire VEVs, these give the right-handed neutrino mass matrix.

Additional Planck-scale operators suppressed by one power of the Planck mass M_P, apart from the ones given in equation 2.7, are forbidden by the symmetries. Further effective operators, suppressed by at least two powers of the Planck mass M_P^2 and involving all allowed contractions of S_4 multiplets ψ and ϕ_i, are expected to arise. The largest of these terms can be $\mathcal{O}(M^2_{\text{GUT}}/M^2_P) \sim 10^{-6}$. We will assume these contributions are negligible; however, such corrections may pollute the texture zero in Y^d.

2.2.3 Clebsch-Gordan relations

We have several adjoint **45** representations of $SO(10)$ in table 2.1. Any adjoint can acquire a VEV aligned in the direction of any of the four $U(1)$ subgroup generators that commute with the Standard Model, or a combination thereof. There are four such $U(1)$ symmetries, labelled $U(1)_X$, $U(1)_Y$, $U(1)_{B-L}$, $U(1)_{T^3_R}$. They arise from the breaking of

$SO(10)$ either through

$$SO(10) \;\to\; SU(5) \times U(1)_X \;\to\; SU(3)_C \times SU(2)_L \times U(1)_Y \times U(1)_X \tag{2.8}$$

or through the Pati-Salam chain

$$\begin{aligned} SO(10) \;&\to\; SU(4)_C \times SU(2)_L \times SU(2)_R \\ &\to\; SU(3)_C \times SU(2)_L \times SU(2)_R \times U(1)_{B-L} \\ &\to\; SU(3)_C \times SU(2)_L \times U(1)_{T_R^3} \times U(1)_{B-L}. \end{aligned} \tag{2.9}$$

The generators of these $U(1)$ symmetries are not linearly independent; two of them may be expressed in terms of the other two. The VEVs of $H_{45}^{X,Y,Z}$ may be written as linear combinations of these alignments. Without loss of generality, we choose $\langle H_{45}^X \rangle$ and $\langle H_{45}^X \rangle$ to be aligned in the "X" and "Y" direction, respectively, while $\langle H_{45}^Z \rangle$ is a combination of both. Fermions couple to these VEVs with strengths that depend on their associated $U(1)$ charges, which are different for quarks and leptons.

Up-type quarks and Dirac neutrinos couple to H_{45}^Z (see figure 2.1). Since $\langle H_{45}^Z \rangle$ is arbitrary, there is no hard prediction for the ratio between quark and neutrino Yukawa couplings within a family. However, the same ratio has to hold for all the families since all the flavons ϕ_a $(a = 1, 2, 3)$ couple to this VEV in the same way. Therefore, once Y^u is determined, Y^ν is also fixed, such that $Y^\nu \propto Y^u$, to good approximation, up to an overall CG factor, with small deviations for the third family.

Meanwhile, the down-type quarks and charged leptons couple to two adjoints H_{45}^X and H_{45}^Y (see figure 2.2). Unlike the up sector, where matter always couples to the same $SO(10)$ VEV, each diagram in figure 2.2 involving a different flavon couples to a distinct linear combination of VEVs $\langle H_{45}^X \rangle$ and $\langle H_{45}^Y \rangle$. This introduces CG factors non-trivially into Y^d and Y^e. As such, there is no fixed relationship between down-type quark and charged lepton Yukawa couplings, neither within a family, nor across families. They are nevertheless expected to be of the same order.

2.2.4 Renormalisability of the third family

In this section we show that naive integration over messenger fields is not possible for the third family, due to the large VEV of ϕ_3. We emphasize that there is an assumed hierarchy of flavon VEVs, such that $v_1 \ll v_2 \ll v_3 \sim M_{\text{GUT}}$, implying it is not possible to formally integrate out the messengers χ_3 which couple to the flavon ϕ_3.

Let us single out the terms in the superpotential W_Y involving the messenger field χ_3, the flavon ϕ_3 and the Higgs field H_{10}^u (the same method applies to terms coupling to

H_{10}^d). Suppressing $\mathcal{O}(1)$ couplings, the relevant terms are

$$W_Y^{(3)} = \psi\phi_3\bar{\chi}_3 + H_{45}^Z\chi_3\bar{\chi}_3 + \chi_3\chi_3 H_{10}^u. \tag{2.10}$$

After the field H_{45}^Z and the flavon field ϕ_3 acquire VEVs, we have

$$W_Y^{(3)} = v_3\psi_3\bar{\chi}_3 + \langle H_{45}^Z\rangle\,\chi_3\bar{\chi}_3 + \chi_3\chi_3 H_{10}^u, \tag{2.11}$$

where the first two terms are of comparable order.

We could have interpreted ψ_3 as the third-family particles. However, there is a large coupling to $\bar{\chi}_3$, which induces a mass for ψ_3 via the second term in equation 2.11. Therefore, ψ_3 cannot be interpreted as the physical third-family states, which are massless above the electroweak scale. To get the physical (massless) states, which we label t, we rotate into a physical basis $(\psi_3, \chi_3) \to (t, \chi)$, such that t does not couple to $\bar{\chi}_3$. This basis change is given by

$$\psi_3 = \frac{\langle H_{45}^Z\rangle\, t + v_3\,\chi}{r}, \quad \chi_3 = \frac{-v_3\, t + \langle H_{45}^Z\rangle\,\chi}{r}; \quad r = \sqrt{v_3^2 + \langle H_{45}^Z\rangle^2}. \tag{2.12}$$

Physically, it may be interpreted as follows: inside the original superpotential W_Y lie the terms

$$\mathcal{W}_Y \supset \chi_3\chi_3 H_{10}^u \supset \frac{v_3^2}{v_3^2 + \langle H_{45}^Z\rangle^2}\, t\, t\, H_{10}^u, \tag{2.13}$$

which generate renormalisable mass terms for the top quark and the third Dirac neutrino at the electroweak scale.

2.2.5 Doublet-triplet and doublet-doublet splitting

As is the case for every broken GUT, the Higgs sector of our model contains more fields than the usual MSSM. The $H_{10}^{u,d}$ multiplets contain colour triplets that mediate proton decay. Since we have two **10**s, there is an additional pair of doublets that, if light, could spoil gauge coupling unification. For these reasons, those extra fields need to be heavy, while ensuring the MSSM doublets are massless. This splitting can be achieved in our model.

The splitting mechanism involves superfields given in table 2.1 as well as the addition of the superfields in table 2.2. The singlet field ξ obtains a VEV slightly above the GUT scale and ensures the correct structure to the masses. The H_{16} generates a mass for the $H_{\overline{16}}$ and also gets a VEV in the right-handed neutrino (ν^c) direction. H_{45}^{B-L} is the only R-charged field that gets a VEV, breaking $\mathbb{Z}_4^R$ to the usual R parity.

Field	Representation				
	S_4	$SO(10)$	$\mathbb{Z}_4$	$\mathbb{Z}_4$	$\mathbb{Z}_4^R$
ξ	1	1	2	2	0
$\bar{\chi}_u$	1	$\overline{16}$	2	1	2
χ_u	1	16	0	1	0
$\bar{\chi}_d$	1	$\overline{16}$	1	0	0
χ_d	1	16	1	2	2
ζ_1	1	45	1	1	2
ζ_2	1	45	1	1	0

Table 2.2: Messengers involved in doublet-triplet splitting.

With the superfields in tables 2.1 and 2.2, we may write the superpotential

$$\begin{aligned}\mathcal{W}_H = {} & H_{45}^{B-L}\left(H_{10}^u H_{10}^d + \zeta_2\zeta_2 + H_{\overline{16}}\chi_u + H_{16}\bar{\chi}_d\right) \\ & + H_{\overline{16}}H_{10}^u\bar{\chi}_u + H_{16}H_{10}^d\chi_d + H_{16}H_{\overline{16}}\zeta_1 + \xi\left(\zeta_1\zeta_2 + \bar{\chi}_u\chi_u + \bar{\chi}_d\chi_d\right) \\ & + H_{45}^{B-L}\left(\frac{H_{\overline{16}}H_{\overline{16}}H_{10}^d}{M_P} + \frac{H_{16}H_{16}H_{10}^u}{M_P} + H_{10}^u H_{10}^d\frac{(H_{45}^{X,Y,Z})^4}{M_P^4}\right),\end{aligned} \tag{2.14}$$

where we have ignored dimensionless couplings. We assume that the VEV $\langle\xi\rangle \gtrsim M_{\text{GUT}}$, so that we may integrate out the messenger fields and obtain the effective superpotential

$$\begin{aligned}\mathcal{W}_H = {} & H_{45}^{B-L}\left(H_{10}^u H_{10}^d + \frac{(H_{16}H_{\overline{16}})^2}{\langle\xi\rangle^2} + \frac{H_{\overline{16}}H_{\overline{16}}H_{10}^u}{\langle\xi\rangle} + \frac{H_{16}H_{16}H_{10}^d}{\langle\xi\rangle}\right. \\ & \left. + \frac{H_{\overline{16}}H_{\overline{16}}H_{10}^d}{M_P} + \frac{H_{16}H_{16}H_{10}^u}{M_P} + H_{10}^u H_{10}^d\frac{(H_{45}^{X,Y,Z})^4}{M_P^4}\right),\end{aligned} \tag{2.15}$$

where we have suppressed dimensionless couplings, and the final term involves all combinations of adjoints allowed by the symmetries, i.e. either $(H_{45}^Z)^4$ or any combination of powers of H_{45}^X and H_{45}^Y totalling four. The three terms suppressed by $\langle\xi\rangle$ are allowed by the integration of three messenger pairs.

We consider that the superfields $H_{\overline{16},16}$, H_{45}^k $(k = X, Y, Z, B-L)$ get GUT-scale VEVs, i.e. $v_{16,\overline{16}} \approx v_{45}^k \approx M_{\text{GUT}}$, through an unspecified mechanism. The fields $H_{\overline{16},16}$ get VEVs in the right-handed neutrino ν^c direction. The field H_{45}^{B-L} gains a VEV aligned in the $B-L$ direction, which splits doublet and triplet Higgs masses through the Dimopoulos-Wilczek (DW) mechanism [190–192]. This can be understood by considering the decomposition of the $H_{10}^{u,d}$ into the Pati-Salam group. The triplets behave as a sextuplet of $SU(4)$ while the doublets are singlets. Since $U(1)_{B-L} \subset SU(4)$, the triplets get a mass from the first term of equation 2.15 while the doublets do not. In the last term, all the $SO(10)$ adjoints can be contracted to a singlet, so they affect doublets and triplets equally.

To show explicitly the mechanism, we construct the doublet and triplet mass matrices.

We define the dimensionless scale parameters $y = M_{\rm GUT}/M_P$, $z = M_{\rm GUT}/\langle\xi\rangle$ and label the up-type doublets inside a given Higgs representation H by $\mathbf{2}_u(H)$, and down-type doublets by $\mathbf{2}_d(H)$. We define triplets $\mathbf{3}_u(H)$ and $\mathbf{3}_d(H)$ analogously. The field H refers either to H^u_{10}, H^d_{10} or $H_{\overline{16},16}$. The doublet mass matrix M_D and the triplet mass matrix M_T are given by

$$M_D = \begin{array}{c} \\ \mathbf{2}_d(H^d_{10}) \\ \mathbf{2}_d(H^u_{10}) \\ \mathbf{2}_d(H_{16}) \end{array} \begin{array}{c} \begin{array}{ccc} \mathbf{2}_u(H^u_{10}) & \mathbf{2}_u(H^d_{10}) & \mathbf{2}_u(H_{\overline{16}}) \end{array} \\ \begin{pmatrix} y^4 & 0 & y \\ 0 & -y^4 & z \\ y & z & z^2 \end{pmatrix} \end{array} M_{\rm GUT}\,,$$

$$M_T = \begin{array}{c} \\ \mathbf{3}_d(H^d_{10}) \\ \mathbf{3}_d(H^u_{10}) \\ \mathbf{3}_d(H_{16}) \end{array} \begin{array}{c} \begin{array}{ccc} \mathbf{3}_u(H^u_{10}) & \mathbf{3}_u(H^d_{10}) & \mathbf{3}_u(H_{\overline{16}}) \end{array} \\ \begin{pmatrix} 1 & 0 & y \\ 0 & -1 & z \\ y & z & z^2 \end{pmatrix} \end{array} M_{\rm GUT}\,. \tag{2.16}$$

The triplets mass matrix M_T has three eigenvalues of $\mathcal{O}(M_{\rm GUT})$. The doublets mass matrix has two eigenvalues at $\mathcal{O}(M_{\rm GUT})$ and one at $\mathcal{O}(y^4 M_{\rm GUT})$, which we identify with the μ term. Since $y \approx 10^{-3}$ we have $\mu \sim 1$ TeV, which is the desired order. Furthermore, the light eigenvectors of M_D define the MSSM doublets $H_{u,d}$ as

$$H_u \approx \mathbf{2}_u(H^u_{10}) + \frac{y}{z}\mathbf{2}_u(H^d_{10}), \quad H_d \approx \mathbf{2}_d(H^d_{10}) + \frac{y}{z}\mathbf{2}_u(H^d_{10}), \tag{2.17}$$

where the contribution of $\mathcal{O}(y)$ is negligible, so that the MSSM doublets are located as required by the Yukawa structure of the model.

2.2.6 Proton decay

One of the characteristic features of GUTs is the prediction of proton decay. It has not been observed and the proton lifetime is constrained to be $\tau_p > 10^{34}$ years [31]. Proton decay can be mediated by the extra gauge bosons and by the triplets accompanying the Higgs doublets. In SUSY $SO(10)$ GUTs the main source for proton decay comes from the triplet Higgsinos. The decay width is dependent on SUSY breaking and the specific coupling texture of the triplets. In general, the constraints are barely met when the triplets are at the GUT scale [194, 195], which is our case as it was shown in section 2.2.5.

Proton decay may also arise from effective terms like

$$gQQQL\frac{\langle X\rangle}{M_P^2}, \tag{2.18}$$

in which case, the constraint $g\langle X\rangle < 3\times 10^9$ GeV [196] must be satisfied to meet the limits on the proton lifetime. In our model, the largest contribution of this type comes from the term

$$\psi\psi\psi\psi\frac{H_{45}^{B-L}(H_{45}^{X,Y}H_{45}^{Z})^2}{M_P^6} \quad \Rightarrow \quad \langle X\rangle = \frac{(M_{\rm GUT})^5}{M_P^4} \sim 10^3 \text{ GeV}. \tag{2.19}$$

The constraint on $g\langle X\rangle$ is easily met, so proton decay from such terms is highly suppressed.

2.3 Yukawa and mass matrices

2.3.1 Complete derivation of Yukawa and mass matrices

In this section we rewrite the renormalisable superpotential in equation 2.6, including the dominant Planck-suppressed terms in equation 2.7, and writing explicitly all $\mathcal{O}(1)$ couplings,

$$\begin{aligned} W_Y = &\sum_{a=1,2,3} \lambda_a^{\phi}\psi\phi_a\bar{\chi}_a + \lambda_a^{\chi}\chi_a\bar{\chi}_a H_{45}^{Z} + \chi_a\chi_a\left(\lambda_a^{u}H_{10}^{u} + \lambda_a^{N}\frac{H_{\overline{16}}H_{\overline{16}}}{M_P}\right) \\ &+ \sum_{b=2,3}\bar{\chi}_b\chi_b'\left(\lambda_b^{X}H_{45}^{X} + \lambda_b^{Y}H_{45}^{Y}\right) + \lambda_b^{d}\chi_b'\chi_b'H_{10}^{d} \\ &+ \lambda_{12}^{d}\chi_1\chi_2H_{10}^{d} + \lambda_3^{\rho}\rho\chi_3H_{\overline{16}} + M_\rho\rho\rho + \lambda_P^{d}\frac{\psi\psi\phi_3H_{10}^{d}}{M_P}. \end{aligned} \tag{2.20}$$

Mass matrices are built from the flavon vacuum alignments in equation 2.2, after constructing singlet products which occur in $\psi\phi_a$ above, i.e. $3'\times 3'\to 1$. The product of two triplets into a singlet is given by

$$(AB) = A_1B_1 + A_2B_3 + A_3B_2. \tag{2.21}$$

To account for this non-trivial product as well as the field redefinition $\psi_2\to-\psi_2$ (this overall sign is unphysical), we define the vectors

$$\langle\tilde{\phi}_i\rangle = I_{S_4}\langle\phi_i\rangle, \quad \text{with} \quad I_{S_4} = \begin{pmatrix}1&0&0\\0&0&-1\\0&1&0\end{pmatrix}. \tag{2.22}$$

In the new variables, the alignments become,

$$\langle\tilde{\phi}_1\rangle = v_1\begin{pmatrix}1\\1\\3\end{pmatrix}, \quad \langle\tilde{\phi}_2\rangle = v_2\begin{pmatrix}0\\1\\1\end{pmatrix}, \quad \langle\tilde{\phi}_3\rangle = v_3\begin{pmatrix}0\\0\\1\end{pmatrix}. \tag{2.23}$$

As explained in section 2.2.3, fermions couple to the VEVs of $\langle H^k_{45} \rangle$ with strengths proportional to unique CG factors. The index k labels the adjoint, i.e. $k = X, Y, Z, B-L$. After the GUT is broken and ψ is decomposed into multiplets of the SM gauge group, the part of an adjoint VEV which couples to a given multiplet f is denoted by

$$H^k_{45} \to \langle H^k_{45} \rangle_f \,, \tag{2.24}$$

where $f = Q, u^c, d^c, L, e^c$, or ν^c. The field $H_{\overline{16}}$ gets a VEV in the direction which preserves $SU(5)$, which we call the (singlet) right-handed neutrino ν^c direction. Its VEV only affects the right-handed neutrino mass matrix and is simply denoted $v_{\overline{16}}$.

The Yukawa matrices are taken from diagrams in figures 2.1-2.3. Taking into account non-trivial S_4 products (as above), we have

$$Y^u_{ij} = \sum_{a=1,2} \lambda^u_a \frac{(\lambda^\phi_a)^2 \langle \tilde{\phi}_a \rangle_i \langle \tilde{\phi}_a \rangle_j}{(\lambda^\chi_a)^2 \langle H^Z_{45} \rangle_Q \langle H^Z_{45} \rangle_{u^c}} + \frac{(\lambda^\phi_3)^2 \langle \tilde{\phi}_3 \rangle_i \langle \tilde{\phi}_3 \rangle_j}{(\lambda^\phi_3)^2 v_3^2 + (\lambda^\chi_3)^2 \langle H^Z_{45} \rangle_Q \langle H^Z_{45} \rangle_{u^c}}, \tag{2.25}$$

$$Y^\nu_{ij} = \sum_{a=1,2} \lambda^u_a \frac{(\lambda^\phi_a)^2 \langle \tilde{\phi}_a \rangle_i \langle \tilde{\phi}_a \rangle_j}{(\lambda^\chi_a)^2 \langle H^Z_{45} \rangle_L \langle H^Z_{45} \rangle_{\nu^c}} + \frac{(\lambda^\phi_3)^2 \langle \tilde{\phi}_3 \rangle_i \langle \tilde{\phi}_3 \rangle_j}{(\lambda^\phi_3)^2 v_3^2 + (\lambda^\chi_3)^2 \langle H^Z_{45} \rangle_L \langle H^Z_{45} \rangle_{\nu^c}}, \tag{2.26}$$

$$\begin{aligned} M^{\mathrm{R}}_{ij} = & \sum_{a=1,2} \frac{\lambda^N_a v^2_{\overline{16}}}{M_P} \frac{(\lambda^\phi_a)^2 \langle \tilde{\phi}_a \rangle_i \langle \tilde{\phi}_a \rangle_j}{(\lambda^\chi_a)^2 \langle H^Z_{45} \rangle_{\nu^c} \langle H^Z_{45} \rangle_{\nu^c}} \\ & + v^2_{\overline{16}} \left(\frac{(\lambda^\rho_3)^2}{M_\rho} + \frac{\lambda^N_3}{M_P} \right) \frac{(\lambda^\phi_3)^2 \langle \tilde{\phi}_3 \rangle_i \langle \tilde{\phi}_3 \rangle_j}{(\lambda^\phi_3)^2 v_3^2 + (\lambda^\chi_3)^2 \langle H^Z_{45} \rangle_{\nu^c} \langle H^Z_{45} \rangle_{\nu^c}}, \end{aligned} \tag{2.27}$$

$$\begin{aligned} Y^d_{ij} = & \lambda^d_2 \frac{(\lambda^\phi_2)^2 \langle \tilde{\phi}_2 \rangle_i \langle \tilde{\phi}_2 \rangle_j}{[\lambda^X_2 \langle H^X_{45} \rangle + \lambda^Y_2 \langle H^Y_{45} \rangle]_Q [\lambda^X_2 \langle H^X_{45} \rangle + \lambda^Y_2 \langle H^Y_{45} \rangle]_{d^c}} \\ & + \lambda^d_3 \frac{(\lambda^\phi_3)^2 \langle \tilde{\phi}_3 \rangle_i \langle \tilde{\phi}_3 \rangle_j}{(\lambda^\phi_3)^2 v_3^2 + [\lambda^X_3 \langle H^X_{45} \rangle + \lambda^Y_3 \langle H^Y_{45} \rangle]_Q [\lambda^X_3 \langle H^X_{45} \rangle + \lambda^Y_3 \langle H^Y_{45} \rangle]_{d^c}} \\ & + \lambda^d_{12} \frac{\lambda^\phi_1 \lambda^\phi_2 \langle \tilde{\phi}_1 \rangle_i \langle \tilde{\phi}_2 \rangle_j}{\lambda^\chi_1 \lambda^\chi_2 \langle H^Z_{45} \rangle_Q \langle H^Z_{45} \rangle_{d^c}} + \lambda^d_P \frac{Y_P v_3}{M_P}, \end{aligned} \tag{2.28}$$

$$\begin{aligned} Y^e_{ij} = & \lambda^d_2 \frac{(\lambda^\phi_2)^2 \langle \tilde{\phi}_2 \rangle_i \langle \tilde{\phi}_2 \rangle_j}{[\lambda^X_2 \langle H^X_{45} \rangle + \lambda^Y_2 \langle H^Y_{45} \rangle]_L [\lambda^X_2 \langle H^X_{45} \rangle + \lambda^Y_2 \langle H^Y_{45} \rangle]_{e^c}} \\ & + \lambda^d_3 \frac{(\lambda^\phi_3)^2 \langle \tilde{\phi}_3 \rangle_i \langle \tilde{\phi}_3 \rangle_j}{(\lambda^\phi_3)^2 v_3^2 + [\lambda^X_3 \langle H^X_{45} \rangle + \lambda^Y_3 \langle H^Y_{45} \rangle]_L [\lambda^X_3 \langle H^X_{45} \rangle + \lambda^Y_3 \langle H^Y_{45} \rangle]_{e^c}} \\ & + \lambda^d_{12} \frac{\lambda^\phi_1 \lambda^\phi_2 \langle \tilde{\phi}_1 \rangle_i \langle \tilde{\phi}_2 \rangle_j}{\lambda^\chi_1 \lambda^\chi_2 \langle H^Z_{45} \rangle_L \langle H^Z_{45} \rangle_{e^c}} + \lambda^d_P \frac{Y_P v_3}{M_P}, \end{aligned} \tag{2.29}$$

where $v_3 = |\langle \phi_3 \rangle|$, $v_u Y^\nu_{ij}$ is the Dirac neutrino mass matrix and M^{R}_{ij} is the right-handed neutrino Majorana matrix. The last term in equation 2.20 is a singlet coming from three S_4 triplets and gives rise to the last terms in equations 2.28 and 2.29, where Y_P is a numerical matrix which is defined below in equation 2.30.

Finally, we take into account the effect of mixing between the state ψ_3 and messenger χ_3,

explained in section 2.2.4. This mixing provides additional contributions to the fermion mass matrices in the form of coefficients multiplying the third rows and columns. The size of each coefficient depends on the CG factors and the ratio(s) of v_3 to adjoint Higgs VEVs v_{45}^k, for $k = X, Y, \chi$. In the limit where $v_3 \ll v_{45}^k$, all these coefficients are 1, corresponding to a negligible amount of χ_3 being mixed into the physical state. This is exactly what occurs for the other two families: the massless states are aligned almost exactly with the states $\psi_{1,2}$. Generally, any significant deviation would require a tuning among CG factors and $\mathcal{O}(1)$ parameters λ. We do not expect these factors to have a large effect on mixing, hence we set them all to one for simplicity.

2.3.2 Numerical Yukawa and neutrino mass matrices

Following the derivation in section 2.3.1, we present here the explicit form of the Yukawa matrices in terms of the numerical matrices

$$Y_{11} = \begin{pmatrix} 1 & 1 & 3 \\ 1 & 1 & 3 \\ 3 & 3 & 9 \end{pmatrix}, \quad Y_{22} = \begin{pmatrix} 0 & 0 & 0 \\ 0 & 1 & 1 \\ 0 & 1 & 1 \end{pmatrix}, \quad Y_{33} = \begin{pmatrix} 0 & 0 & 0 \\ 0 & 0 & 0 \\ 0 & 0 & 1 \end{pmatrix},$$
$$Y_{12} = \begin{pmatrix} 0 & 1 & 1 \\ 1 & 2 & 4 \\ 1 & 4 & 6 \end{pmatrix}, \quad Y_P = \begin{pmatrix} 0 & 0 & -1 \\ 0 & 2 & 0 \\ -1 & 0 & 0 \end{pmatrix}, \tag{2.30}$$

which are constructed from the products $\langle\tilde{\phi}_i\rangle \langle\tilde{\phi}_i\rangle^T$ (see equation 2.23). We remind that the tilde on the flavon VEVs takes into account the S_4 singlet contractions in the triplet products like $(\psi\phi_i)(\psi\phi_j)$. Y_P derives from the Planck-suppressed operator $\psi\psi\phi_3 H_{10}^d$.

The up, down, charged lepton and Dirac neutrino Yukawa matrices (Y^u, Y^d, Y^e and Y^ν, respectively) and right-handed neutrino mass matrix M^{R} may be expressed as

$$Y^u = y_1^u e^{i\eta} Y_{11} + y_2^u Y_{22} + y_3^u e^{i\eta'} Y_{33}, \tag{2.31}$$
$$Y^\nu = y_1^\nu e^{i\eta} Y_{11} + y_2^\nu Y_{22} + y_3^\nu e^{i\eta'} Y_{33}, \tag{2.32}$$
$$M^{\mathrm{R}} = M_1^{\mathrm{R}} e^{i\eta} Y_{11} + M_2^{\mathrm{R}} Y_{22} + M_3^{\mathrm{R}} e^{i\eta'} Y_{33}, \tag{2.33}$$
$$Y^d = y_{12}^d e^{i\frac{\eta}{2}} Y_{12} + y_2^d e^{i\alpha_d} Y_{22} + y_3^d e^{i\beta_d} Y_{33} + y^P e^{i\gamma} Y_P, \tag{2.34}$$
$$Y^e = y_{12}^e e^{i\frac{\eta}{2}} Y_{12} + y_2^e e^{i\alpha_e} Y_{22} + y_3^e e^{i\beta_e} Y_{33} + y^P e^{i\gamma} Y_P, \tag{2.35}$$

since the MSSM Higgs doublets H_u and H_d arise from H_{10}^u and H_{10}^d, respectively, as shown in section 2.2.5.

The flavon VEVs v_a ($a = 1, 2, 3$) are complex, with the fixed phase relation

$$\eta = \arg\left(\frac{v_1}{v_2}\right)^2 = -\frac{2\pi}{3}, \tag{2.36}$$

given (up to a sign) by the superpotential that fixes the alignments. The remaining phase η' is determined by the fit.

The light neutrino mass matrix is obtained by the seesaw mechanism. Both Y^ν and $M^{\rm R}$ have the same structure, namely both are sums over the same rank-1 matrices Y_{11}, Y_{22} and Y_{33}. By a proof given in [197], the light neutrino matrix m_ν will also have this structure, i.e.

$$\begin{aligned} m_\nu &= \mu_1 e^{i\eta} Y_{11} + \mu_2 Y_{22} + \mu_3 e^{i\eta'} Y_{33} \\ &= \mu_1 e^{i\eta} \begin{pmatrix} 1 & 1 & 3 \\ 1 & 1 & 3 \\ 3 & 3 & 9 \end{pmatrix} + \mu_2 \begin{pmatrix} 0 & 0 & 0 \\ 0 & 1 & 1 \\ 0 & 1 & 1 \end{pmatrix} + \mu_3 e^{i\eta'} \begin{pmatrix} 0 & 0 & 0 \\ 0 & 0 & 0 \\ 0 & 0 & 1 \end{pmatrix}, \end{aligned} \tag{2.37}$$

where the parameters μ_i are given in terms of the parameters y_i^ν and $M_i^{\rm R}$ simply by

$$\mu_i = v_u^2 \frac{(y_i^\nu)^2}{M_i^{\rm R}}. \tag{2.38}$$

As shown in section 2.1, the flavons yield a light neutrino mass matrix m_ν, where the normal hierarchy $m_1 \ll m_2 \ll m_3$ then corresponds to $\mu_3 \lesssim \mu_1 \ll \mu_2$. Achieving this hierarchy after seesaw implies that the right-handed neutrino masses are very hierarchical, as we will see below.[5]

2.3.3 Analytic estimates

The parameters y_i^u, y_i^d, y_i^e, μ_i, and y^P (a total of 13) appearing in the Yukawa and mass matrices 2.31-2.35 are free real parameters of the model. Recalling that η is fixed by flavon vacuum alignment, we have the following further free parameters: η', $\alpha_{d,e}$, $\beta_{d,e}$, and γ (a total of 6). The scales of the real parameters are mostly fixed by the scales of the flavon VEVs, $v_{1,2,3}$. We set the flavon VEV scales to some appropriate values,

$$v_1 \approx 0.002 M_{\rm GUT}, \qquad v_2 \approx 0.05 M_{\rm GUT}, \qquad v_3 \approx 0.5 M_{\rm GUT}, \tag{2.39}$$

where we set $M_{\rm GUT} \simeq 10^{16}$ GeV. The terms giving $M_{1,2}^{\rm R}$ and y^P in equations 2.33 and 2.34-2.35, respectively, derive from terms suppressed by one Planck mass M_P. As they arise from unspecified dynamics, the scale of these parameters is not very well defined. For definiteness, we set $M_P \simeq 10^{19}$ GeV and again assume that the associated coefficients are close to one. We consider that $M_\rho \sim M_{\rm GUT}$ and therefore M_3^R is also at the GUT scale due to the term $\rho\chi_3 H_{\overline{16}}$, see also figure 2.3.

We examine the parameters of the matrices defined in equations 2.31-2.35 setting all

[5] While the model does not mathematically forbid an inverted hierarchy, we have checked that the corresponding predictions for neutrino masses and mixing angles would always give a bad fit to data. It would also require parameter choices that strongly violate the naturalness principle employed here.

$\mathcal{O}(1)$ coefficients to exactly one, and ignoring CG factors by setting all adjoint Higgs VEVs to $M_{\rm GUT} \simeq 10^{16}$ GeV. Then the Yukawa couplings are estimated to be

$$\begin{aligned} y_1^u \sim y_1^\nu \sim\ & v_1^2/M_{\rm GUT}^2 && \approx 4\times 10^{-6}, \\ y_2^u \sim y_2^\nu \sim y_2^d \sim\ & y_2^e \sim\ v_2^2/M_{\rm GUT}^2 && \approx 2.5\times 10^{-3}, \\ y_3^u \sim y_3^\nu \sim y_3^d \sim\ & y_3^e \sim\ v_3^2/M_{\rm GUT}^2 && \approx 0.25, \\ y_{12}^d \sim\ & y_{12}^e \sim v_1 v_2/M_{\rm GUT}^2 && \approx 1\times 10^{-4}, \\ y^P \sim\ & v_3/M_P && \approx 5\times 10^{-4}. \end{aligned} \tag{2.40}$$

The right-handed neutrino mass parameters are estimated to be

$$M_1^{\rm R} \sim 4\times 10^7 \text{ GeV}, \quad M_2^{\rm R} \sim 2.5\times 10^{10} \text{ GeV}, \quad M_3^{\rm R} \sim 10^{16} \text{ GeV}. \tag{2.41}$$

This very strong hierarchy implies negligible right-handed neutrino mixing, such that the mass eigenvalues closely correspond to the above values. As each parameter contains several $\mathcal{O}(1)$ coefficients and CG factors, the above numbers only represent order of magnitude estimates.

The numerical fit in section 2.4 shows that the above estimates are in good agreement with the values that produce a good fit to data except only for the parameter $M_1^{\rm R}$, which is primarily responsible for the lightest right-handed neutrino mass. It should be a factor $\mathcal{O}(0.01)$ times the estimate above in order to give the correct light neutrino mass spectrum. This can be understood by inserting the above estimates for y_1^ν and $M_1^{\rm R}$ into the expression for μ_1 in equation 2.38, which suggests $\mu_1 \sim 0.01$ meV, whereas we will see the fit prefers a value of $\mathcal{O}(1)$ meV. The necessary factor can be achieved by assuming that one or more coefficients deviate from unity.

One can also get approximate expressions for the quark mixing angles in terms of quark Yukawa couplings as follows. The very strong hierarchy in the three real parameters of Y^u is correlated with that in the physical Yukawa eigenvalues of up, charm and top quarks. We therefore expect negligible contributions from the up sector to quark mixing. This implies that not only do the four real parameters in the down sector, y_i^d and y^P, fix the down-type Yukawa eigenvalues, they also must reproduce the observed CKM mixing angles.

Let us keep only the leading terms in each element of Y^d and ignore free phases. As noted above, $y_{12}^d \sim y^P < y_2^d \ll y_3^d$. We also define $y_2' = y_2^d + 2y_{12}^d + 2y^P$. Then

$$Y^d \approx \begin{pmatrix} 0 & y_{12}^d & y_{12}^d - y^P \\ y_{12}^d & y_2' & y_2' + 2(y_{12}^d - y^P) \\ y_{12}^d - y^P & y_2' + 2(y_{12}^d - y^P) & y_3^d \end{pmatrix}. \tag{2.42}$$

In the small angle approximation, the mixing angles can be estimated by

$$\theta_{12}^q \approx \frac{Y_{12}^d}{Y_{22}^d} = \frac{y_{12}^d}{y_2'}, \quad \theta_{13}^q \approx \frac{Y_{13}^d}{Y_{33}^d} = \frac{y_{12}^d - y^P}{y_3^d}, \quad \theta_{23}^q \approx \frac{Y_{23}^d}{Y_{33}^d} = \frac{y_2' + 2(y_{12}^d - y^P)}{y_3^d}. \tag{2.43}$$

The down-type Yukawa eigenvalues are given by $y_d \approx (y_{12}^d)^2/y_2'$, $y_s \approx y_2'$, $y_b \approx y_3^d$. Solving for y_{12}^d, y_2' and y_3^d, we have, to good approximation, $y_{12}^d \approx \sqrt{y_d y_s}$, $y_2' \approx y_s$, $y_3^d \approx y_b$. Reintroducing these into our estimates for mixing angles, we get

$$\theta_{12}^q \approx \sqrt{\frac{y_d}{y_s}}, \quad \theta_{13}^q \approx \frac{\sqrt{y_d y_s} - y^P}{y_b}, \quad \theta_{23}^q \approx \frac{y_s + 2(\sqrt{y_s y_d} - y^P)}{y_b}. \tag{2.44}$$

The first equality is exactly the GST relation [144], which is in good agreement with data. In fact, the GST relation, which predicts $\theta_{12}^q \simeq 0.224$ for the central values of y_d and y_s, is in mild tension with experimental data, which gives $\theta_{12}^q \simeq 0.227$. Possible modifications to the GST result have been proposed [198], e.g. adding a correction like $\sqrt{y_u/y_c}$, which can be realised by a texture zero also in Y^u. Alternatively, one may exploit the statistical uncertainties on each of the down and strange quark masses. A small deviation from their central values can predict a slightly different θ_{12}^q.

On the other hand, the mixing angles θ_{13}^q and θ_{23}^q are less precisely estimated, as the parameter y^P can be as large as y_{12}^d, and the final result will depend on the relative phase between y_{12}^d and y^P. Note however that both mixing angles depend in the same way on $y_{12}^d - y^P$. Generally, the approximations in equation 2.44 predict some tension between θ_{13}^q and θ_{23}^q, which are too large and too small, respectively. This tension cannot be resolved simply by tuning y^P.

2.4 Numerical fit

Our model determines the Yukawa couplings and mixing parameters at the GUT scale, which is also the highest flavour-breaking scale. The values from experiments must therefore be run up to the GUT scale. Moreover, when matching the SM to the MSSM at the scale M_{SUSY}, supersymmetric radiative threshold corrections have to be included. The GUT scale values after the running of quark and lepton parameters together with the inclusion of one-loop supersymmetric threshold correction have been computed in [199] and we use their results. The parametrisation of these corrections is summarised in appendix B. Most parameters do not significantly affect the fit, so are simply set to reasonable values. Specifically, we set $M_{\text{SUSY}} = 1$ TeV, $\tan\beta = 5$ and $\bar{\eta}_q = \bar{\eta}_\ell = 0$. We also find that a good fit can be achieved for a rather large value $\bar{\eta}_b = -0.8$. The choices of SUSY parameters $\tan\beta$ and $\bar{\eta}_b$ are here empirically determined to give a good fit of the model to data. It is clear from the fit that large (negative) $\bar{\eta}_b$ is required, affecting primarily the bottom quark Yukawa coupling y_b. In order to keep y_b perturbative, we

must assume $\tan\beta < 30$. In the region of $5 < \tan\beta < 10$ or so, the fit is rather insensitive to the exact choice. Neutrino data is taken from the NuFit global fit [200].

To find the best fit of the model to data, we minimise a χ^2 function, defined in the standard way: for a given set of input parameters x, we calculate the n observables $P_n(x)$. These are then compared to the observed values P_n^{obs}, which have associated statistical errors σ_n.[6] Then

$$\chi^2 = \sum_n \left(\frac{P_n(x) - P_n^{\text{obs}}}{\sigma_n} \right)^2 . \tag{2.45}$$

For our model, the input parameters are $x = \{y_i^u, y_i^d, y_i^e, y_P, \mu_i, \eta', \alpha_{d,e}, \beta_{d,e}, \gamma\}$, and the observables are given by $P_n \in \{\theta_{ij}^q, \delta^q, y_{u,c,t}, y_{d,s,b}, \theta_{ij}^\ell, y_{e,\mu,\tau}, \Delta m_{ij}^2\}$. Note that as the lepton CP phase δ^ℓ is not yet well measured, we do not include it in the fit, rather we prefer to leave it as a pure prediction. Furthermore, only the neutrino mass-squared differences are measured in oscillation experiments (as opposed to the masses themselves), while our model predicts the masses outright, including the lightest neutrino mass m_1.

Observable	Data		Model
	Central value	1σ range	Best fit
θ_{12}^ℓ /°	33.57	$32.81 \to 34.32$	33.62
θ_{13}^ℓ /°	8.460	$8.310 \to 8.610$	8.455
θ_{23}^ℓ /°	41.75	$40.40 \to 43.10$	41.96
δ^ℓ /°	261.0	$202.0 \to 312.0$	300.9
y_e /10^{-5}	1.017	$1.011 \to 1.023$	1.017
y_μ /10^{-3}	2.147	$2.134 \to 2.160$	2.147
y_τ /10^{-2}	3.654	$3.635 \to 3.673$	3.654
$\Delta m_{21}^2/(10^{-5}\,\text{eV}^2)$	7.510	$7.330 \to 7.690$	7.515
$\Delta m_{31}^2/(10^{-3}\,\text{eV}^2)$	2.524	$2.484 \to 2.564$	2.523
m_1 /meV			0.441
m_2 /meV			8.680
m_3 /meV			50.24
$\sum m_i$ /meV		< 230	59.36
α_{21}			67.90
α_{31}			164.2

Table 2.3: Model predictions in the lepton sector for $\tan\beta = 5$, $M_{\text{SUSY}} = 1$ TeV and $\bar{\eta}_b = -0.8$. The observables are at the GUT scale. The lepton contribution to the total χ^2 is 0.03. δ^ℓ as well as the neutrino masses m_i are pure predictions of our model. The bound on $\sum m_i$ is taken from [59].

We present the best fit (minimum χ^2) of the model to physical observables (Yukawa couplings and neutrino mass and mixing parameters) in tables 2.3 and 2.4, which also include the central values and 1σ ranges from data. Figure 2.4 shows the associated pulls, and table 2.5 shows the corresponding input parameter values. The fit gives

[6] In order for a minimum χ^2 to correspond to the maximum likelihood, the statistical uncertainties should be symmetric (Gaussian). This is essentially satisfied for all parameters except θ_{23}^ℓ, where current experimental data cannot conclusively resolve the octant, i.e whether it is larger or smaller than 45°. Currently, the data favours $\theta_{23}^\ell < 45°$, with a central value 41.6° [200]. We will assume this is the true value.

Observable	Data		Model
	Central value	1σ range	Best fit
θ^q_{12} /°	13.03	12.99 → 13.07	13.02
θ^q_{13} /°	0.039	0.037 → 0.040	0.039
θ^q_{23} /°	0.445	0.438 → 0.452	0.439
δ^q /°	69.22	66.12 → 72.31	69.21
y_u /10^{-6}	2.988	2.062 → 3.915	3.012
y_c /10^{-3}	1.462	1.411 → 1.512	1.493
y_t	0.549	0.542 → 0.556	0.547
y_d /10^{-5}	2.485	2.212 → 2.758	2.710
y_s /10^{-4}	4.922	4.656 → 5.188	5.168
y_b	0.141	0.136 → 0.146	0.137

Table 2.4: Model predictions in the quark sector for $\tan\beta = 5$, $M_{\rm SUSY} = 1$ TeV and $\bar{\eta}_b = -0.8$. The observables are at the GUT scale. The quark contribution to the total χ^2 is 3.38.

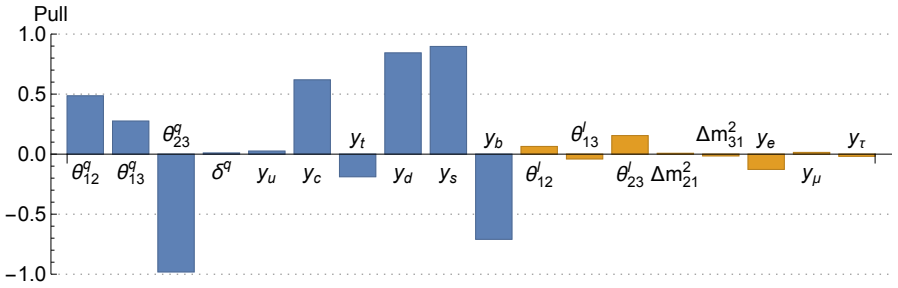

Figure 2.4: Pulls for the best fit of model to data, as shown in tables 2.3-2.4, for quark (blue) and lepton (yellow) parameters.

$\chi^2 \approx 3.4$.[7] A second minimum with $\chi^2 \approx 4$ was also found, leading primarily to a different prediction for δ^ℓ, as discussed below, although we shall not present the full fit parameters for this case.

We see from tables 2.3, 2.4 and figure 2.4 that both quark and lepton sectors are fitted to within 1σ of the values predicted by global fits to experiment. The biggest pulls are in down-type quark Yukawa couplings $y_{d,s,b}$ and θ^q_{23}. As shown in section 2.3.3, θ^q_{23} is approximately given by the ratio y_s/y_b, which is typically too small. Furthermore, attempts to increase θ^q_{23}, e.g. by tuning y^P, tends to increase θ^q_{13}, which is then too large. This tension can be ameliorated by assuming large threshold corrections, i.e. by setting $\bar{\eta}_b = -0.8$, although some tension remains among the above parameters, which deviate by about 1σ.

We find two different minima with best fit values for δ^l of 300.9° with $\chi^2 \approx 3.4$ (as seen in table 2.3) and 233.9° corresponding to a second best fit point with $\chi^2 \approx 4$. We note that both values are far from maximal CP violation $\delta^\ell = 270°$, which is close to the prediction from CSD3 with diagonal charged leptons. In short, charged-lepton

[7] The best fit predicts a strong neutrino hierarchy, with $m_1 < 1$ meV. It is possible to achieve a milder hierarchy, although the numerical fit gives $\chi^2 \gtrsim 20$ in such cases, predicting neutrino masses of approximately 5, 10 and 51 meV. Additionally it predicts $\delta^\ell \approx +25°$, currently disfavoured by experiment.

Parameter	Value
$y_1^u\,/10^{-6}$	3.009
$y_2^u\,/10^{-3}$	1.491
y_3^u	0.549
$y_{12}^d\,/10^{-4}$	-1.186
$y_2^d\,/10^{-4}$	6.980
y_3^d	0.137
$y^P\,/10^{-4}$	1.243

Parameter	Value
$y_{12}^e\,/10^{-4}$	1.558
$y_2^e\,/10^{-3}$	2.248
$y_3^e\,/10^{-2}$	3.318
μ_1 /meV	2.413
μ_2 /meV	27.50
μ_3 /meV	2.900

Parameter	Value
α_d	0.043π
β_d	0.295π
α_e	1.692π
β_e	1.755π
γ	0.918π
η'	1.053π

Table 2.5: Best fit input parameter values. The model has 13 real parameters: y_i^u, y_i^d, y_i^e, μ_i and y^P. While η is fixed by flavon alignment to $-2\pi/3$, there are six additional free phases: η', $\alpha_{d,e}$, $\beta_{d,e}$ and γ. The total χ^2 is 3.4.

corrections induce a deviation from maximal CP phase, which can either be positive or negative, depending on the phases of Y^e.

One may be tempted to calculate a reduced chi-squared χ^2_ν, i.e. the χ^2 per degree of freedom (d.o.f.), where the number of d.o.f. is naively given by the number of observables minus the number of input parameters. In the conventional picture, a good fit has $\chi^2_\nu \simeq 1$. However, as discussed in [201], this interpretation is only valid for linear models, which our model is not. Indeed, when evaluating χ^2 we fit 19 inputs to 18 observables, which in a linear model would suggest a perfect fit is always possible; this is certainly not the case. While χ^2 is a valid tool for comparing models to each other, since it is not possible to establish an exact number of d.o.f., we cannot reliably define χ^2_ν.

2.5 Summary

We try to address the flavour puzzle in the Standard Model, which is the source of a majority of the Standard Model free parameters, characterised by different mixing behaviours for quarks and leptons, and very hierarchical masses. The most minimal solution to the problem of neutrino masses remains the seesaw mechanism with heavy right-handed neutrinos, which arise automatically in $SO(10)$, with naturally large masses. This motivates $SO(10)$ above other popular gauge groups, such as $SU(5)$, where right-handed neutrinos are added by hand. All three families of SM fermions in the **16** of $SO(10)$ are here also unified in a single triplet of S_4. This very elegant picture presents model-building challenges, many of which we have tackled in this chapter.

We have constructed a rather simple, natural and complete $SO(10)$ model of flavour with a discrete $S_4 \times \mathbb{Z}_4^2 \times \mathbb{Z}_4^R$ symmetry, where all Yukawa matrices derive from the VEVs of triplet flavons, in the CSD3 alignment. It is simple in the sense that the field content is reasonably minimal, with small Higgs representations of $SO(10)$ consisting of two **10**s which contain the MSSM doublets, a Higgs spinor pair **16** and $\overline{\mathbf{16}}$ responsible for Majorana masses and four adjoint Higgs **45**s, which provide necessary Clebsch-Gordan

factors that distinguish charged leptons and down-type quarks. It is natural in the sense that Yukawa and mass matrices consist of sums of low-rank matrices, each of which contributes dominantly to a particular family, i.e. "universal sequential dominance". It is complete in the sense that we address the μ-problem, Higgs mixing and doublet-triplet splitting, and provide an ultraviolet renormalisable model, with Planck-suppressed operators controlled by symmetry. However, we do not discuss the origin of the hierarchy of flavon VEVs, nor do we repeat the discussion of flavon vacuum alignment, which can be found in [142].

We believe this model represents a significant step forward in the quest for a complete and correct description of fermions within SUSY GUTs. For instance, we have demonstrated the correct procedure for treating the third family couplings and how to generate an electroweak-scale renormalisable third-family Yukawa coupling. We also emphasise that the principle of universal sequential dominance is a simple and effective way to understand fermion hierarchies. Although the origin of such family hierarchies has not been fully resolved, as the scales of flavon VEVs v_a $(a = 1, 2, 3)$ are assumed rather than proven, the problem has been ameliorated, since the hierarchy is given by the squares of these VEVs.

The model successfully reproduces the observed fermion masses and mixing, even in the quark sector, where the CKM parameters are measured to very high precision. Analytical estimates are underpinned by a detailed numerical analysis, demonstrating the viability of the model. Moreover, there is no tuning of $\mathcal{O}(1)$ parameters necessary to explain the mass hierarchies of charged fermions, accounting also for the milder hierarchy in down-type quarks compared to up-type quarks. The model simultaneously realises large lepton mixing and small quark mixing, as well as the GST relation for the Cabibbo angle, $\theta_{12}^q \approx \sqrt{y_d/y_s}$ via a texture zero in the down-type Yukawa matrix Y^d. In the lepton sector an excellent fit to data is found, predicting a normal neutrino hierarchy and lightest neutrino mass $m_1 \lesssim 0.5$ meV. The CP phase δ^ℓ was not fitted, but left as a pure prediction. Two distinct fits are found, with corresponding best fit values $\delta^\ell \approx 301^\circ$ and 234°. We emphasise that the model predicts significant deviation from both zero and maximal CP violation.

Chapter 3

$S_4 \times SO(10)$ grand unified theory of flavour and leptogenesis

To further explore the phenomenological implications of $S_4 \times SO(10)$ models, in this chapter we present a more complete version involving an additional $Z_4^R \times Z_4^3$ controlling the Higgs and flavon symmetry breaking sectors. In the model here, we prefer the simpler constrained sequential dominance-2 (CSD2) [202] vacuum alignments since it also allows successful leptogenesis, as discussed below. Interestingly we find that leptogenesis is not consistent with the earlier model based on CSD3 vacuum alignments, which is a significant motivation for considering the new model based on CSD2. Additionally, we explicitly show the superpotential leading to the CSD2 vacuum alignments and the origin of the hierarchies between the flavon VEVs. This chapter is primarily derived from [2].

3.1 The model

3.1.1 Overview of the model

The symmetry of the model is $S_4 \times SO(10) \times \mathbb{Z}_4^R \times \mathbb{Z}_4^3$. The model has a gauge symmetry $SO(10)$ which is the GUT symmetry. The symmetry S_4 is the flavour symmetry which gives the specific CSD2 structure to the fermion mass matrices. The $\mathbb{Z}_4^R$ is an R symmetry while the other three $\mathbb{Z}_4$'s are shaping symmetries. Furthermore, we assume that the GUT theory is invariant under trivial CP symmetry, which is spontaneously broken by the complex VEVs of the flavons.

We present table 3.1 with the Higgs, flavons and matter superfields relevant to the Yukawa sector. The superfield ψ accommodates the full Standard Model fermion content and is a spinorial **16** of $SO(10)$ and a triplet $\mathbf{3'}$ of S_4. The superfields $H_{10}^{u,d}$ contain the MSSM Higgs doublets $H_{u,d}$ respectively. The $H_{\overline{16}}$ breaks $SO(10) \to SU(5)$ and gives

Field	Representation					
	S_4	$SO(10)$	$\mathbb{Z}_4^R$	$\mathbb{Z}_4$	$\mathbb{Z}_4$	$\mathbb{Z}_4$
ψ	$3'$	16	1	0	0	0
H_{10}^u	1	10	0	0	0	0
H_{10}^d	1	10	0	0	2	0
$H_{\overline{16}}$	1	$\overline{16}$	0	0	0	0
H_{16}	1	16	0	0	1	0
$H_{45}^{X,Y}$	1	45	0	0	1	0
$H_{45}^{W,Z}$	1	45	0	2	0	0
H_{45}^{B-L}	1	45	2	0	2	0
ζ	1	1	0	0	2	0

(a) Matter and Higgs superfields.

Field	Representation					
	S_4	$SO(10)$	$\mathbb{Z}_4^R$	$\mathbb{Z}_4$	$\mathbb{Z}_4$	$\mathbb{Z}_4$
ϕ_1	$3'$	1	0	2	2	0
ϕ_2	$3'$	1	0	2	0	0
ϕ_3	$3'$	1	0	0	2	0
$\phi_{S,U}$	$3'$	1	0	0	0	1
ϕ_T	3	1	0	1	0	1
ξ	1	1	0	3	0	2
ϕ_t	3	1	0	0	1	3

(b) Flavon superfields.

Table 3.1: Superfield content of the model that relates directly to the low energy fields.

masses to the right-handed neutrinos. The superfields on the adjoint **45** representation H_{45}'s break $SU(5) \to SM$ and introduce the necessary Clebsch-Gordan (CG) relations to generate correct charged lepton and down quark masses. The flavon superfields ϕ_i, with $i = 1, 2, 3$ break S_4 completely and they acquire the specific CSD2 vacuum alignments [202] given by

$$\langle \phi_1 \rangle = v_1 \begin{pmatrix} 1 \\ 0 \\ 2 \end{pmatrix}, \quad \langle \phi_2 \rangle = v_2 \begin{pmatrix} 0 \\ 1 \\ -1 \end{pmatrix}, \quad \langle \phi_3 \rangle = v_3 \begin{pmatrix} 0 \\ 1 \\ 0 \end{pmatrix}, \tag{3.1}$$

with $|v_1| \ll |v_2| \ll |v_3|$. In this chapter, CSD2 is simply used as a label which refers to this particular flavon vacuum alignment in equation 3.1. The superpotential that fixes the CSD2 flavon alignments is presented in section 3.1.3, while the superpotential responsible of the hierarchy between the flavon VEVs is shown in section 3.1.4.

The symmetries of the model and the superfield content in table 3.1 lead to a very specific mass structure for the Standard Model fermion fields. The up-type quark and the neutrino Yukawa matrices arise from terms like

$$H_{10}^u(\psi\phi_1)(\psi\phi_1) + H_{10}^u(\psi\phi_2)(\psi\phi_2) + H_{10}^u(\psi\phi_3)(\psi\phi_3), \tag{3.2}$$

where the brackets denote S_4 singlet contractions. Similarly to chapter 2, each term in equation 3.2 generates a rank-1 matrix. Therefore, the hierarchy between the flavon VEVs gives a natural explanation of the hierarchical Yukawa couplings, i.e. $y_u \sim v_1^2/M_{\rm GUT}^2$, $y_c \sim v_2^2/M_{\rm GUT}^2$ and $y_t \sim v_3^2/M_{\rm GUT}^2$. In this chapter, we explicitly show a superpotential which fixes the hierarchy between the flavon VEVs $|v_1| \ll |v_2| \ll |v_3|$ in section 3.1.4. The right-handed neutrino Majorana masses are similar to equation 3.2 but replacing H_{10}^u by $H_{\overline{16}}H_{\overline{16}}$. The right-handed neutrino mass matrices have the same structure as the Dirac neutrino masses since they are dictated by the same flavon vac-

uum alignments. This fact gives rise to exactly the same structure for the left-handed neutrino Majorana masses after the seesaw mechanism, as shown in section 3.2.3.

The down-type quark and the charged lepton Yukawa matrices emerge from terms like

$$H_{10}^d(\psi\phi_1)(\psi\phi_2) + H_{10}^d(\psi\phi_2)(\psi\phi_2) + H_{10}^d(\psi\phi_3)(\psi\phi_3) + H_{10}^d(\psi\psi)_{3'}\phi_3, \tag{3.3}$$

where the brackets denote S_4 singlet contractions apart from the last term in which the $\mathbf{3'}$ contraction is necessary to subsequently combine it with the flavon ϕ_3 into a singlet. These Yukawa matrices have a different structure compared to the up sector, due to a mixing term between the flavons ϕ_1 and ϕ_2, which explains why there is a milder hierarchy in the down and charged lepton sectors compared to the up one. It also introduces a texture zero in the (1,1) element of the down Yukawa matrix, reproducing the GST relation [144], i.e. the Cabibbo angle is predicted to be $\theta_{12}^q \simeq \sqrt{y_d/y_s}$.

With this setup the full Standard Model fermion masses are generated in a very specific and predictive way, this being the main aim of chapter 3. Furthermore, all the messenger superfields and adjoints obtain a GUT scale mass after GUT symmetry breaking. The triplets inside the Higgs superfields $H_{10}^{u,d}$ also get a GUT scale mass through the Dimopoulos-Wiclzeck mechanism [190–192], as shown in section 3.1.5. This way we make sure that at low energies, only the MSSM remains.

3.1.2 Effective Yukawa structure

Field	Representation					
	S_4	$SO(10)$	$\mathbb{Z}_4^R$	$\mathbb{Z}_4$	$\mathbb{Z}_4$	$\mathbb{Z}_4$
$\bar{\chi}_1$	1	$\overline{16}$	1	2	2	0
χ_1	1	16	1	0	2	0
$\bar{\chi}_2$	1	$\overline{16}$	1	2	0	0
χ_2	1	16	1	0	0	0
$\bar{\chi}_3$	1	$\overline{16}$	1	0	2	0
χ_3	1	16	1	2	2	0
χ_3^d	1	16	1	0	1	0
χ_2^d	1	16	1	2	3	0
$\bar{\chi}_u$	1	$\overline{16}$	2	0	0	0
χ_u	1	16	0	0	2	0
$\bar{\chi}_d$	1	$\overline{16}$	0	0	1	0
χ_d	1	16	2	0	1	0
ζ_1	1	45	2	0	3	0
ζ_2	1	45	0	0	3	0

(a) Messenger superfields.

Field	Representation					
	S_4	$SO(10)$	$\mathbb{Z}_4^R$	$\mathbb{Z}_4$	$\mathbb{Z}_4$	$\mathbb{Z}_4$
$X_{3'}$	$3'$	1	2	0	0	2
X_2	2	1	2	2	0	2
$\tilde{X}_2$	2	1	2	0	1	1
X_1	1	1	2	0	2	2
$\tilde{X}_1$	1	1	2	3	3	0
$X_{1'}$	$1'$	1	2	3	2	2
$Z_{3'}$	$3'$	1	2	3	0	2
$\tilde{Z}_{3'}$	$3'$	1	2	2	2	0
$\tilde{Z}$	1	1	2	3	2	3
Z	1	1	2	0	0	0

(b) Driving superfields.

Table 3.2: Superfields that appear only at high energies. Together with the ones in table 3.1 they list the complete field content of the model.

We now present the effective Yukawa terms in more detail, with the full field content of the model listed in tables 3.1 and 3.2. The superpotential relevant to the Yukawa terms, including terms $\mathcal{O}(1/M_P)$, is given by

$$\begin{aligned} W_Y \sim & \frac{H^u_{10}(\psi\phi_1)(\psi\phi_1)}{\langle H^{W,Z}_{45}\rangle^2} + \frac{H^u_{10}(\psi\phi_2)(\psi\phi_2)}{\langle H^{W,Z}_{45}\rangle^2} + \frac{H^u_{10}(\psi\phi_3)(\psi\phi_3)}{\langle H^{W,Z}_{45}\rangle^2} \\ & + \frac{H^d_{10}(\psi\phi_1)(\psi\phi_2)}{\langle H^{W,Z}_{45}\rangle^2} + \frac{H^d_{10}(\psi\phi_2)(\psi\phi_2)}{\langle H^{X,Y}_{45}\rangle^2} + \frac{H^d_{10}(\psi\phi_3)(\psi\phi_3)}{\langle H^{X,Y}_{45}\rangle^2} \\ & + \frac{H_{\overline{16}}H_{\overline{16}}(\psi\phi_1)(\psi\phi_1)}{M_P\langle H^{W,Z}_{45}\rangle^2} + \frac{H_{\overline{16}}H_{\overline{16}}(\psi\phi_2)(\psi\phi_2)}{M_P\langle H^{W,Z}_{45}\rangle^2} + \frac{H_{\overline{16}}H_{\overline{16}}(\psi\phi_3)(\psi\phi_3)}{M_P\langle H^{W,Z}_{45}\rangle^2} \\ & + \frac{H^d_{10}(\psi\psi)_{3'}(\phi_3)}{M_P}, \end{aligned} \tag{3.4}$$

where $(\ )_{3'}$ means a $\mathbf{3'}$ contraction, while $(\ )$ without any subscript means the singlet contraction of S_4 and we have ignored all the $\mathcal{O}(1)$ dimensionless couplings for simplicity. There are plenty of terms suppressed by M_P^2 and they are expected to make small mass contributions of $\mathcal{O}(M^2_{GUT}/M^2_P) < 10^{-6}$, and therefore negligible. The most important correction, of $\mathcal{O}(10^{-6})$, is made to the up-quark Yukawa coupling. In section 3.3 we perform a fit ignoring these corrections, however from table 3.5, we see that this contribution is of comparable magnitude. If they were to be included, they would only shift the fit parameters and therefore we can safely ignore them. The largest contribution to the electron Yukawa coupling is of $\mathcal{O}(10^{-8})$ and is therefore negligible.

The diagrams that generate the terms in equation 3.4 are shown in figures 3.1-3.3, where they include the messengers χ listed in table 3.2.

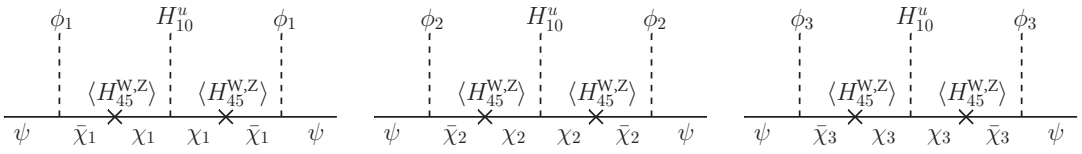

Figure 3.1: Diagrams coupling ψ to H^u_{10}. When flavons acquire VEVs, these give the up-type quark and Dirac neutrino Yukawa matrices.

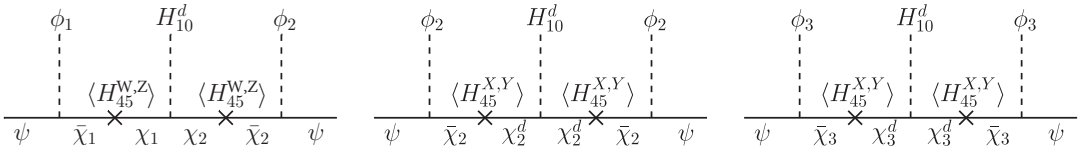

Figure 3.2: Diagrams coupling ψ to H^d_{10}. These generate the down-type quark and charged lepton Yukawa matrices.

In section 3.2, we present the renormalisable terms involving the heavy messenger fields in table 3.2.

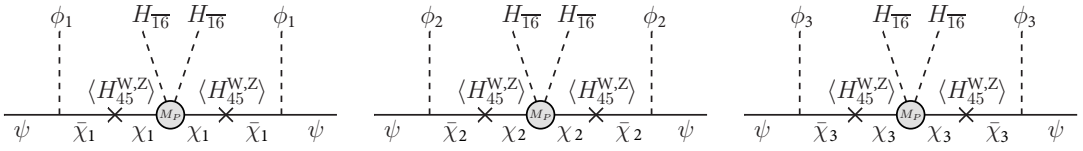

Figure 3.3: Diagrams coupling ψ to $H_{\overline{16}}$. These give the right-handed neutrino mass matrix.

3.1.3 Vacuum alignment

We introduce the flavon superpotential that fixes the symmetry breaking flavon VEVs in equation 3.1. To derive these alignments, we need to add a set of driving fields, listed in table 3.2, which couple to the flavon fields in table 3.1. We follow a sequence of steps using supersymmetric F-terms equations to align all the flavons. The letter subscript (S, U, T and t) in the flavons refers to the symmetry preserving generator, where t correspond to T multiplied by a Z_3 generator which is not part of S_4. The alignments depend on the S_4 representation of the driving field, denoted by its subscript X_i, Z_i. The superpotential is given by

$$\begin{aligned} W_\phi \sim\ & X_{3'}(\phi_{S,U})^2 + X_2(\phi_T)^2 + X_1(\phi_t)^2 + \tilde{X}_1\phi_T\phi_t + X_{1'}\phi_T\phi_3 + \tilde{X}_2\phi_t\phi_3 \\ & + Z_{3'}(\phi_{S,U}\phi_T + \xi\phi_2) + \tilde{Z}_{3'}\xi\left(\frac{\phi_2\phi_3}{M_P} - \phi_1\right), \end{aligned} \tag{3.5}$$

where we have ignored dimensionless $\mathcal{O}(1)$ parameters since they are not relevant. Solving the F-term equations from the driving fields fixes the flavon VEV alignments, while the F-term equations from flavons forbid the driving fields from getting a VEV.

The three S_4 generators, working in the T-diagonal basis as in appendix A.1, are

$$S = \frac{1}{3}\begin{pmatrix} -1 & 2 & 2 \\ 2 & -1 & 2 \\ 2 & 2 & -1 \end{pmatrix}, \quad T = \begin{pmatrix} 1 & 0 & 0 \\ 0 & \omega^2 & 0 \\ 0 & 0 & \omega \end{pmatrix} \quad \text{for } \mathbf{3} \text{ or } \mathbf{3'}\,, \tag{3.6}$$

and

$$U = \mp\begin{pmatrix} 1 & 0 & 0 \\ 0 & 0 & 1 \\ 0 & 1 & 0 \end{pmatrix}, \quad SU = US = \mp\frac{1}{3}\begin{pmatrix} -1 & 2 & 2 \\ 2 & 2 & -1 \\ 2 & -1 & 2 \end{pmatrix}, \quad \text{for } \mathbf{3}, \mathbf{3'} \text{ respectively.} \tag{3.7}$$

The first three terms in the superpotential in equation 3.5 couple the square of a flavon triplet to a single driving field X_i. The different representations of X_i result on distinct

flavon alignments such that they are fixed as

$$X_{3'}(\phi_{S,U})^2 \longrightarrow \begin{pmatrix} 1 \\ \omega^n \\ \omega^{2n} \end{pmatrix} , \tag{3.8}$$

$$X_2(\phi_T)^2 \longrightarrow \begin{pmatrix} 1 \\ 0 \\ 0 \end{pmatrix} , \begin{pmatrix} 1 \\ -2\omega^n \\ -2\omega^{2n} \end{pmatrix} , \tag{3.9}$$

$$X_1(\phi_t)^2 \longrightarrow \begin{pmatrix} 0 \\ 0 \\ 1 \end{pmatrix} , \begin{pmatrix} 0 \\ 1 \\ 0 \end{pmatrix} , \begin{pmatrix} 2 \\ 2x \\ -1/x \end{pmatrix} , \tag{3.10}$$

up to an integer ($n \in \mathbb{Z}$) or continuous ($x \in \mathbb{R}$) parameter, with $\omega = e^{2\pi i/3}$.

The $\langle \phi_T \rangle$ has four different solutions. The last three solutions are related by a T transformation. From these three, the one without any ω is related to the first solution by an S transformation. Since all the solutions for $\langle \phi_T \rangle$ are related by S_4 transformations, we may choose $(1,0,0)^T$ without loss of generality. Moreover, we may notice that the alignments for $\langle \phi_{S,U} \rangle$ can be brought to the standard $(1,1,1)^T$ form by a T transformation which does not affect the $\langle \phi_T \rangle$ alignment.

Finally, the $\langle \phi_t \rangle$ has three different solutions. The third solution is removed by the fourth term in the superpotential 3.5 which requires orthogonality with $\langle \phi_T \rangle$. This fixes the solution to be either $(0,0,1)^T$ or $(0,1,0)^T$, which are related by an U transformation. Since the so-selected alignments of $\langle \phi_T \rangle$ and $\langle \phi_{S,U} \rangle$ do not change their form (up to possible overall sign) under application of a U transformation, we choose $\langle \phi_t \rangle \propto (0,0,1)^T$ without loss of generality,.

The fifth and sixth terms in equation 3.5 fix the alignment of ϕ_3 to be orthogonal to $\langle \phi_t \rangle$ and $\langle \phi_T \rangle$ so that it is fixed to be $(0,1,0)^T$.

The term $Z_{3'}(\phi_{S,U}\phi_T + \xi\phi_2)$ in equation 3.5 involves

$$(\langle \phi_{S,U} \rangle \cdot \langle \phi_T \rangle)_{3'} \propto \begin{pmatrix} 0 \\ -1 \\ 1 \end{pmatrix} , \tag{3.11}$$

and fixes $\langle \phi_2 \rangle$ into this direction. Equivalently, the last term in the superpotential 3.5 contains the product

$$(\langle \phi_2 \rangle \cdot \langle \phi_3 \rangle)_{3'} \propto \begin{pmatrix} 1 \\ 0 \\ 2 \end{pmatrix} , \tag{3.12}$$

and fixes $\langle \phi_1 \rangle$ into this direction. The ξ field does not add anything to the flavon alignments but it does play a role in driving the hierarchy between the flavon VEVs as

explained below in section 3.1.4.

In summary, the F-term equations from the driving fields X_i, Z_i fix the alignments to be

$$\begin{aligned} \langle \phi_{S,U} \rangle &= v_1 \begin{pmatrix} 1 \\ 1 \\ 1 \end{pmatrix}, \ \langle \phi_T \rangle = v_2 \begin{pmatrix} 1 \\ 0 \\ 0 \end{pmatrix}, \ \langle \phi_t \rangle = v_t \begin{pmatrix} 0 \\ 0 \\ 1 \end{pmatrix} \\ \langle \phi_1 \rangle &= v_1 \begin{pmatrix} 1 \\ 0 \\ 2 \end{pmatrix}, \ \langle \phi_2 \rangle = v_2 \begin{pmatrix} 0 \\ 1 \\ -1 \end{pmatrix}, \ \langle \phi_3 \rangle = v_3 \begin{pmatrix} 0 \\ 1 \\ 0 \end{pmatrix}, \end{aligned} \tag{3.13}$$

where the last three flavons couple to the matter superfield ψ and determine the fermion mass matrix structure. The flavon VEVs v_i are, in general, complex, and spontaneously break the assumed CP symmetry of the high energy theory.

3.1.4 Symmetry breaking

The model gives a natural understanding of the Standard Model fermion masses through the hierarchy between the flavon VEVs $|v_1| \ll |v_2| \ll |v_3|$. Here, we show the symmetry breaking superpotential that produces such hierarchy between the VEVs,

$$\begin{aligned} \mathcal{W}_{DV} \sim\ & \tilde{Z}_3 \xi \left(\phi_1 - \frac{\phi_2 \phi_3}{M_P} \right) + \tilde{Z} \frac{\phi_T}{M_P} \left(\phi_1 \phi_2 - \frac{\phi_3 \sum_i \phi_i^2}{M_P} + \mathcal{O}(1/M_P^2) \right) \\ & + Z \left(M_{GUT}^2 + \sum_i \phi_i^2 + (H_{45}^{W,Z})^2 + (H_{45}^{B-L})^2 + \zeta^2 + Z^2 + \mathcal{O}(1/M_P) \right) \\ & + H_{45}^{B-L} \left((H_{45}^{X,Y})^2 + \frac{\zeta}{M_P} \left((H_{45}^{W,Z})^2 + (H_{45}^{B-L})^2 \right) + H_{45}^{X,Y} \frac{H_{\overline{16}} H_{16}}{M_P} + DT + \mathcal{O}(1/M_P^2) \right), \end{aligned} \tag{3.14}$$

where we have ignored dimensionless couplings for simplicity.

The first term of equation 3.14 also appears in the alignment superpotential in equation 3.5 and fixes

$$|\tilde{\kappa}_1 v_1| = \left| \frac{v_2 v_3}{M_P} \right|, \tag{3.15}$$

where $\tilde{\kappa}_1$ denotes an effective dimensionless coupling coming from the ones in the superpotential. Note that we have written this equation as only fixing the modulus. This happens due to the appearance of the field ξ. We assume that there are two copies of that field, which get a VEV with an arbitrary phase. This phase, together with the dimensionless couplings for each term, does not allow to relate the phases of the v_i.

The second term of equation 3.14 fixes the VEVs

$$\tilde{\kappa}_2 \; v_1 v_2 = \frac{v_3}{M_P} \sum_i v_i^2, \tag{3.16}$$

where $\tilde{\kappa}_2$ denotes an effective dimensionless coupling coming from the ones in the superpotential. This equation, together with the previous one, require a hierarchy in the v_i's. Specifically it requires $v_{2,3} \gg v_1$.

The field $\tilde{Z}$ does not obtain a VEV to comply with the F-term equations from the flavons.

The second line of equation 3.14 drives the linear combination

$$M_{GUT}^2 \sim \sum_i v_i^2 + \langle H_{45}^{W,Z} \rangle^2 + \langle H_{45}^{B-L} \rangle^2 + \langle \zeta \rangle^2 + \langle Z \rangle^2 , \tag{3.17}$$

where we assume that the sum of v_i and the all adjoints get a GUT scale VEV. The field Z does not get a VEV due to the F-term equations coming from the adjoints. This equation does not fix the phases of the VEVs. We assume that the $\langle H_{45}^{W,Z} \rangle$ are real while the phase of the sum of flavon VEVs is unconstrained (only related to the one of $\langle \zeta \rangle$ which does not appear at low energies). We assume that the flavons obtain a VEV that break the CP symmetry with an arbitrary phase.

The third line of equation 3.14 drives

$$\frac{\langle \zeta \rangle}{M_P} \left(\langle H_{45}^{W,Z} \rangle^2 + \langle H_{45}^{B-L} \rangle^2 \right) \sim \langle H_{45}^{X,Y} \rangle^2 + \langle H_{45}^{X,Y} \rangle \frac{\langle H_{\overline{16}} H_{16} \rangle}{M_P}, \tag{3.18}$$

where we assume that the $\langle H_{45}^{X,Y} \rangle$ is real. The term DT appearing in equation 3.14 represents all the terms involved in the doublet-triplet splitting (shown in section 3.1.5) that do not contribute to the F-term equation, but they are there nonetheless. The F-term equations coming from the adjoints $H_{45}^{X,Y}$ force the messengers $\chi_{u,d}$ to also acquire a VEV and does not change any low energy phenomenology.

The F-term equations previously discussed can give a VEV to the adjoint fields but do not fix their direction. The adjoint fields can get a VEV in any SM preserving direction. In general they can be written as a linear combination of the $U(1)_{X,Y}$ directions. We do not assume any specific direction for the VEVs $\langle H_{45}^{W,X,Y,Z}, \zeta \rangle$. We assume that $\langle H_{45}^{B-L} \rangle$ lies in the $U(1)_{B-L}$ direction[1]. We assume that the $\langle H_{\overline{16},16} \rangle$ lie in the right-handed neutrino direction.

Using the first three equations 3.15-3.17, we may find that the flavon VEVs are given by

$$v_1 = \frac{\tilde{\kappa}_3^2 M_{GUT}^2}{\sqrt{\tilde{\kappa}_1 \tilde{\kappa}_2} M_P} \; v_2, \quad v_2 = \frac{\sqrt{\tilde{\kappa}_1} \tilde{\kappa}_3 M_{GUT}}{\sqrt{\tilde{\kappa}_2}}, \quad v_3 = \tilde{\kappa}_3 M_{GUT}. \tag{3.19}$$

[1] It can be written as the linear combination $B - L = (-X + 4Y)/5$.

In this way, if we assume that $\tilde{\kappa}_1 \simeq 0.1,\ \tilde{\kappa}_2 \simeq 10,\ \tilde{\kappa}_3 \simeq 1$, we have

$$v_1 \simeq 0.001\ M_{GUT}, \quad v_2 \simeq 0.1\ M_{GUT}, \quad v_3 \simeq M_{GUT}, \tag{3.20}$$

which generates the hierarchy between the fermion families. We note that the hierarchy between v_1 and v_2 is given by the structure of the F-term equations. The hierarchy between v_2 and v_3 is assumed and realized by a much milder hierarchy between the couplings in the superpotential.

Using equation 3.16 and knowing that $v_3 \gg v_{1,2}$, we approximately get

$$\tilde{\kappa}_2\ v_1 v_2 \simeq \frac{v_3^3}{M_P}, \tag{3.21}$$

which also fixes the VEV phases to be

$$\arg v_1 + \arg v_2 \simeq 3 \arg v_3. \tag{3.22}$$

In terms of the physical phases, which we define in section 3.2.2 this means

$$\eta \simeq 4\eta' - 2\gamma, \tag{3.23}$$

and, therefore, there are only two free physical phases.

3.1.5 Doublet-triplet splitting

We need to address the fact that the Higgs superfields $H_{10}^{u,d}$ and $H_{16,\overline{16}}$ contain $SU(2)$ doublets and $SU(3)$ triplets. The triplets have to be heavy since they mediate proton decay, while two of the doublets need to remain light so they can be associated to the MSSM Higgs doublets. This is known as the doublet-triplet splitting problem and can be solved using the Dimopolous-Wilczek mechanism [190–192]. In our case this mechanism is in place since we assume that $\langle H_{45}^{B-L} \rangle$ lies in the $U(1)_{B-L}$ direction. Furthermore, there are extra pairs of doublets, and they are required to be heavy to preserve gauge coupling unification. Using the fields in tables 3.1-3.2, we may write the superpotential involving the Higgs fields (ignoring dimensionless parameters) as

$$\begin{aligned}\mathcal{W}_H = H_{45}^{B-L} &\left(H_{10}^u H_{10}^d + \zeta_2 \zeta_2 + H_{\overline{16}} \chi_u + H_{16} \overline{\chi}_d \right) \\ &+ H_{\overline{16}} H_{10}^u \overline{\chi}_u + H_{16} H_{10}^d \chi_d + H_{16} H_{\overline{16}} \zeta_1 + \zeta \left(\zeta_1 \zeta_2 + \overline{\chi}_u \chi_u + \overline{\chi}_d \chi_d \right) \\ &+ H_{45}^{B-L} \left(\frac{H_{\overline{16}} H_{\overline{16}} H_{10}^d}{M_P} + \frac{H_{16} H_{16} H_{10}^u}{M_P} + H_{10}^u H_{10}^d \frac{(H_{45}^{X,Y,W,Z})^4}{M_P^4} \right).\end{aligned} \tag{3.24}$$

After integrating out the messengers ζ_i, χ_j, the superpotential becomes

$$\mathcal{W}_H = H_{45}^{B-L}\left(\kappa_1 H_{10}^u H_{10}^d + \kappa_2 \frac{(H_{16}H_{\overline{16}})^2}{\langle\zeta\rangle^2} + \kappa_7 H_{10}^u H_{10}^d \frac{(H_{45}^{X,Y,W,Z})^4}{M_P^4} + \kappa_3 \frac{H_{\overline{16}}H_{\overline{16}}H_{10}^u}{\langle\zeta\rangle} + \kappa_4 \frac{H_{\overline{16}}H_{\overline{16}}H_{10}^d}{M_P} + \kappa_5 \frac{H_{16}H_{16}H_{10}^u}{M_P} + \kappa_6 \frac{H_{16}H_{16}H_{10}^d}{\langle\zeta\rangle}\right). \tag{3.25}$$

We remember that the magnitude of the VEVs is assumed to be

$$\langle H_{16}\rangle \simeq \langle H_{\overline{16}}\rangle \simeq \langle H_{45}\rangle = M_{GUT}. \tag{3.26}$$

We define the dimensionless parameters $z = M_{GUT}/\langle\zeta\rangle$ and $y = M_{GUT}/M_P$ and denote the up (down)-type doublet inside each H_{10} as $\mathbf{2}_{u(d)}(H_{10}^{u,(d)})$, and similarly for the triplets. Then, the mass matrix for the triplets can be written as

$$M_T \sim \begin{array}{c} \\ \mathbf{3}_d(H_{10}^d) \\ \mathbf{3}_d(H_{10}^u) \\ \mathbf{3}_d(H_{16}) \end{array} \begin{array}{c} \begin{array}{ccc} \mathbf{3}_u(H_{10}^u) & \mathbf{3}_u(H_{10}^d) & \mathbf{3}_u(H_{\overline{16}}) \end{array} \\ \begin{pmatrix} \kappa_1 & 0 & \kappa_4 y \\ 0 & -\kappa_1 & \kappa_3 z \\ \kappa_5 y & \kappa_6 z & \kappa_2 z^2 \end{pmatrix} \end{array} M_{GUT}. \tag{3.27}$$

The mass matrix for the triplets in equation 3.27 has approximate eigenvalues given by

$$m_T \sim \quad \kappa_1 M_{GUT}, \quad \kappa_1 M_{GUT}, \quad \kappa_2 z^2 M_{GUT}, \tag{3.28}$$

such that the triplets are at the GUT scale if one requires $\kappa_1 \sim \kappa_2 z^2 \sim 1$.

The mass matrix for the doublets is given by

$$M_D \sim \begin{array}{c} \\ \mathbf{2}_d(H_{10}^d) \\ \mathbf{2}_d(H_{10}^u) \\ \mathbf{2}_d(H_{16}) \end{array} \begin{array}{c} \begin{array}{ccc} \mathbf{2}_u(H_{10}^u) & \mathbf{2}_u(H_{10}^d) & \mathbf{2}_u(H_{\overline{16}}) \end{array} \\ \begin{pmatrix} -\kappa_7 y^4 & 0 & \kappa_4 y \\ 0 & \kappa_7 y^4 & \kappa_3 z \\ \kappa_5 y & \kappa_6 z & \kappa_2 z^2 \end{pmatrix} \end{array} M_{GUT}, \tag{3.29}$$

with approximate eigenvalues

$$m_D \sim \quad -y^4 M_{GUT}, \quad \kappa_6\kappa_3 z^2 M_{GUT}, \quad \kappa_2 z^2 M_{GUT}. \tag{3.30}$$

In this case, two doublet pairs are at the GUT scale if $\kappa_6\kappa_3 z^2 \sim \kappa_2 z^2 \sim 1$. Furthermore, there is a μ term generated by

$$\mu \sim y^4 M_{GUT} \sim 1 \text{ TeV}, \tag{3.31}$$

which happens at the correct order.

The light MSSM doublets are given by

$$H_u \simeq \mathbf{2}_u(H_{10}^u) + \frac{\kappa_4 y}{\kappa_3 z}\mathbf{2}_u(H_{10}^d), \qquad H_d \simeq \mathbf{2}_d(H_{10}^d) + \frac{\kappa_5 y}{\kappa_6 z}\mathbf{2}_u(H_{10}^d), \tag{3.32}$$

so that the second term is suppressed to be $< 10^{-3}$ and we may safely assume that the MSSM Higgs doublets $H_{u(d)}$ lie only inside $H_{10}^{u(d)}$.

3.1.6 Proton decay

One of the characteristic features of GUTs is the prediction of proton decay. It has not been experimentally observed and the proton lifetime is constrained to be $\tau_p > 10^{34}$ years [31].

Within the model, proton decay can be mediated by the extra gauge bosons of the GUT symmetry and by the triplets accompanying the Higgs doublets. In SUSY $SO(10)$ GUTs, the main source for proton decay comes from the triplet Higgsinos. The decay width is dependent on SUSY breaking and the specific coupling texture of the triplets and determining it exactly lies beyond the scope of this chapter. In general the constraints are barely met when the triplets have a mass at the GUT scale [194–196], and in section 3.1.5 we have shown this is our case.

Furthermore, the existence of additional fields in the model may allow proton decay to arise from effective terms of the type

$$gQQQL\frac{\langle X\rangle}{M_P^2}. \tag{3.33}$$

Such terms must obey the constraint $g\langle X\rangle < 3 \times 10^9$ GeV [196]. In our model, the largest contribution of this type comes from the term

$$\psi\psi\psi\psi\frac{\langle H_{45}^{B-L}(H_{45}^{X,Y})^2\rangle}{M_P^4} \quad \Rightarrow \quad \langle X\rangle = \frac{(M_{\mathrm{GUT}})^3}{M_P^2} \sim 10^{10}\ \mathrm{GeV}. \tag{3.34}$$

The constraints are met when $g < 0.3$. With an $\mathcal{O}(1)$ g parameter, the contributions coming from these terms are the same order as the ones coming from the Higgs triplets. In this model, proton decay complies with experimental constraints but lies fairly close to detection.

3.2 Detailed Yukawa structure

In this section, we introduce the fully detailed Yukawa structure. The complete superfield content of the model is given by the superfields in table 3.1, together with the

messenger superfields in table 3.2. With the symmetries of the model and these superfields, we may write the superpotential relevant to the Yukawa terms, up to $\mathcal{O}(1/M_P)$,

$$W_Y = \sum_{a=1,2,3} \left(\lambda_a^{\phi} (\psi\phi_a)\, \bar{\chi}_a + (\lambda_a^W H_{45}^W + \lambda_a^Z H_{45}^Z)\chi_a\bar{\chi}_a + \lambda_a^u \chi_a\chi_a H_{10}^u + \lambda_a^N \chi_a\chi_a \frac{H_{\overline{16}} H_{\overline{16}}}{M_P} \right) + \sum_{b=2,3} \left(\bar{\chi}_b \chi_b^d (\lambda_b^X H_{45}^X + \lambda_b^Y H_{45}^Y) + \lambda_b^d \chi_b^d \chi_b^d H_{10}^d \right) + \lambda_{12}^d \chi_1\chi_2 H_{10}^d + \lambda_t^d \frac{(\psi\psi)_{3'}\, \phi_3 H_{10}^d}{M_P}, \tag{3.35}$$

where $(\,)$, $(\,)_{3'}$ means an S_4 singlet or $\mathbf{3'}$ contraction respectively. The λ's are dimensionless and real coupling constants, due to CP conservation, and are all expected to be $\mathcal{O}(1)$.

After integrating out the messengers χ, we obtain the superpotential

$$W_Y = \sum_{a=1,2,3} \left(\frac{(\lambda_a^{\phi})^2 (\psi \langle\phi_a\rangle)(\psi \langle\phi_a\rangle)}{(\lambda_a^W \langle H_{45}^W\rangle + \lambda_a^Z \langle H_{45}^Z\rangle)^2} \lambda_a^u H_{10}^u + \frac{(\lambda_a^{\phi})^2 (\psi \langle\phi_a\rangle)(\psi \langle\phi_a\rangle)}{(\lambda_a^W \langle H_{45}^W\rangle + \lambda_a^Z \langle H_{45}^Z\rangle)^2} \frac{\lambda_a^N}{M_P} \langle H_{\overline{16}}\rangle \langle H_{\overline{16}}\rangle \right) + \left(\sum_{b=2,3} \lambda_b^d \frac{(\lambda_b^{\phi})^2 (\psi \langle\phi_b\rangle)(\psi \langle\phi_b\rangle)}{(\lambda_b^X \langle H_{45}^X\rangle + \lambda_b^Y \langle H_{45}^Y\rangle)^2} + \lambda_{12}^d \frac{\lambda_1^{\phi}\lambda_2^{\phi} (\psi \langle\phi_1\rangle)(\psi \langle\phi_2\rangle)}{(\lambda_1^W \langle H_{45}^W\rangle + \lambda_1^Z \langle H_{45}^Z\rangle)(\lambda_2^W \langle H_{45}^W\rangle + \lambda_2^Z \langle H_{45}^Z\rangle)} + \lambda_t^d \frac{(\psi\psi)_{3'} \langle\phi_3\rangle}{M_P} \right) H_{10}^d, \tag{3.36}$$

that generates all the Standard Model fermion masses. The structure of the mass matrices is dictated by the flavon alignments in equation 3.1. Furthermore, the adjoints **45** provide the necessary CG coefficients to distinguish between each fermion type and give the correct masses to Standard Model fermions, as we show in section 3.2.2.

3.2.1 Renormalisability of the third family

In equation 3.36, all the terms suppressed by $\langle H_{45}^{X,Y,W,Z}\rangle$ involve integrating out the messengers by assuming $M_{GUT} \gg v_i$. This naive integration is not possible for the third flavon since it has a much larger VEV $v_3 \sim M_{GUT}$. Let us single out the terms in W_Y involving these fields. Ignoring $\mathcal{O}(1)$ couplings, and after the fields get their VEV, the relevant terms are

$$W_Y^{(3)} \sim v_3 \psi_3 \bar{\chi}_3 + \langle H_{45}^{W,Z}\rangle\, \chi_3 \bar{\chi}_3. \tag{3.37}$$

Naively, one would interpret ψ_3 as the set of third-family particles, but the first term in equation 3.37 generates mixing with $\bar{\chi}_3$. To obtain the physical (massless) states, which we label t, we rotate into a physical basis $(\psi_3, \chi_3) \to (t, \chi)$

$$\psi_3 = \frac{\langle H_{45}^{W,Z}\rangle\, t + v_3\, \chi}{r}, \quad \chi_3 = \frac{-v_3\, t + \langle H_{45}^{W,Z}\rangle\, \chi}{r}; \quad r = \sqrt{v_3^2 + \langle H_{45}^{W,Z}\rangle^2}. \tag{3.38}$$

Physically, it may be interpreted as follows: inside the original superpotential W_Y lie the terms

$$\mathcal{W}_Y \supset \chi_3 \chi_3 H^u_{10} \supset \frac{v_3^2}{v_3^2 + \langle H_{45}^{W,Z} \rangle^2}\, t\, t\, H^u_{10}, \tag{3.39}$$

which generate renormalisable mass terms for the third family at the electroweak scale.

3.2.2 Mass matrix structure

The superpotential in equation 3.36 generates all the Standard Model fermion mass matrices. The structure of the mass matrices is fixed by the flavon VEV structure shown in equation 3.1. We may redefine the dimensionless couplings to obtain the mass structure of the Standard Model fermions at low energies

$$\begin{aligned}
y^u_a &= \lambda^u_a \frac{(\lambda^\phi_a)^2 |v_a|^2}{[\lambda^W_a \langle H^W_{45} \rangle + \lambda^Z_a \langle H^Z_{45} \rangle]_Q [\lambda^W_a \langle H^W_{45} \rangle + \lambda^Z_a \langle H^Z_{45} \rangle]_{u^c}}, \\
y^u_3 &= \frac{(\lambda^\phi_3)^2 |v_3|^2}{(\lambda^\phi_3)^2 v_3^2 + [\lambda^W_3 \langle H^W_{45} \rangle + \lambda^Z_3 \langle H^Z_{45} \rangle]_Q [\lambda^W_3 \langle H^W_{45} \rangle + \lambda^Z_3 \langle H^Z_{45} \rangle]_{u^c}}, \\
y^\nu_a &= \lambda^u_a \frac{(\lambda^\phi_a)^2 |v_a|^2}{[\lambda^W_a \langle H^W_{45} \rangle + \lambda^Z_a \langle H^Z_{45} \rangle]_L [\lambda^W_a \langle H^W_{45} \rangle + \lambda^Z_a \langle H^Z_{45} \rangle]_{\nu^c}}, \\
y^\nu_3 &= \frac{(\lambda^\phi_3)^2 |v_3|^2}{(\lambda^\phi_3)^2 v_3^2 + (\lambda^\chi_3)^2 [\lambda^W_3 \langle H^W_{45} \rangle + \lambda^Z_3 \langle H^Z_{45} \rangle]_L [\lambda^W_3 \langle H^W_{45} \rangle + \lambda^Z_3 \langle H^Z_{45} \rangle]_{\nu^c}}, \\
y^e_2 &= \lambda^d_2 \frac{(\lambda^\phi_2)^2 |v_2|^2}{[\lambda^X_2 \langle H^X_{45} \rangle + \lambda^Y_2 \langle H^Y_{45} \rangle]_L [\lambda^X_2 \langle H^X_{45} \rangle + \lambda^Y_2 \langle H^Y_{45} \rangle]_{e^c}}, \\
y^e_3 &= \lambda^d_3 \frac{(\lambda^\phi_3)^2 |v_3|^2}{(\lambda^\phi_3)^2 v_3^2 + [\lambda^X_3 \langle H^X_{45} \rangle + \lambda^Y_3 \langle H^Y_{45} \rangle]_L [\lambda^X_3 \langle H^X_{45} \rangle + \lambda^Y_3 \langle H^Y_{45} \rangle]_{e^c}}, \\
y^d_2 &= \lambda^d_2 \frac{(\lambda^\phi_2)^2 |v_2|^2}{[\lambda^X_2 \langle H^X_{45} \rangle + \lambda^Y_2 \langle H^Y_{45} \rangle]_Q [\lambda^X_2 \langle H^X_{45} \rangle + \lambda^Y_2 \langle H^Y_{45} \rangle]_{d^c}}, \\
y^d_3 &= \lambda^d_3 \frac{(\lambda^\phi_3)^2 |v_3|^2}{(\lambda^\phi_3)^2 v_3^2 + [\lambda^X_3 \langle H^X_{45} \rangle + \lambda^Y_3 \langle H^Y_{45} \rangle]_Q [\lambda^X_3 \langle H^X_{45} \rangle + \lambda^Y_3 \langle H^Y_{45} \rangle]_{d^c}}, \\
y^e_{12} &= \lambda^d_{12} \frac{\lambda^\phi_1 \lambda^\phi_2 |v_1 v_2|}{[\lambda^W_1 \langle H^W_{45} \rangle + \lambda^Z_1 \langle H^Z_{45} \rangle]_{L+e^c} [\lambda^W_2 \langle H^W_{45} \rangle + \lambda^Z_2 \langle H^Z_{45} \rangle]_{L+e^c}}, \\
y^d_{12} &= \lambda^d_{12} \frac{\lambda^\phi_1 \lambda^\phi_2 |v_1 v_2|}{[\lambda^W_1 \langle H^W_{45} \rangle + \lambda^Z_1 \langle H^Z_{45} \rangle]_{Q+d^c} [\lambda^W_2 \langle H^W_{45} \rangle + \lambda^Z_2 \langle H^Z_{45} \rangle]_{Q+d^c}}, \\
M^{\mathrm{R}}_a &= \frac{\lambda^N_a v_{\overline{16}}^2}{M_P} \frac{(\lambda^\phi_a)^2 |v_a|^2}{[\lambda^W_a \langle H^W_{45} \rangle + \lambda^Z_a \langle H^Z_{45} \rangle]^2_{\nu^c}}, \\
M^{\mathrm{R}}_3 &= \frac{\lambda^N_3 v_{\overline{16}}^2}{M_P} \frac{(\lambda^\phi_3)^2 |v_3|^2}{(\lambda^\phi_3)^2 v_3^2 + [\lambda^W_3 \langle H^W_{45} \rangle + \lambda^Z_3 \langle H^Z_{45} \rangle]^2_{\nu^c}}, \\
y^P &= \lambda^d_t \frac{v_3}{M_P},
\end{aligned} \tag{3.40}$$

where $a = 1, 2$ and $\langle H_{45}^{X,Y,W,Z} \rangle_f$ denotes the adjoint VEV with the corresponding CG coefficients for each Standard Model fermion f. This allows for each y, M parameter in equation 3.40 to be independent. The VEVs $\langle H^{X,Y} \rangle$ obtain a VEV in an arbitrary $SO(10)$ breaking direction and they need to be different from one another.

For a better understanding we show an explicit example. Let us assume that $\langle H_{45}^{X,Y} \rangle$ is aligned in the $U(1)_{X,Y}$ direction respectively with an M_{GUT} magnitude. In this case, the effective Yukawa couplings $y_2^{e,d}$ would be

$$y_2^e = \lambda_2^d \frac{(\lambda_2^\phi)^2 |v_2|^2}{[3\lambda_2^X - \lambda_2^Y/2][-\lambda_2^X + \lambda_2^Y] M_{GUT}^2}, \quad y_2^d = \lambda_2^d \frac{(\lambda_2^\phi)^2 |v_2|^2}{[-\lambda_2^X + \lambda_2^Y/6][3\lambda_2^X + \lambda_2^Y/3] M_{GUT}^2}, \tag{3.41}$$

where the coefficients multiplying each $\lambda^{X,Y}$ are the $U(1)_{X,Y}$ charges of the corresponding Standard Model field. Since the $\lambda_2^{X,Y}$ appear with different coefficients in $y_2^{e,d}$, we can use them to obtain a arbitrarily different effective Yukawa coupling for charged leptons and down type quarks.

Assuming that all the adjoints have real VEVs, the physical phases are

$$\begin{aligned} \eta &= 2 \arg v_1 - 2 \arg v_2 \\ \eta' &= 2 \arg v_3 - 2 \arg v_2 \\ \gamma &= \arg v_3 - 2 \arg v_2, \end{aligned} \tag{3.42}$$

while all the $y's$ and $M's$ are real.

With these definitions we may write the fermion mass matrices

$$\begin{aligned}
M^e/v_d &= y_{12}^e e^{i\eta/2} \begin{pmatrix} 0 & 1 & 1 \\ 1 & 4 & 2 \\ 1 & 2 & 0 \end{pmatrix} + y_2^e \begin{pmatrix} 0 & 0 & 0 \\ 0 & 1 & 1 \\ 0 & 1 & 1 \end{pmatrix} + y_3^e e^{i\eta'} \begin{pmatrix} 0 & 0 & 0 \\ 0 & 0 & 0 \\ 0 & 0 & 1 \end{pmatrix} + y^P e^{i\gamma} \begin{pmatrix} 0 & 0 & 1 \\ 0 & 2 & 0 \\ 1 & 0 & 0 \end{pmatrix}, \\
M^d/v_d &= y_{12}^d e^{i\eta/2} \begin{pmatrix} 0 & 1 & 1 \\ 1 & 4 & 2 \\ 1 & 2 & 0 \end{pmatrix} + y_2^d \begin{pmatrix} 0 & 0 & 0 \\ 0 & 1 & 1 \\ 0 & 1 & 1 \end{pmatrix} + y_3^d e^{i\eta'} \begin{pmatrix} 0 & 0 & 0 \\ 0 & 0 & 0 \\ 0 & 0 & 1 \end{pmatrix} + y^P e^{i\gamma} \begin{pmatrix} 0 & 0 & 1 \\ 0 & 2 & 0 \\ 1 & 0 & 0 \end{pmatrix}, \\
M^u/v_u &= y_1^u e^{i\eta} \begin{pmatrix} 1 & 2 & 0 \\ 2 & 4 & 0 \\ 0 & 0 & 0 \end{pmatrix} + y_2^u \begin{pmatrix} 0 & 0 & 0 \\ 0 & 1 & 1 \\ 0 & 1 & 1 \end{pmatrix} + y_3^u e^{i\eta'} \begin{pmatrix} 0 & 0 & 0 \\ 0 & 0 & 0 \\ 0 & 0 & 1 \end{pmatrix}, \\
M_D/v_u &= y_1^\nu e^{i\eta} \begin{pmatrix} 1 & 2 & 0 \\ 2 & 4 & 0 \\ 0 & 0 & 0 \end{pmatrix} + y_2^\nu \begin{pmatrix} 0 & 0 & 0 \\ 0 & 1 & 1 \\ 0 & 1 & 1 \end{pmatrix} + y_3^\nu e^{i\eta'} \begin{pmatrix} 0 & 0 & 0 \\ 0 & 0 & 0 \\ 0 & 0 & 1 \end{pmatrix}, \\
M_R &= M_1^R e^{i\eta} \begin{pmatrix} 1 & 2 & 0 \\ 2 & 4 & 0 \\ 0 & 0 & 0 \end{pmatrix} + M_2^R \begin{pmatrix} 0 & 0 & 0 \\ 0 & 1 & 1 \\ 0 & 1 & 1 \end{pmatrix} + M_3^R e^{i\eta'} \begin{pmatrix} 0 & 0 & 0 \\ 0 & 0 & 0 \\ 0 & 0 & 1 \end{pmatrix}.
\end{aligned} \tag{3.43}$$

We note the remarkable universal structure of the matrices in the up and neutrino sectors, which differ from the down and charged lepton sectors.

The y and M parameters are all free and independent while there is a constraint in the phases

$$\eta \simeq 4\eta' - 2\gamma, \tag{3.44}$$

as shown in section 3.1.4. We have in total 18 free parameters that fix the whole spectrum of fermion masses and mixing angles, as discussed in section 3.3.1.

In section 3.1.4, it is shown that the flavons get a VEV $v_1 \simeq 0.001 M_{GUT}$, $v_2 \simeq 0.1\ M_{GUT}$, and $v_3 \simeq M_{GUT}$, while the adjoint **45** fields and $\overline{\mathbf{16}}$ are assumed to get a GUT scale VEV, i.e. $v_{45}^{X,Y,W,Z} \simeq v_{\overline{16}} \simeq M_{GUT}$. We assume that all the dimensionless parameters in the superpotential are $\mathcal{O}(1)$, and using $\tan\beta \sim 20$, the mass matrix parameters are expected to be

$$\begin{aligned}
y_1^u \sim y_1^\nu \sim v_1^2/v_{45}^2 \sim 10^{-6}, \quad & y_2^u \sim y_2^\nu \sim v_2^2/v_{45}^2 \sim 10^{-2}, \\
y_3^u \sim y_3^\nu \sim v_3^2/v_{45}^2 \sim 1, \quad & y_{12}^d \sim y_{12}^e \sim \cos\beta\ v_1 v_2/v_{45}^2 \sim 10^{-5}, \\
y_2^d \sim y_2^e \sim \cos\beta\ v_2^2/v_{45}^2 \sim 10^{-3}, \quad & y_3^d \sim y_3^e \sim \cos\beta\ v_3^2/v_{45}^2 \sim 0.1, \\
y^P \sim \cos\beta\ v_3/M_P \sim 10^{-4}, \quad & M_1^R \sim v_{\overline{16}}^2 v_1^2/v_{45}^2 M_P \sim 10^7\ GeV, \\
M_2^R \sim v_{\overline{16}}^2 v_2^2/v_{45}^2 M_P \sim 10^{11}\ GeV, \quad & M_3^R \sim v_{\overline{16}}^2 v_3^2/v_{45}^2 M_P \sim 10^{13}\ GeV.
\end{aligned} \tag{3.45}$$

These values denote only an approximate order of magnitude for each parameter and are expected to be different due to the appearance of dimensionless couplings. This applies specially to the last 4 parameters that come from unknown Planck suppressed physics and may deviate significantly from our naive expectation.

3.2.3 Seesaw mechanism

Since we have heavy right-handed neutrino Majorana masses, the left handed neutrinos get a small Majorana mass through the type-I seesaw

$$m_\nu = -M_D M_R^{-1} (M_D)^T. \tag{3.46}$$

As we see in equation 3.43, the Dirac neutrino masses M_D and the right-handed neutrino Majorana masses M_R have the same matrix structure. These are rank one matrices so that we may write them as

$$\begin{aligned}
M_D/v_u &= y_1^\nu e^{i\eta}\ \varphi_1\varphi_1^T + y_2^\nu\ \varphi_2\varphi_2^T + y_3^\nu e^{i\eta'}\ \varphi_3\varphi_3^T, \\
M_R &= M_1^R e^{i\eta}\ \varphi_1\varphi_1^T + M_2^R\ \varphi_2\varphi_2^T + M_3^R e^{i\eta'}\ \varphi_3\varphi_3^T,
\end{aligned} \tag{3.47}$$

with

$$\varphi_1^T = (1,2,0), \quad \varphi_2^T = (0,1,1), \quad \varphi_3^T = (0,0,1). \tag{3.48}$$

We may always find vectors $\tilde{\varphi}_a$ such that

$$\tilde{\varphi}_i^T \varphi_j = \delta_{ij}, \tag{3.49}$$

this way we may write the inverse matrix as

$$M_R^{-1} = \frac{e^{-i\eta}}{M_1^R}\tilde{\varphi}_1\tilde{\varphi}_1^T + \frac{1}{M_2^R}\tilde{\varphi}_2\tilde{\varphi}_2^T + \frac{e^{-i\eta'}}{M_3^R}\tilde{\varphi}_3\tilde{\varphi}_3^T. \tag{3.50}$$

Plugging this into the seesaw mechanism 3.46, we obtain the light effective left-handed Majorana neutrino mass matrix m_ν as

$$m_\nu = \mu_1 e^{i\eta}\ \varphi_1\varphi_1^T + \mu_2\ \varphi_2\varphi_2^T + \mu_3 e^{i\eta'}\ \varphi_3\varphi_3^T, \quad \text{with} \quad \mu_a = \frac{(y_a^\nu v_u)^2}{M_a^R}. \tag{3.51}$$

We may conclude that the small left-handed neutrino mass matrix has the same universal structure

$$m_\nu = \mu_1 e^{i\eta}\begin{pmatrix} 1 & 2 & 0 \\ 2 & 4 & 0 \\ 0 & 0 & 0 \end{pmatrix} + \mu_2\begin{pmatrix} 0 & 0 & 0 \\ 0 & 1 & 1 \\ 0 & 1 & 1 \end{pmatrix} + \mu_3 e^{i\eta'}\begin{pmatrix} 0 & 0 & 0 \\ 0 & 0 & 0 \\ 0 & 0 & 1 \end{pmatrix}, \tag{3.52}$$

after the seesaw mechanism.

3.3 Numerical fit

To test our model we perform a numerical fit using a χ^2 test function. We have a set of input parameters $x = \{y_i^u, y_i^d, y_i^e, y^P, \mu_i, \eta', \gamma\}$, from which we obtain a set of observables $P_n(x)$. We minimize the function defined as

$$\chi^2 = \sum_n \left(\frac{P_n(x) - P_n^{\text{obs}}}{\sigma_n}\right)^2, \tag{3.53}$$

where the 19 observables are given by $P_n^{\text{obs}} \in \{\theta_{ij}^q, \delta^q, y_{u,c,t}, y_{d,s,b}, \theta_{ij}^\ell, \delta^l, y_{e,\mu,\tau}, \Delta m_{ij}^2\}$ with statistical errors σ_n. This test assumes data is normally (Gaussian) distributed, which is true for most of the observables except for θ_{23}^ℓ. The atmospheric mixing angle octant, i.e. $\theta_{23}^\ell < 45^\circ$ or $\theta_{23}^\ell > 45^\circ$, has not been determined yet. Current data favours $\theta_{23}^\ell = 41.6$ from Nufit 3.0 [200] and we assume such scenario.

We need to run up all the measured Yukawa couplings and mixing angles up to the GUT scale in order to compare it with the predictions of our model.[2] In doing so, we need to match the SM to the MSSM at the SUSY scale, M_{SUSY}, which involves adding the

[2] Note that we are performing the numerical fit in terms of the effective neutrino mass parameters μ_i defined in equation 3.52. We are ignoring any renormalisation group running corrections in the neutrino sector.

Observable	Data		Model
	Central value	1σ range	Best fit
θ_{12}^{ℓ} /°	33.57	$32.81 \to 34.33$	33.53
θ_{13}^{ℓ} /°	8.460	$8.310 \to 8.610$	8.452
θ_{23}^{ℓ} /°	41.75	$40.40 \to 43.10$	41.88
δ^{ℓ} /°	261.0	$206.0 \to 316.0$	200.3
y_e /10^{-5}	6.023	$5.987 \to 6.059$	6.023
y_μ /10^{-2}	1.272	$1.264 \to 1.280$	1.272
y_τ	0.222	$0.219 \to 0.225$	0.222
$\Delta m_{21}^2/(10^{-5}\,\mathrm{eV}^2)$	7.510	$7.330 \to 7.690$	7.507
$\Delta m_{31}^2/(10^{-3}\,\mathrm{eV}^2)$	2.524	$2.484 \to 2.564$	2.524
m_1 /meV			10.94
m_2 /meV			13.95
m_3 /meV			51.42
$\sum m_i$ /meV		< 230	76.31
α_{21} /°			134.3
α_{31} /°			6.415
$m_{\beta\beta}$ /meV		$< 61\text{-}165$	11.10

Table 3.3: Model predictions in the lepton sector for $\tan\beta = 20$, $M_{\mathrm{SUSY}} = 1$ TeV and $\bar{\eta}_b = -0.9$. The observables are at the GUT scale. The lepton contribution to the total χ^2 is 1.2. The neutrino masses m_i as well as the Majorana phases are pure predictions of our model. The bound on $\sum m_i$ is taken from[59]. The bound on $m_{\beta\beta}$ is taken from [61].

supersymmetric radiative threshold corrections. This has been done in [199]. At the GUT scale, the values depend to a good approximation only on $\bar{\eta}_b$ and $\tan\beta$. A good fit is found for large $\bar{\eta}_b$, which can be explained if $\tan\beta \gtrsim 5$, as shown in appendix B. We also need $\tan\beta < 30$ to keep Yukawa couplings perturbative. The best fit is found for $\bar{\eta}_b = -0.9$ and $\tan\beta = 20$. The SUSY scale does not affect the fit and we choose $M_{SUSY} = 1$ TeV. The fit has been performed using the Mixing Parameter Tools (MPT) package [203].

The best fit found has a $\chi^2 = 11.9$. Table 2.3 shows the best fit to the charged leptons and neutrinos observables. Neutrino data is taken from the Nufit 3.0 global fit [200]. Only the neutrino mass-squared differences are known but the model also predicts the neutrino masses themselves as well as the Majorana phases. The model predicts normal ordered neutrino masses and we also give the effective Majorana mass $m_{\beta\beta}$. All the lepton sector is fitted to within 1σ except for the leptonic CP phase. δ^{ℓ} is not yet well measured, although a negative CP phase is preferred [204].

In table 2.4, we have all the quark Yukawa couplings and mixing parameters for the minimum χ^2. The biggest contribution to the χ^2 is coming from this sector, as shown in figure. 3.4. This figure shows the corresponding pulls for lepton (light orange) and quark (blue) observables. As we can see, all parameters lie inside the 2σ region and the biggest pulls are in the quark Yukawa couplings.

Table 2.5 shows the input parameter values.[3] There are 13 real parameters plus two

[3] Assuming the Dirac neutrino Yukawa parameters y_i^{ν} in equation 3.45, we can compute the right-

Observable	Data		Model
	Central value	1σ range	Best fit
θ_{12}^q /°	13.03	$12.99 \to 13.07$	13.02
θ_{13}^q /°	0.016	$0.016 \to 0.017$	0.016
θ_{23}^q /°	0.189	$0.186 \to 0.192$	0.186
δ^q /°	69.22	$66.12 \to 72.31$	70.66
y_u /10^{-6}	3.060	$2.111 \to 4.009$	3.253
y_c /10^{-3}	1.497	$1.444 \to 1.549$	1.567
y_t	0.666	$0.637 \to 0.694$	0.611
y_d /10^{-4}	1.473	$1.311 \to 1.635$	1.614
y_s /10^{-3}	2.918	$2.760 \to 3.075$	3.098
y_b	2.363	$2.268 \to 2.457$	2.238

Table 3.4: Model predictions in the quark sector for $\tan\beta = 20$, $M_{\rm SUSY} = 1$ TeV and $\bar{\eta}_b = -0.9$. The observables are at the GUT scale. The quark contribution to the total χ^2 is 10.7.

additional phases, a total of 15 input parameters to fit 19 data points, which remarks the predictivity of the model, not only fitting to all available quark and lepton data but also fixing the neutrino masses and Majorana phases.

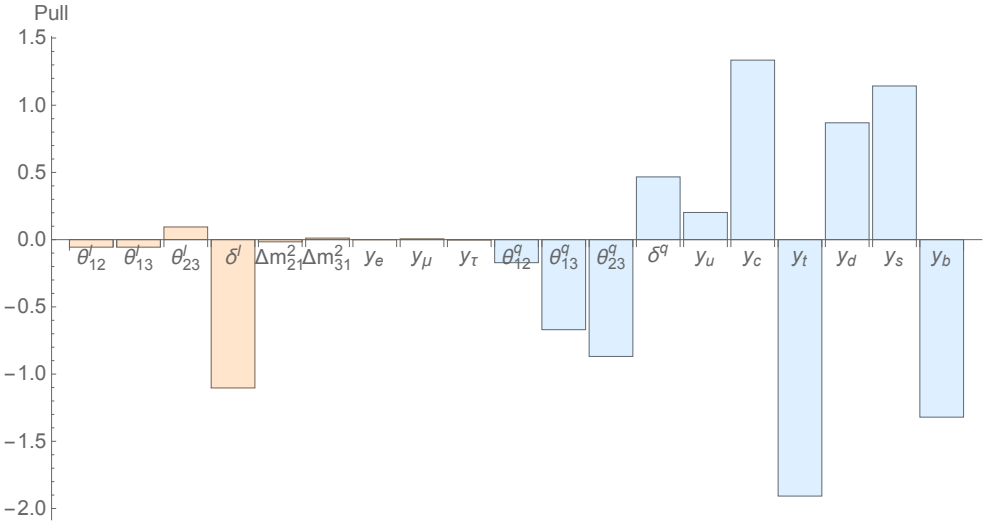

Figure 3.4: Pulls for the best fit of model to data, as shown in Tables 3.3-3.4, for lepton (light orange) and quark (blue) parameters.

3.3.1 Parameter counting

In this section we explain and clarify the number of parameters in our model. Clearly at the high energy scale there are many parameters associated with the undetermined $\mathcal{O}(1)$ Yukawa couplings of the 43 superfields of the model. For example the renormalisable Yukawa superpotential in equation 3.35 contains 23 parameters alone. Then we must

handed neutrino masses, using the seesaw formula in equation 3.51 and taking the μ_i values from the fit, such that $M_1^R \sim 10^4$ GeV, $M_2^R \sim 10^{11}$ GeV and $M_3^R \sim 10^{15}$ GeV. Only M_2 has the expected natural value given in equation 3.45. We remark that right-handed neutrino Majorana masses come from unknown Planck suppressed physics, which is presumably responsible for the mismatch.

Parameter	Value
$y_1^u\,/10^{-6}$	3.232
$y_2^u\,/10^{-3}$	1.580
y_3^u	-0.610
$y_{12}^d\,/10^{-4}$	-7.068
$y_2^d\,/10^{-4}$	-8.737
y_3^d	-2.238

Parameter	Value
$y_{12}^e\,/10^{-4}$	8.616
$y_2^e\,/10^{-2}$	1.013
y_3^e	0.229
μ_1 /meV	6.845
μ_2 /meV	27.18
μ_3 /meV	42.17

Parameter	Value
$y^P\,/10^{-4}$	2.475
γ	1.968π
η'	0.790π

Table 3.5: Best fit input parameter values. The model has 13 real parameters: y_i^u, y_i^d, y_i^e, μ_i and y^P and two additional free phases: η' and γ. The total χ^2 is 11.9.

add to this all the $\mathcal{O}(1)$ Yukawa couplings associated with vacuum alignment, GUT symmetry breaking and doublet-triplet splitting, many of which we have not defined explicitly. Despite this, we are claiming that our model is predictive at low energies. How can this be? The short answer is that most of these parameters are irrelevant for physics below the GUT scale, as discussed in detail below.

The effective fermion mass matrices generated below the GUT scale are given in equation 3.43 as function of 18 free effective parameters (remembering the constraint on η) that will fix all the fermion masses and mixing angles, including right-handed neutrino Majorana masses and Majorana phases. This compares favourably to the 31 parameters of a general high energy model, comprising 21 parameters in the lepton sector of a general three right-handed neutrinos seesaw model [205], plus the 6 quark masses and 4 CKM parameters. However, below the seesaw scale of right-handed neutrino masses, the effective parameter counting is different again and requires further discussion below.

In order to perform the fit and compare our model with available data, we apply the seesaw mechanism to write the light effective left-handed Majorana neutrino mass matrix as a function of the new parameters μ_i in equation 3.51. Therefore, we have 15 effective parameters at low energy (shown in table 3.5) that fit the 19 so far measured or constrained observables in figure 3.4.[4] After the fit is performed, the model predicts all the three light neutrino masses with a normal ordering, a CP oscillation phase of 200° and both the Majorana phases, corresponding to a total of 22 low energy observables which will be eventually observable (10 from the quark sector discussed above and 12 from the lepton sector, including the two Majorana phases). Therefore we see that, below the seesaw scales, the model contains 15 effective parameters which generate 22 observables, making the model eminently testable, as these observables become better determined.

[4] We need to run up to the GUT scale these observables and, therefore, we need to include SUSY threshold corrections. The fit is therefore also dependent on $\bar{\eta}_b$ and $\tan\beta$. As shown earlier, we find a good fit for $\bar{\eta}_b = -0.9$ and $\tan\beta = 20$.

3.4 N_2 leptogenesis

The source of the Baryon Asymmetry of the Universe (BAU)

$$\eta_B = (6.1 \pm 0.1) \times 10^{-10}, \tag{3.54}$$

remains unexplained in the Standard Model. One of the most convincing sources for it is leptogenesis, where the asymmetry is generated through CP breaking decays of heavy right-handed neutrinos into leptons, then converted into baryons through sphalerons.

The simplest mechanism to generate the correct BAU, happens when the lightest right-handed neutrino has CP breaking decays and a mass of about $\sim 10^{10}$ GeV. In our model, according to equation 3.45, it is the second right-handed neutrino the one that is expected to be at that scale. When leptogenesis is generated mainly by the decays of the second right-handed neutrino, it is called N_2 leptogenesis. This has already been calculated in [206] and we will apply such calculations to our specific model.

3.4.1 General N_2 leptogenesis

Leptogenesis calculations are done in the so called flavour basis, where the charged lepton and right-handed neutrino mass matrices are both diagonal. In this basis, the Dirac neutrino mass matrix is given by

$$\begin{gathered} m_D = V_{eL} M_D U_N^T, \text{ where} \\ V_{eL} M^{e\dagger} M^e V_{eL}^\dagger = diag(y_e^2, y_\mu^2, y_\tau^2) v_d^2, \qquad U_N M_R U_N^T = diag(M_1, M_2, M_3). \end{gathered} \tag{3.55}$$

The final asymmetry can be computed using simple approximate analytic equations derived in [206]. The total and flavoured decay parameters, K_i and $K_{i\alpha}$ respectively, can be written as

$$K_{i\alpha} = \frac{|m_{D\alpha i}|^2}{m_\star^{MSSM} M_i} \quad \text{and} \quad K_i = \sum_\alpha K_{i\alpha} = \frac{(m_D^\dagger m_D)_{ii}}{m_\star^{MSSM} M_i}, \tag{3.56}$$

where the equilibrium neutrino mass is given by

$$m_\star^{MSSM} \simeq 0.78 \times 10^{-3}\,\text{eV}\, \sin^2\beta. \tag{3.57}$$

The wash-out at the production is described by the efficiency factor $\kappa(K_{2\alpha})$ that for an initial thermal N_2 abundance can be calculated as

$$\kappa(K_{2\alpha}) = \frac{2}{z_B(K_{2\alpha})\, K_{2\alpha}} \left(1 - e^{-\frac{K_{2\alpha}\, z_B(K_{2\alpha})}{2}}\right), \quad z_B(K_{2\alpha}) \simeq 2 + 4\, K_{2\alpha}^{0.13}\, e^{-\frac{2.5}{K_{2\alpha}}}. \tag{3.58}$$

In the hierarchical right-handed neutrino mass limit, as our model is, the CP asymme-

tries can be approximated to

$$\varepsilon_2 = \sum_\alpha \varepsilon_{2\alpha}, \quad \varepsilon_{2\alpha} \simeq \frac{3}{8\,\pi}\frac{M_2}{v^2}\frac{\mathrm{Im}\Big[\big(m_D^\dagger\big)_{i\alpha}\big(m_D\big)_{\alpha 3}\big(m_D^\dagger m_D\big)_{i3}\Big]}{M_2\,M_3\,\widetilde{m}_2}, \tag{3.59}$$

where $\widetilde{m}_2 \equiv (m_D^\dagger\, m_D)_{22}/M_2$.

In the regime where $5\times 10^{11}\,\mathrm{GeV}\,(1+\tan^2\beta) \gg M_2 \gg 5\times 10^{8}\,\mathrm{GeV}\,(1+\tan^2\beta)$, the final $B-L$ asymmetry can be calculated using

$$\begin{aligned} N^{\mathrm{f}}_{B-L} \;\simeq\; & \left[\frac{K_{2e}}{K_{2\tau_2^\perp}}\,\varepsilon_{2\tau_2^\perp}\kappa(K_{2\tau_2^\perp}) + \left(\varepsilon_{2e} - \frac{K_{2e}}{K_{2\tau_2^\perp}}\,\varepsilon_{2\tau_2^\perp}\right)\kappa(K_{2\tau_2^\perp}/2)\right] e^{-\frac{3\pi}{8}K_{1e}} + \\ + \; & \left[\frac{K_{2\mu}}{K_{2\tau_2^\perp}}\,\varepsilon_{2\tau_2^\perp}\,\kappa(K_{2\tau_2^\perp}) + \left(\varepsilon_{2\mu} - \frac{K_{2\mu}}{K_{2\tau_2^\perp}}\,\varepsilon_{2\tau_2^\perp}\right)\kappa(K_{2\tau_2^\perp}/2)\right] e^{-\frac{3\pi}{8}K_{1\mu}} + \\ + \; & \varepsilon_{2\tau}\,\kappa(K_{2\tau})\,e^{-\frac{3\pi}{8}K_{1\tau}}\,, \end{aligned} \tag{3.60}$$

where we indicated with $\tau_2^\perp$ the electron plus muon component of the quantum flavour states produced by the N_2-decays defining $K_{2\tau_2^\perp} \equiv K_{2e} + K_{2\mu}$ and $\varepsilon_{2\tau_2^\perp} \equiv \varepsilon_{2e} + \varepsilon_{2\mu}$. The final asymmetry, in terms of the baryon to photon number ratio is

$$\eta_B \simeq 2\; a_{sph}\frac{N_{B-L}}{N_\gamma^{rec}}, \tag{3.61}$$

where $\alpha_{sph} = 8/23$ is the fraction of $B-L$ asymmetry converted into baryon asymmetry by sphalerons. The photon asymmetry at recombination is $(N_\gamma^{rec})^{MSSM} \simeq 78$. The factor of 2 accounts for the asymmetry generated by the right-handed neutrinos plus the superpartners sneutrinos.

3.4.2 Leptogenesis in our model

Using the matrices in equation 3.43 and the fit in table 3.5, we may calculate the BAU generated through N_2 leptogenesis in our model. The first thing to note is that the parameters are quite hierarchical so that the rotation angles of the diagonalizing matrices can be neglected since they only give 1% contributions

$$V_{eL} \simeq \mathbb{1}, \qquad U_N \simeq diag(e^{-i\eta/2}, 0, e^{-i\eta'/2}), \tag{3.62}$$

and the neutrino mass matrix in the flavour basis becomes

$$m_{Dij} \simeq \begin{pmatrix} y_1^\nu e^{i\eta/2} & 2y_1^\nu e^{i\eta} & 0 \\ 2\; y_1^\nu e^{i\eta/2} & y_2^\nu & y_2^\nu e^{-i\eta'/2} \\ 0 & y_2^\nu & y_3^\nu e^{i\eta'/2} \end{pmatrix} v_u. \tag{3.63}$$

Also, due to the hierarchical nature of the couplings we may safely assume that the right-handed neutrino mass parameters are equal to their mass eigenvalues, i.e. $M_a^R \simeq M_a$.

One of the features of the matrix structure in equation 3.63 is an approximate zero in the (3,1) entry of the Dirac mass matrix, meaning that the wash-out due to τ's decaying into the first right-handed neutrino N_1 is suppressed. In terms of decaying parameters, it implies that $K_{1\tau}$ vanishes and the last term in equation 3.60 is greatly enhanced since it overcomes the exponential suppression. The zero in the Dirac mass matrix 3.63 is a consequence of the CSD2 vacuum alignments; it would not be zero for CSD3 vacuum alignments and this is why leptogenesis is not possible within the model introduced in chapter 2. With these approximations, the baryon asymmetry becomes

$$\begin{gathered} \eta_B \simeq \frac{2\alpha_{sph}}{N_\gamma^{rec}}\,\kappa(K_{2\tau})\,\varepsilon_{2\tau}, \text{ where} \\ K_{2\tau} = \frac{(y_2^\nu)^2 v_u^2}{m_\star^{MSSM} M_2} \quad \text{and} \quad \epsilon_{2\tau} = \sin\eta' \frac{3}{8\pi}\frac{M_2}{M_3}\frac{(y_3^\nu)^2}{2}\sin^2\beta. \end{gathered} \tag{3.64}$$

We note that η' is identified with the leptogenesis phase. Using equation 3.51, we may write the neutrino Yukawa couplings as $y_a^\nu = \sqrt{\mu_a M_a^R}/v_u$ so that

$$\eta_B \simeq \sin\eta' \frac{3}{8\pi}\frac{\alpha_{sph}}{N_\gamma^{rec}}\,\kappa\left(\frac{\mu_2}{m_\star^{MSSM}}\right)\frac{\mu_3 M_2}{v^2}, \tag{3.65}$$

where we note that the only free parameter is M_2. Using the parameters from the fit, in table 3.5, the correct BAU is generated when[5]

$$M_2 \simeq 1.9 \times 10^{11}\ GeV. \tag{3.66}$$

From equation 3.45 we see that this is the natural value for the second right-handed neutrino mass, so that the model naturally explains the origin of the BAU through N_2 leptogenesis without any need for tuning.

3.5 Summary

We have constructed a SUSY GUT of flavour based on the symmetry $S_4 \times SO(10) \times \mathbb{Z}_4^3 \times \mathbb{Z}_4^R$ that is relatively simple, predictive and fairly complete. The Higgs sector of the model involves two $SO(10)$ **10**-plets, a **16**-plet and its conjugate $\overline{\mathbf{16}}$ representation, and three **45**-plets. These low dimensional Higgs representations are all that is required to break the GUT symmetry, yield the Clebsch-Gordan relations responsible for the difference of the charged fermion masses, and account for heavy right-handed neutrino Majorana masses. In order to account for the hierarchical mixing structure of the Yukawa

[5] M_2 has been computed numerically, including the rotation angles of the diagonalizing matrices in equation 3.63.

matrices, we also need a particular set of S_4 triplet flavons with hierarchical VEVs and particular CSD2 vacuum alignments, where both features are fully discussed here. To complete the model we also require a rather rich spectrum of high energy messenger and driving superfields, which, like most of the Higgs fields, do not appear in the low energy effective theory.

We highlight and summarise the main successes and features of the model as follows:

- The model is successfully built with an $SO(10)$ gauge symmetry where all of the fields belong to the small "named" representations: fundamental, spinorial and adjoints; this could be helpful for a possible future string embedding.
- It contains a superpotential that spontaneously breaks the original symmetry: $S_4 \times SO(10) \times \mathbb{Z}_4^3 \times \mathbb{Z}_4^R \to SU(3)_C \times SU(2)_L \times U(1)_Y \times \mathbb{Z}_2^R$. The model also spontaneously breaks CP.
- The S_4 breaking superpotential that yields the CSD2 vacuum alignment is fairly simple.
- All the GUT scale parameters are natural and $\sim \mathcal{O}(1)$, explaining the hierarchy of the low energy parameters, where the family mass hierarchy is due to the derived hierarchy of flavon VEVs $|v_1| \ll |v_2| \ll |v_3|$, rather than by Froggatt-Nielsen.
- The model contains a working doublet-triplet mechanism, that yields exactly two light Higgs doublets from two $SO(10)$ Higgs multiplets, respectively and without mixing, apart from the μ term which is generated at the correct scale. It also has well behaved proton decay.
- The model naturally generates sufficient BAU through N_2 leptogenesis, which fixes the second right-handed neutrino mass $M_2 \simeq 2 \times 10^{11}$ GeV, in the natural range predicted by the model.
- At low energies, the model contains 15 free parameters that generate 19 presently constrained observables so that it is quite predictive. The model achieves an excellent fit of the Standard Model fermion masses and mixing angles, with $\chi^2 = 11.9$.

We find it remarkable that all of the above can be achieved consistently within a single model. It contains 43 supermultiplet fields, which is the minimal number for any such complete model in the literature so far.

Despite the above successes of the model, it also has a few drawbacks. It does not explain SUSY breaking, and it relies on specific threshold corrections. Even though it has an almost complete UV completion, it still relies on $\mathcal{O}(1/M_P)$ terms for the right-handed neutrino masses. Indeed M_1 and M_3 apparently do not have such natural values as

M_2, and we are forced to explain this away by appealing to the unknown physics at the Planck scale. The symmetry breaking superpotential gives VEVs to most of the GUT breaking fields but it does not drive all of them. Also we do not address the strong CP problem, inflation or Dark Matter (DM) (which may in principle be due to the lightest SUSY particle, stabilised by the R-parity). Indeed we have not considered the SUSY spectrum at all. Such issues are beyond the stated aims of the present thesis and the idea of this chapter is to propose a complete grand unified theory of flavour and leptogenesis, consistent with the data on quark and lepton masses and mixing parameters, in which the three families of quarks and leptons are unified into a single $(\mathbf{3'}, \mathbf{16})$ representation of $S_4 \times SO(10)$.

Importantly, the model can be tested due to its robust predictions of a normal neutrino mass ordering, a CP oscillation phase of 200°, an atmospheric angle of 42° in the first octant and a neutrinoless double beta decay parameter $m_{\beta\beta} = 11$ meV, with the sum of neutrino masses being 76 meV. These predictions, together with the other lepton mixing angles given earlier, will enable the model to be tested by the forthcoming neutrino experiments.

Chapter 4

$SU(5)$ grand unified theory with A_4 modular symmetry

Given the success of chapters 2 and 3, we aim to build a new model based on supersymmetric $SU(5)$ in 6-dimensions. In this chapter, we include extra dimensions for several reasons. First, we choose to compactify the two extra dimensions on a $T^2/\mathbb{Z}_2$ orbifold, in which the tetrahedral symmetry of A_4 arises naturally and plays the roll of the flavour symmetry. Furthermore, we show that, if there is a finite modular symmetry, then it can only be A_4 with fixed modulus $\tau = \omega = e^{i2\pi/3}$ or $\tau = \omega + 1$, where we focus on the first possibility. Secondly, the GUT symmetry is broken to the Standard Model by using GUT-symmetry violating boundary conditions on the orbifold compactification and the doublet-triplet splitting problem is easily solved by leaving only the light Higgs doublets after orbifolding. All these features reduce significantly the number of superfields, the structure of the Yukawa matrices is now dictated by modular forms and there is no need for alignment superpotentials since the flavon alignments are fixed by the orbifold boundary conditions. The contents of this chapter are primarily established from the work in [3].

4.1 Motivation

It is well known that orbifold GUTs in extra dimensions (ED) can provide an elegant explanation of GUT breaking and Higgs doublet-triplet spitting [120]. Similarly, theories involving GUTs and flavour symmetries have been formulated in ED [123, 126, 165, 168, 173, 207–209]. The extra dimensions can help to understand the origin of the discrete non-Abelian group symmetry, such as A_4 and S_4, which may then be identified as a remnant symmetry of the extended Poincaré group after orbifolding, as discussed in section 1.7.3.

Some time ago it was suggested that modular symmetry, when interpreted as a family symmetry, might help to provide a possible explanation for the neutrino mass matrices [210, 211]. Recently it has been suggested that neutrino masses might be modular forms [212], with constraints on the Yukawa couplings. This has led to a revival of the idea that modular symmetries are symmetries of the extra dimensional space-time with Yukawa couplings determined by their modular weights [213–218]. However to date, no attempt has been made to combine this idea with orbifold GUTs in order to provide a unified framework for quark and lepton masses and mixings.

In this chapter, we present the first example in the literature of a grand unified theory (GUT) with a modular symmetry interpreted as a family symmetry. The theory is based on a 6-dimensional (6D) supersymmetric $SU(5)$, where the two extra dimensions are compactified on a $T_2/\mathbb{Z}_2$ orbifold. Such constructions suggest an underlying modular A_4 symmetry with fixed modulus $\tau = \omega = e^{i2\pi/3}$ or $\tau = \omega + 1$, and we choose to construct the model based on the first possibility $\tau = \omega$. This is one of the main differences of the present chapter as compared to recent works with modular symmetries which regard the modulus τ as a free phenomenological parameter [212, 215]. We construct a detailed model along these lines, where the brane fields on the fixed points are assumed to respect a generalised CP symmetry $A_4 \ltimes \mathbb{Z}_2$ which leads to an effective $\mu-\tau$ reflection symmetry at low energies, implying maximal atmospheric mixing and maximal leptonic CP violation. The model introduces two triplet flavons in the bulk, whose vacuum alignments are determined by orbifold boundary conditions, analogous to those used for $SU(5)$ breaking with doublet-triplet splitting. There are also two right-handed neutrinos on the branes whose Yukawa couplings are determined by modular weights. The charged lepton and down-type quarks have diagonal and hierarchical Yukawa matrices, with quark mixing due to a hierarchical up-quark Yukawa matrix with high modular weight to provide quark CP violation.

4.2 Orbifold $T^2/\mathbb{Z}_2$ and symmetries

4.2.1 Review of modular transformations

We presented the general theory of modular transformations and modular forms in section 1.7.4. For completeness, we remind that the modular group $\Gamma \equiv PSL(2,\mathbb{Z})$ is generated by

$$S : \tau \to -1/\tau \quad \text{and} \quad T : \tau \to \tau + 1, \tag{4.1}$$

satisfying the relation

$$\Gamma \simeq \{S, T | S^2 = (ST)^3 = 1\}/\{\pm 1\}, \tag{4.2}$$

where the mod out by $\{\pm 1\}$ reflects the fact that an $SL(2,\mathbb{Z})$ transformation on the modulus parameter τ and its negative are equivalent, see equations 1.77 and 1.78. The

finite modular group Γ_N is realized when the generator T also complies with $T^N = 1$, i.e.

$$\Gamma_N \simeq \{S, T | S^2 = (ST)^3 = T^N = 1\}/\{\pm 1\}. \tag{4.3}$$

In the following, we choose the (non-unique) representation

$$S = \begin{pmatrix} 0 & 1 \\ -1 & 0 \end{pmatrix} \quad \text{and} \quad T_{(N)} = \begin{pmatrix} e^{-i2\pi/N} & 0 \\ 1 & e^{i2\pi/N} \end{pmatrix}, \tag{4.4}$$

which is consistent with the presentation of the finite modular group Γ_N in equation 4.3 for any integer $N > 2$.

4.2.2 Modular symmetry of the orbifold $T^2/\mathbb{Z}_2$

We assume that the two extra dimensions are compactified on a $T^2/\mathbb{Z}_2$ orbifold. We combine the two extra dimensions coordinates, x_5 and x_6, in the complex coordinate $z = x_5 + ix_6$. The action of the orbifold is given by

$$\begin{aligned} z &= z + \omega_1, \\ z &= z + \omega_2, \\ z &= -z, \end{aligned} \tag{4.5}$$

where ω_1 and ω_2 are the two lattice vectors defining the torus T^2, while the last equation is due to the $\mathbb{Z}_2$ action. This orbifold contains four invariant fixed points

$$\bar{z} = \left\{0, \frac{\omega_1}{2}, \frac{\omega_2}{2}, \frac{\omega_1 + \omega_2}{2}\right\}, \tag{4.6}$$

where $\bar{z}$ refers to the set of fixed points, i.e. $\bar{z} = \{\bar{z}_1, \bar{z}_2, \bar{z}_3, \bar{z}_4\}$.

Any model built in the 6D space-time with the two extra dimensions compactified on a $T^2/\mathbb{Z}_2$ orbifold, will have fields living at the fixed points, known as 4D 'brane' fields, and will also have 'bulk' fields, depending on both the uncompactified coordinates and the complex coordinate z. Therefore, it is relevant to study if, after compactification, there is any symmetry left unbroken among the fixed points, which will afterwards affect the fields allocated on them. In this section, we want to find out for which values of ω_1 and ω_2, if any, the set of fixed points is invariant under the general modular transformations in equation 4.4. For doing so, we will apply these transformations on the set of fixed points $\bar{z}$ in equation 4.6, and see if there is any solution, i.e. if there exits any value of ω_1, ω_2 and N under which the set is left invariant up to permutations of the fixed points. We will also assume that $|\omega_1| = |\omega_2|$ as it is usually done in orbifold theories.

The action of the general modular transformations in equation 4.4 on the lattice vectors

ω_1 and ω_2 is given by

$$S\begin{pmatrix}\omega_1\\ \omega_2\end{pmatrix}=\begin{pmatrix}\omega_2\\ -\omega_1\end{pmatrix},\qquad T_{(N)}\begin{pmatrix}\omega_1\\ \omega_2\end{pmatrix}=\begin{pmatrix}e^{-i2\pi/N}\omega_1\\ \omega_1+e^{i2\pi/N}\omega_2\end{pmatrix}. \tag{4.7}$$

Therefore, after an S-transformation, the set of fixed points is transformed to

$$\bar{z}_S=\left\{0,\ \frac{\omega_2}{2},\ \frac{-\omega_1}{2},\ \frac{\omega_2-\omega_1}{2}\right\}. \tag{4.8}$$

However, we can use the orbifold transformations in equation 4.5, i.e. we can add ω_1 to the second and fourth fixed points in $\bar{z}_S$, and obtain the original set $\bar{z}$. Therefore, the set of fixed points, up to permutations, is always invariant under an S-transformation, for any value of ω_1 and ω_2.

The T-transformed fixed points are given by

$$\bar{z}_T=\left\{0,\ \frac{e^{-i2\pi/N}\omega_1}{2},\ \frac{\omega_1+e^{i2\pi/N}\omega_2}{2},\ \frac{e^{-i2\pi/N}\omega_1+\omega_1+e^{i2\pi/N}\omega_2}{2}\right\}. \tag{4.9}$$

If the set is to be invariant, up to permutations of the fixed points, the second term in equation 4.9 must correspond to one of the original fixed points in $\bar{z}$. Since there is no orbifold transformation or value of N that can relate it to the $\omega_1/2$ nor the 0 branes, then it must correspond to $\omega_2/2$ or $(\omega_1+\omega_2)/2$, up to orbifold transformations. Therefore, we find the constraints $\pm\omega_2=\omega_1 e^{-2i\pi/N}$ or $\pm\omega_2=\omega_1(e^{-2i\pi/N}+1)$. The $\pm$ sign is due to the $\mathbb{Z}_2$ orbifold symmetry. For the fixed points, both signs are equivalent since one $(-\omega_2/2)$ is related to the other $(\omega_2/2)$ by adding an extra ω_2, which is a symmetry of the torus. Without loss of generality, we choose to use the negative sign.

For $\omega_2=-\omega_1 e^{-2i\pi/N}$, the set ot T-transformed fixed points become

$$\bar{z}_{T(\omega_2=-\omega_1 e^{-2i\pi/N})}=\left\{0,\ \frac{e^{-i2\pi/N}\omega_1}{2},\ 0,\ \frac{e^{-i2\pi/N}\omega_1}{2}\right\}, \tag{4.10}$$

which removes two fixed points, so this choice of ω_2 does not leave a set of invariant fixed points.

The second choice is $\omega_2=-\omega_1(e^{-2i\pi/N}+1)$ and the T-transformed set is

$$\bar{z}_{T(\omega_2=-\omega_1(e^{-i2\pi/N}+1))}=\left\{0,\ \frac{\omega_1 e^{-i2\pi/N}}{2},\ \frac{-\omega_1 e^{i2\pi/N}}{2},\ \frac{\omega_1 e^{-i2\pi/N}-\omega_1 e^{i2\pi/N}}{2}\right\}. \tag{4.11}$$

We are looking for an invariant set of branes, therefore from equation 4.6, we see that $\omega_1/2$ must be in the set. The second and third terms in equation 4.11 multiply $\omega_1/2$ by a phase so it can not correspond to the original one. Therefore, the only possibility is that the last term in equation 4.11 is identical to the brane $\omega_1/2$, up to orbifold transformations. We can add integer n times ω_2 and integer m times ω_1 or change an

overall sign and it will correspond to the same point. Taking this into account, then the requirement that the second fixed point from equation 4.6 corresponds to the fourth one from equation 4.11 gives

$$\omega_1 e^{-i2\pi/N} - \omega_1 e^{i2\pi/N} = \omega_1 + m\omega_1 + n\omega_2. \tag{4.12}$$

If now we also take into account that $\omega_2 = -\omega_1(e^{-i2\pi/N} + 1)$, equation 4.12 can be rewritten as

$$-e^{2i\pi/N} + e^{-2i\pi/N}(1-2n) - 2n + 2m = 1, \tag{4.13}$$

for arbitrary integers n, m, N. Since both sides are real, this fixes $n = 1$ and we end up with

$$-2\cos\left(\frac{2\pi}{N}\right) = 3 - 2m, \tag{4.14}$$

which only has solutions for $m = 1$ and $N = 3$ or $m = 2$ and $N = 6$.

The $T_{(N)}$ generators for $N = 3$ and $N = 6$, in equation 4.4, satisfy

$$T_{(3)}^3 = T_{(6)}^6 = 1, \quad T_{(6)}^3 = -1, \tag{4.15}$$

that, due to the modding out of the $\pm\{1\}$ sign in the presentation of the finite modular group Γ_N in equation 4.3, Γ_3 and Γ_6 are both equivalent and for now we will only refer to $\Gamma_3 \simeq A_4$ modular symmetry.

Therefore, we have shown that for the $T^2/\mathbb{Z}_2$ orbifold, the set of fixed points is invariant under modular transformations only if the modular group is $\Gamma_3 \simeq A_4$ and when the lattice vectors satisfy the relation $\omega_2 = \omega_1\ \omega$, for $N = 3$, or $\omega_2 = \omega_1(\omega + 1)$, for $N = 6$, where $\omega = e^{i2\pi/3}$.

Without loss of generality, we can always rescale the lattice vectors such that the torus is equivalent to one whose periods are 1 and $\tau = \omega_2/\omega_1$. In the following, we work on the orbifold $T^2/\mathbb{Z}_2$ with the torus defined by 1 and twist angle $\tau = \omega$. If we would have chosen the $N = 6$ case, the basis vectors would be $\omega_1 = 1$ and $\omega_2 = \omega + 1$ with the same A_4 modular symmetry. This is a choice that we follow in the rest of the chapter. The above argument suggests that brane fields allocated on the fixed points must respect a $\Gamma_3 \simeq A_4$ modular symmetry, with fixed modulus $\tau = \omega = e^{i2\pi/3}$. We emphasize that this is one of the main differences of the present chapter as compared to recent works with modular symmetries that regard the modulus τ as a free phenomenological parameter [212, 215]. In our work, we assume a specific orbifold structure which fixes the angle $\tau = \omega = e^{i2\pi/3}$ from the outset, although we shall not address the problem of moduli stabilisation.

4.2.3 Remnant symmetry of the orbifold $T^2/\mathbb{Z}_2$ with twist $\omega = e^{i2\pi/3}$

In this section, we study the extra dimensional space-time as the orbifold $T^2/\mathbb{Z}_2$ with twist angle $\omega = e^{i2\pi/3}$ independently of any modular symmetry considerations. This orbifold corresponds to the identification

$$\begin{aligned} z &\sim z+1, \\ z &\sim z+\omega, \\ z &\sim -z, \end{aligned} \tag{4.16}$$

where the first two equations are the periodic conditions from the torus T^2 and the third one is the action generated by the orbifolding symmetry $\mathbb{Z}_2$. The orbifold symmetry transformations leave four invariant fixed points

$$\bar{z} = \left\{0,\ \frac{1}{2},\ \frac{\omega}{2},\ \frac{1+\omega}{2}\right\}, \tag{4.17}$$

shown in figure 4.1.

We analyse the remnant symmetry of the space-time symmetry after it is broken down to the 4D Poincaré symmetry through orbifold compactification, as in section 1.7.3. We assume that the space-time symmetry before compactification is a 6D Poincaré symmetry. The compactification breaks part of this symmetry, however, due to the geometry of our $T^2/\mathbb{Z}_2$ orbifold with twist angle $\omega = e^{i2\pi/3}$, a discrete subgroup is left unbroken. This group may be generated by the space-time transformations

$$\begin{aligned} &S : z \to z+1/2 \quad \text{or} \quad z \to z+\omega/2, \\ &T : z \to \omega^2 z, \\ &U : z \to z^* \quad \text{or} \quad z \to -z^*, \end{aligned} \tag{4.18}$$

which permute the fixed points and leave invariant the set of four fixed points in equation 4.17. These transformations satisfy

$$\begin{aligned} S^2 = T^3 = (ST)^3 = 1, \\ U^2 = (SU)^2 = (TU)^2 = (STU)^4 = 1, \end{aligned} \tag{4.19}$$

where the first line is the presentation of the group A_4 and both lines complete the presentation of S_4. In figure 4.1, we show how these transformations act on the extra dimensional space and how the A_4 symmetry is realized.

The $T^2/\mathbb{Z}_2$ orbifold with twist angle ω has four fixed points and they are permuted by the discrete subgroup of rotations and translation in the extra space, A_4 or S_4. This symmetry, together with 4D Poincaré transformations, is a subgroup of the 6D Poincaré symmetry that survives compactification. Any brane field living in the fixed points will

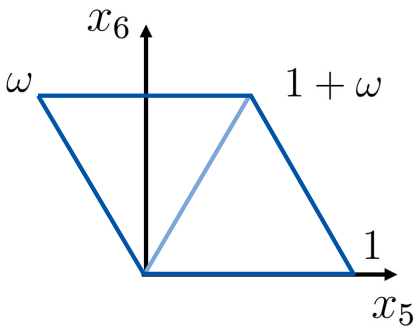

(a) The extra dimensional space. Opposite sides are identified to form a torus. The orbifolding $\mathbb{Z}_2$ identifies both equilateral triangles. These are the identifications in equation 4.16.

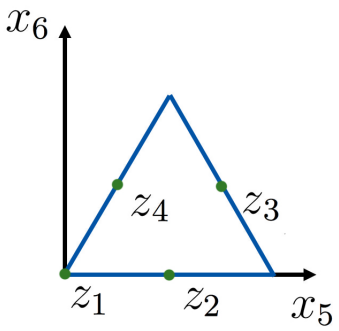

(b) The effective extra dimensional space $T^2/(\mathbb{Z}_2)$. This is the whole bulk. The four invariant fixed points $z_{1,2,3,4}$ are shown.

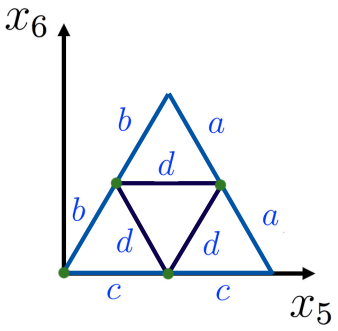

(c) The four fixed points are permuted by the symmetries S, T, U in equation 4.18. The transformations S, U identify the sides a, b, c while T rotates everything by identifying sides d.

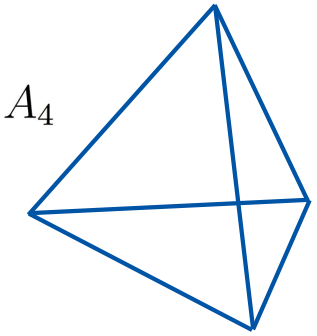

(d) By actually folding to identify sides a, b, c we obtain a tetrahedron, whose vertices are related by the symmetry group A_4.

Figure 4.1: Visualization on the remnant A_4 symmetry after orbifolding.

transform under the 4D Poincaré group as usual and additionally under the remnant A_4 or S_4 symmetry. We choose the embedding of the representation $4 \to 3 + 1$ so that the brane fields can only transform under those irreducible representations [208].

With these type of models one chooses the bulk fields to follow the space-time symmetry transformations in equation 4.18, so that this symmetry becomes the flavour symmetry of the model [123, 126, 207]. For example, this approach has been followed for A_4 or S_4 combined with $SU(5)$ Grand Unified Theories (GUTs) in 6d or 8d [166, 168, 173, 208, 209].

4.2.4 Connection between the modular and the remnant symmetries

In this section, we connect and identify the two symmetries that we have been discussing so far: the modular symmetry $\Gamma_3 \simeq A_4$ in section 4.2.2 and the remnant A_4 symmetry, as a subgroup of the space-time 6D Poincaré symmetry, in section 4.2.3 (we shall return to the remnant S_4 symmetry in section 4.2.5). At this point, the reader might have noticed that, indeed, the two symmetries are identical when acting on the fixed points.

The modular symmetry is just a passive transformation, acting on the lattice vectors defining the torus. Under these passive transformations, we have checked that the set of fixed points is permuted but left invariant. The remnant A_4 symmetry is an active transformation, acting on the extra space and again inducing permutations of the four fixed points. It is just a choice of "picture" (active or passive) which we choose.

Modular symmetry acting on brane fields behave as any usual discrete flavour symmetry (i.e. modular forms are not relevant), since the fields living on the fixed points do not depend on the extra dimensional coordinate. We checked that on the orbifold $T_2/\mathbb{Z}_2$, the fixed points can only be consistent with the modular group Γ_3 iff $\tau = \omega$ or $\tau = \omega + 1$ and no other. In this setup, the fixed points feel the finite modular A_4 symmetry as simply equivalent to a remnant A_4 symmetry, a subgroup of the extra dimensional Poincaré group.

We can see from equation 4.7, that the S and $T_{(3)}$ transformations (the Γ_3 modular transformations) correspond to specific passive reflections, rotations and translations. This way this must be a subgroup of the 6d Poincaré group.

Bulk fields will transform under some representation of the 6D Poincaré, however they will transform under a non linear representation of the modular symmetry Γ_3, the modular forms [212]. We can then conclude that we can have the modular symmetry Γ_3 as a non linear realization of the remnant A_4 symmetry.

4.2.5 Enhanced $A_4 \ltimes \mathbb{Z}_2$ symmetry of the fixed points

In section 4.2.3, we have seen that the orbifold has a remnant symmetry S_4 on the fixed points. We note here that $S_4 \simeq A_4 \ltimes \mathbb{Z}_2$. We have also discussed in section 4.2.4, that if we impose a modular symmetry $\Gamma_3 \simeq A_4$ on the whole space, its action on the brane fields is the same action as the remnant space-time symmetry, i.e. it permutes the fixed points but leaves invariant the whole set. The modular symmetry acts on the basis vectors of the torus while the remnant symmetry is a space-time symmetry, therefore the first one can be seen as passive transformation while the second one is an active transformation. This way we may identify the remnant A_4 symmetry of the brane fields as a modular symmetry.

We know, from section 4.2.3 that the full symmetry of the fixed points is S_4, however we can not interpret it as a modular symmetry since we proved in section 4.2.2, that the fixed points can only be invariant under the modular transformations corresponding to $\Gamma_3 \simeq A_4$, i.e. we only found a solution for $N = 3$ or $N = 6$.

The symmetry generated by U in equation 4.18 is a remnant symmetry of the orbifolding process, but it can not be interpreted as a modular transformation. We conclude that the remnant symmetry of the branes is $\Gamma_3 \ltimes \mathbb{Z}_2 \simeq A_4 \ltimes \mathbb{Z}_2$. The $\mathbb{Z}_2$ symmetry is

generated by $C \cdot U$ where U is the usual matrix representation of the generator from S_4 and C stands for complex conjugation of the complex coordinate, which is equivalent to a change of sign in x_6, i.e. the parity transformation of the 6^{th} dimension P_6. The $\mathbb{Z}_2$ is not a modular symmetry while the A_4 is. The product of both symmetries is not direct since the generator U does not commute with all A_4 generators and is reminiscent of the corresponding S_4 generator.

The A_4 modular symmetry will require the Yukawa couplings to be specific modular forms, see appendix A.2.2. The $\mathbb{Z}_2$ symmetry will further restrict the possible mass matrix structure so that the theory has strong predictions for leptons [219]. As we shall see later, the up quarks will lie in different A_4 singlets, so that only the subgroup $\mathbb{Z}_3$ is remnant while the $\mathbb{Z}_2$ behaves trivially. This forces stringent relations for the lepton mass matrices but not for the quarks.

After compactification, the $\mathbb{Z}_2$ behaves like a generalized CP symmetry where the transformations $C, P_1, ..., P_5$ are trivial while $\tilde{P}_6 = P_6\, U$, where P_6 is the trivial parity transformation, while the U is a family transformation [220]. Although this is not a usual generalized CP symmetry. There is no C transformation involved, only P_6. However, after compactification this symmetry appears as an effective generalized CP symmetry. As stated before, this effective symmetry transformations only affects non trivially on the brane fields and the fields on the bulk are unaffected.

We have shown that the remnant $\mathbb{Z}_2$ symmetry on the branes behaves as an effective generalized CP transformation. In appendix A.2.1, we check its compatibility with the A_4 flavour symmetry, and find that it is consistent, as indeed it must be.

4.3 The model

4.3.1 Field content

In this section we construct a supersymmetric $SU(5)$ GUT model on a 6D orbifold $T^2/\mathbb{Z}_2$ with twist $\omega = e^{i2\pi/3}$, with an A_4 modular symmetry as a flavour symmetry, extended by the $\mathbb{Z}_2$ symmetry on the fixed points. Furthermore we impose a global $U(1)$ as a shaping symmetry. We assume different boundary conditions at each invariant fixed point. These conditions break the original symmetry into the MSSM.

All the fields in the bulk ψ will transform under the modular transformations

$$\tau \to \frac{a\tau + b}{c\tau + d} \quad \text{as} \quad \psi \to (c\tau + d)^{-k} \rho \psi, \tag{4.20}$$

where ρ is the usual matrix representation of the corresponding A_4 transformation. Each field has an arbitrary weight $-k$. The fields are not modular forms and can have any

Field	Representation		
	$A_4 \ltimes \mathbb{Z}_2$	$SU(5)$	$U(1)$
F	**3**	$\bar{\mathbf{5}}$	$a+2c$
N_s^c	**1**	**1**	a
N_a^c	**1**	**1**	$4a$
ξ	**1**	**1**	$-2a$

Table 4.1: Brane fields living on the fixed points, including matter and right-handed neutrino superfields. A working set of charges is $\{a,b,c\} = \{2,0,1\}$. Note that the **3** representations on the brane transform under $A_4 \ltimes \mathbb{Z}_2$ as shown in table A.2 and equation A.9.

Field	Representation			Localization			
	A_4	$SU(5)$	$U(1)$	Weight	P_0	$P_{1/2}$	$P_{\omega/2}$
$T_1^{\pm}$	$\mathbf{1''}$	**10**	$c+4a$	$-\gamma$	$+1$	±1	±1
$T_2^{\pm}$	$\mathbf{1'}$	**10**	$c+2a$	$-\gamma$	$+1$	±1	±1
$T_3^{\pm}$	**1**	**10**	c	$-\gamma$	$+1$	±1	±1
H_5	**1**	**5**	$-2c$	$-\alpha$	$+1$	$+1$	$+1$
$H_{\bar{5}}$	$\mathbf{1'}$	$\bar{\mathbf{5}}$	b	$\alpha+\gamma$	$+1$	$+1$	$+1$
ϕ_1	**3**	**1**	$-b-a-3c$	$-\alpha$	$+1$	$+1$	$+1$
ϕ_2	**3**	**1**	$-3a$	$\alpha-\beta$	$+1$	-1	$+1$

Table 4.2: Bulk fields used in constructing the model, including matter, Higgs and flavon superfields. A working set of charges is $\{a,b,c\} = \{2,0,1\}$. The complete theory must also contain three $\overline{T}_i$, being the complex conjugate representation of T_i so that it is anomaly free.

weight k_i. The brane superfields that are located on the fixed points do not depend on the extra dimensions and therefore they must have weight zero [212].

The whole field content is listed in tables 4.1 and 4.2. The fields that do not have weight nor parity under the boundary conditions are located on the fixed points and feel the symmetry $A_4 \ltimes \mathbb{Z}_2$, see table 4.1. The transformations of the fields under this symmetry are discussed in appendix A.2. The **3** representations of the brane fields transform under $A_4 \ltimes \mathbb{Z}_2$ as shown in table A.2 and equation A.9.

The field F contains the MSSM fields L and d_R, it is a flavour triplet **3** and is located on the fixed points. The fields $T_i^{\pm}$ contain the MSSM u_R, e_R, Q, they are 3 flavour singlets. There are two copies of each T with different parities under the boundary conditions, as we shall see in the next section, this allows different masses for down quarks and charged leptons. There are only two right handed neutrinos $N_{a,s}^c$. The MSSM Higgs fields $h_{u,d}$ are inside the $H_{5,\bar{5}}$, respectively. We have two flavons $\phi_{1,2}$ that help to give structure to the fermion masses. Finally, the field ξ generates the hierarchy between the masses à la Froggatt-Nielsen [104].

4.3.2 GUT and flavour breaking by orbifold compactification

In section 1.7.2, we briefly introduced orbifold compactifications and how the action of orbifold compactification on field space can break the original gauge group to a smaller subgroup. Here, we apply the same procedure choosing a set of boundary conditions that break A_4 completely and $SU(5)$ into the Standard Model. We also break the extended $\mathcal{N} = 2$ SUSY to $\mathcal{N} = 1$ SUSY.

The compactification on the $T^2/\mathbb{Z}_2$ orbifold implies that the extra dimensional space has the symmetry given in equation 4.16. This geometric orbifold action is now embedded into an action on field space

$$\begin{aligned} \phi(x,z) &\to G_5\ \phi(x,z-1), \\ \phi(x,z) &\to G_6\ \phi(x,z-\omega), \\ \phi(x,z) &\to G\ \phi(x,-z), \end{aligned} \tag{4.21}$$

where $\phi(x,z)$ is a general field of the theory and G_5, G_6 and G are elements of the symmetry group of the theory. The action on field space in equation 4.21 is equivalent to the action on the extra dimensional space in equation 4.16, with the difference that since we are in a gauge theory, the equations do not need to be fulfilled exactly but only up to a gauge transformation.

The gauge transformations G_5, G_6 and G are also matrix representations of the symmetries in equation 4.16 and therefore they must comply with

$$G^2 = 1, \quad G_5 G_6 = G_6 G_5, \quad G G_{5,6} G = G_{5,6}^{-1}, \tag{4.22}$$

where the first equation comes from the fact that it belongs to the parity operator, the second is due to the fact of the commutativity of the translations and the third one denotes the relation between parity and translations.

Additionally, we know that the orbifold $T^2/\mathbb{Z}_2$ contains four fixed points given by $\bar{z}$ in equation 4.17, i.e. these points are invariant under the symmetry transformations in equation 4.16. At the fixed points $\bar{z}_i$ with $i = 1, \ldots, 4$, we impose the following boundary conditions

$$\phi(x, z + \bar{z}_i) \to P_{\bar{z}_i} \phi(x, -z + \bar{z}_i), \tag{4.23}$$

which corresponds to a reflection at each of the fixed points. In combination with the gauge transformations in equation 4.21, they have to satisfy

$$P_0 = G, \quad P_{1/2} = G_5 G, \quad P_{\omega/2} = G_6 G, \quad P_{(1+\omega)/2} = G_5 G_6 G = P_{1/2} P_0 P_{\omega/2}. \tag{4.24}$$

By choosing all $G's$ to commute, all boundary conditions become matrices of order 2. The boundary conditions must belong to the symmetry group $A_4 \times SU(5)$ of the SUSY

model, and are chosen to break the symmetry in a particular way as follows

$$\begin{aligned} P_0 &= 1_3 \times 1_5, \\ P_{1/2} &= T_1 \times \mathrm{diag}(-1,-1,-1,1,1), \\ P_{\omega/2} &= T_2 \times \mathrm{diag}(-1,-1,-1,1,1), \end{aligned} \tag{4.25}$$

where 1_3 is the 3×3 identity matrix while 1_5 is the 5×5 identity matrix and the matrices T_1 and T_2 are given by

$$T_1 = \begin{pmatrix} 1 & 0 & 0 \\ 0 & -1 & 0 \\ 0 & 0 & -1 \end{pmatrix} \text{ and } T_2 = \begin{pmatrix} 1 & 0 & 0 \\ 0 & 0 & 1 \\ 0 & 1 & 0 \end{pmatrix} = U. \tag{4.26}$$

The last boundary condition is defined by the others as $P_{(1+\omega)/2} = P_{1/2}P_0P_{\omega/2} = T_1T_2 \times 1_5$.

The boundary condition P_0 breaks the effective extended $\mathcal{N}=2 \to \mathcal{N}=1$ SUSY. The boundary conditions $P_{1/2,\omega/2}$ break A_4 completely and $SU(5) \to SU(3)\times SU(2)\times U(1)$. As in the example given in the introduction, equation 1.68, depending on how the parity assignments are chosen we can break the $SU(5)$ multiplets into different multiplets of the Standard Model gauge group.

The parity assignments are given in table 4.2. The superfields $F, N^c_{a,s}, \xi$ live on the fixed points and are unaffected by the boundary conditions. The fields $T^{\pm}$ are A_4 singlets and do not feel the A_4 breaking conditions, although they do feel the $SU(5)$ breaking condition according to their parity. The fields T^+ contain the light MSSM u_R, e_R fields, while the fields T^- encompass the light fields Q. This allows for independent masses for charged leptons and down quarks since they come from different fields. The Higgs fields feel the $SU(5)$ breaking condition leaving only the light doublets, solving the doublet-triplet splitting problem [207] (for a recent discussion see for example [208]).

The flavons $\phi_{1,2}$ feel the A_4 breaking conditions. They have different parities under the conditions and this fixes their alignments to be

$$\langle\phi_1\rangle = v_1 \begin{pmatrix} 1 \\ 0 \\ 0 \end{pmatrix}, \quad \langle\phi_2\rangle = v_2 \begin{pmatrix} 0 \\ 1 \\ 1 \end{pmatrix}. \tag{4.27}$$

We may remark that these flavon VEV alignments do not break the $\mathbb{Z}_2$ symmetry generated by U, even though they are in the bulk.

We see that the orbifolding breaks the symmetry $SU(5)\times A_4 \ltimes \mathbb{Z}_2 \to SU(3)\times SU(2)\times U(1)\times\mathbb{Z}_2$ while solving the doublet-triplet splitting, separating charged lepton and down quark masses and completely aligning flavon VEVs.

We do not show an explicit driving mechanism for the VEVs $v_{1,2,\xi}$. We assume that they are driven radiatively [152, 153, 221–225].

4.3.3 Effective Yukawa superpotential

In 6D, the superpotential has dimension 5 while each superfield has dimension 2. A 6D interacting superpotential is inherently non-renormalizable. We work with the effective 4D superpotential, which happens after compactification and we assume the compactification scale is close to the original cutoff scale. We use Λ to denote both, the compactification scale and the GUT scale, which is taken to be the cut-off of the effective theory.

With the fields in tables 4.1 and 4.2, we can write the effective 4D Yukawa terms

$$\begin{aligned}\mathcal{W}_Y = {} & y_s^N \xi N_s^c N_s^c + y_a^N \xi \frac{\xi^3}{\Lambda^3} N_a^c N_a^c \\ & + y_s^\nu \frac{\xi}{\Lambda} F H_5 N_s^c + y_a^\nu \frac{\phi_2 \xi}{\Lambda^2} F H_5 N_a^c \\ & + y_3^e \frac{\phi_1}{\Lambda} F H_{\bar{5}} T_3^+ + y_2^e \frac{\phi_1 \xi}{\Lambda^2} F H_{\bar{5}} T_2^+ + y_1^e \frac{\phi_1 \xi^2}{\Lambda^3} F H_{\bar{5}} T_1^+ \\ & + y_3^d \frac{\phi_1}{\Lambda} F H_{\bar{5}} T_3^- + y_2^d \frac{\phi_1 \xi}{\Lambda^2} F H_{\bar{5}} T_2^- + y_1^d \frac{\phi_1 \xi^2}{\Lambda^3} F H_{\bar{5}} T_1^- \\ & + y_{ij}^u H_5 T_i^+ T_j^- \frac{\xi^{6-i-j}}{\Lambda^{6-i-j}},\end{aligned} \tag{4.28}$$

where $i, j = 1, 2, 3$. Due to the stringent $U(1)$ shaping symmetry, there are no higher order terms. The field ξ has a VEV and generates hierarchies between families à la Froggatt-Nielsen [104].

The first line in equation 4.28 gives the two right-handed neutrino Majorana masses without any mixing. The fields in both terms have zero weight so the modular symmetry does not add anything new. The second line generate Dirac neutrino masses. They have non trivial weights and their structure will be discussed in section 4.3.4. The third line gives masses to charged leptons. They are all weight zero automatically and the mass matrix is diagonal. The fourth line generates a diagonal down quark mass matrix. Since it involves a different field (T^- instead of T^+) the coupling constants are independent. Finally the fifth line gives masses to the up-type quarks, which is a general non-symmetric mass matrix. Since the fields in these terms have a non trivial weight but the $T^\pm$ are singlets, the modular symmetry does not change the matrix structure. We remark that the top quark mass term is renormalizable.

At the GUT level, the μ term is forbidden, so it should be generated by another mechanism at a much smaller scale [92].

4.3.4 Effective alignments from modular forms

In this section, we discuss the couplings in equation 4.28 with weight different from zero, i.e. y_s^ν, y_a^ν and y_{ij}^u. Their weight is given to compensate the weight of the terms they couple to, such that they become modular forms transforming according to

$$\tau \to \frac{a\tau + b}{c\tau + d}, \quad Y \to (c\tau + d)^{k_Y} \rho_Y Y, \tag{4.29}$$

where k_Y is the weight and must be a positive even integer [226] and ρ_Y is the representation under the modular A_4 symmetry. In the case of $\Gamma_3 \simeq A_4$, the modular forms can be constructed as a function of the Dedekind eta-function $\eta(\tau)$ and the exact form can be found in appendix A.2.2.

The modular forms are functions of the lattice basis vector parameter $\tau = \omega_2/\omega_1$. Usually, this parameter is chosen to give a good fit to the flavour parameters. In our case, the specific orbifold our model is set to fix

$$\tau = \omega = e^{2i\pi/3} \tag{4.30}$$

and the modular form structure is fixed up to a real constant.

The modular form y_s^ν must be a triplet under A_4 to construct an invariant singlet with the triplet field F. Furthermore, it has weight α to compensate the overall weight of the corresponding term. We show the effective triplet alignments it can have in table 4.3, for different weights α. The possibilities are very limited since many modular forms vanish when $\tau = \omega$, as shown in appendix A.2.2. Larger weight modular forms repeat the same structure so that this table is exhaustive, as discussed in appendix A.2.2.

α	$(y_s^\nu)_{\mathbf{3}}$
0	0
2	$y \begin{pmatrix} 2 \\ 2\omega \\ -\omega^2 \end{pmatrix}$
4	$y \begin{pmatrix} 2 \\ -\omega \\ 2\omega^2 \end{pmatrix}$
6	$y \begin{pmatrix} -1 \\ 2\omega \\ 2\omega^2 \end{pmatrix}$

Table 4.3: The effective alignments of the modular form y_s^ν as a triplet, depending on its weight α. The parameter y is an arbitrary constant.

The modular form y_a^ν must have weight β. It multiplies the flavon ϕ_2, so that they must be contracted into a triplet $(y_a^\nu \langle\phi_2\rangle)_{\mathbf{3}}$ which will generate the effective alignment.

In the case of y_a^ν being a singlet under A_4, the effective alignment is simply given the flavon VEV $\langle\phi_2\rangle$ in equation 4.27, which was fixed by the orbifold boundary conditions. When y_a^ν is a triplet under A_4, it must be contracted with ϕ_2 as shown in appendix A.2, $\mathbf{3}\times\mathbf{3}\to\mathbf{1}+\mathbf{1'}+\mathbf{1''}+\mathbf{3_a}+\mathbf{3_s}$. This gives different possible products for the effective triplet. The actual effective alignment is an arbitrary linear combination of all possibilities and can be found in table 4.4. For $\beta=0$ the only modular form is a singlet, so the only triplet that can be built is $\langle\phi_2\rangle$. For $\beta=2$, the only modular form is the triplet $Y_{\mathbf{3}}^{(2)}$ shown in the appendix A.2.2. The effective triplet is the linear combination of the symmetric and antisymmetric product of the modular form with the flavon VEV, $\langle\phi_2\rangle\times Y_{\mathbf{3}}^{(2)}\to\mathbf{3_a}+\mathbf{3_s}$. For $\beta=4,6$ the modular form can be the singlet $Y_{\mathbf{1'}}^{(4)}, Y_{\mathbf{1}}^{(6)}$ respectively and the corresponding triplets $Y_{\mathbf{3}}^{(4)}, Y_{\mathbf{3},2}^{(6)}$, so that the actual alignment comes from the linear combination of $\langle\phi_2\rangle\times Y_{\mathbf{1},\mathbf{1'}}\to\mathbf{3}$ and $\langle\phi_2\rangle\times Y_{\mathbf{3}}\to\mathbf{3_a}+\mathbf{3_s}$.

β	$(y_a^\nu\,\langle\phi_2\rangle)_3/v_2$
0	$y_1\begin{pmatrix}0\\1\\1\end{pmatrix}$
2	$y_1\begin{pmatrix}\omega^2-2\omega\\-2\omega-2\\4\omega-2\end{pmatrix}+y_2\begin{pmatrix}-\omega^2-2\omega\\-2\\2\end{pmatrix}$
4	$y_1\omega\begin{pmatrix}1\\0\\1\end{pmatrix}+y_2\begin{pmatrix}-2\omega^2+\omega\\2\omega^2-2\\-2\omega^2-2\end{pmatrix}+y_3\begin{pmatrix}2\omega^2+\omega\\-2\\2\end{pmatrix}$
6	$y_1\begin{pmatrix}0\\1\\1\end{pmatrix}+y_2\begin{pmatrix}2\\4\omega^2+1\\4\omega+1\end{pmatrix}+y_3\begin{pmatrix}2\omega^2-2\omega\\1\\-1\end{pmatrix}$

Table 4.4: The effective alignments of the modular form y_a^ν contracted with $\langle\phi_2\rangle$ into a triplet, depending on its weight β. The parameters y_i are constants constrained by the $A_4\ltimes\mathbb{Z}_2$ symmetry.

By choosing the weights α and β, the structure of the neutrino mass matrix is completely defined. The y in table 4.3 and y_1,y_2,y_3 in table 4.4 correspond to general complex numbers that comply with the non trivial CP symmetry of the model.

We have obtained all the possible A_4 invariant modular forms. However, we have to comply with the extended symmetry $A_4\ltimes\mathbb{Z}_2$. The U generator only transforms non trivially the triplet field F which is contracted to a triplet modular form. An U transformation of the field F can be reabsorbed by transforming the modular form by

$$C\begin{pmatrix}1&0&0\\0&0&1\\0&1&0\end{pmatrix} \tag{4.31}$$

where the C stands for complex conjugation. Invariant terms under the full symmetry must involve modular forms that are also invariant under the $\mathbb{Z}_2$ transformation. From

table 4.3, the only invariant case is when $\alpha = 6$ with real y. From table 4.4, the only invariant cases happen when $\beta = 0$ with real y_1 or $\beta = 6$ with $y_{1,2}$ real and y_3 imaginary.

The triplet field F is not only taking part in the Dirac neutrino mass terms but also in the down quark and charged leptons mass terms, therefore they also must be invariant under the enhanced symmetry $A_4 \ltimes \mathbb{Z}_2$. In this case, the field F is contracted with the flavon field ϕ_1 and it is easy to check that the transformation in equation 4.31 leaves the VEV invariant when real and therefore the charged lepton and down quark mass terms when the parameters y_i^d and y_i^e involved are real.

Finally, the modular form y_{ij}^u must have weight $\alpha + 2\gamma$ to build an invariant. All the fields in the corresponding terms are singlets, so these modular forms must be singlets also and do not change the structure. Depending on i and j, the modular form y_{ij}^u must be a different type of singlet. The weight $\alpha + 2\gamma$ has to be large enough so that the space contains the three types of singlets. This modular form does not add anything to the structure of the up-type quark mass matrix but allows to build the A_4 invariants for all T_iT_j combinations. The smallest weight that allows modular forms of all 3 types of singlets is 20, as discussed in appendix A.2.2. These modular forms y_{ij}^u are in general complex.

The case $\beta = 0$ has not enough freedom to fit the neutrino data with only two free parameters. We conclude that the smallest phenomenologically viable choice for weights is

$$\alpha = \beta = 6 \quad \text{and} \quad \gamma = 7. \tag{4.32}$$

4.3.5 Mass matrices

We are now able to express the mass matrices following equation 4.28 and the effective alignments given in section 4.3.4. First, we define the dimensionless parameters

$$\langle \xi \rangle / \Lambda = \tilde{\xi} \quad \text{and} \quad v_i/\Lambda = \tilde{v}_i, \tag{4.33}$$

where Λ is the original cutoff scale. The down quark and charged lepton mass matrices are diagonal

$$\begin{aligned} M^d =& v_d \begin{pmatrix} y_1^d \tilde{\xi}^2 & 0 & 0 \\ 0 & y_2^d \tilde{\xi} & 0 \\ 0 & 0 & y_3^d \end{pmatrix} \tilde{v}_1, \\ M^e =& v_d \begin{pmatrix} y_1^e \tilde{\xi}^2 & 0 & 0 \\ 0 & y_2^e \tilde{\xi} & 0 \\ 0 & 0 & y_3^e \end{pmatrix} \tilde{v}_1, \end{aligned} \tag{4.34}$$

while the up quark mass matrix can be written as

$$M_u = v_u \begin{pmatrix} y^u_{11}\,\tilde{\xi}^4 & y^u_{12}\,\tilde{\xi}^3 & y^u_{13}\,\tilde{\xi}^2 \\ y^u_{21}\,\tilde{\xi}^3 & y^u_{22}\,\tilde{\xi}^2 & y_{23}\tilde{\xi} \\ y^u_{31}\,\tilde{\xi}^2 & y^u_{32}\,\tilde{\xi} & y^u_{33} \end{pmatrix} \tilde{v}_2, \tag{4.35}$$

where the parameters y^d_i and y^d_i are real due to the enhanced symmetry on the fixed points $A_4 \ltimes \mathbb{Z}_2$ while y^u_{ij} are in general complex.

The down-type quark and charged lepton mass matrices in equation 4.34 are diagonal so the fit to the observed masses is straightforward. The hierarchy between the masses of the different families is understood through the powers of $\tilde{\xi}$ and can be achieved assuming the dimensionless couplings to be of order $\mathcal{O}(1)$. All the contributions to quark mixing is coming from the up sector. The complex parameters in the up-type mass matrix, see equation 4.35, fix the up, charm and top quark masses as well as the observed CKM mixing angles. We can obtain a perfect fit for weight $\gamma = 7$. Different values of $\tilde{v}_1$, $\tilde{v}_2$ and $\tilde{\xi}$ can fit the observed masses using different dimensionless couplings still of order $\mathcal{O}(1)$.

The form of the Dirac neutrino mass matrix depends on the weights α and β. All the possible alignments are given in tables 4.3 and 4.4. The $\mathbb{Z}_2$ symmetry restricts ourselves to the case $\alpha = 6$ and $\beta = 0$ or $\beta = 6$. In the case of $\beta = 0$, we only have two free parameters $\{y, y_1\}$ and we can not find a good fit. Therefore, the only phenomenologically viable case is for $\alpha = \beta = 6$ and we restrict ourselves to this case in the following.

As shown in the appendix A.2, we have to take into account the Clebsch-Gordan coefficients when contracting the modular form $(y^\nu_s F)_{\mathbf{1}}$ and $(y^\nu_a \langle\phi_2\rangle F)_{\mathbf{1}}$ into singlets, i.e. $\mathbf{3} \times \mathbf{3} \to \mathbf{1}$, given by

$$(\varphi\psi)_{\mathbf{1}} = \varphi_1\psi_1 + \varphi_2\psi_3 + \varphi_3\psi_2, \tag{4.36}$$

after which the effective alignments for $\alpha = 6$ and $\beta = 6$ look like

$$\alpha_6 = y \begin{pmatrix} -1 \\ 2\omega^2 \\ 2\omega \end{pmatrix}, \quad \beta_6 = \begin{pmatrix} 2y_2 + y_3(2\omega^2 - 2\omega) \\ y_1 + y_2(4\omega + 1) - y_3 \\ y_1 + y_2(4\omega^2 + 1) + y_3 \end{pmatrix}, \tag{4.37}$$

respectively. The Dirac neutrino mass matrix is then given by

$$M^\nu_D = v_u \begin{pmatrix} \left(2y_2 + y_3(2\omega^2 - 2\omega)\right)\tilde{v}_2 & -y \\ \left(y_1 + y_2(4\omega + 1) - y_3\right)\tilde{v}_2 & 2\omega^2 y \\ \left(y_1 + y_2(4\omega^2 + 1) + y_3\right)\tilde{v}_2 & 2\omega y \end{pmatrix} \tilde{\xi}. \tag{4.38}$$

The right-handed neutrino Majorana mass matrix is diagonal

$$M_R = \langle \xi \rangle \begin{pmatrix} y_a^N \tilde{\xi}^3 & 0 \\ 0 & y_s^N \end{pmatrix}, \tag{4.39}$$

with hierarchical right-handed neutrino masses given by the different powers of the field ξ. Furthermore, we have heavy right-handed neutrino Majorana masses such that the left-handed neutrinos get a small Majorana mass through type I seesaw [22]

$$m_L^\nu = M_\nu^D M_R^{-1} (M_\nu^D)^T. \tag{4.40}$$

The neutrino mass matrix looks like

$$m_\nu = \left(\frac{v_u^2}{\langle \xi \rangle} \frac{\tilde{\xi}^2}{y_s^N} \right) \alpha_6 (\alpha_6)^T + \left(\frac{v_u^2}{\langle \xi \rangle} \frac{\tilde{v}_2^2}{\tilde{\xi} y_a^N} \right) \beta_6 (\beta_6)^T, \tag{4.41}$$

where α_6 and β_6 are the alignments defined in equation 4.37. The effective parameters at low energy are $\{y, y_1, y_2, y_3\}$, previously defined in tables 4.3 and 4.4. The $\mathbb{Z}_2$ symmetry fixes the parameters $\{y, y_1, y_2\}$ to be real while y_3 is purely imaginary.

4.3.6 $\mu - \tau$ reflection symmetry

The neutrino mass matrix in equation 4.41 is $\mu - \tau$ reflection symmetric ($\mu\tau$-R symmetric). This corresponds to the interchange symmetry between the muon neutrino ν_μ and the tau neutrino ν_τ combined with CP symmetry, namely

$$\nu_e \to \nu_e^c, \quad \nu_\mu \to \nu_\tau^c, \quad \nu_\tau \to \nu_\mu^c, \tag{4.42}$$

where the superscript denotes the charge conjugation of the neutrino field. This can be easily seen from the alignments in equation 4.37 which construct the neutrino mass matrix in equation 4.41. The $\mathbb{Z}_2$ symmetry fixes the parameters $\{y, y_1, y_2\}$ to be real while y_3 is purely imaginary, therefore the transformation in equation 4.42 leaves the alignments invariant and accordingly the neutrino mass matrix. For a review of $\mu\tau$ symmetry see e.g. [227] and references therein, also see the recent discussion [228].

It is known that having a neutrino mass matrix $\mu\tau$-R symmetric in the flavour basis (which is our case) is equivalent to $\mu - \tau$ universal ($\mu\tau$-U) mixing in the PMNS matrix, see reference [229]. The consequences of having $\mu - \tau$ symmetry is that it leads to having non zero reactor angle, θ_{13}, together with maximal atmospheric mixing angle and maximal Dirac CP phase:

$$\theta_{13} \neq 0, \quad \theta_{23} = 45^\circ, \quad \delta^l = \pm 90^\circ \tag{4.43}$$

We remark that this is a prediction of the model due to having $A_4 \ltimes \mathbb{Z}_2$ symmetry on

the fixed points.

4.3.7 Numerical fit

The parameters $\{y, y_1, y_2, y_3\}$ in the neutrino mass matrix 4.41 will fit the rest of the PMNS observables, namely $\{\theta_{12}^l, \theta_{13}^l, \Delta m_{21}^2, \Delta m_{31}^2\}$ together with the prediction of the $\mu-\tau$ symmetry, $\theta_{23} = 45^\circ$ and $\delta^l = -90^\circ$. The contribution to a χ^2 test function comes only from these predictions and we use the recent global fit values of neutrino data from NuFit4.0 [32]. The best fit points together with the 1σ ranges are $\theta_{23}/^\circ = 49.6^{+1.0}_{-1.2}$ and $\delta^l/^\circ = 215^{+40}_{-29}$ for normal mass ordering and without the Super-Kamiokande atmospheric neutrino data analysis. However, the distribution of these two observables are far from Gaussian and the predictions of having maximal atmospheric mixing angle $\theta_{23} = 45^\circ$ and maximal CP violation $\delta^l = -90^\circ$, still lie inside the $3\sigma(4\sigma)$ region with a $\chi^2 = 5.48(6.81)$ without (with) Super-Kamiokande. We show two numerical fits below, although this is only an example as we can find a good fit for a large range of parameters y, y_1, y_2 and y_3.[1] The predictions of the model $\theta_{23} = 45^\circ$ and $\delta^l = -90^\circ$ are due to the $\mu\tau$-R symmetry and the four free parameters are used to fit the rest of the observables in the PMNS matrix.

We perform a χ^2 test function when fitting the effective neutrino mass matrix in equation 4.41 with input parameters $x = y, y_1, y_2, y_3$, from which we obtain a set of observables $P_n(x)$. We minimize the function defined as

$$\chi^2 = \sum_n \left(\frac{P_n(x) - P_n^{obs}}{\sigma_n} \right)^2 , \tag{4.44}$$

where the observables are given by $P_n^{\text{obs}} \in \{\theta_{12}^l, \theta_{13}^l, \theta_{23}^l, \delta^l, \Delta m_{21}^2, \Delta m_{31}^2\}$ with statistical errors σ_n. We use the recent global fit values of neutrino data from NuFit4.0 [32]. Most of the observables follow an almost Gaussian distribution and we take a conservative approach using the smaller of the given uncertainties in our computations except for θ_{23}^l and δ^l. The best fit from NuFit4.0 is for normal mass ordering with inverted ordering being disfavoured with a $\Delta\chi^2 = 4.7(9.3)$ without (with) the Super-Kamiokande atmospheric neutrino data analysis. We tried a fit to inverted mass ordering and we found a $\chi^2 \sim 6800$, therefore in the following results we only focus in the case of normal mass ordering.

The model predictions are shown in table 4.5. The neutrino mass matrix in equation 4.41 predicts maximal atmospheric mixing angle, $\theta_{23}^l = 45^\circ$, and maximal CP violation, $\delta^l = -90^\circ$, within the 3σ region from the latest neutrino oscillation data. This is a consequence of the $\mu\tau$-R symmetric form of the neutrino mass matrix when y, y_1, y_2 are

[1] Although the model only allows the weights $\alpha = 0$ and $\beta = 0, 6$, we tried a numerical fit with all possible combination of weights with the alignments in tables 4.3 and 4.4, and the only one that worked is the $\mu\tau$-R symmetric for $\alpha = \beta = 6$.

Observable	Data		Model
	Central value	1σ range	$\alpha = \beta = 6$
θ_{12}^{ℓ} /°	33.82	$33.06 \to 34.60$	33.82
θ_{13}^{ℓ} /°	8.610	$8.480 \to 8.740$	8.610
θ_{23}^{ℓ} /°	49.60	$48.40 \to 50.60$	45.
δ^{ℓ} /°	215.0	$186.0 \to 255.0$	270.
$\Delta m_{21}^2/(10^{-5}\,\mathrm{eV}^2)$	7.390	$7.190 \to 7.600$	7.390
$\Delta m_{31}^2/(10^{-3}\,\mathrm{eV}^2)$	2.525	$2.493 \to 2.558$	2.525
m_1 /meV			0
m_2 /meV			8.597
m_3 /meV			50.25
$\sum m_i$ /meV	$\lesssim 230$		58.85
α_{23} /°			180.
$m_{\beta\beta}$ /meV	$\lesssim$ 60-200		2.587

Table 4.5: Model predictions in the neutrino sector for weights $\alpha = \beta = 6$. The neutrino masses m_i as well as the Majorana phases are pure predictions of our model. We also predict maximal atmospheric mixing angle $\theta_{23}^{l} = 45^{\circ}$ and maximal CP phase $\delta^{l} = 270^{\circ}$. The bound on $\sum m_i$ is taken from[59]. The bound on $m_{\beta\beta}$ is taken from [60]. There is only one physical Majorana phase α_{23} since $m_1 = 0$.

real while y_3 is imaginary. Furthermore, since we only have two right-handed neutrinos, we predict a massless left-handed neutrino $m_1 = 0$ and there is only one physical Majorana phase α_{23} [230]. The bound on effective Majorana mass $m_{\beta\beta}$ [60] as well as the predicted value are also given in table 4.5.

The fit has been performed using the Mixing Parameter Tools (MPT) package [203]. The values of y, y_1, y_2 and y_3 are shown in table 4.6. Fit 1 shows a good fit where all of the dimensionless real parameters y are of $\mathcal{O}(1)$, however a large range of parameters can give an equally good fit, see for example Fit 2. The VEV ratios $|\tilde{\xi}, \tilde{v}_i|$ are parameters that do not enter the fit directly and they are chosen to reproduce the hierarchy between the fermion Yukawa couplings, making them more natural numbers. These VEV ratios also appear in the quark and charged-lepton mass matrices in equations 4.34 and 4.35. For different values of $|\tilde{\xi}|$ and $|\tilde{v}_2|$, as in Fit 1 and 2 in table 4.6, different dimensionless $\mathcal{O}(1)$ parameters y_i^d, y_i^e and y_{ij}^u can be used to give the correct mass of the down- and up-type quarks and charged leptons. In the case of the neutrino mass matrix, even for fixed $|\tilde{\xi}|$ and $|\tilde{v}_2|$, there is a large range of parameters y, y_1, y_2 and y_3 that can give a good fit to the observables, meaning that the modular forms for weight $\alpha = 6$ and $\beta = 6$ give a constrained form of the neutrino mass matrix which is phenomenologically suitable. For comparison, we also give the value of the χ^2 test function in the case of $\beta = 0$, in which we only have two free parameters y and y_1, and it goes up to $\chi^2 \sim 1500$, while for $\beta = 6$ with four free parameters we have found a perfect fit for a variety of values of y, y_1, y_2 and y_3.

Fit 1	
Parameter	Value
y	-1.28
y_1	0.66
y_2	-1.05
y_3	i 1.07
y_s^N	1
y_a^N	1
$\|\tilde{\xi}\|$	0.01
$\|\tilde{v}_2\|$	0.001

Fit 2	
Parameter	Value
y	-1.00
y_1	-1.00
y_2	-0.08
y_3	i 0.08
y_s^N	1
y_a^N	1
$\|\tilde{\xi}\|$	0.02
$\|\tilde{v}_2\|$	0.004

Table 4.6: Two different sets with the four input parameters y, y_1, y_2 and y_3 that enter into the neutrino mass matrix in equation 4.41, giving the correct PMNS observables.

4.4 Summary

In this chapter, we have presented the first example in the literature of a grand unified theory with a modular symmetry interpreted as a family symmetry. The theory is based on supersymmetric $SU(5)$ in 6D, where the two extra dimensions are compactified on a $T_2/\mathbb{Z}_2$ orbifold. We have shown that, if there is a finite modular symmetry, then it can only be A_4 with fixed modulus $\tau = \omega = e^{i2\pi/3}$ or $\tau = \omega + 1$. We emphasize that this is one of the main differences of the present chapter as compared to recent works with modular symmetries which regard the modulus τ as a free phenomenological parameter [212, 215]. By contrast, in the present chapter we assume a specific orbifold structure which fixes the modulus to one of only two values, where we focus on the case $\tau = \omega = e^{i2\pi/3}$, although we do not address the problem of moduli stabilisation.

We have shown that it is possible to construct a consistent model along these lines, which successfully combines an $SU(5)$ GUT group with the A_4 modular symmetry and a $U(1)$ shaping symmetry. In this model, the matter F brane field on the fixed points is assumed to respect an enhanced symmetry $A_4 \ltimes \mathbb{Z}_2$ which leads to an effective $\mu - \tau$ reflection symmetry at low energies, predicting maximal atmospheric angle and maximal CP phase. In addition, there are two right-handed neutrinos on the fixed points whose Yukawa couplings are determined by modular weights, leading to specific alignments that fix the Dirac mass matrix. The model also introduces two triplet flavons in the bulk, whose vacuum alignments are determined by orbifold boundary conditions, analogous to those responsible for Higgs doublet-triplet splitting. The charged lepton and down-type quarks have diagonal and hierarchical Yukawa matrices, with quark mixing due to a hierarchical up-quark Yukawa matrix with sufficiently high modular weight to provide quark CP violation.

The resulting model, summarised in tables 4.1 and 4.2, provides an economical and successful description of quark and lepton (including neutrino) masses and mixing angles

and CP phases. Indeed the quarks can be fit perfectly, consistently with $SU(5)$, using only $\mathcal{O}(1)$ parameters. In addition we obtain a very good fit for the lepton observables with $\chi^2 \approx 5(7)$ without (with) Super-Kamiokande data, using four $\mathcal{O}(1)$ parameters which determine the entire lepton mixing matrix U_{PMNS} and the light neutrino masses (8 observables), which implies that that the theory is quite predictive. The main predictions of the model are a normal neutrino mass hierarchy with a massless neutrino, and the $\mu - \tau$ reflection symmetry predictions $\theta_{23}^l = 45^\circ$ and CP phase $\delta^l = -90^\circ$, which will be tested soon.

Chapter 5

Flavourful Z' model to accommodate $R_{K^{(*)}}$ anomalies

Previously, we have been interested in flavour models at the grand unification scale, in which the Standard Model is embedded into a larger group such as $SO(10)$ in chapters 2 and 3 or $SU(5)$ in chapter 4. In general, one of the simplest extensions of the Standard Model that one could do is to introduce an additional gauged $U(1)'$, which could emerge as a remnant of larger group embeddings of the SM gauge group, with rank larger than 4. In this chapter, we are motivated to present one of such models to examine flavour at the electroweak scale and give a possible explanation to the present anomalies in semi-leptonic B-meson decays. The ideas presented in this chapter are mainly based on [4].

5.1 Introduction

Recently, the phenomenological motivation for considering non-universal Z' models has increased due to mounting evidence for semi-leptonic B-meson decays whose rates and differential distributions are inconsistent with those predicted by the Standard Model [231–233]. In particular, the LHCb Collaboration has reported a number of deviations from μ-e universality in $B \to K^{(*)} l^+ l^-$ decays. These decays are $b \to s$ flavour-changing neutral-current (FCNC) processes which in the Standard Model are only allowed involving electroweak loop Feynman diagrams, see figure 5.1a. Since FCNCs are forbidden at tree-level in the SM, they become sensitive to any new physics that introduce additional tree-level FCNC interactions as in figure 5.1b.

The couplings of leptons to electroweak gauge bosons are independent of their flavour, this is known as lepton universality (LU) in the Standard Model. The flavour-changing neutral-currents are a good way to test LU. Particularly, the ratios within a given range

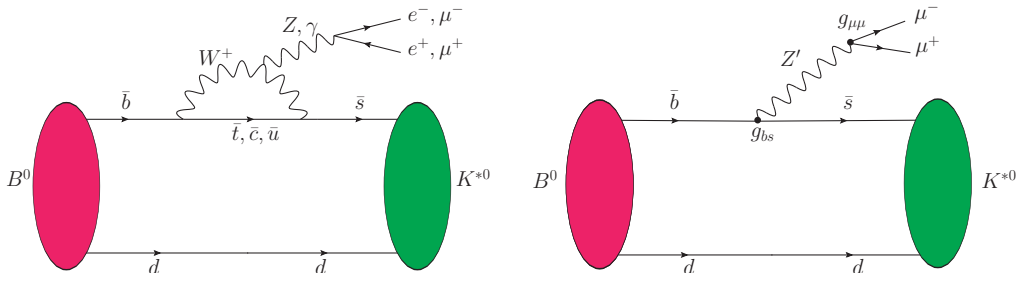

(a) One of the possible diagrams leading to B decays within the Standard Model.

(b) Tree-level contribution to B decays from a new Z' gauge boson.

Figure 5.1: Some of the diagrams responsible for B-meson decays in the model presented. On the left we show one of the the Standard Model contributions, while on the right we present the new tree-level contribution due to a new Z' gauge boson.

of the dilepton mass squared from q^2_{min} to q^2_{max} given by

$$R_{K^{(*)}} = \frac{\int_{q^2_{\text{min}}}^{q^2_{\text{max}}} \frac{\mathrm{d}\Gamma[B \to K^{(*)}\mu^+\mu^-]}{\mathrm{d}q^2}\mathrm{d}q^2}{\int_{q^2_{\text{min}}}^{q^2_{\text{max}}} \frac{\mathrm{d}\Gamma[B \to K^{(*)}e^+e^-]}{\mathrm{d}q^2}\mathrm{d}q^2}, \tag{5.1}$$

where Γ is the q^2-dependent partial width of the decay, are a reliable way to probe deviations from the SM predictions since some theoretical uncertainties cancel out in the ratio. Due to lepton universality, the ratios of $\mu^+\mu^-$ to e^+e^- final states R_K and R_{K^*} are expected to be close to unity in the Standard Model, however, these are observed to be about 70% of their expected values. The measurement of R_K [234] is reported for $1 < q < 6$ GeV^2 while the R_{K^*} [235] ratio is measured in two regions $0.045 < q^2 < 1.1$ GeV^2 and $1.1 < q^2 < 6.0$ GeV^2:

$$\begin{aligned} R_K &= 0.745^{+0.090}_{-0.074}(\text{stat}) \pm 0.036(\text{syst}) \quad \text{for } 1 < q < 6 \text{ GeV}^2 \,, \\ R_{K^*} &= \begin{cases} 0.66^{+0.11}_{-0.07}(\text{stat}) \pm 0.03(\text{syst}) & \text{for } 0.045 < q^2 < 1.1 \text{ GeV}^2, \\ 0.69^{+0.11}_{-0.07}(\text{stat}) \pm 0.05(\text{syst}) & \text{for } 1.1 < q^2 < 6.0 \text{ GeV}^2. \end{cases} \end{aligned} \tag{5.2}$$

Each measurement is displaying a 2.5σ deviation from the SM and combining that with the input from other $b \to s\ell^+\ell^-$ processes, the SM is disfavoured by 4 to 5 standard deviations [236, 237].

The R_K and R_{K^*} anomalies if confirmed, or equivalently, any conclusive observation of LU violation would indicate the evidence of new physics beyond the Standard Model (BSM). The B decay rates may be affected by the presence of new heavy BSM particles, which could couple differently to electrons and muons, violating lepton universality, and therefore could be responsible for the deviation between the $R_{K^{(*)}}$ measurements and the SM prediction.

A number of recent phenomenological analyses, see e.g. [236–244], conclude that these data can be well fit when the low-energy Lagrangian below the weak scale contains a

new physics operator of the $C_{9\mu}^{\rm NP} = -C_{10\mu}^{\rm NP}$ form, where $C_{9\mu}^{\rm NP}$ and $C_{10\mu}^{\rm NP}$ are the corresponding Wilson coefficients of the effective four-fermion contact interactions $O_{9\mu}^{\rm NP} = (\bar{b}\gamma^\mu P_L s)(\bar{\mu}\gamma^\mu \mu)$ and $O_{10\mu}^{\rm NP} = (\bar{b}\gamma^\mu P_L s)(\bar{\mu}\gamma^\mu\gamma_5 \mu)$. An operator of the form $C_{9\mu}^{\rm NP} = -C_{10\mu}^{\rm NP}$ leads to

$$\Delta\mathcal{L}_{\rm eff} \supset G_{bs\mu}(\bar{b}_L\gamma^\mu s_L)(\bar{\mu}_L\gamma_\mu \mu_L) + \text{H.c.}, \tag{5.3}$$

which fits the $R_{K^{(*)}}$ anomalies for

$$G_{bs\mu} \sim \frac{1}{(30\ \text{TeV})^2}. \tag{5.4}$$

In a flavourful Z' model, the new physics operator in equation 5.3 will arise from tree-level Z' exchange: $G_{bs\mu} = -\frac{g_{bs}g_{\mu\mu}}{M_{Z'}^2}$, where g_{bs} is the flavour-violating Z' coupling to left-handed b- and s-quarks, and $g_{\mu\mu}$ is the couplings to left-handed muons. There is already a vast literature discussing the Z' explanation of the B-anomalies and phenomenological constraints on the parameter space of such models, see e.g. [245–275]. In realistic models of this kind, the coupling g_{bs} is strongly constrained by precision measurements of the B_s meson mass difference. Taking that into account, one can derive the constraint $M_{Z'} \lesssim 1.2 g_{\mu\mu}$ TeV, implying that $M_{Z'}$ must be close to the weak scale in weakly coupled models. The corollary is that the Z' is in the correct mass range to act as mediator between the SM and thermally produced dark matter [276–282]. In this chapter we only discuss how this Z' model can account for the B-anomalies while in reference [4] it is shown that the same model can simultaneously explain the observed relic abundance via a weakly interacting massive particle (WIMP) communicating with the SM through the same Z'.

We follow reference [283], which introduces a fourth vector-like family with non-universal gauged $U(1)'$ charges. The idea is that the Z' couples universally to the three chiral families, which then mix with the non-universal fourth family to induce effective non-universal couplings in the physical light mixed quarks and leptons. Such a mechanism has wide applicability, for example it was recently discussed in the context of F-theory models with non-universal gauginos [284]. Two explicit examples were discussed in [283]. Firstly an $SO(10) \to SU(5) \times U(1)_X$ model, where we identified $U(1)' \equiv U(1)_X$, which however was subsequently shown to be not consistent with both explaining R_{K^*} and respecting the B_s mass difference [285]. Reference [283] also discussed a fermiophobic model where the gauged $U(1)'$ charges are not carried by the three chiral families, only by fourth vector-like family. In the absence of mixing, the Z' is fermiophobic, having no couplings to the three chiral families, but does couple to a fourth vector-like family. Due to mixing effects, we shall suppose that the Z' gets induced couplings to the second family of left-handed lepton doublets (containing the left-handed muon and its neutrino) and to the third family of left-handed quark doublets (containing the left-handed top and bottom quarks). Including only such couplings is enough to address the B-anomalies, in analogy to related scenarios where new vector-like fermions mix with

the SM ones [250, 253, 256, 258, 261, 268, 270, 275]. In addition, this set-up provides a natural WIMP dark matter candidate: the neutrino residing in the fourth family. We are interested in the parameter space of this model where the B-anomalies are explained, while in [4] it is shown that both B-anomalies and the relic abundance of dark matter can be simultaneously explained. Since the study of dark matter is not the aim of this thesis neither of this chapter, we shall not say anything else about it and we refer to [4] for the full analysis in which direct and indirect dark matter constraints are taken into account. Here, we present the model capable of explaining the B-anomalies and we show that this can be achieved without conflicting experimental constraints such as B_s mixing, LHC searches, neutrino trident, and so on.

5.2 The model

We consider a model in which, in addition to the Standard Model with the usual three chiral families of left-handed quarks and leptons, including the right-handed neutrinos, we add a dark $U(1)'$ gauge symmetry and a fourth vector-like family of fermions. The idea is to have the SM quarks and leptons neutral under the $U(1)'$ while the vector-like family has the SM quantum numbers and is charged under the $U(1)'$, leading to a dark matter candidate and flavour-changing Z' operators after the vector-like fermion mass term mix with the SM fermions.

Table 5.1 shows all the particle content and their corresponding representations and charges. The non-universal $U(1)'$ charges forbid mixing between the fourth family and the chiral families via the usual Higgs Yukawa couplings. Therefore, we need to add new singlet scalars, with appropriate $U(1)'$ charges, to generate mass mixing of quarks and leptons with the vector-like family. The $U(1)'$ is broken by the VEVs of the new Higgs singlets ϕ_ψ to yield a massive Z'.

The Higgs Yukawa couplings of the first three chiral families can be written in a 4×4 matrix notation

$$\mathcal{L}^{\text{Yukawa}} = y^u \bar{Q}_L \tilde{H} u_R + y^d \bar{Q}_L H d_R + y^e \bar{L}_L H e_R + y^\nu \bar{L}_L \tilde{H} \nu_R + \text{H.c.} \,, \tag{5.5}$$

where $\tilde{H} = i\sigma_2 H^*$ and y^u, y^d, y^e, y^ν are 4×4 matrices with the fourth row and columns consisting of all zeros, since the fourth family does not couple to the Higgs doublets. The $U(1)'$ charges allow Yukawa couplings between the singlet fields ϕ, the fourth family $\tilde{\psi}_4$ and the first three chiral families ψ_i. Furthermore, there is an explicit mass term between the opposite chirality fourth family fields ψ_4 and $\tilde{\psi}_4$,

$$\begin{aligned}\mathcal{L}^{\text{mass}} = {} & x_i^Q \phi_Q \bar{Q}_{Li} \tilde{Q}_{R4} + x_i^u \phi_u \bar{\tilde{u}}_{L4} u_{Ri} + x_i^d \phi_d \bar{\tilde{d}}_{L4} d_{Ri} + x_i^L \phi_L \bar{L}_{Li} \tilde{L}_{R4} + x_i^e \phi_e \bar{\tilde{e}}_{L4} e_{Ri} \\ & + M_4^Q \bar{Q}_{L4} \tilde{Q}_{R4} + M_4^u \bar{\tilde{u}}_{L4} u_{R4} + M_4^d \bar{\tilde{d}}_{L4} d_{R4} + M_4^L \bar{L}_{L4} \tilde{L}_{R4} + M_4^e \bar{\tilde{e}}_{L4} e_{R4} \\ & + M_4^\nu \bar{\tilde{\nu}}_{L4} \nu_{R4} + \text{H.c.} \,,\end{aligned} \tag{5.6}$$

Field	Representation/charge			
	$SU(3)_c$	$SU(2)_L$	$U(1)_Y$	$U(1)'$
Q_{Li}	**3**	**2**	$1/6$	0
u_{Ri}	**3**	**1**	$2/3$	0
d_{Ri}	**3**	**1**	$-1/3$	0
L_{Li}	**1**	**2**	$-1/2$	0
e_{Ri}	**1**	**1**	-1	0
ν_{Ri}	**1**	**1**	0	0
H	**1**	**2**	$1/2$	0
$Q_{L4}, \tilde{Q}_{R4}$	**3**	**2**	$1/6$	q_{Q4}
$u_{R4}, \tilde{u}_{L4}$	**3**	**1**	$2/3$	q_{u4}
$d_{R4}, \tilde{d}_{L4}$	**3**	**1**	$-1/3$	q_{d4}
$L_{L4}, \tilde{L}_{R4}$	**1**	**2**	$-1/2$	q_{L4}
$e_{R4}, \tilde{e}_{L4}$	**1**	**1**	-1	q_{e4}
$\nu_{R4}, \tilde{\nu}_{L4}$	**1**	**1**	0	$q_{\nu 4}$
$\phi_{Q,u,d,L,e}$	**1**	**1**	0	$-q_{Q_4,u_4,d_4,L_4,e_4}$

Table 5.1: The model consists of the usual three chiral families of quarks and leptons ψ_i ($i = 1, 2, 3$), including the right-handed neutrino, a Higgs doublet H, plus a fourth vector-like family of fermions $\psi_4, \tilde{\psi}_4$ and new Higgs singlets ϕ_ψ which mix fourth family fermions with the three chiral families. Note that we exclude ϕ_ν so that $\nu_{R4}, \tilde{\nu}_{L4}$ do not mix and are stable.

where $i = 1, ..., 3$.

The fourth-family vector-like singlet neutrinos $\nu_{R4}, \tilde{\nu}_{L4}$ are special since we do not have a singlet field ϕ_ν that couples them to the other families, which is why such terms are absent in the above equation. This implies that $\nu_{R4}, \tilde{\nu}_{L4}$ are absolutely stable, with their stability guaranteed by an unbroken global $U(1)_{\nu_{R4}}$ and, since they do not carry any Standard Model quantum numbers, they may play the role of dark matter. Note that we also impose lepton number conservation $U(1)_L$ for all four families of leptons which forbids Majorana mass terms. Hence all neutrinos (including those in the fourth vector-like family) will have purely Dirac masses.[1]

After the singlet scalar fields ϕ obtain a non-zero vacuum expectation value (VEV), we may rewrite the Lagrangian in terms of new mass parameters $M_i^Q = x_i^Q \langle \phi_Q \rangle$, similarly for the other mass parameters, such that

$$\begin{aligned}\mathcal{L}^{\text{mass}} = {} & M_\alpha^Q \bar{Q}_{L\alpha} \tilde{Q}_{R4} + M_\alpha^u \bar{\tilde{u}}_{L4} u_{R\alpha} + M_\alpha^d \bar{\tilde{d}}_{L4} d_{R\alpha} + M_\alpha^L \bar{L}_{L\alpha} \tilde{L}_{R4} + M_\alpha^e \bar{\tilde{e}}_{L4} e_{R\alpha} \\ & + M_4^\nu \bar{\tilde{\nu}}_{L4} \nu_{R4} + \text{H.c.} \,,\end{aligned} \tag{5.7}$$

where $\alpha = 1, ..., 4$. We may diagonalize the mass matrix before electroweak symmetry

[1] Alternatively it is possible to introduce various seesaw mechanisms into this kind of model, leading to Majorana masses, as recently discussed [285]. However in this chapter we only consider Dirac neutrinos.

breaking, when only the fourth family is massive

$$\begin{aligned}\mathcal{L}^{\text{mass}} = \tilde{M}_4^Q \bar{Q'}_{L4} \tilde{Q}_{R4} + \tilde{M}_4^u \bar{\tilde{u}}_{L4} u'_{R4} + \tilde{M}_4^d \bar{\tilde{d}}_{L4} d'_{R4} + \tilde{M}_4^L \bar{L'}_{L4} \tilde{L}_{R4} + \tilde{M}_4^e \bar{\tilde{e}}_{L4} e'_{R4} \\ + M_4^\nu \bar{\tilde{\nu}}_{L4} \nu_{R4} + \text{H.c.}\end{aligned} \tag{5.8}$$

The prime states for the heavy mass basis where only the fourth family has explicit vector-like Dirac mass terms and it is related to the original charge basis by unitary mixing matrices,

$$Q'_L = V_{Q_L} Q_L, \quad u'_R = V_{u_R} u_R, \quad d'_R = V_{d_R} d_R, \quad L'_L = V_{L_L} L_L, \quad e'_R = V_{e_R} e_R, \tag{5.9}$$

while for the neutrino states $\tilde{\nu}_{L4}$ and ν_{R4} the original and the mass basis coincides. In this basis, the Yukawa couplings in equation 5.5 become

$$\mathcal{L}^{\text{Yukawa}} = y'^u \bar{Q'}_L \tilde{H} u'_R + y'^d \bar{Q'}_L H d'_R + y'^e \bar{L'}_L H e'_R + y'^\nu \bar{L'}_L \tilde{H} \nu_R + \text{H.c.}\ , \tag{5.10}$$

where

$$y'^u = V_{Q_L} y^u V_{u_R}^\dagger, \quad y'^d = V_{Q_L} y^d V_{d_R}^\dagger, \quad y'^e = V_{L_L} y^e V_{e_R}^\dagger \quad y'^\nu = V_{L_L} y^\nu. \tag{5.11}$$

This shows that there is a coupling between the heavy fourth family and the Higgs due to their mixing with the first three chiral families. However, this coupling will be small since the original y^u, y^d, y^e, y^ν contain zeroes in the fourth row and column and they are mixing suppressed. Therefore, we can integrate out the fourth family and look at the low energy effective theory by simply removing the fourth rows and columns of the primed Yukawa matrices in equation 5.10. The three massless families, below the heavy mass scale, are described by

$$\mathcal{L}^{\text{Yukawa}}_{\text{light}} = y'^u_{ij} \bar{Q'}_{Li} \tilde{H} u'_{Rj} + y'^d_{ij} \bar{Q'}_{Li} H d'_{Rj} + y'^e_{ij} \bar{L'}_{Li} H e'_{Rj} + y'^\nu_{ij} \bar{L'}_{Li} \tilde{H} \nu_{Rj} + \text{H.c.}\ , \tag{5.12}$$

where

$$y'^u_{ij} = (V_{Q_L} y^u V_{u_R}^\dagger)_{ij}, \quad y'^d_{ij} = (V_{Q_L} y^d V_{d_R}^\dagger)_{ij}, \quad y'^e_{ij} = (V_{L_L} y^e V_{e_R}^\dagger)_{ij}, \quad y'^\nu_{ij} = (V_{L_L} y^\nu)_{ij} \tag{5.13}$$

and $i, j = 1, ..., 3$. The Yukawa matrices for the quarks and charged leptons can be now diagonalized

$$V'_{uL} y'^u V'^\dagger_{uR} = \text{diag}(y_u, y_c, y_t), \quad V'_{dL} y'^d V'^\dagger_{dR} = \text{diag}(y_d, y_s, y_b), \quad V'_{eL} y'^e V'^\dagger_{eR} = \text{diag}(y_e, y_\mu, y_\tau). \tag{5.14}$$

The unitary CKM matrix is then given by

$$V_{\text{CKM}} = V'_{uL} V'^\dagger_{dL}. \tag{5.15}$$

In the case of neutrinos, since we are forbidding Majorana masses, the light physical

neutrinos have Dirac mass eigenvalues given by,

$$vV'_{\nu L}y'^{\nu}V'^{\dagger}_{\nu R} = \text{diag}(m_1, m_2, m_3). \tag{5.16}$$

The lepton mixing matrix or PMNS matrix can be constructed from the transformations in equations 5.14 and 5.16

$$V_{\text{PMNS}} = V'_{eL}V'^{\dagger}_{\nu L}. \tag{5.17}$$

To look at the Lagrangian involving the SM gauge couplings, we emphasize that all the four families have the same charges under the SM. The unitary transformations in equation 5.9 cancel as in the usual GIM mechanism [21] and the gauge couplings in the heavy mass basis remains the same as in the SM. After integrating out the fourth family and electroweak symmetry is broken, and the light Yukawa matrices are diagonalised, the couplings to the $W^{\pm}$ gauge bosons are

$$\begin{aligned}\mathcal{L}_W^{\text{int}} = &\frac{g}{\sqrt{2}}\begin{pmatrix}\bar{u}_L & \bar{c}_L & \bar{t}_L\end{pmatrix}V_{\text{CKM}}W^+_\mu\gamma^\mu\begin{pmatrix}d_L\\ s_L\\ b_L\end{pmatrix}\\ &+\frac{g}{\sqrt{2}}\begin{pmatrix}\bar{e}_L & \bar{\mu}_L & \bar{\tau}_L\end{pmatrix}V_{\text{PMNS}}W^+_\mu\gamma^\mu\begin{pmatrix}\nu_{1L}\\ \nu_{2L}\\ \nu_{3L}\end{pmatrix}+\text{H.c.},\end{aligned} \tag{5.18}$$

where g is the usual $SU(2)_L$ gauge coupling. For the couplings to the Z gauge boson, the same happens, the charges are the same for the fourth families and the transformations in equation 5.9 cancel, such that in the heavy mass basis, after electroweak symmetry breaking, we are left with

$$\mathcal{L}_Z^{\text{int}} = \frac{e}{2s_W c_W}\bar{\psi}'_\alpha Z_\mu\gamma^\mu(C_V^\psi - C_A^\psi\gamma_5)\psi'_\alpha \tag{5.19}$$

where

$$\psi'_\alpha = u'_\alpha, d'_\alpha, e'_\alpha, \nu'_\alpha \quad \alpha = 1, ..., 4 \tag{5.20}$$

and

$$C_A^\psi = t_3, \quad C_V^\psi = t_3 - 2s_W^2 Q. \tag{5.21}$$

The electric charge of the fermions is denoted by Q and t_3 are the eigenvalues of $\sigma_3/2$. The couplings to the Z boson are flavour diagonal, even after diagonalization of the light fermion mass matrices, due to the unitary transformations cancelling. The interactions will be the same as in equation 5.19, replacing the fields ψ'_α by their three family mass eigenstates.

In the case of the couplings to the Z' gauge bosons, we have non-universal couplings that lead to flavour changing. In the original basis, after the $U(1)'$ symmetry is broken, we have diagonal gauge couplings between the massive Z' gauge boson and the four

families

$$\mathcal{L}^{\text{gauge}}_{Z'} = g' Z'_\mu (\bar{Q}_L D_Q \gamma^\mu Q_L + \bar{u}_R D_u \gamma^\mu u_R + \bar{d}_R D_d \gamma^\mu d_R + \bar{L}_L D_L \gamma^\mu L_L + \bar{e}_R D_e \gamma^\mu e_R) \quad (5.22)$$

where,

$$\begin{aligned} D_Q &= \text{diag}(0,0,0,q_{Q4}), \quad D_u = \text{diag}(0,0,0,q_{u4}), \quad D_d = \text{diag}(0,0,0,q_{d4}) \\ D_L &= \text{diag}(0,0,0,q_{L4}), \quad D_e = \text{diag}(0,0,0,q_{e4}), \quad D_\nu = \text{diag}(0,0,0,q_{d4}). \end{aligned} \quad (5.23)$$

In addition there are the fourth family couplings involving the opposite chirality states $\tilde{\psi}_4$. Using the transformations in equation 5.9, we get the Z' couplings in the diagonal heavy mass basis

$$\mathcal{L}^{\text{gauge}}_{Z'} = g' Z'_\mu (\bar{Q'}_L D'_Q \gamma^\mu Q'_L + \bar{u'}_R D'_u \gamma^\mu u'_R + \bar{d'}_R D'_d \gamma^\mu d'_R + \bar{L'}_L D'_L \gamma^\mu L'_L + \bar{e'}_R D'_e \gamma^\mu e'_R) \quad (5.24)$$

where $D'_Q = V_{Q_L} D_Q V^\dagger_{Q_L}$, and similarly with $Q \to L$, etc. Ignoring phases, these matrices can be parametrized as

$$D'_Q = q_{Q_4} \begin{pmatrix} s^2_{14} & c_{14}s_{14}s_{24} & c_{14}c_{24}s_{14}s_{34} & c_{14}c_{24}c_{34}s_{14} \\ c_{14}s_{14}s_{24} & c^2_{14}s^2_{24} & c^2_{14}c_{24}s_{24}s_{34} & c^2_{14}c_{24}c_{34}s_{24} \\ c_{14}c_{24}s_{14}s_{34} & c^2_{14}c_{24}s_{24}s_{34} & c^2_{14}c^2_{24}s^2_{34} & c^2_{14}c^2_{24}c_{34}s_{34} \\ c_{14}c_{24}c_{34}s_{14} & c^2_{14}c_{24}c_{34}s_{24} & c^2_{14}c^2_{24}c_{34}s_{34} & c^2_{14}c^2_{24}c^2_{34} \end{pmatrix} \quad (5.25)$$

where s_{ij} and c_{ij} refer to $\sin\theta_{ij}$ and $\cos\theta_{ij}$ (we have also suppressed the superscript in the angles $s^Q_{14} \to s_{14}$ for simplicity). Since the $U(1)'$ charges differ for the fourth family, the unitary transformations do not cancel and the matrices D'_Q, etc., are not generally diagonal. Therefore, Z' exchange can couple to light families of different flavour.

We are interested in the $\bar{s}bZ'$ and $\bar{\mu}\mu Z'$ couplings, needed for the $R_{K^{(*)}}$ anomalies. Assuming that only the mixing angles $\theta^{Q_L}_{34}$ and $\theta^{L_L}_{24}$ are different from zero[2] the mixing mass matrices become

$$D'_Q = q_{Q_4} \begin{pmatrix} 0 & 0 & 0 & 0 \\ 0 & 0 & 0 & 0 \\ 0 & 0 & (s^Q_{34})^2 & c^Q_{34}s^Q_{34} \\ 0 & 0 & c^Q_{34}s^Q_{34} & (c^Q_{34})^2 \end{pmatrix}, \quad D'_L = q_{L_4} \begin{pmatrix} 0 & 0 & 0 & 0 \\ 0 & (s^L_{24})^2 & 0 & c^L_{24}s^L_{24} \\ 0 & 0 & 0 & 0 \\ 0 & c^L_{24}s^L_{24} & 0 & (c^L_{24})^2 \end{pmatrix}, \quad (5.26)$$

while the rest of them being zero. In the low energy effective theory, after integrating out the fourth heavy family, the Z' couplings to the three massless families of quarks

[2] A more natural possibility would be to assume that the new vector-like fermions have a large mixing only with the 3rd generation of the SM doublet, that is with taus instead of muons. Then the coupling to muons could arise due to a mixing between the SM charged leptons, as in [283]. However, explaining the B-meson anomalies in such a set-up runs in conflict with the strong bounds from non-observation of $\tau \to 3\mu$.

and leptons are

$$\mathcal{L}_{Z'}^{\text{gauge}} = g' Z'_\mu \left(q_{Q_4} (s_{34}^Q)^2 \bar{Q}'_{L_3} \gamma^\mu Q'_{L_3} + q_{L_4} (s_{24}^L)^2 \bar{L}'_{L_2} \gamma^\mu L'_{L_2} \right), \tag{5.27}$$

where $Q'_{L3} = (t'_L, b'_L)$ and $L'_{L2} = (\nu'_{\mu L}, \mu'_L)$. Using now the diagonalization of the Yukawa matrices in equation 5.14, we can expand the primed fields in terms of the mass eigenstates,

$$\begin{aligned} b'_L &= (V'^\dagger_{dL})_{31} d_L + (V'^\dagger_{dL})_{32} s_L + (V'^\dagger_{dL})_{33} b_L \\ t'_L &= (V'^\dagger_{uL})_{31} u_L + (V'^\dagger_{uL})_{32} c_L + (V'^\dagger_{uL})_{33} t_L \\ \nu'_{\mu L} &= (V'^\dagger_{\nu L})_{21} \nu_{1L} + (V'^\dagger_{\nu L})_{22} \nu_{2L} + (V'^\dagger_{\nu L})_{23} \nu_{3L} \\ \mu'_L &= (V'^\dagger_{eL})_{21} e_L + (V'^\dagger_{eL})_{22} \mu_L + (V'^\dagger_{eL})_{23} \tau_L. \end{aligned} \tag{5.28}$$

For simplicity, we assume that the charged lepton mass matrix is diagonal so that we may drop the primes on the muon field so that $\mu'_L = \mu_L$. Under this assumption, in the lepton sector, the Z' only couples to muon mass eigenstates μ_L and muon neutrinos $\nu_{\mu L}$, where the latter are related to neutrino mass eigenstates by the PMNS matrix,

$$\nu'_{\mu L} = (V_{\text{PMNS}})_{21} \nu_{1L} + (V_{\text{PMNS}})_{22} \nu_{2L} + (V_{\text{PMNS}})_{23} \nu_{3L} \tag{5.29}$$

Given the hierarchies of the CKM matrix, we will assume similar hierarchies of the rotation matrix elements:

$$|(V'_{(d,u)L})_{31}|^2 \ll |(V'_{(d,u)L})_{32}|^2 \ll |(V'_{(d,u)L})_{33}|^2 \approx 1 \tag{5.30}$$

The vector-like neutrino ν_4 is not charged under the SM and can be considered as a dark matter candidate [4]. The portal that allows it to annihilate into ordinary matter is the Z' mediator. The explicit coupling between the Z' and the dark matter candidate ν_4 is

$$\mathcal{L}_{Z'}^{\nu_4} = g' q_{\nu_4} Z'_\mu \bar{\nu}_4 \gamma^\mu \nu_4, \tag{5.31}$$

where the Dirac dark matter field is given by $\nu_4 = \tilde{\nu}_{4L} + \nu_{4R}$ with a Dirac mass $m_\nu \bar{\nu}_4 \nu_4$ where we have defined $m_\nu \equiv M_4^\nu$.

We finish this section by summarizing all non-SM interactions that will later be relevant for our phenomenological analysis, introducing the notation that we shall subsequently use:

$$\mathcal{L} \supset Z'_\mu \left(g_{bb} \bar{q}_L \gamma^\mu q_L + g_{bs} \bar{b}_L \gamma^\mu s_L + g_{\mu\mu} \bar{\ell}_L \gamma^\mu \ell_L + g_{\nu\nu} \bar{\nu}_4 \gamma^\mu \nu_4 \right), \tag{5.32}$$

where $q_L = (t_L, b_L)^T$, $\ell_L = (\nu_{\mu\, L}, \mu_L)^T$, $g_{bb} = g' q_{Q4} (s_{34}^Q)^2$, $g_{bs} = g_{bb} (V'^\dagger_{dL})_{32}$, $g_{\mu\mu} = g' q_{L_4} (s_{24}^L)^2$, $g_{\nu\nu} = g' q_{\nu_4}$. We expect $|(V'^\dagger_{dL})_{32}| \lesssim |V_{ts}|$, where $|V_{ts}| \approx 0.04$ is the 3-2

entry of the CKM matrix, as otherwise unnatural cancellations would be required. It follows that $|g_{bs}| \lesssim |V_{ts} g_{bb}|$; in the following for simplicity we assume $g_{bs} = V_{ts} g_{bb}$, and that g_{bb} and $g_{\mu\mu}$ have the same sign. Thus, the relevant parameter space is 5-dimensional: 3 couplings (g_{bb}, $g_{\mu\mu}$, $g_{\nu\nu}$) and 2 masses ($M_{Z'}$ and the dark matter mass m_ν). From the theory point of view these are all essentially free parameters, although one naturally expects $g_{\nu\nu} \gg g_{bb}, g_{\mu\mu}$ in the absence of large mixings or large hierarchies of $U(1)'$ charges. These parameters are then constrained by flavour physics, multiple low-energy precision measurements, colliders, and dark matter detection experiments. In the following section we identify the regions of the parameter space where the B-anomalies can be explained without conflicting any existing experimental data, considering only a three-dimensional parameter space: $(g_{bb}, g_{\mu\mu}, M_{Z'})$. The whole analysis including the dark matter constraints can be found in [4]. We note that Z' models simultaneously addressing the B-anomalies and dark matter have been previously discussed in [276–282]. In particular, reference [279] performed a detailed analysis of collider, precision, dark matter constraints in a similar model based on gauged $L_\mu - L_\tau$ symmetry. The main practical difference between our setup and that model is the presence of Z' couplings to b-quarks in equation 5.32, which affects the LHC phenomenology.

5.3 $R_{K^{(*)}}$ anomalies and flavour constraints

In this section we review and update the constraints on the parameter space of Z' models motivated by the current B-meson anomalies. One possible explanation of the R_K and R_{K^*} measurements in LHCb is that the low-energy Lagrangian below the weak scale contains an additional contribution to the effective 4-fermion operator with left-handed muon, b-quark, and s-quark fields:

$$\Delta\mathcal{L}_{\text{eff}} \supset G_{bs\mu}(\bar{b}_L \gamma^\mu s_L)(\bar{\mu}_L \gamma_\mu \mu_L) + \text{H.c.}, \qquad G_{bs\mu} \approx \frac{1}{(31.5\ \text{TeV})^2}. \tag{5.33}$$

Above, the numerical value of the effective coefficient corresponds to the best fit quoted in [237]. In our model, this operator arises from tree-level Z' exchange and the analogous operator with μ_L replaced by e_L does not appear due to vanishing charged lepton mixing. We can express the coefficient $G_{bs\mu}$ as function of the couplings in equation 5.32,

$$G_{bs\mu} = -\frac{g_{bs} g_{\mu\mu}}{M_{Z'}^2} = -\frac{V_{ts} g_{bb} g_{\mu\mu}}{M_{Z'}^2}. \tag{5.34}$$

Together, equations (5.33) and (5.34) imply the constraint on the parameters g_{bb}, $g_{\mu\mu}$ and $M_{Z'}$:

$$\frac{g_{bb} g_{\mu\mu}}{M_{Z'}^2} \approx \frac{1}{(6.4\ \text{TeV})^2}. \tag{5.35}$$

There are additional constraints on these parameters coming from flavour physics and

low-energy precision measurements. In the following we determine the region of the parameter space where the $R_{K^{(*)}}$ anomalies can be explained without conflicting other experimental data.

5.3.1 $B_s - \overline{B}_s$ mixing

The Z' coupling to bs leads to an additional tree-level contribution to $B_s - \overline{B}_s$ mixing. Low-energy observables are affected by the effective operator arising from integrating out the Z' at tree level:

$$\Delta\mathcal{L}_{\text{eff}} \supset -\frac{G_{bs}}{2}(\bar{s}_L\gamma^\mu b_L)^2 + \text{h.c}, \qquad G_{bs} = \frac{g_{bs}^2}{M_{Z'}^2} = \frac{g_{bb}^2 V_{ts}^2}{M_{Z'}^2}. \tag{5.36}$$

Such a new contribution is highly constrained by the measurements of the mass difference ΔM_s of neutral B_s mesons. In this chapter we follow the recent analysis of reference [286] which, using updated lattice results, obtains a stronger bound on G_{bs}:

$$-\frac{1}{(180\text{ TeV})^2} \lesssim G_{bs} \lesssim \frac{1}{(770\text{ TeV})^2}, \qquad @\,95\%\text{CL}. \tag{5.37}$$

The resulting constraints in the $(g_{\mu\mu}, g_{bb})$ plane are shown as the light blue region in figure 5.2. The updated constraint is particularly strong for the models that generate a strictly positive G_{bs} [286] (as is the case in Z' models) due to the $\sim 1.8\sigma$ discrepancy between the measured ΔM_s and the updated SM predictions which favours $G_{bs} < 0$. As a consequence, Z' models explaining the B-meson anomalies requires $M_{Z'} \lesssim 1$ TeV, assuming weak coupling $g_{\mu\mu} \lesssim 1$. For easy reference, we also show the B_s mixing constraints based on the previous SM determination of ΔM_s [287], $-\frac{1}{(160\text{ TeV})^2} \lesssim G_{bs} \lesssim \frac{1}{(140\text{ TeV})^2}$, see the dark blue region in figure 5.2 labelled "B_s mixing 2015".

5.3.2 Neutrino trident

The Z' coupling to left-handed muons leads to a new tree-level contribution to the effective 4-lepton interaction

$$\Delta\mathcal{L}_{\text{eff}} \supset -\frac{G_\mu}{2}(\bar{\ell}_L\gamma^\mu\ell_L)^2, \qquad G_\mu = \frac{g_{\mu\mu}^2}{M_{Z'}^2}. \tag{5.38}$$

This operator is constrained by the trident production $\nu_\mu\gamma^* \to \nu_\mu\mu^+\mu^-$ [288–290]. Using the results of the global fit in [291], the bound on the effective coefficient is given by

$$-\frac{1}{(390\text{ GeV})^2} \lesssim G_\mu \lesssim \frac{1}{(370\text{ GeV})^2}, \qquad @\,95\%\text{CL}. \tag{5.39}$$

The limits in the $(g_{\mu\mu}, g_{bb})$ plane are shown as the orange region in figure 5.2. Since the trident constraints probe much lower scales than the B_s mixing, a much larger Z'

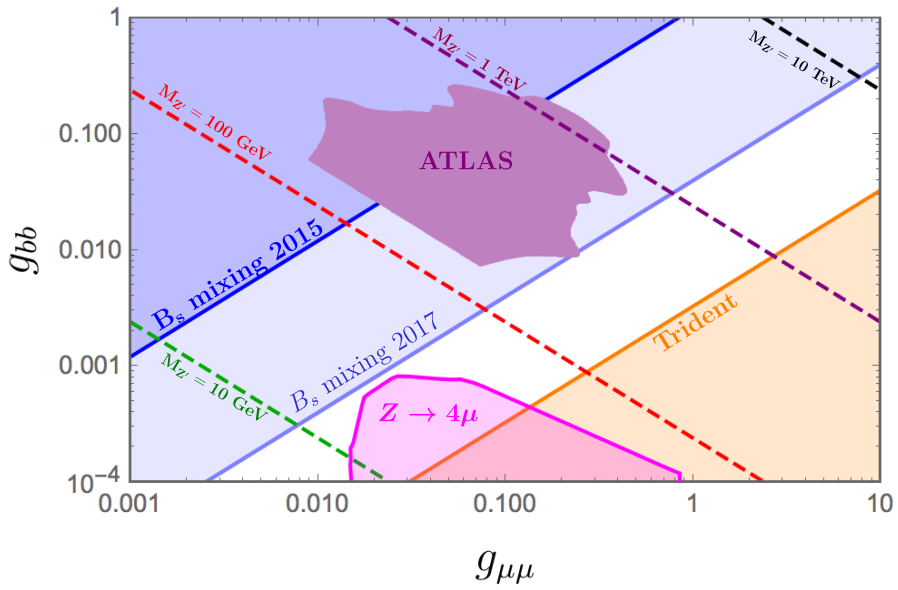

Figure 5.2: The parameter space in the $(g_{\mu\mu}, g_{bb})$ plane compatible with $R_{K^{(*)}}$ anomalies and flavour constraints (white). The Z' mass varies over the plane, with a unique Z' mass for each point in the plane as determined by equation 5.35. We show the recent B_s mixing constraints (light blue), the trident bounds (orange), the $Z \to 4\mu$ constraints (pink), and the ATLAS constraints from dimuon resonances $Z' \to \mu\mu$ (purple); for reference we also display the previous weaker B_s mixing bounds (dark blue). The green, red, purple and black lines correspond to $M_{Z'} = 10, 100, 1000, 10000$ GeV respectively.

coupling to muons is allowed, $g_{\mu\mu} \gtrsim 1$ for a heavy enough Z'. Nevertheless, together with the B_s mixing constraints, the trident leaves only a narrow sliver of the parameter space that could address the B meson anomalies.

5.3.3 LHC searches

Further constraints on our model come from collider searches. For light Z' masses, the LHC measurements of the Z decays to four muons, with the second muon pair produced in the SM via a virtual photon [292, 293], $pp \to Z \to 4\mu$, sets relevant constraints in the low mass region of Z' models, $5 \lesssim M_{Z'} \lesssim 70$ GeV. The $Z \to 4\mu$ constraints on the magnitude of the Z' coupling to muons were analysed in [247, 279, 290]. Projecting these results onto our model, the excluded parameter space is marked as the pink regions in figures 5.2 and 5.3 and in the upper-left panel of figure 5.4. All in all, the $Z \to 4\mu$ constraint is non-trivial but for any Z' mass it always leaves some available parameter space to explain the B-meson anomalies.

For a heavier Z', the strongest constraints comes from LHC dimuon resonance searches, $pp \to Z' \to \mu^+\mu^-$, see also [269]. In our model the Z' is dominantly produced at the LHC through its couplings to bottom quarks, $b\bar{b} \to Z'$. The cross section $\sigma(pp \to Z')$ from $b\bar{b}$ collisions is taken from figure 3 of reference [294]. The contribution of bottom-strange collisions, which is secondary in our model, is estimated using `Madgraph` [295].

The Z' boson can subsequently decay into muons, muon neutrinos, bottom or strange quarks, and also into top quarks and dark matter when kinematically allowed. The partial decay widths are given by

$$\begin{aligned}
\Gamma_{Z'\to\mu\bar{\mu}} &= \frac{1}{24\pi} g_{\mu\mu}^2 M_{Z'} = \Gamma_{Z'\to\nu_\mu\bar{\nu}_\mu}, \\
\Gamma_{Z'\to b\bar{b}} &= \frac{1}{8\pi} g_{bb}^2 M_{Z'}, \qquad \Gamma_{Z'\to b\bar{s}} = \frac{1}{8\pi} g_{bb}^2 V_{ts}^2 M_{Z'}, \\
\Gamma_{Z'\to t\bar{t}} &= \frac{1}{8\pi} g_{bb}^2 M_{Z'} \left(1 - \frac{m_t^2}{M_{Z'}^2}\right) \sqrt{1 - \frac{4m_t^2}{M_{Z'}^2}}, \\
\Gamma_{Z'\to\nu_4\bar{\nu}_4} &= \frac{1}{24\pi} g_{\nu\nu}^2 M_{Z'} \left(1 - \frac{m_\nu^2}{M_{Z'}^2}\right) \sqrt{1 - \frac{4m_\nu^2}{M_{Z'}^2}},
\end{aligned} \tag{5.40}$$

from which we calculate $\mathrm{Br}(Z' \to \mu\mu)$ analytically. Then $\sigma(pp \to Z' \to \mu\mu)$ is estimated using the narrow-width approximation, and compared with the limits from the recent dimuon resonance search by ATLAS [296], which allows us to constrain Z' masses between 150 GeV and 5 TeV. We verified that the analogous Tevatron analyses give weaker constraints, also in the low mass regime. Figure 5.4 shows the ATLAS constraints for specific Z' masses (200, 500 and 1000 GeV) with dark matter couplings set to zero and arbitrary $(g_{\mu\mu}, g_{bb})$ couplings. Figure 5.2 shows the same limits for the Z' mass fixed in function of $(g_{\mu\mu}, g_{bb})$ by the condition in equation 5.35. In the plane $(g_{\mu\mu}, g_{bb})$, the Z' mass is fixed to explain the observed $R_{K^{(*)}}$ anomalies, therefore for each $g_{\mu\mu}$, g_{bb} and Z' mass we compute the cross section and we check if this is excluded by ATLAS or not. We conclude that in the parameter space of our model relevant for explaining the B-meson anomalies the ATLAS dimuon limits are always weaker that the new B_s mixing constraints.

5.3.4 Constraints from lepton-flavour violation

So far we were assuming zero mixing in the charged-lepton sector. It is interesting to discuss the constraints resulting from relaxing that assumption. In particular, for a non-vanishing mixing angle between charged leptons of the second and first generations $(V'_{eL})_{21} \neq 0$, a non-diagonal Z' coupling to left-handed muons and electrons would be present

$$\mathcal{L} \supset g_{\mu\mu} (V'_{eL})_{21} \bar{\mu}_L \gamma^\mu e_L Z'_\mu + \text{H.c.} \,, \tag{5.41}$$

which could generate an additional contribution to the transition $\mu \to e\gamma$ whose partial decay width can be estimated, according to [270], as

$$\Gamma(\mu \to e\gamma) \simeq \frac{\alpha\, m_\mu^5}{1024\pi^4 M_{Z'}^4} g_{\mu\mu}^4 |V'_{eL}|_{21}^2 F^2(m_\mu^2/M_{Z'}^2) \,, \tag{5.42}$$

where $F(x)$ is a loop function, as defined in [270], whose limit for $M_{Z'} \gg m_\mu$ is $\lim_{x\to 0} F(x) = 2/3$. The branching ratio of $\mu \to e\gamma$ is severely constrained by the

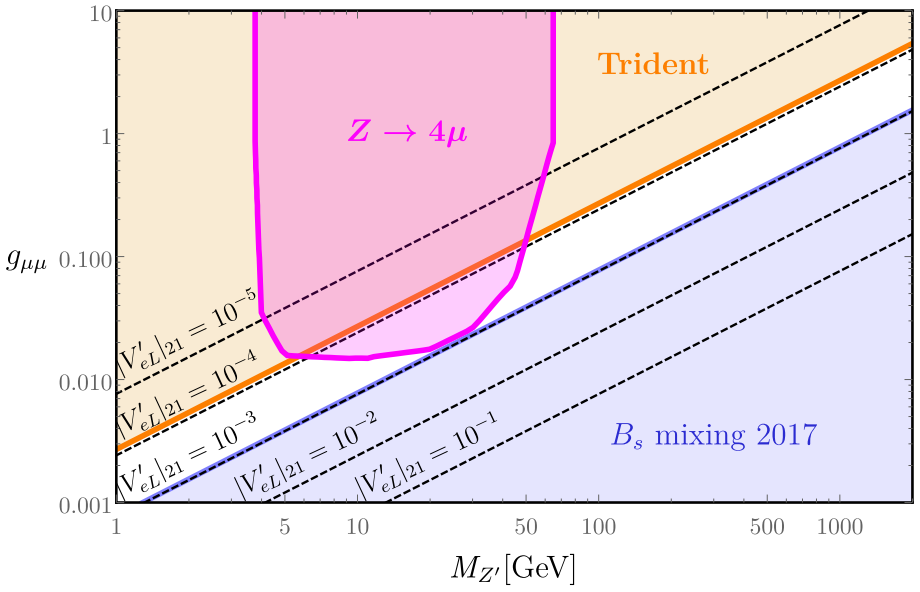

Figure 5.3: The parameter space in the $(g_{\mu\mu}, M_{Z'})$ plane compatible with $R_{K^{(*)}}$ anomalies and flavour constraints (white). We show the recent B_s mixing constraints (light blue), the trident bounds (orange), the $Z \to 4\mu$ limits (pink) as well as the expected limits from $\mu \to e\gamma$ for several values of $|V'_{eL}|_{21}$ (black dashed).

MEG experiment [297] which set the bound $\text{BR}(\mu \to e\gamma) \leq 4.2 \times 10^{-13}$ at 90%CL. An analytical approximation of this branching ratio is given by

$$\text{BR}(\mu \to e\gamma) \simeq 1.24 \times 10^{-6}\ g_{\mu\mu}^4 |V'_{eL}|_{21}^2 \left(\frac{M_{Z'}}{1\ \text{TeV}}\right)^{-4}\ , \tag{5.43}$$

implying that $\mu \to e\gamma$ is expected to set a stronger constraint than the neutrino trident production for values of the mixing angle $|V'_{eL}|_{21} \gtrsim 10^{-4}$ as represented in figure 5.3, while $|V'_{eL}|_{21} \gtrsim 10^{-3}$ would rule out the entire parameter space. As a result, in the viable parameter space of our setup, the mixing angle $|V'_{eL}|_{21}$ is expected to be $|V'_{eL}|_{21} \lesssim 10^{-4}$. Similarly, the experimental limit on the lepton-flavour-violating of the tau lepton into 3 muons, $\text{BR}(\tau \to 3\mu) \leq 2 \times 10^{-8}$ [298], constrains the mixing angle between charged leptons of the second and third generation $(V'_{eL})_{32}$: $\frac{g_{\mu\mu}^2 |V'_{eL}|_{32}}{M_{Z'}^2} \lesssim \frac{1}{(16\ \text{TeV})^2}$. This is stronger than the trident bound in equation (5.39) for $(V'_{eL})_{32} \gtrsim 3 \times 10^{-4}$, while $(V'_{eL})_{32} \gtrsim 3 \times 10^{-3}$ would rule out the entire parameter space.

5.3.5 Other constraints

Finally we comment on other precision observables which yield secondary constraints on our model.

The contribution of Z' to the muon magnetic moment is given by

$$\Delta_{g-2}^{\mu} = \frac{1}{12\pi^2} m_{\mu}^2 \left(\frac{g_{\mu\mu}}{M_{Z'}}\right)^2 . \tag{5.44}$$

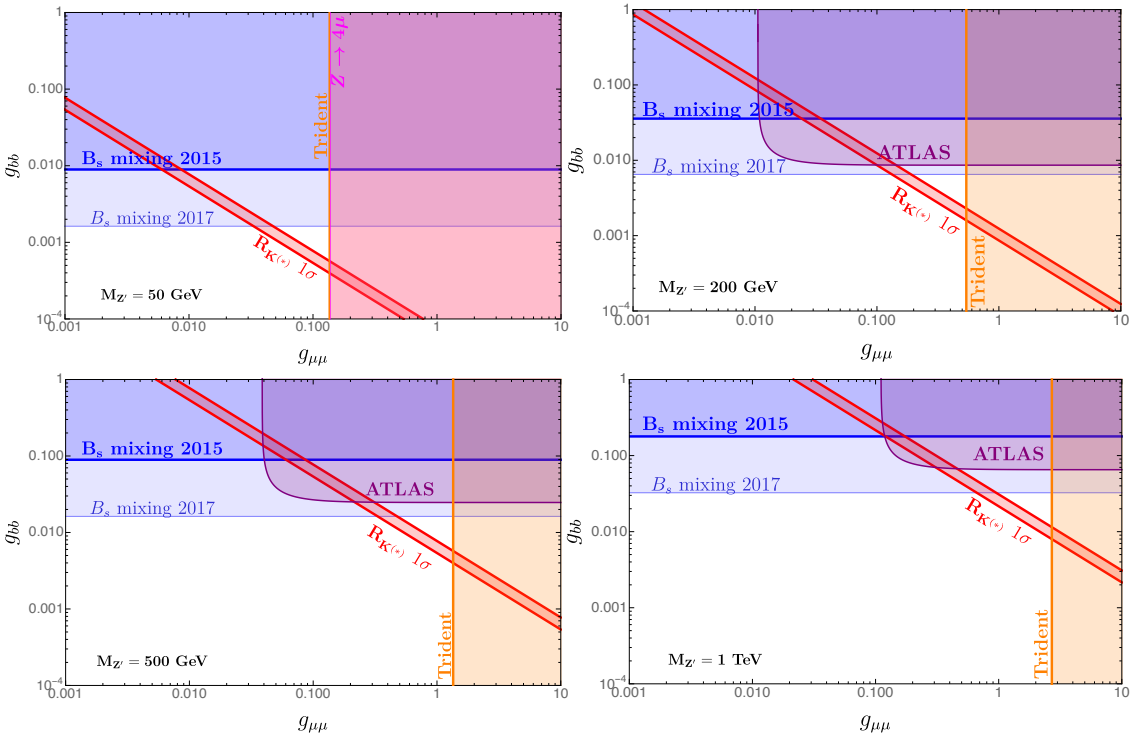

Figure 5.4: Bounds on the parameter space in the $(g_{\mu\mu}, g_{bb})$ plane for fixed Z' masses: 50, 200, 500 and 1000 GeV, as indicated on each panel. The red bands explain $R_{K^{(*)}}$ at 1σ. The blue and orange areas show the $B_s - \overline{B}_s$ mixing [286] and neutrino trident [291] 2σ exclusions, respectively. For low Z' masses we have additional constraints from $Z \to 4\mu$ as shown in pink. The ATLAS limits [296] from dimuon resonance searches for 36 fb^{-1}luminosity are given in purple for larger Z' masses.

The measured discrepancy of the muon magnetic moment is $\Delta^{\mu}_{g-2} = (290 \pm 90) \times 10^{-11}$ [299]. This sets weaker limits on the ratio $g_{\mu\mu}/M_{Z'}$ than the trident production.

Next, Z' exchange generates the effective interaction between b-quarks and muons:

$$\mathcal{L}_{\text{eff}} \supset G_{b\mu}(\bar{b}_L\gamma^{\mu}b_L)(\bar{\mu}_L\gamma_{\mu}\mu_L), \qquad G_{b\mu} = -\frac{g_{bb}g_{\mu\mu}}{M^2_{Z'}} = -\frac{1}{(6.4\text{ TeV})^2}, \tag{5.45}$$

where we used equation 5.35. The operator in equation 5.45 is constrained by lepton flavour universality of upsilon meson decays [300]. Focusing on the Υ_{1s} state, given the measured ratio [301]

$$R^{\tau/\mu}_{1s} = \frac{\Gamma(\Upsilon_{1s} \to \tau^+\tau^-)}{\Gamma(\Upsilon_{1s} \to \mu^+\mu^-)} = 1.008 \pm 0.023, \tag{5.46}$$

and the SM prediction $R^{\tau/\mu}_{1s} = 0.9924$, one finds the constraint

$$-\frac{1}{(150\text{ GeV})^2} < G_{b\mu} < \frac{1}{(190\text{ GeV})^2} \qquad @\,95\%\text{CL}. \tag{5.47}$$

This is automatically satisfied in our model in the parameter space where the $R_{K^{(*)}}$ anomalies are explained.

5.4 Summary

We have presented a new Z' model to accommodate the observed $R_{K^{(*)}}$ anomalies. We extend the Standard Model, including three right-handed neutrinos, with an $U(1)'$ gauge symmetry and a fourth family of vector-like fermions. In the absence of mixing, the Z' is fermiophobic, having no couplings to the SM three chiral families, but does couple to a fourth vector-like family. Due to mixing effects, the Z' gets induced couplings to second family left-handed lepton doublets and third family left-handed quark doublets. These couplings add a tree-level contribution to the $b \to s$ flavour-changing neutral-current process, as shown in figure 5.1b. Since the Z' couples to muons but it does not couple to electrons, this model can account for the measured B-meson decay ratios R_K and R_{K^*}.

We identify the parameter space where this explanation is consistent with existing experimental constraints from LHC searches, precision measurements of flavour mixing and neutrino processes. In this chapter, the relevant parameter space is effectively three-dimensional, and spanned by the Z' couplings to muons ($g_{\mu\mu}$) and b-quarks (g_{bb}) and by the mass of the Z' gauge boson ($M_{Z'}$). For each $g_{\mu\mu}$ and $M_{Z'}$, g_{bb} is fixed according to equation 5.35 to the best fit value reproducing the $R_{K^{(*)}}$ measurements. The coupling g_{bb} is further strongly constrained by precision measurements of the B_s meson mass difference leading to $M_{Z'} \lesssim 1.2 g_{\mu\mu}$ TeV. In our model, the Z' coupling to muons is suppressed by a mixing angle between the SM 2nd generation lepton doublet and the 4th generation vector-like lepton doublet, and thus $M_{Z'}$ is expected to be close to the weak scale. The coupling $g_{\mu\mu}$ is also constrained by neutrino trident production. Further restrictions from LHC searches are shown to be weaker than the B_s mixing constraints, see figure 5.2. Figures 5.2 and 5.4 show that there is narrow band in which $R_{K^{(*)}}$ anomalies can be understood for Z' masses between 10 GeV $\lesssim M_{Z'} \lesssim$ 1 TeV. Larger Z' masses would require a large Z' couplings to muons $g_{\mu\mu} > 1$, which seems unnatural, and smaller Z' masses are allowed for $g_{bb} \lesssim 10^{-3}$.

Incidentally, that parameter space can be probed by several distinct methods. First of all, the allowed window can be further squeezed by better precision measurements of the trident $\nu_\mu N \to \mu^+\mu^-\nu_\mu N$ process, and by improving the theoretical precision of the SM prediction for the B_s meson mass difference. The above statement is in fact valid for all models where the B-anomalies are addressed by a tree-level Z' exchange. What is more specific to models where the Z' interactions with the SM fermions originates from mixing of the latter with vector-like fermions is a non-vanishing Z' coupling not only to muons but also to b-quarks. This results in a non-negligible rate of the partonic process $b\bar{b} \to Z' \to \mu^+\mu^-$ which can be probed by dimuon resonance searches at the LHC. In fact, the preferred $M_{Z'}$ range is where the LHC sensitivity is optimal. Targeted searches for b-quark-collision initiated process (rather than recast of generic dimuon searches) could lead to a discovery signal in the near future, or to better constraints that are more stringent than the B_s mixing one.

Even though, in this chapter, we do not discuss the dark matter candidate naturally arising in this model, i.e. the fourth vector-like neutrino, the analysis has been performed in [4]. Here, it is shown that the model is compatible with both, fitting $R_{K^{(*)}}$ anomalies and reproducing the correct relic abundance of dark matter while satisfying all experimental and cosmological constraints. To summarize the results shown in [4], assuming our model is indeed the correct explanation of the observed $R_{K^{(*)}}$ anomalies and dark matter relic abundance, the analysis hints at a particular corner of the parameter space where 300 GeV $\lesssim M_{Z'} \lesssim$ 1 TeV, $m_\nu \gtrsim 1$ TeV, $g_{\nu\nu} \gtrsim 1$, $g_{bb} \sim 0.1 g_{\mu\mu}$ and $0.1 \lesssim g_{\mu\mu} \lesssim 1$.

Chapter 6

Conclusions

In this thesis we have addressed the flavour puzzle and the origin of neutrino masses within a SUSY flavour GUT framework in chapters 2-4, while the last chapter 5 was dedicated to flavour at the electroweak scale. In the following, we summarize the main successes of each chapter as well as some drawbacks that in most of the cases motivated the subsequent chapter.

Chapters 2-4 were based on flavour SUSY GUTs, driven by the aim of resolving as many open questions in particle physics as possible simultaneously. We followed a guiding principle, given by the discrete family symmetry group, to tackle the flavour puzzle. We introduced flavon fields that after acquiring VEVs give a dynamical origin to the Yukawa parameters of the Standard Model. We have also addressed neutrino masses and mixing within a type-I seesaw mechanism. Charge quantisation and gauge coupling unification were assured by the GUT group and we ensured that only the two MSSM Higgs doublets remained at low scales.

In chapter 2, we constructed a model based on an $S_4 \times SO(10)$ grand unified theory of flavour. $SO(10)$ was chosen since it predicts three right-handed neutrinos and makes neutrino mass inevitable. In the model, the flavon vacuum alignments preserve the SU generator of S_4, leading to the CSD3 vacuum alignments. All known fermions are contained at the high scale within a single representation ψ which is $(\mathbf{3'}, \mathbf{16})$ representation of $S_4 \times SO(10)$.

The model relies on "universal sequential dominance", meaning that the Yukawa matrices are sums of low-rank matrices and each matrix in the sum naturally accounts for the mass of a particular family. The hierarchy between all fermion masses is explained by assuming only a rather mild hierarchy in the flavons VEVs, i.e. $\langle\phi_1\rangle < \langle\phi_2\rangle < \langle\phi_3\rangle$, with differences of an order of magnitude between each flavon VEV. With this set up, the model successfully reproduces all the observed fermion masses and mixing, even in the quark sector, although we had to assume some SUSY threshold corrections to the

running of Yukawa parameters. The milder hierarchy in the down-type quarks compared to the up-type quarks is explained by a mixed term involving $\phi_1\phi_2$, which introduces a texture zero in the $(1,1)$ element of the down-type Yukawa matrix Y^d. This feature leads to the GST relation for the Cabibbo angle $\theta_{12}^q \approx \sqrt{y_d/y_s}$. In the lepton sector, an excellent fit to data was performed and we gave some predictions as normal hierarchy and CP phase deviating both from zero and maximal CP violation.

To achieve fermion masses and mixing, there is no need of tuning of $\mathcal{O}(1)$ parameters. We ensured naturalness within the model with all dimensionless parameters in the renormalisable superpotential being $\mathcal{O}(1)$. The model is also simple, meaning that we employed the smallest possible field content. We also addressed the doublet-triplet splitting and the μ problem and we provided an ultraviolet renormalisable model. However, we did not discuss the origin of the hierarchy of flavon VEVs, nor did we derive the CSD3 vacuum alignments which would require additional field content. Similarly, we did not show explicitly how $SO(10)$ was broken to the MSSM. Furthermore, even though the second right-handed neutrino has a mass of $\mathcal{O}(10^{10})$ GeV, which is in the preferred range to reproduce the observed BAU, N_2 leptogenesis does not survive the washout due to the inverse decays into the lightest right-handed neutrino N_1. These features motivated us to construct a new model presented in chapter 3, which is still based on an $S_4 \times SO(10)$ symmetry but with different CSD2 vacuum alignments.

In chapter 3, we also unified the fermions in a **16** representation of $SO(10)$ and a triplet $\mathbf{3'}$ of S_4. The Yukawa couplings are given again a dynamical origin and arise from the CSD2 vacuum alignments of the flavon fields. The model contains similar characteristics to the ones in chapter 2, the Yukawa matrices are derived from sum of low-rank matrices, where each matrix accounts for a particular fermion, while the hierarchy between different fermions is due to a milder hierarchy between the flavon VEVs. Similarly, the CSD2 structure and the mixing term $\phi_1\phi_2$ in the down-type quark Yukawa matrix give rise to the GST relation and to a milder hierarchy in the down-type quarks compared to the up-type quarks.

Additionally, in this model a set of driving fields was added which together with the supersymmetric F-term equations fix the CSD2 vacuum alignments. We also showed the symmetry breaking superpotential that fixes the hierarchy between the flavon VEVs $\langle\phi_1\rangle < \langle\phi_2\rangle < \langle\phi_3\rangle$ as well as a working doublet-triplet splitting mechanism and a μ term generated at the correct scale.

In this model, the second right-handed neutrino N_2 has an expected natural mass value of the order $\mathcal{O}(10^{11})$ GeV, in the favoured range to produce the observed BAU through N_2 thermal leptogenesis. To verify if it is feasible to obtain the measured baryon asymmetry, we took into account the washout due to inverse decays into N_1 and we computed all relevant parameters, i.e. decay asymmetries, efficiency factors and flavour effects. Interestingly, the CSD2 vacuum alignments lead to a zero in the $(3,1)$ entry of the Dirac

neutrino mass matrix in the flavour basis so that there is not suppression due to taus decaying into N_1. Therefore, this model naturally generates sufficient BAU through N_2 leptogenesis, fixing the second right-handed neutrino mass $M_2 \simeq 1.9 \times 10^{11}$ GeV, in the natural range predicted by the model.

We also performed a fit to the Standard Model fermion masses and mixing angles with some predictions such as normal neutrino mass ordering and a CP violating phase of 200°. However, the fit relies on specific large SUSY threshold corrections and it still depends on $\mathcal{O}(1/M_P)$ terms for the right-handed neutrinos.

The main difference between chapters 2 and 3 is given by the distinct flavon alignments which results in different predictions in the Yukawa couplings and mixing parameters. Chapter 2 is based on CSD3 while chapter 3 is based on CSD2. In chapter 2, we have 19 free parameters to fit 18 data points (we decided not to include δ^l in the fit and we left it as a pure prediction of the model since it was not yet well measured) and we found a $\chi^2 \approx 3.4$ with all the predictions within the 1σ range. In chapter 3, we have a larger $\chi^2 \approx 11.9$, with the leptonic sector perfectly fit while we found larger pulls in the quark sector, for example, the top Yukawa coupling deviates almost 2σ. However, in chapter 3 the number of free parameters is reduced to 15 and additionally we can find the correct baryon asymmetry of the Universe through leptogenesis what was not possible in chapter 2. In both cases most of the contribution to the χ^2 function comes from the quark sector and we still have to rely in large SUSY threshold corrections.

Heretofore, in chapter 2 our guiding principles were naturalness, with only $\mathcal{O}(1)$ dimensionless parameters and minimality, with only low-dimensional representations and a minimal field content. In chapter 3, we went one step further and we focused also in completeness, where we added a set of driving fields to reproduce the desired flavon vacuum alignments and we also showed an explicit symmetry breaking leading to the hierarchy between flavon VEVs. Then, in chapter 4 we aimed at combining all these guiding principles in a useful way with the introduction of extra dimensions. In this case, the number of fields was largely reduced since the boundary conditions on the orbifold compactification introduce GUT-symmetry breaking, reproduce a doublet-triplet splitting and additionally align the flavon VEVs.

In chapter 4 we focused on a supersymmetric $SU(5)$ theory in 6-dimensions, where the two extra dimensions were compactified on a $T^2/\mathbb{Z}_2$ orbifold. We showed that within this orbifold, if there is a finite modular symmetry, it can only be A_4 with fixed modulus $\tau = \omega = e^{i2\pi/3}$ or $\tau = \omega + 1$, where we focused on the first possibility. However, we did not address the problem of moduli stabilisation. The finite modular symmetry A_4 plays the roll of the flavour symmetry and the structure of the matrices is dictated not only by the flavon VEVs but also by the Yukawa couplings which become modular forms.

In this model, the hierarchy between fermions is understood through the Froggatt-Nielsen mechanism. The down-type quarks and the charged leptons have diagonal and

hierarchical Yukawa matrices, with quark mixing due to a hierarchical up-type quark Yukawa matrix. The neutrino mass matrix is $\mu-\tau$ reflection symmetric at low energies, predicting maximal atmospheric mixing angle and maximal leptonic CP violation. The model also predicts normal neutrino mass hierarchy. The rest of the PMNS observables are fit to the best present measured values, while the quarks can be perfectly fit using only $\mathcal{O}(1)$ parameters.

Finally, chapter 5 was devoted to flavour physics at the electroweak scale. In this chapter, we abandoned the idea of solving simultaneously most of the open questions of the Standard Model presented in chapter 1, and we focused on explaining the present anomalies in semi-leptonic B-meson decays, which if confirmed, may be the first signal of new physics beyond the Standard Model, apart from neutrino masses. In particular, we accounted for the deviations from $\mu - e$ universality, predicted by the Standard Model, which have been reported by the LHCb Collaboration in B-meson decays. Since these decays are $b \to s$ flavour-changing neutral-currents, forbidden at tree-level in the SM, they become sensitive to any new physics that introduce additional tree-level interactions.

In the model presented, we introduced an additional $U(1)'$ symmetry to the SM (including three right-handed neutrinos) and a fourth family of vector-like fermions. The only fermions charged under the new $U(1)'$ are the ones in the fourth family. However, due to mixing effects, the Z' gets induced couplings to the second family of left-handed lepton doublets and to the third family of left-handed quark doublets. We showed that the model can account for the measured B-decay ratios consistently with existing experimental constrains from LHC searches and precision measurements of flavour mixing and neutrino processes. Additionally, the model provides a natural dark matter candidate, the neutrino in the fourth family, although we did not discuss the relic abundance neither the dark matter direct and indirect experimental constraints on this thesis.

Beyond the above successes of the different chapters, there are still a few drawbacks that deserve further study. Chapter 2-4 did not explain SUSY breaking. A more detailed phenomenological study will take into account experimental constraints on SUSY observables. Furthermore, to achieve a good fit large SUSY threshold corrections were necessary, studying the underlying SUSY model which can reproduce the required corrections is beyond the stated aims of this thesis. Furthermore, we did not discuss the strong CP problem, inflation or Dark Matter (which may in principle be the lightest SUSY particle, stabilised by the R-parity).

In chapter 5, the available parameter space of the model can be proved in the future since the preferred $M_{Z'}$ range is within the LHC sensitivity scope. Better precision measurements and resonance searches at the LHC can test the allowed window as well as an improvement in the theoretical precision of the SM prediction for the B_s mass difference can further squeeze the parameter space.

In summary, we have presented three different SUSY flavour GUT models in chapters 2-4 addressing some of the known Standard Model open questions such us neutrino masses, the flavour puzzle, charge quantization and gauge coupling unification, and the baryon asymmetry of the universe, among many others. In chapter 5, we introduced an extension of the Standard Model which has implications at the electroweak scale, in particular, it may explain the recent anomalies in B-meson decays.

I hope that the results presented in this thesis give a deeper insight into physics beyond the Standard Model and that they will be helpful for future research.

Appendix A

S_4 and A_4 group theory

In this section, we introduce the group theory properties of S_4 and A_4. S_4 is the symmetric group consisting of all possible permutations among 4 objects and it also corresponds to the rigid rotational symmetries of a cube. A_4 is a subgroup of S_4 and consists of all even permutations in S_4. A_4 is also given by the rigid rotational symmetries of a tetrahedron. There are 24 independent transformations (group elements of S_4) of which 12 are symmetries of A_4 (group elements of A_4). We will define the groups in terms of their presentation, where the generators (subsets of elements from which we can obtain all elements of the group by multiplication) have to satisfy certain rules. In the case of S_4, we need three generators S, T and U which satisfy the presentation rules [302]

$$S^2 = T^3 = U^2 = (ST)^3 = (SU)^2 = (TU)^2 = (STU)^4 = 1. \tag{A.1}$$

If we drop the generator U, this reduces to the presentation of A_4 [303]. All group elements can be constructed from these generators, following the rules above.

A.1 S_4 symmetry group

We shall now present the irreducible matrix representations for S_4 in the T-diagonal basis, see [101, 304, 305] for proofs and other bases. S_4 has the following irreducible representations: two singlet representations $\mathbf{1}$ and $\mathbf{1'}$, one doublet representation $\mathbf{2}$ and two triplets denoted by $\mathbf{3}$ and $\mathbf{3'}$ which are independent. The matrix representations in the T-diagonal basis are given in table A.1 [102] (where $\omega = e^{i2\pi/3}$).

The Kronecker product rules are basis independent but the Clebsch-Gordan coefficients depend on the basis. We list the Kronecker products and Clebsch-Gordan coefficients of S_4 in the T-diagonal basis given by table A.1 [129], where n counts the number of primes which appear, e.g. $\mathbf{3} \otimes \mathbf{3'} \to \mathbf{3'}$ has $n = 2$ primes. The products involving at

S_4	$\mathbf{1}$,$\mathbf{1'}$	$\mathbf{2}$	$\mathbf{3}$,$\mathbf{3'}$
S	1	$\begin{pmatrix} 1 & 0 \\ 0 & 1 \end{pmatrix}$	$\frac{1}{3}\begin{pmatrix} -1 & 2 & 2 \\ 2 & -1 & 2 \\ 2 & 2 & -1 \end{pmatrix}$
T	1	$\begin{pmatrix} \omega & 0 \\ 0 & \omega^2 \end{pmatrix}$	$\begin{pmatrix} 1 & 0 & 0 \\ 0 & \omega^2 & 0 \\ 0 & 0 & \omega \end{pmatrix}$
U	± 1	$\begin{pmatrix} 0 & 1 \\ 1 & 0 \end{pmatrix}$	$\mp\begin{pmatrix} 1 & 0 & 0 \\ 0 & 0 & 1 \\ 0 & 1 & 0 \end{pmatrix}$

Table A.1: Generators S, T and U in the irreducible representations of S_4, where $\omega = e^{i2\pi/3}$.

least one singlet or doublet are given by

$$
\begin{aligned}
\mathbf{1}^{(\prime)} \otimes \mathbf{1}^{(\prime)} \to \mathbf{1}^{(\prime)} \quad & \left\{ \begin{array}{ll} & \mathbf{1}\otimes\mathbf{1}\to\mathbf{1} \\ n=\text{even} & \mathbf{1'}\otimes\mathbf{1'}\to\mathbf{1} \\ & \mathbf{1}\otimes\mathbf{1'}\to\mathbf{1'} \end{array} \right\} \quad \alpha\beta, \\
\mathbf{1}^{(\prime)} \otimes \mathbf{2} \to \mathbf{2} \quad & \left\{ \begin{array}{ll} n=\text{even} & \mathbf{1}\otimes\mathbf{2}\to\mathbf{2} \\ n=\text{odd} & \mathbf{1'}\otimes\mathbf{2}\to\mathbf{2} \end{array} \right\} \quad \alpha \begin{pmatrix} \beta_1 \\ (-1)^n\beta_2 \end{pmatrix}, \\
\mathbf{1}^{(\prime)} \otimes \mathbf{3}^{(\prime)} \to \mathbf{3}^{(\prime)} \quad & \left\{ \begin{array}{ll} & \mathbf{1}\otimes\mathbf{3}\to\mathbf{3} \\ n=\text{even} & \mathbf{1'}\otimes\mathbf{3'}\to\mathbf{3} \\ & \mathbf{1}\otimes\mathbf{3'}\to\mathbf{3'} \\ & \mathbf{1'}\otimes\mathbf{3}\to\mathbf{3'} \end{array} \right\} \quad \alpha \begin{pmatrix} \beta_1 \\ \beta_2 \\ \beta_3 \end{pmatrix}, \\
\mathbf{2}\otimes\mathbf{2} \to \mathbf{1}^{(\prime)} \quad & \left\{ \begin{array}{ll} n=\text{even} & \mathbf{2}\otimes\mathbf{2}\to\mathbf{1} \\ n=\text{odd} & \mathbf{2}\otimes\mathbf{2}\to\mathbf{1'} \end{array} \right\} \quad \alpha_1\beta_2 + (-1)^n\alpha_2\beta_1, \\
\mathbf{2}\otimes\mathbf{2} \to \mathbf{2} \quad & \left\{ n=\text{even} \quad \mathbf{2}\otimes\mathbf{2}\to\mathbf{2} \right\} \quad \begin{pmatrix} \alpha_2\beta_2 \\ \alpha_1\beta_1 \end{pmatrix}, \\
\mathbf{2}\otimes\mathbf{3}^{(\prime)} \to \mathbf{3}^{(\prime)} \quad & \left\{ \begin{array}{ll} n=\text{even} & \mathbf{2}\otimes\mathbf{3}\to\mathbf{3} \\ & \mathbf{2}\otimes\mathbf{3'}\to\mathbf{3'} \\ n=\text{odd} & \mathbf{2}\otimes\mathbf{3}\to\mathbf{3'} \\ & \mathbf{2}\otimes\mathbf{3'}\to\mathbf{3} \end{array} \right\} \quad \alpha_1 \begin{pmatrix} \beta_2 \\ \beta_3 \\ \beta_1 \end{pmatrix} + (-1)^n\alpha_2 \begin{pmatrix} \beta_3 \\ \beta_1 \\ \beta_2 \end{pmatrix},
\end{aligned}
\tag{A.2}
$$

while the products of two triplets going into either a singlet, a doublet or a triplet are

given by

$$
\begin{aligned}
&\mathbf{3}^{(\prime)} \otimes \mathbf{3}^{(\prime)} \to \mathbf{1}^{(\prime)} && \left\{ \begin{array}{ll} & \mathbf{3} \otimes \mathbf{3} \to \mathbf{1} \\ n = \text{even} & \mathbf{3}' \otimes \mathbf{3}' \to \mathbf{1} \\ & \mathbf{3} \otimes \mathbf{3}' \to \mathbf{1}' \end{array} \right\} && \alpha_1\beta_1 + \alpha_2\beta_3 + \alpha_3\beta_2, \\
&\mathbf{3}^{(\prime)} \otimes \mathbf{3}^{(\prime)} \to \mathbf{2} && \left\{ \begin{array}{ll} n = \text{even} & \mathbf{3} \otimes \mathbf{3} \to \mathbf{2} \\ & \mathbf{3}' \otimes \mathbf{3}' \to \mathbf{2} \\ n = \text{odd} & \mathbf{3} \otimes \mathbf{3}' \to \mathbf{2} \end{array} \right\} && \begin{pmatrix} \alpha_2\beta_2 + \alpha_3\beta_1 + \alpha_1\beta_3 \\ (-1)^n(\alpha_3\beta_3 + \alpha_2\beta_1 + \alpha_1\beta_2) \end{pmatrix}, \\
&\mathbf{3}^{(\prime)} \otimes \mathbf{3}^{(\prime)} \to \mathbf{3}^{(\prime)} && \left\{ \begin{array}{ll} & \mathbf{3} \otimes \mathbf{3} \to \mathbf{3}' \\ n = \text{odd} & \mathbf{3} \otimes \mathbf{3}' \to \mathbf{3} \\ & \mathbf{3}' \otimes \mathbf{3}' \to \mathbf{3}' \end{array} \right\} && \begin{pmatrix} 2\alpha_1\beta_1 - \alpha_2\beta_3 - \alpha_3\beta_2 \\ 2\alpha_3\beta_3 - \alpha_1\beta_2 - \alpha_2\beta_1 \\ 2\alpha_2\beta_2 - \alpha_3\beta_1 - \alpha_1\beta_3 \end{pmatrix}, \\
&\mathbf{3}^{(\prime)} \otimes \mathbf{3}^{(\prime)} \to \mathbf{3}^{(\prime)} && \left\{ \begin{array}{ll} & \mathbf{3} \otimes \mathbf{3} \to \mathbf{3} \\ n = \text{even} & \mathbf{3} \otimes \mathbf{3}' \to \mathbf{3}' \\ & \mathbf{3}' \otimes \mathbf{3}' \to \mathbf{3} \end{array} \right\} && \begin{pmatrix} \alpha_2\beta_3 - \alpha_3\beta_2 \\ \alpha_1\beta_2 - \alpha_2\beta_1 \\ \alpha_3\beta_1 - \alpha_1\beta_3 \end{pmatrix},
\end{aligned}
\tag{A.3}
$$

where α_i and β_i refers to the components of each multiplet such that no index is needed when referring to the singlet multiplet.

A.2 A_4 symmetry group

A_4 is the even permutation group of four objects, which is isomorphic to the symmetry group of a regular tetrahedron. It has 12 elements that can be generated by two generators, S and T, with the presentation

$$S^2 = T^3 = (ST)^3 = 1. \tag{A.4}$$

A_4 has four inequivalent irreducible representations: three singlet $\mathbf{1}, \mathbf{1}', \mathbf{1}''$ and one triplet $\mathbf{3}$ representations. The one-dimensional representations are determined uniquely by the conditions in A.4, while the three-dimensional representation is determined up to an unitary transformation, representing a change of basis. We choose to work with the same complex basis as [212] and the representation matrices of the generators are shown in table A.2.

The product of two triplets $\varphi = (\varphi_1, \varphi_2, \varphi_3)$ and $\psi = (\psi_1, \psi_2, \psi_3)$, decomposes as $\mathbf{3} \times \mathbf{3} = \mathbf{1} + \mathbf{1}' + \mathbf{1}'' + \mathbf{3_s} + \mathbf{3_a}$, where $\mathbf{3_{s,a}}$ denote the symmetric or antisymmetric product, respectively. The component decomposition of the products are shown in table A.3.

The 12 elements of A_4 are obtained as $1, S, T, ST, TS, T^2, ST^2, STS, TST, T^2S, TST^2$

A_4	$\mathbf{1}$	$\mathbf{1'}$	$\mathbf{1''}$	$\mathbf{3}$
S	1	1	1	$\frac{1}{3}\begin{pmatrix} -1 & 2 & 2 \\ 2 & -1 & 2 \\ 2 & 2 & -1 \end{pmatrix}$
T	1	ω	ω^2	$\begin{pmatrix} 1 & 0 & 0 \\ 0 & \omega & 0 \\ 0 & 0 & \omega^2 \end{pmatrix}$

Table A.2: Generators S and T in the irreducible representations of A_4, where $\omega = e^{i2\pi/3}$.

	Component decomposition
$(\varphi\psi)_{\mathbf{1}}$	$\varphi_1\psi_1 + \varphi_2\psi_3 + \varphi_3\psi_2$
$(\varphi\psi)_{\mathbf{1'}}$	$\varphi_3\psi_3 + \varphi_1\psi_2 + \varphi_2\psi_1$
$(\varphi\psi)_{\mathbf{1''}}$	$\varphi_2\psi_2 + \varphi_3\psi_1 + \varphi_1\psi_3$
$(\varphi\psi)_{\mathbf{3_s}}$	$\frac{1}{\sqrt{3}}\begin{pmatrix} 2\varphi_1\psi_1 - \varphi_2\psi_3 - \varphi_3\psi_2 \\ 2\varphi_3\psi_3 - \varphi_1\psi_2 - \varphi_2\psi_1 \\ 2\varphi_2\psi_2 - \varphi_3\psi_1 - \varphi_1\psi_3 \end{pmatrix}$
$(\varphi\psi)_{\mathbf{3_a}}$	$\begin{pmatrix} \varphi_2\psi_3 - \varphi_3\psi_2 \\ \varphi_1\psi_2 - \varphi_2\psi_1 \\ \varphi_3\psi_1 - \varphi_1\psi_3 \end{pmatrix}$

Table A.3: Decomposition of the product of two A_4 triplets φ, ψ in the T-diagonal basis. The subscript of the bracket refers to the representation in which the product is contracted since $\mathbf{3} \times \mathbf{3} = \mathbf{1} + \mathbf{1'} + \mathbf{1''} + \mathbf{3_s} + \mathbf{3_a}$.

and T^2ST. The A_4 elements belong to 4 conjugacy classes

$$\begin{aligned} &1C_1 : 1 \\ &4C_3 : T,\ ST,\ TS,\ STS \\ &4C_3^2 : T^2,\ ST^2,\ T^2S,\ ST^2S \\ &3C_2 : S,\ T^2ST,\ TST^2, \end{aligned} \tag{A.5}$$

where mC_n^k refers to the Schoenflies notation where m is the number of elements of rotations by an angle $2\pi k/n$.

A.2.1 Generalised *CP* consistency conditions for A_4

In this section, we check the compatibility of the $\mathbb{Z}_2$ symmetry on the fixed points with the A_4 flavour symmetry in chapter 4. The remnant $\mathbb{Z}_2$ symmetry behaves as an effective generalized CP transformation and the brane fields will transform under $\mathbb{Z}_2$ as

$$\psi(x) \to X_{\mathbf{r}}\psi^*(x'), \tag{A.6}$$

where $x' = (t, x_1, x_2, x_3, x_5, -x_6)$ and $X_{\mathbf{r}}$ is the representation matrix in the irreducible representation r. To combine the flavour symmetry A_4 with the $\mathbb{Z}_2$ symmetry, the transformations have to satisfy certain consistency conditions [306, 307], which were specifically applied to A_4 flavour symmetry in [219]. These conditions assure that if we perform a $\mathbb{Z}_2$ transformation, then apply a family symmetry transformation, and finally an inverse $\mathbb{Z}_2$ transformation is followed, the resulting net transformation should be equivalent to a family symmetry transformation. It is sufficient to only impose the consistency conditions on the group generators:

$$X_{\mathbf{r}}\rho^*_{\mathbf{r}}(S)X_{\mathbf{r}}^{-1} = \rho_{\mathbf{r}}(S'), \quad X_{\mathbf{r}}\rho^*_{\mathbf{r}}(T)X_{\mathbf{r}}^{-1} = \rho_{\mathbf{r}}(T'), \tag{A.7}$$

where $\rho_{\mathbf{r}}$ denotes the representation matrix for the generators S and T, see table A.2. As shown in [219], S' and T' can only belong to certain conjugacy classes of A_4

$$S' \in 3C_2, \quad T' \in 4C_3 \cup 4C_3^2, \tag{A.8}$$

(see equation A.5 to find out the elements in each conjugacy class). The transformations under the generalised CP symmetry $\mathbb{Z}_2$ are then:

$$\psi_{\mathbf{1'}} \to \psi^*_{\mathbf{1''}}, \quad \psi_{\mathbf{1''}} \to \psi^*_{\mathbf{1'}}, \quad \psi_{\mathbf{3}} \to \begin{pmatrix} 1 & 0 & 0 \\ 0 & 0 & 1 \\ 0 & 1 & 0 \end{pmatrix} \psi^*_{\mathbf{3}}, \tag{A.9}$$

which are consistent with equations A.7 and A.8 for $S' = S$ and $T' = T$. However in the model under consideration in chapter 4, we do not have any brane field transforming under the $\mathbf{1'}$ and $\mathbf{1''}$ representation. Thus the $\mathbb{Z}_2$ transformation only affects the $\mathbf{3}$ representations.

We conclude that the $\mathbf{3}$ representations on the fixed points transform under $A_4 \ltimes \mathbb{Z}_2$ as shown in table A.2 and equation A.9.

A.2.2 Modular forms for $\Gamma_3 \simeq A_4$

In this section, we explicitly show the construction of modular forms for $\Gamma_3 \simeq A_4$ following reference [212]. These modular forms are necessary to understand the structure of the Yukawa couplings in chapter 4.

To build invariant terms under the modular group Γ_3, the couplings have to become modular forms with weight k_Y [127], transforming according to

$$Y(\tau') \to (c\tau + d)^{k_Y} \rho Y(\tau), \tag{A.10}$$

where ρ is the representation under the modular group and τ' is the transformed modular

parameter after a modular transformation, given by

$$\tau \to \tau' = \frac{a\tau + b}{c\tau + d}. \tag{A.11}$$

To get an invariant term, we need to satisfy two conditions, first the weight k_Y has to cancel the overall weights of the fields and second the product of ρ times the representation matrices of the fields has to contain an invariant singlet. When $k_Y = 0$ for every constant, we have the usual discrete symmetry. Therefore, the modular form with weight 0 is simply a constant and a singlet under A_4.

In reference [212], it is shown that a weight 2 form can only transform in the three-dimensional representation of Γ_3 and each component of the triplet $Y_{\mathbf{3}}^T = (Y_1, Y_2, Y_3)$ is given by

$$\begin{aligned}
Y_1(\tau) &= \frac{i}{2\pi}\left(\frac{\eta'\left(\frac{\tau}{3}\right)}{\eta\left(\frac{\tau}{3}\right)} + \frac{\eta'\left(\frac{\tau+1}{3}\right)}{\eta\left(\frac{\tau+1}{3}\right)} + \frac{\eta'\left(\frac{\tau+2}{3}\right)}{\eta\left(\frac{\tau+2}{3}\right)} - \frac{27\eta'(3\tau)}{\eta(3\tau)}\right), \\
Y_2(\tau) &= \frac{-i}{\pi}\left(\frac{\eta'\left(\frac{\tau}{3}\right)}{\eta\left(\frac{\tau}{3}\right)} + \omega^2\,\frac{\eta'\left(\frac{\tau+1}{3}\right)}{\eta\left(\frac{\tau+1}{3}\right)} + \omega\,\frac{\eta'\left(\frac{\tau+2}{3}\right)}{\eta\left(\frac{\tau+2}{3}\right)}\right), \\
Y_3(\tau) &= \frac{-i}{\pi}\left(\frac{\eta'\left(\frac{\tau}{3}\right)}{\eta\left(\frac{\tau}{3}\right)} + \omega\,\frac{\eta'\left(\frac{\tau+1}{3}\right)}{\eta\left(\frac{\tau+1}{3}\right)} + \omega^2\,\frac{\eta'\left(\frac{\tau+2}{3}\right)}{\eta\left(\frac{\tau+2}{3}\right)}\right),
\end{aligned} \tag{A.12}$$

where $\eta(\tau)$ denotes the Dedekind function

$$\eta(\tau) = q^{1/24}\prod_{n=1}^{\infty}(1-q^n), \qquad q \equiv e^{i2\pi\tau}. \tag{A.13}$$

Therefore, there are no weight 2 singlets. In the model presented in chapter 4, the modulus is fixed by the orbifold to be $\tau = \omega$. In this case, up to an overall coefficient, we have

$$Y_1(\omega) = 2, \quad Y_2(\omega) = 2\omega, \quad Y_3(\omega) = -\omega^2, \tag{A.14}$$

and the triplet for weight 2 is

$$Y_{\mathbf{3}}^{(2)} = (2,\ 2\omega,\ -\omega^2), \tag{A.15}$$

where the superscript refers to the weight and the subscript to the representation under A_4.

Higher weight modular forms can be written in terms of the weight 2 forms by taking products of them following the decomposition rules in table A.3. Then, the weight 4

modular forms are written as

$$\begin{aligned} Y^{(4)}_{\mathbf{3}} &= (Y_1^2 - Y_2Y_3, Y_3^2 - Y_1Y_2, Y_2^2 - Y_1Y_3), \\ Y^{(4)}_{\mathbf{1}} &= Y_1^2 + 2Y_2Y_3, \\ Y^{(4)}_{\mathbf{1'}} &= Y_3^2 + 2Y_1Y_2, \\ Y^{(4)}_{\mathbf{1''}} &= Y_2^2 + 2Y_1Y_3, \end{aligned} \tag{A.16}$$

where the subscript corresponds to the representation under A_4. In our model, the modulus field is fixed by the orbifold to be $\tau = \omega$. In this case, the only non-zero weight 4 modular forms are

$$Y^{(4)}_{\mathbf{3}}|_{\tau=\omega} = (2, \ -\omega, \ 2\omega^2), \quad Y^{(4)}_{\mathbf{1'}} = \omega \tag{A.17}$$

The weight 6 modular forms can be found in a similar way and are written as

$$\begin{aligned} Y^{(6)}_{\mathbf{1}} &= Y_1^3 + Y_2^3 + Y_3^3 - 3Y_1Y_2Y_3, \\ Y^{(6)}_{\mathbf{3},1} &= (Y_1^3 + 2Y_1Y_2Y_3, Y_1^2Y_2 + 2Y_2^2Y_3, Y_1^2Y_3 + 2Y_3^2Y_2), \\ Y^{(6)}_{\mathbf{3},2} &= (Y_3^3 + 2Y_1Y_2Y_3, Y_3^2Y_1 + 2Y_1^2Y_2, Y_3^2Y_2 + 2Y_2^2Y_1), \\ Y^{(6)}_{\mathbf{3},3} &= (Y_2^3 + 2Y_1Y_2Y_3, Y_2^2Y_3 + 2Y_3^2Y_1, Y_2^2Y_1 + 2Y_1^2Y_3), \end{aligned} \tag{A.18}$$

where we have three different triplet representations labelled by the subscript $3, i$ for $i = 1, 2, 3$. Due to relations of the Dedekind functions, the modular forms satisfy [212]

$$Y_2^2 + 2Y_1Y_3 = 0, \tag{A.19}$$

which reduce the number of possible modular forms. Furthermore, in our case with the modulus parameter being fixed to $\tau = \omega$, we also have the constraint

$$(Y_1^2 + 2Y_2Y_3)|_{\tau=\omega} = 0, \tag{A.20}$$

which reduces even further the possible modular forms. Therefore, the only triplet of weight 6 that is different from zero in equation A.18 is

$$Y^{(6)}_{\mathbf{3},2}|_{\tau=\omega} = (-1, \ 2\omega^2, \ 2\omega). \tag{A.21}$$

All modular forms are built from products of the weight 2 triplet. We can build the modular forms for weight 8. Following [212], this is a 15 dimensional space that must be decomposed as $\mathbf{2} \times \mathbf{1} + \mathbf{2} \times \mathbf{1'} + \mathbf{2} \times \mathbf{1''} + \mathbf{3} \times \mathbf{3}$. For simplicity we can work out only the specific case where $\tau = \omega$. This case is greatly restricted and can be checked by doing all possible multiplications of $\mathbf{3} \times \mathbf{3} \times \mathbf{3} \times \mathbf{3}$ that the only non zero modular forms are

$$Y^{(8)}_{\mathbf{3}} = (2, \ 2\omega, \ -\omega^2) \quad \text{and} \quad Y^{(8)}_{\mathbf{1''}} = \omega^2, \tag{A.22}$$

where we can see that the triplet has the same structure as the weight 2 one. From this, we conclude that any higher weight triplet would only repeat the previous structures without having any new one.

For weight 10 we would have the same triplet as in weight 4 but two singlets since we can have the non-trivial products

$$Y^{(6)}_{\mathbf{1}} \times Y^{(4)}_{\mathbf{1'}} \to \mathbf{1'}, \quad \text{and} \quad Y^{(6)}_{\mathbf{3}} \times Y^{(4)}_{\mathbf{3}} \to \mathbf{1''}, \tag{A.23}$$

such that this is the first weight that has two singlets. The next weight that has the three singlets is built from powers of these singlets, so the modular form must have weight 20. This is important in chapter 4 when building the up-type quark Yukawa matrix since we need the three types of singlets to construct the invariant term and therefore the up Yukawa coupling y^u_{ij} must have weight 20, constraining the value of γ in table 4.2 to be $\gamma = 7$.

Appendix B

Running Yukawa parameters

The models in chapters 2-4 are defined at the GUT scale, while experimental data is available at the Standard Model scale. Therefore, to test the model we need to have the running from fermion masses and mixing parameters at the high energy scale where the model is defined. Additionally, one needs to include the supersymmetric radiative threshold corrections when deriving the running parameters at M_{GUT}.

An analysis of the running of MSSM Yukawa parameters up to the GUT scale has been performed in [199], where they propose a useful parametrisation of $\tan\beta$ enhanced 1-loop threshold corrections to the charged fermion Yukawa couplings and quark mixing angles.

The analysis assumes that, when matching the SM to its SUSY extension, all superpartners are integrated out at once at a single threshold scale $M_{\rm SUSY}$. The matching conditions at the SUSY scale $M_{\rm SUSY}$ are parametrised in terms of four parameters $\bar{\eta}_{q,b,\ell}$, which take into account the contribution from loops involving SUSY particles, and $\bar{\beta}$, as

$$\begin{aligned}
y_{u,c,t}^{\rm MSSM} &\simeq y_{u,c,t}^{\rm SM} \csc\bar{\beta},\\
y_{d,s}^{\rm MSSM} &\simeq (1+\bar{\eta}_q)^{-1}\, y_{d,s}^{\rm SM} \sec\bar{\beta},\\
y_{b}^{\rm MSSM} &\simeq (1+\bar{\eta}_b)^{-1}\, y_{b}^{\rm SM} \sec\bar{\beta},\\
y_{e,\mu}^{\rm MSSM} &\simeq (1+\bar{\eta}_\ell)^{-1}\, y_{e,\mu}^{\rm SM} \sec\bar{\beta},\\
y_{\tau}^{\rm MSSM} &\simeq y_{\tau}^{\rm MSSM} \sec\bar{\beta}.
\end{aligned} \tag{B.1}$$

The CKM parameters also get corrections

$$\begin{aligned}
\theta_{i3}^{q,\rm MSSM} &\simeq \frac{1+\bar{\eta}_b}{1+\bar{\eta}_q}\,\theta_{i3}^{q,\rm SM},\\
\theta_{12}^{q,\rm MSSM} &\simeq \theta_{12}^{q,\rm SM},\\
\delta^{q,\rm MSSM} &\simeq \delta^{q,\rm SM}.
\end{aligned} \tag{B.2}$$

To a very good approximation θ_{12}^q and δ^q are not affected by the threshold corrections. The running of couplings $y_i^{\rm MSSM}$ up to the GUT scale, $y_i^{\rm MSSM} \to y_i^{\rm MSSM@GUT}$, depends to a good approximation only on $\bar{\eta}_b$ and $\tan\bar{\beta}$. In the limit where threshold corrections to y_τ are negligible, $\bar{\beta}$ reduces to the usual β. We will assume just such a scenario. We will also set $\bar{\eta}_q = \bar{\eta}_\ell = 0$ for simplicity, as these are found not to affect the quality of the fits. Meanwhile, the neutrino masses and mixing angles are expected to be largely insensitive to group running.

Conversely, the remaining SUSY parameter, $\bar{\eta}_b$, will be important and prefers a large (negative) value for both fits in chapters 2 and 3. The leading contributions to this parameter come from loops either sbottoms and gluinos or stops and higgsinos that add up to [308]

$$\bar{\eta}_b \simeq \frac{\tan\beta}{16\pi^2}\left(\frac{8}{3}g_3^2\frac{m_{\tilde{g}}\mu}{2m_0^2} + \lambda_t^2\frac{\mu A_t}{m_0^2}\right), \tag{B.3}$$

where m_0 represents the squark masses, g_3 the strong coupling, $m_{\tilde{g}}$ the gluino mass and A_t the SUSY softly breaking trilinear coupling involving the stops. We see that a large contribution can be achieved when

$$m_{\tilde{g}}, \mu, A_t > m_0, \qquad \tan\beta \gtrsim 5. \tag{B.4}$$

Since SUSY breaking lies beyond the scope of this thesis, it is sufficient for us to show that there is a parameter space in the softly broken SUSY that generates the necessary corrections.

Appendix C

Conventions

C.1 Dirac gamma matrices

First, we introduce the notation that will follow for the rest of the appendix. We define 1_n as the $n \times n$ identity matrix and when no subindex is added, we will be assuming 1 as the integer number. We present the Weyl or chiral representation of the Dirac gamma matrices γ^μ in 2×2 block form:

$$\gamma^0 = \begin{pmatrix} 0 & 1_2 \\ 1_2 & 0 \end{pmatrix}, \quad \gamma^i = \begin{pmatrix} 0 & \sigma^i \\ -\sigma^i & 0 \end{pmatrix}, \tag{C.1}$$

where $i = 1, 2, 3$ and σ^i are the Pauli matrices

$$\sigma^1 = \begin{pmatrix} 0 & 1 \\ 1 & 0 \end{pmatrix}, \quad \sigma^2 = \begin{pmatrix} 0 & -i \\ i & 0 \end{pmatrix}, \quad \sigma^3 = \begin{pmatrix} 1 & 0 \\ 0 & -1 \end{pmatrix}. \tag{C.2}$$

The additional gamma matrix γ^5 in a 2×2 block diagonal form is given by

$$\gamma^5 = i\gamma^0\gamma^1\gamma^2\gamma^3 = \begin{pmatrix} -1_2 & 0 \\ 0 & 1_2 \end{pmatrix}. \tag{C.3}$$

The gamma matrices satisfy the anticommutation relations

$$\{\gamma^\mu, \gamma^\nu\} = 2\eta^{\mu\nu} 1_4, \quad \{\gamma^5, \gamma^\mu\} = 0, \tag{C.4}$$

where $\mu, \nu = 0, 1, 2, 3$ and $\eta^{\mu\nu} = diag(1, -1, -1, -1)$ is the Minkowski metric. Additionally, in the Weyl basis the gamma matrices comply with

$$\begin{aligned} &\gamma^{0*} = (\gamma^0)^T = \gamma^{0\dagger} = \gamma^0, \\ &\gamma^{i\dagger} = -\gamma^i, \quad \gamma^{5\dagger} = \gamma^5, \\ &(\gamma^0)^2 = 1, \quad (\gamma^i)^2 = -1, \quad (\gamma^5)^2 = 1, \\ &\gamma^0\gamma^{\mu\dagger}\gamma^0 = \gamma^\mu. \end{aligned} \tag{C.5}$$

The chiral projectors are defined as

$$P_L \equiv \frac{1_4 - \gamma^5}{2} = \begin{pmatrix} 1_2 & 0 \\ 0 & 0 \end{pmatrix}, \quad P_R \equiv \frac{1_4 + \gamma^5}{2} = \begin{pmatrix} 0 & 0 \\ 0 & 1_2 \end{pmatrix}. \tag{C.6}$$

Left-(right-) handed fields are eigenvectors of the operator γ^5 with eigenvalues $-1(+1)$. We define the left-handed ψ_L and right-handed ψ_R fields from the four-component fields ψ as

$$\psi_L := P_L\psi, \quad \psi_R := P_R\psi. \tag{C.7}$$

The fields ψ_L and ψ_R are known as chiral fields.

C.2 Charge conjugation matrix

Charge conjugation is defined to take a solution of the Dirac equation

$$(i\gamma^\mu(\partial_\mu - ieQA_\mu) - m)\psi(x) = 0 \tag{C.8}$$

into a solution ψ^c of the charge conjugate Dirac equation

$$(i\gamma^\mu(\partial_\mu + ieQA_\mu) - m)\psi^c(x) = 0. \tag{C.9}$$

A solution is given by

$$\psi^c = C\overline{\psi(x)}^T, \tag{C.10}$$

where $\overline{\psi} = \psi^\dagger\gamma^0$ and the charge conjugation matrix C must fulfil $C(\gamma^\mu)^T C^{-1} = -\gamma^\mu$. In the chiral representation of the gamma matrices given in equation C.1, one finds that $C = e^{i\alpha}\gamma^2\gamma^0$ for $\alpha \in \mathbb{R}$ (arbitrary) is a solution.

If ψ is a chiral field, then the charged conjugated field ψ^c has the opposite chirality. For example, if ψ_L is a left-handed chiral field, under conjugation the chirality of the field changes, i.e. ψ_L^c transforms as a right-handed field.

Bibliography

[1] F. Björkeroth, F. J. de Anda, S. F. King, and E. Perdomo. A natural S_4 SO(10) model of flavour. *JHEP*, 10:148, 2017. doi: 10.1007/JHEP10(2017)148.

[2] F. J. de Anda, S. F. King, and E. Perdomo. $SO(10) \times S_4$ grand unified theory of flavour and leptogenesis. *JHEP*, 12:075, 2017. doi: 10.1007/JHEP12(2017)075.

[3] F. J. de Anda, S. F. King, and E. Perdomo. $SU(5)$ Grand Unified Theory with A_4 Modular Symmetry. 2018.

[4] A. Falkowski, S. F. King, E. Perdomo, and M. Pierre. Flavourful Z' portal for vector-like neutrino Dark Matter and $R_{K^{(*)}}$. *JHEP*, 08:061, 2018. doi: 10.1007/JHEP08(2018)061.

[5] H. Fritzsch, Murray Gell-Mann, and H. Leutwyler. Advantages of the Color Octet Gluon Picture. *Phys. Lett.*, 47B:365–368, 1973. doi: 10.1016/0370-2693(73)90625-4.

[6] H. David Politzer. Reliable Perturbative Results for Strong Interactions? *Phys. Rev. Lett.*, 30:1346–1349, 1973. doi: 10.1103/PhysRevLett.30.1346. [,274(1973)].

[7] David J. Gross and Frank Wilczek. Ultraviolet Behavior of Nonabelian Gauge Theories. *Phys. Rev. Lett.*, 30:1343–1346, 1973. doi: 10.1103/PhysRevLett.30.1343. [,271(1973)].

[8] S. L. Glashow. Partial Symmetries of Weak Interactions. *Nucl. Phys.*, 22:579–588, 1961. doi: 10.1016/0029-5582(61)90469-2.

[9] Abdus Salam and John Clive Ward. Electromagnetic and weak interactions. *Phys. Lett.*, 13:168–171, 1964. doi: 10.1016/0031-9163(64)90711-5.

[10] Steven Weinberg. A Model of Leptons. *Phys. Rev. Lett.*, 19:1264–1266, 1967. doi: 10.1103/PhysRevLett.19.1264.

[11] Abdus Salam. Weak and Electromagnetic Interactions. *Conf. Proc.*, C680519:367–377, 1968.

[12] Peter W. Higgs. Broken symmetries, massless particles and gauge fields. *Phys. Lett.*, 12:132–133, 1964. doi: 10.1016/0031-9163(64)91136-9.

[13] F. Englert and R. Brout. Broken Symmetry and the Mass of Gauge Vector Mesons. *Phys. Rev. Lett.*, 13:321–323, 1964. doi: 10.1103/PhysRevLett.13.321. [,157(1964)].

[14] Peter W. Higgs. Broken Symmetries and the Masses of Gauge Bosons. *Phys. Rev. Lett.*, 13:508–509, 1964. doi: 10.1103/PhysRevLett.13.508. [,160(1964)].

[15] G. S. Guralnik, C. R. Hagen, and T. W. B. Kibble. Global Conservation Laws and Massless Particles. *Phys. Rev. Lett.*, 13:585–587, 1964. doi: 10.1103/PhysRevLett.13.585. [,162(1964)].

[16] Peter W. Higgs. Spontaneous Symmetry Breakdown without Massless Bosons. *Phys. Rev.*, 145:1156–1163, 1966. doi: 10.1103/PhysRev.145.1156.

[17] T. W. B. Kibble. Symmetry breaking in nonAbelian gauge theories. *Phys. Rev.*, 155:1554–1561, 1967. doi: 10.1103/PhysRev.155.1554. [,165(1967)].

[18] N. Cabibbo. Unitary Symmetry and Leptonic Decays. *Phys. Rev. Lett.*, 10:531–533, 1963. doi: 10.1103/PhysRevLett.10.531. [,648(1963)].

[19] Makoto Kobayashi and Toshihide Maskawa. CP Violation in the Renormalizable Theory of Weak Interaction. *Prog. Theor. Phys.*, 49:652–657, 1973. doi: 10.1143/PTP.49.652.

[20] Ling-Lie Chau and Wai-Yee Keung. Comments on the Parametrization of the Kobayashi-Maskawa Matrix. *Phys. Rev. Lett.*, 53:1802, 1984. doi: 10.1103/PhysRevLett.53.1802.

[21] S. L. Glashow, J. Iliopoulos, and L. Maiani. Weak Interactions with Lepton-Hadron Symmetry. *Phys. Rev.*, D2:1285–1292, 1970. doi: 10.1103/PhysRevD.2.1285.

[22] P. Minkowski. $\mu \to e\gamma$ at a Rate of One Out of 10^9 Muon Decays? *Phys. Lett.*, 67B:421–428, 1977. doi: 10.1016/0370-2693(77)90435-X.

[23] T. Yanagida. Proceedings of the workshop on unified theory and baryon number in the universe. O. Sawata and A. Sugamoto eds., KEK report:79–18, 1979.

[24] S.L. Glashow. Quarks and leptons, proceedings of the advanced study institute (Cargèse, Corsica, 1979). J.-L. Basdevant *et al.* eds., Plenum, New York, 1981.

[25] Murray Gell-Mann, Pierre Ramond, and Richard Slansky. Complex Spinors and Unified Theories. *Conf. Proc.*, C790927:315–321, 1979.

[26] Rabindra N. Mohapatra and Goran Senjanovic. Neutrino Mass and Spontaneous Parity Nonconservation. *Phys. Rev. Lett.*, 44:912, 1980. doi: 10.1103/PhysRevLett.44.912. [,231(1979)].

[27] B. Pontecorvo. Mesonium and anti-mesonium. *Sov. Phys. JETP*, 6:429, 1957. [Zh. Eksp. Teor. Fiz.33,549(1957)].

[28] B. Pontecorvo. Inverse beta processes and nonconservation of lepton charge. *Sov. Phys. JETP*, 7:172–173, 1958. [Zh. Eksp. Teor. Fiz.34,247(1957)].

[29] Z. Maki, M. Nakagawa, and S. Sakata. Remarks on the unified model of elementary particles. *Prog. Theor. Phys.*, 28:870–880, 1962. doi: 10.1143/PTP.28.870. [,34(1962)].

[30] B. Pontecorvo. Neutrino Experiments and the Problem of Conservation of Leptonic Charge. *Sov. Phys. JETP*, 26:984–988, 1968. [Zh. Eksp. Teor. Fiz.53,1717(1967)].

[31] M. Tanabashi et al. Review of particle physics. *Phys. Rev. D*, 98:030001, Aug 2018. doi: 10.1103/PhysRevD.98.030001. URL `https://link.aps.org/doi/10.1103/PhysRevD.98.030001`.

[32] I. Esteban, M. C. Gonzalez-Garcia, A. Hernandez-Cabezudo, M. Maltoni, and T. Schwetz. Global analysis of three-flavour neutrino oscillations: synergies and tensions in the determination of θ_{23}, δ_{CP}, and the mass ordering. *JHEP*, 01:106, 2019. doi: 10.1007/JHEP01(2019)106.

[33] N. Vinyoles, A. M. Serenelli, F. L. Villante, S. Basu, J. Bergstrm, M. C. Gonzalez-Garcia, M. Maltoni, C. Pea-Garay, and N. Song. A new Generation of Standard Solar Models. *Astrophys. J.*, 835(2):202, 2017. doi: 10.3847/1538-4357/835/2/202.

[34] B. T. Cleveland, Timothy Daily, Raymond Davis, Jr., James R. Distel, Kenneth Lande, C. K. Lee, Paul S. Wildenhain, and Jack Ullman. Measurement of the solar electron neutrino flux with the Homestake chlorine detector. *Astrophys. J.*, 496:505–526, 1998. doi: 10.1086/305343.

[35] F. Kaether, W. Hampel, G. Heusser, J. Kiko, and T. Kirsten. Reanalysis of the GALLEX solar neutrino flux and source experiments. *Phys. Lett.*, B685:47–54, 2010. doi: 10.1016/j.physletb.2010.01.030.

[36] J. N. Abdurashitov et al. Measurement of the solar neutrino capture rate with gallium metal. III: Results for the 2002–2007 data-taking period. *Phys. Rev.*, C80: 015807, 2009. doi: 10.1103/PhysRevC.80.015807.

[37] J. Hosaka et al. Solar neutrino measurements in super-Kamiokande-I. *Phys. Rev.*, D73:112001, 2006. doi: 10.1103/PhysRevD.73.112001.

[38] J. P. Cravens et al. Solar neutrino measurements in Super-Kamiokande-II. *Phys. Rev.*, D78:032002, 2008. doi: 10.1103/PhysRevD.78.032002.

[39] K. Abe et al. Solar neutrino results in Super-Kamiokande-III. *Phys. Rev.*, D83: 052010, 2011. doi: 10.1103/PhysRevD.83.052010.

[40] Yuuki Nakano. *8B solar neutrino spectrum measurement using Super-Kamiokande IV*. PhD thesis, U. Tokyo (main). URL `http://www-sk.icrr.u-tokyo.ac.jp/sk/_pdf/articles/2016/doc_thesis_naknao.pdf`.

[41] M. Ikeda. Solar neutrino measurements with Super-Kamiokande. doi: 10.5281/zenodo.1286857.

[42] B. Aharmim et al. Combined Analysis of all Three Phases of Solar Neutrino Data from the Sudbury Neutrino Observatory. *Phys. Rev.*, C88:025501, 2013. doi: 10.1103/PhysRevC.88.025501.

[43] G. Bellini et al. Precision measurement of the 7Be solar neutrino interaction rate in Borexino. *Phys. Rev. Lett.*, 107:141302, 2011. doi: 10.1103/PhysRevLett.107.141302.

[44] G. Bellini et al. Measurement of the solar 8B neutrino rate with a liquid scintillator target and 3 MeV energy threshold in the Borexino detector. *Phys. Rev.*, D82:033006, 2010. doi: 10.1103/PhysRevD.82.033006.

[45] G. Bellini et al. Neutrinos from the primary protonproton fusion process in the Sun. *Nature*, 512(7515):383–386, 2014. doi: 10.1038/nature13702.

[46] M. Honda, M. Sajjad Athar, T. Kajita, K. Kasahara, and S. Midorikawa. Atmospheric neutrino flux calculation using the NRLMSISE-00 atmospheric model. *Phys. Rev.*, D92(2):023004, 2015. doi: 10.1103/PhysRevD.92.023004.

[47] M. G. Aartsen et al. Determining neutrino oscillation parameters from atmospheric muon neutrino disappearance with three years of IceCube DeepCore data. *Phys. Rev.*, D91(7):072004, 2015. doi: 10.1103/PhysRevD.91.072004.

[48] K. Abe et al. Atmospheric neutrino oscillation analysis with external constraints in Super-Kamiokande I-IV. *Phys. Rev.*, D97(7):072001, 2018. doi: 10.1103/PhysRevD.97.072001.

[49] A. Gando et al. Reactor On-Off Antineutrino Measurement with KamLAND. *Phys. Rev.*, D88(3):033001, 2013. doi: 10.1103/PhysRevD.88.033001.

[50] Feng Peng An et al. Improved Measurement of the Reactor Antineutrino Flux and Spectrum at Daya Bay. *Chin. Phys.*, C41(1):013002, 2017. doi: 10.1088/1674-1137/41/1/013002.

[51] A. Cabrera Serra. Double Chooz Improved Multi-Detector Measurements.

[52] D. Adey et al. Measurement of the Electron Antineutrino Oscillation with 1958 Days of Operation at Daya Bay. *Phys. Rev. Lett.*, 121(24):241805, 2018. doi: 10.1103/PhysRevLett.121.241805.

[53] G. Bak et al. Measurement of Reactor Antineutrino Oscillation Amplitude and Frequency at RENO. *Phys. Rev. Lett.*, 121(20):201801, 2018. doi: 10.1103/PhysRevLett.121.201801.

[54] P. Adamson et al. Measurement of Neutrino and Antineutrino Oscillations Using Beam and Atmospheric Data in MINOS. *Phys. Rev. Lett.*, 110(25):251801, 2013. doi: 10.1103/PhysRevLett.110.251801.

[55] P. Adamson et al. Electron neutrino and antineutrino appearance in the full MINOS data sample. *Phys. Rev. Lett.*, 110(17):171801, 2013. doi: 10.1103/PhysRevLett.110.171801.

[56] A. Izmaylov. T2K Neutrino Experiment. Recent Results and Plans.

[57] T. Koga. *Measurement of neutrino interactions on water and search for electron anti-neutrino appearance in the T2K experiment.* PhD thesis, U. Tokyo. URL `https://www.t2k.org/docs/thesis/090/Doctor%20thesis`.

[58] M. Sanchez. Nova results and prospects. doi: 10.5281/zenodo.1286758.

[59] P. A. R. Ade et al. Planck 2015 results. XIII. Cosmological parameters. *Astron. Astrophys.*, 594:A13, 2016. doi: 10.1051/0004-6361/201525830.

[60] M. Agostini et al. Improved Limit on Neutrinoless Double-β Decay of ^{76}Ge from GERDA Phase II. *Phys. Rev. Lett.*, 120(13):132503, 2018. doi: 10.1103/PhysRevLett.120.132503.

[61] A. Gando et al. Search for Majorana Neutrinos near the Inverted Mass Hierarchy Region with KamLAND-Zen. *Phys. Rev. Lett.*, 117(8):082503, 2016. doi: 10.1103/PhysRevLett.117.109903,10.1103/PhysRevLett.117.082503. [Addendum: Phys. Rev. Lett.117,no.10,109903(2016)].

[62] P. Ramond. Dual Theory for Free Fermions. *Phys. Rev.*, D3:2415–2418, 1971. doi: 10.1103/PhysRevD.3.2415.

[63] A. Neveu and J. H. Schwarz. Quark Model of Dual Pions. *Phys. Rev.*, D4:1109–1111, 1971. doi: 10.1103/PhysRevD.4.1109.

[64] Jean-Loup Gervais and B. Sakita. Field Theory Interpretation of Supergauges in Dual Models. *Nucl. Phys.*, B34:632–639, 1971. doi: 10.1016/0550-3213(71)90351-8. [,154(1971)].

[65] Yu. A. Golfand and E. P. Likhtman. Extension of the Algebra of Poincare Group Generators and Violation of p Invariance. *JETP Lett.*, 13:323–326, 1971. [Pisma Zh. Eksp. Teor. Fiz.13,452(1971)].

[66] J. Wess and B. Zumino. Supergauge Transformations in Four-Dimensions. *Nucl. Phys.*, B70:39–50, 1974. doi: 10.1016/0550-3213(74)90355-1. [,24(1974)].

[67] S. Weinberg. Implications of Dynamical Symmetry Breaking. *Phys. Rev.*, D13:974–996, 1976. doi: 10.1103/PhysRevD.19.1277,10.1103/PhysRevD.13.974. [Addendum: Phys. Rev.D19,1277(1979)].

[68] E. Gildener. Gauge Symmetry Hierarchies. *Phys. Rev.*, D14:1667, 1976. doi: 10.1103/PhysRevD.14.1667.

[69] L. Susskind. Dynamics of Spontaneous Symmetry Breaking in the Weinberg-Salam Theory. *Phys. Rev.*, D20:2619–2625, 1979. doi: 10.1103/PhysRevD.20.2619.

[70] G. 't Hooft, C. Itzykson, A. Jaffe, H. Lehmann, P. K. Mitter, I. M. Singer, and R. Stora. Recent Developments in Gauge Theories. Proceedings, Nato Advanced Study Institute, Cargese, France, August 26 - September 8, 1979. *NATO Sci. Ser. B*, 59:pp.1–438, 1980. doi: 10.1007/978-1-4684-7571-5.

[71] A. Salam and J. A. Strathdee. On Superfields and Fermi-Bose Symmetry. *Phys. Rev.*, D11:1521–1535, 1975. doi: 10.1103/PhysRevD.11.1521.

[72] Marcus T. Grisaru, W. Siegel, and M. Rocek. Improved Methods for Supergraphs. *Nucl. Phys.*, B159:429, 1979. doi: 10.1016/0550-3213(79)90344-4.

[73] G. R. Farrar and P. Fayet. Phenomenology of the Production, Decay, and Detection of New Hadronic States Associated with Supersymmetry. *Phys. Lett.*, 76B: 575–579, 1978. doi: 10.1016/0370-2693(78)90858-4.

[74] P. Langacker. Precision Tests Of The Standard Model. *Proceedings of the PASCOS90 Symposium*, World Scientific, 1990.

[75] J. R. Ellis, S. Kelley, and Dimitri V. Nanopoulos. Probing the desert using gauge coupling unification. *Phys. Lett.*, B260:131–137, 1991. doi: 10.1016/0370-2693(91)90980-5.

[76] U. Amaldi, W. de Boer, and H. Furstenau. Comparison of grand unified theories with electroweak and strong coupling constants measured at LEP. *Phys. Lett.*, B260:447–455, 1991. doi: 10.1016/0370-2693(91)91641-8.

[77] P. Langacker and M. Luo. Implications of precision electroweak experiments for M_t, ρ_0, $\sin^2\theta_W$ and grand unification. *Phys. Rev.*, D44:817–822, 1991. doi: 10.1103/PhysRevD.44.817.

[78] C. Giunti, C. W. Kim, and U. W. Lee. Running coupling constants and grand unification models. *Mod. Phys. Lett.*, A6:1745–1755, 1991. doi: 10.1142/S0217732391001883.

[79] D. Z. Freedman, P. van Nieuwenhuizen, and S. Ferrara. Progress Toward a Theory of Supergravity. *Phys. Rev.*, D13:3214–3218, 1976. doi: 10.1103/PhysRevD.13.3214.

[80] S. Deser and B. Zumino. Consistent Supergravity. *Phys. Lett.*, B62:335, 1976. doi: 10.1016/0370-2693(76)90089-7. [,335(1976)].

[81] P. Van Nieuwenhuizen. Supergravity. *Phys. Rept.*, 68:189–398, 1981. doi: 10.1016/0370-1573(81)90157-5.

[82] Abdus Salam and J. A. Strathdee. Supergauge Transformations. *Nucl. Phys.*, B76: 477–482, 1974. doi: 10.1016/0550-3213(74)90537-9.

[83] S. Ferrara, J. Wess, and B. Zumino. Supergauge Multiplets and Superfields. *Phys. Lett.*, 51B:239, 1974. doi: 10.1016/0370-2693(74)90283-4.

[84] S. Dimopoulos and H. Georgi. Softly Broken Supersymmetry and SU(5). *Nucl. Phys.*, B193:150–162, 1981. doi: 10.1016/0550-3213(81)90522-8.

[85] S. Weinberg. Supersymmetry at Ordinary Energies. 1. Masses and Conservation Laws. *Phys. Rev.*, D26:287, 1982. doi: 10.1103/PhysRevD.26.287.

[86] N. Sakai and T. Yanagida. Proton Decay in a Class of Supersymmetric Grand Unified Models. *Nucl. Phys.*, B197:533, 1982. doi: 10.1016/0550-3213(82)90457-6.

[87] S. Dimopoulos, S. Raby, and F. Wilczek. Proton Decay in Supersymmetric Models. *Phys. Lett.*, 112B:133, 1982. doi: 10.1016/0370-2693(82)90313-6.

[88] H. Goldberg. Constraint on the Photino Mass from Cosmology. *Phys. Rev. Lett.*, 50:1419, 1983. doi: 10.1103/PhysRevLett.103.099905,10.1103/PhysRevLett.50.1419. [,219(1983)].

[89] John R. Ellis, J. S. Hagelin, Dimitri V. Nanopoulos, Keith A. Olive, and M. Srednicki. Supersymmetric Relics from the Big Bang. *Nucl. Phys.*, B238:453–476, 1984. doi: 10.1016/0550-3213(84)90461-9. [,223(1983)].

[90] H. Georgi and S. L. Glashow. Unity of All Elementary Particle Forces. *Phys. Rev. Lett.*, 32:438–441, 1974. doi: 10.1103/PhysRevLett.32.438.

[91] Jogesh C. Pati and Abdus Salam. Lepton Number as the Fourth Color. *Phys. Rev.*, D10:275–289, 1974. doi: 10.1103/PhysRevD.10.275,10.1103/PhysRevD.11.703.2. [Erratum: Phys. Rev.D11,703(1975)].

[92] Stephen P. Martin. A Supersymmetry primer. pages 1–98, 1997. doi: 10.1142/9789812839657_0001,10.1142/9789814307505_0001. [Adv. Ser. Direct. High Energy Phys.18,1(1998)].

[93] H. Georgi. The State of the ArtGauge Theories. *AIP Conf. Proc.*, 23:575–582, 1975. doi: 10.1063/1.2947450.

[94] H. Fritzsch and P. Minkowski. Unified Interactions of Leptons and Hadrons. *Annals Phys.*, 93:193–266, 1975. doi: 10.1016/0003-4916(75)90211-0.

[95] R. N. Mohapatra. Supersymmetric grand unification. In *Supersymmetry, supergravity and supercolliders. Proceedings, Theoretical Advanced Study Institute in*

elementary particle physics, TASI'97, Boulder, USA, June 2-27, 1997, pages 601–657, 1997.

[96] J. H. Christenson, J. W. Cronin, V. L. Fitch, and R. Turlay. Evidence for the 2π Decay of the K_2^0 Meson. *Phys. Rev. Lett.*, 13:138–140, 1964. doi: 10.1103/PhysRevLett.13.138.

[97] J. Goldstone. Field Theories with Superconductor Solutions. *Nuovo Cim.*, 19: 154–164, 1961. doi: 10.1007/BF02812722.

[98] Y. Nambu and G. Jona-Lasinio. Dynamical Model of Elementary Particles Based on an Analogy with Superconductivity. 1. *Phys. Rev.*, 122:345–358, 1961. doi: 10.1103/PhysRev.122.345. [,127(1961)].

[99] Y. Nambu and G. Jona-Lasinio. Dynamical Model of Elementary Particles Based on an Analogy with Superconductivity. 2. *Phys. Rev.*, 124:246–254, 1961. doi: 10.1103/PhysRev.124.246. [,141(1961)].

[100] G. Altarelli and F. Feruglio. Discrete Flavor Symmetries and Models of Neutrino Mixing. *Rev. Mod. Phys.*, 82:2701–2729, 2010. doi: 10.1103/RevModPhys.82.2701.

[101] H. Ishimori, T. Kobayashi, H. Ohki, Y. Shimizu, H. Okada, and M. Tanimoto. Non-Abelian Discrete Symmetries in Particle Physics. *Prog. Theor. Phys. Suppl.*, 183:1–163, 2010. doi: 10.1143/PTPS.183.1.

[102] S. F. King and C. Luhn. Neutrino Mass and Mixing with Discrete Symmetry. *Rept. Prog. Phys.*, 76:056201, 2013. doi: 10.1088/0034-4885/76/5/056201.

[103] S. F. King, A. Merle, S. Morisi, Y. Shimizu, and M. Tanimoto. Neutrino Mass and Mixing: from Theory to Experiment. *New J. Phys.*, 16:045018, 2014. doi: 10.1088/1367-2630/16/4/045018.

[104] C. D. Froggatt and H. B. Nielsen. Hierarchy of Quark Masses, Cabibbo Angles and CP Violation. *Nucl. Phys.*, B147:277–298, 1979. doi: 10.1016/0550-3213(79)90316-X.

[105] P. F. Harrison, D. H. Perkins, and W. G. Scott. Tri-bimaximal mixing and the neutrino oscillation data. *Phys. Lett.*, B530:167, 2002. doi: 10.1016/S0370-2693(02)01336-9.

[106] P. F. Harrison and W. G. Scott. Permutation symmetry, tri - bimaximal neutrino mixing and the S3 group characters. *Phys. Lett.*, B557:76, 2003. doi: 10.1016/S0370-2693(03)00183-7.

[107] G. Lemaitre. The expanding universe. *Gen. Rel. Grav.*, 29:641–680, 1997. doi: 10.1023/A:1018855621348. [Annales Soc. Sci. Bruxelles A53,51(1933)].

[108] A. G. Riess et al. Observational evidence from supernovae for an accelerating universe and a cosmological constant. *Astron. J.*, 116:1009–1038, 1998. doi: 10.1086/300499.

[109] A. H. Guth. The Inflationary Universe: A Possible Solution to the Horizon and Flatness Problems. *Phys. Rev.*, D23:347–356, 1981. doi: 10.1103/PhysRevD.23.347. [Adv. Ser. Astrophys. Cosmol.3,139(1987)].

[110] A. D. Linde. A New Inflationary Universe Scenario: A Possible Solution of the Horizon, Flatness, Homogeneity, Isotropy and Primordial Monopole Problems. *Phys. Lett.*, 108B:389–393, 1982. doi: 10.1016/0370-2693(82)91219-9. [Adv. Ser. Astrophys. Cosmol.3,149(1987)].

[111] A. Albrecht and P. J. Steinhardt. Cosmology for Grand Unified Theories with Radiatively Induced Symmetry Breaking. *Phys. Rev. Lett.*, 48:1220–1223, 1982. doi: 10.1103/PhysRevLett.48.1220. [Adv. Ser. Astrophys. Cosmol.3,158(1987)].

[112] A. D. Sakharov. Violation of CP Invariance, C asymmetry, and baryon asymmetry of the universe. *Pisma Zh. Eksp. Teor. Fiz.*, 5:32–35, 1967. doi: 10.1070/PU1991v034n05ABEH002497. [Usp. Fiz. Nauk161,no.5,61(1991)].

[113] F. R. Klinkhamer and N. S. Manton. A Saddle Point Solution in the Weinberg-Salam Theory. *Phys. Rev.*, D30:2212, 1984. doi: 10.1103/PhysRevD.30.2212.

[114] M. Fukugita and T. Yanagida. Baryogenesis Without Grand Unification. *Phys. Lett.*, B174:45–47, 1986. doi: 10.1016/0370-2693(86)91126-3.

[115] W. Buchmuller, P. Di Bari, and M. Plumacher. Leptogenesis for pedestrians. *Annals Phys.*, 315:305–351, 2005. doi: 10.1016/j.aop.2004.02.003.

[116] S. Yu. Khlebnikov and M. E. Shaposhnikov. The Statistical Theory of Anomalous Fermion Number Nonconservation. *Nucl. Phys.*, B308:885–912, 1988. doi: 10.1016/0550-3213(88)90133-2.

[117] J. A. Harvey and M. S. Turner. Cosmological baryon and lepton number in the presence of electroweak fermion number violation. *Phys. Rev.*, D42:3344–3349, 1990. doi: 10.1103/PhysRevD.42.3344.

[118] T. Kaluza. Zum Unittsproblem der Physik. *Sitzungsber. Preuss. Akad. Wiss. Berlin (Math. Phys.)*, 1921:966–972, 1921. doi: 10.1142/S0218271818700017. [Int. J. Mod. Phys.D27,no.14,1870001(2018)].

[119] O. Klein. Quantum Theory and Five-Dimensional Theory of Relativity. *Z. Phys.*, 37:895–906, 1926. doi: 10.1007/BF01397481. [,76(1926)].

[120] Y. Kawamura. Gauge symmetry breaking from extra space $S^1/Z(2)$. *Prog. Theor. Phys.*, 103:613–619, 2000. doi: 10.1143/PTP.103.613.

[121] Y. Kawamura. Triplet doublet splitting, proton stability and extra dimension. *Prog. Theor. Phys.*, 105:999–1006, 2001. doi: 10.1143/PTP.105.999.

[122] Y. Kawamura. Split multiplets, coupling unification and extra dimension. *Prog. Theor. Phys.*, 105:691–696, 2001. doi: 10.1143/PTP.105.691.

[123] G. Altarelli, F. Feruglio, and Y. Lin. Tri-bimaximal neutrino mixing from orbifolding. *Nucl. Phys.*, B775:31–44, 2007. doi: 10.1016/j.nuclphysb.2007.03.042.

[124] A. Hebecker and J. March-Russell. The structure of GUT breaking by orbifolding. *Nucl. Phys.*, B625:128–150, 2002. doi: 10.1016/S0550-3213(02)00016-0.

[125] M. Quiros. New ideas in symmetry breaking. In *Summer Institute 2002 (SI 2002) Fuji-Yoshida, Japan, August 13-20, 2002*, pages 549–601, 2003. [,549(2003)].

[126] A. Adulpravitchai, A. Blum, and M. Lindner. Non-Abelian Discrete Flavor Symmetries from T**2/Z(N) Orbifolds. *JHEP*, 07:053, 2009. doi: 10.1088/1126-6708/2009/07/053.

[127] S. Ferrara, D. Lust, Alfred D. Shapere, and S. Theisen. Modular Invariance in Supersymmetric Field Theories. *Phys. Lett.*, B225:363, 1989. doi: 10.1016/0370-2693(89)90583-2.

[128] S. Ferrara, .D. Lust, and S. Theisen. Target Space Modular Invariance and Low-Energy Couplings in Orbifold Compactifications. *Phys. Lett.*, B233:147–152, 1989. doi: 10.1016/0370-2693(89)90631-X.

[129] S. F. King. Unified Models of Neutrinos, Flavour and CP Violation. *Prog. Part. Nucl. Phys.*, 94:217–256, 2017. doi: 10.1016/j.ppnp.2017.01.003.

[130] S. F. King. Atmospheric and solar neutrinos with a heavy singlet. *Phys. Lett.*, B439:350–356, 1998. doi: 10.1016/S0370-2693(98)01055-7.

[131] S. F. King. Atmospheric and solar neutrinos from single right-handed neutrino dominance and U(1) family symmetry. *Nucl. Phys.*, B562:57–77, 1999. doi: 10.1016/S0550-3213(99)00542-8.

[132] S. F. King. Large mixing angle MSW and atmospheric neutrinos from single right-handed neutrino dominance and U(1) family symmetry. *Nucl. Phys.*, B576:85–105, 2000. doi: 10.1016/S0550-3213(00)00109-7.

[133] S. F. King. Constructing the large mixing angle MNS matrix in seesaw models with right-handed neutrino dominance. *JHEP*, 09:011, 2002. doi: 10.1088/1126-6708/2002/09/011.

[134] F. P. An et al. Observation of electron-antineutrino disappearance at Daya Bay. *Phys. Rev. Lett.*, 108:171803, 2012. doi: 10.1103/PhysRevLett.108.171803.

[135] J. K. Ahn et al. Observation of Reactor Electron Antineutrino Disappearance in the RENO Experiment. *Phys. Rev. Lett.*, 108:191802, 2012. doi: 10.1103/PhysRevLett.108.191802.

[136] Y. Abe et al. Indication of Reactor $\bar{\nu}_e$ Disappearance in the Double Chooz Experiment. *Phys. Rev. Lett.*, 108:131801, 2012. doi: 10.1103/PhysRevLett.108.131801.

[137] S. F. King. Predicting neutrino parameters from SO(3) family symmetry and quark-lepton unification. *JHEP*, 08:105, 2005. doi: 10.1088/1126-6708/2005/08/105.

[138] S. F. King. Minimal predictive see-saw model with normal neutrino mass hierarchy. *JHEP*, 07:137, 2013. doi: 10.1007/JHEP07(2013)137.

[139] S. F. King. Minimal see-saw model predicting best fit lepton mixing angles. *Phys. Lett.*, B724:92–98, 2013. doi: 10.1016/j.physletb.2013.06.013.

[140] F. Björkeroth and S. F. King. Testing constrained sequential dominance models of neutrinos. *J. Phys.*, G42(12):125002, 2015. doi: 10.1088/0954-3899/42/12/125002.

[141] S. F. King. Littlest Seesaw. *JHEP*, 02:085, 2016. doi: 10.1007/JHEP02(2016)085.

[142] S. F. King and C. Luhn. Littlest Seesaw model from $S_4\times$ U(1). *JHEP*, 09:023, 2016. doi: 10.1007/JHEP09(2016)023.

[143] Peter Ballett, Stephen F. King, Silvia Pascoli, Nick W. Prouse, and TseChun Wang. Precision neutrino experiments vs the Littlest Seesaw. *JHEP*, 03:110, 2017. doi: 10.1007/JHEP03(2017)110.

[144] R. Gatto, G. Sartori, and M. Tonin. Weak Selfmasses, Cabibbo Angle, and Broken SU(2) x SU(2). *Phys. Lett.*, 28B:128–130, 1968. doi: 10.1016/0370-2693(68)90150-0.

[145] C. Hagedorn, M. Lindner, and R. N. Mohapatra. S(4) flavor symmetry and fermion masses: Towards a grand unified theory of flavor. *JHEP*, 06:042, 2006. doi: 10.1088/1126-6708/2006/06/042.

[146] B. Dutta, Y. Mimura, and R. N. Mohapatra. An SO(10) Grand Unified Theory of Flavor. *JHEP*, 05:034, 2010. doi: 10.1007/JHEP05(2010)034.

[147] P. S. Bhupal Dev, B. Dutta, R. N. Mohapatra, and Matthew Severson. θ_{13} and Proton Decay in a Minimal $SO(10)\times S_4$ model of Flavor. *Phys. Rev.*, D86:035002, 2012. doi: 10.1103/PhysRevD.86.035002.

[148] K. M. Patel. An SO(10)XS4 Model of Quark-Lepton Complementarity. *Phys. Lett.*, B695:225–230, 2011. doi: 10.1016/j.physletb.2010.11.024.

[149] D.-G. Lee and R. N. Mohapatra. An SO(10) x S(4) scenario for naturally degenerate neutrinos. *Phys. Lett.*, B329:463–468, 1994. doi: 10.1016/0370-2693(94)91091-X.

[150] Y. Cai and H.-B. Yu. A SO(10) GUT Model with S4 Flavor Symmetry. *Phys. Rev.*, D74:115005, 2006. doi: 10.1103/PhysRevD.74.115005.

[151] P. S. Bhupal D., R. N. Mohapatra, and M. Severson. Neutrino Mixings in SO(10) with Type II Seesaw and θ_{13}. *Phys. Rev.*, D84:053005, 2011. doi: 10.1103/PhysRevD.84.053005.

[152] I. de Medeiros Varzielas, S. F. King, and G. G. Ross. Neutrino tri-bi-maximal mixing from a non-Abelian discrete family symmetry. *Phys. Lett.*, B648:201–206, 2007. doi: 10.1016/j.physletb.2007.03.009.

[153] S. F. King and M. Malinsky. A(4) family symmetry and quark-lepton unification. *Phys. Lett.*, B645:351–357, 2007. doi: 10.1016/j.physletb.2006.12.006.

[154] S. Morisi, M. Picariello, and E. Torrente-Lujan. Model for fermion masses and lepton mixing in SO(10) x A(4). *Phys. Rev.*, D75:075015, 2007. doi: 10.1103/PhysRevD.75.075015.

[155] F. Bazzocchi, M. Frigerio, and S. Morisi. Fermion masses and mixing in models with SO(10) x A(4) symmetry. *Phys. Rev.*, D78:116018, 2008. doi: 10.1103/PhysRevD.78.116018.

[156] C. Hagedorn, M. A. Schmidt, and A. Yu. Smirnov. Lepton Mixing and Cancellation of the Dirac Mass Hierarchy in SO(10) GUTs with Flavor Symmetries T(7) and Sigma(81). *Phys. Rev.*, D79:036002, 2009. doi: 10.1103/PhysRevD.79.036002.

[157] F. Bazzocchi and I. de Medeiros Varzielas. Tri-bi-maximal mixing in viable family symmetry unified model with extended seesaw. *Phys. Rev.*, D79:093001, 2009. doi: 10.1103/PhysRevD.79.093001.

[158] S. F. King and C. Luhn. A New family symmetry for SO(10) GUTs. *Nucl. Phys.*, B820:269–289, 2009. doi: 10.1016/j.nuclphysb.2009.05.020.

[159] S. F. King and C. Luhn. A Supersymmetric Grand Unified Theory of Flavour with PSL(2)(7) x SO(10). *Nucl. Phys.*, B832:414–439, 2010. doi: 10.1016/j.nuclphysb.2010.02.019.

[160] I. de Medeiros Varzielas and G. G. Ross. Discrete family symmetry, Higgs mediators and $theta_{13}$. *JHEP*, 12:041, 2012. doi: 10.1007/JHEP12(2012)041.

[161] A. Anandakrishnan, S. Raby, and A. Wingerter. Yukawa Unification Predictions for the LHC. *Phys. Rev.*, D87(5):055005, 2013. doi: 10.1103/PhysRevD.87.055005.

[162] S. F. King and G. G. Ross. Fermion masses and mixing angles from SU (3) family symmetry and unification. *Phys. Lett.*, B574:239–252, 2003. doi: 10.1016/j.physletb.2003.09.027.

[163] Ivo de Medeiros Varzielas and Graham G. Ross. SU(3) family symmetry and neutrino bi-tri-maximal mixing. *Nucl. Phys.*, B733:31–47, 2006. doi: 10.1016/j.nuclphysb.2005.10.039.

[164] I. de Medeiros Varzielas, S. F. King, and G. G. Ross. Tri-bimaximal neutrino mixing from discrete subgroups of SU(3) and SO(3) family symmetry. *Phys. Lett.*, B644:153–157, 2007. doi: 10.1016/j.physletb.2006.11.015.

[165] S. F. King and M. Malinsky. Towards a Complete Theory of Fermion Masses and Mixings with SO(3) Family Symmetry and 5-D SO(10) Unification. *JHEP*, 11: 071, 2006. doi: 10.1088/1126-6708/2006/11/071.

[166] G. Altarelli, F. Feruglio, and C. Hagedorn. A SUSY SU(5) Grand Unified Model of Tri-Bimaximal Mixing from A_4. *JHEP*, 03:052, 2008. doi: 10.1088/1126-6708/2008/03/052.

[167] P. Ciafaloni, M. Picariello, E. Torrente-Lujan, and A. Urbano. Neutrino masses and tribimaximal mixing in Minimal renormalizable SUSY SU(5) Grand Unified Model with A(4) Flavor symmetry. *Phys. Rev.*, D79:116010, 2009. doi: 10.1103/PhysRevD.79.116010.

[168] T. J. Burrows and S. F. King. A(4) Family Symmetry from SU(5) SUSY GUTs in 6d. *Nucl. Phys.*, B835:174–196, 2010. doi: 10.1016/j.nuclphysb.2010.04.002.

[169] I. K. Cooper, S. F. King, and C. Luhn. SUSY SU(5) with singlet plus adjoint matter and A4 family symmetry. *Phys. Lett.*, B690:396–402, 2010. doi: 10.1016/j.physletb.2010.05.066.

[170] S. Antusch, S. F. King, and M. Spinrath. Measurable Neutrino Mass Scale in $A_4\times$ SU(5). *Phys. Rev.*, D83:013005, 2011. doi: 10.1103/PhysRevD.83.013005.

[171] S. Antusch, S. F. King, C. Luhn, and Martin Spinrath. Right Unitarity Triangles and Tri-Bimaximal Mixing from Discrete Symmetries and Unification. *Nucl. Phys.*, B850:477–504, 2011. doi: 10.1016/j.nuclphysb.2011.05.005.

[172] D. Meloni. Bimaximal mixing and large theta13 in a SUSY SU(5) model based on S4. *JHEP*, 10:010, 2011. doi: 10.1007/JHEP10(2011)010.

[173] T. J. Burrows and S. F. King. A_4 x SU(5) SUSY GUT of Flavour in 8d. *Nucl. Phys.*, B842:107–121, 2011. doi: 10.1016/j.nuclphysb.2010.08.018.

[174] C. Hagedorn, S. F. King, and C. Luhn. SUSY $S_4\times$ SU(5) revisited. *Phys. Lett.*, B717:207–213, 2012. doi: 10.1016/j.physletb.2012.09.026.

[175] J. P. Gehrlein, J.and Oppermann, D. Schfer, and M. Spinrath. An SU(5) $\times$ A_5 golden ratio flavour model. *Nucl. Phys.*, B890:539–568, 2014. doi: 10.1016/j.nuclphysb.2014.11.023.

[176] B. D. Callen and R. R. Volkas. Large lepton mixing angles from a 4+1-dimensional SU(5) x A(4) domain-wall braneworld model. *Phys. Rev.*, D86:056007, 2012. doi: 10.1103/PhysRevD.86.056007.

[177] A. Meroni, S. T. Petcov, and M. Spinrath. A SUSY SU(5)xT' Unified Model of Flavour with large θ_{13}. *Phys. Rev.*, D86:113003, 2012. doi: 10.1103/PhysRevD.86.113003.

[178] M.-C. Chen, J. Huang, K. T. Mahanthappa, and A. M. Wijangco. Large $\theta_1 3$ in a SUSY $SU(5) \times T'$ Model. *JHEP*, 10:112, 2013. doi: 10.1007/JHEP10(2013)112.

[179] S. F. King, C. Luhn, and A. J. Stuart. A Grand Delta(96) x SU(5) Flavour Model. *Nucl. Phys.*, B867:203–235, 2013. doi: 10.1016/j.nuclphysb.2012.09.021.

[180] S. Antusch, C. Gross, V. Maurer, and C. Sluka. A flavour GUT model with $\theta_{13}^{PMNS} \simeq \theta_C/\sqrt{2}$. *Nucl. Phys.*, B877:772–791, 2013. doi: 10.1016/j.nuclphysb.2013.11.003.

[181] S. Antusch, C. Gross, V. Maurer, and C. Sluka. Inverse neutrino mass hierarchy in a flavour GUT model. *Nucl. Phys.*, B879:19–36, 2014. doi: 10.1016/j.nuclphysb.2013.11.017.

[182] S. Antusch, I. de Medeiros Varzielas, V. Maurer, C. Sluka, and M. Spinrath. Towards predictive flavour models in SUSY SU(5) GUTs with doublet-triplet splitting. *JHEP*, 09:141, 2014. doi: 10.1007/JHEP09(2014)141.

[183] S. F. King. A model of quark and lepton mixing. *JHEP*, 01:119, 2014. doi: 10.1007/JHEP01(2014)119.

[184] S. F. King. A to Z of Flavour with Pati-Salam. *JHEP*, 08:130, 2014. doi: 10.1007/JHEP08(2014)130.

[185] R. de Adelhart Toorop, F. Bazzocchi, and L. Merlo. The Interplay Between GUT and Flavour Symmetries in a Pati-Salam x S4 Model. *JHEP*, 08:001, 2010. doi: 10.1007/JHEP08(2010)001.

[186] T. Feldmann, F. Hartmann, W. Kilian, and C. Luhn. Combining Pati-Salam and Flavour Symmetries. *JHEP*, 10:160, 2015. doi: 10.1007/JHEP10(2015)160.

[187] I. de Medeiros Varzielas. Non-Abelian family symmetries in Pati-Salam unification. *JHEP*, 01:097, 2012. doi: 10.1007/JHEP01(2012)097.

[188] I. P. Ivanov and L. Lavoura. SO(10) models with flavour symmetries: Classification and examples. *J. Phys.*, G43(10):105005, 2016. doi: 10.1088/0954-3899/43/10/105005.

[189] H. Lee, S. Raby, M. Ratz, G. G. Ross, R. Schieren, K. Schmidt-Hoberg, and P. K. S. Vaudrevange. A unique $\mathbb{Z}_4^R$ symmetry for the MSSM. *Phys. Lett.*, B694: 491–495, 2011. doi: 10.1016/j.physletb.2010.10.038.

[190] S. Dimopoulos and F. Wilczek. Incomplete Multiplets in Supersymmetric Unified Models. 1981.

[191] K. S. Babu and S. M. Barr. Natural suppression of Higgsino mediated proton decay in supersymmetric SO(10). *Phys. Rev.*, D48:5354–5364, 1993. doi: 10.1103/PhysRevD.48.5354.

[192] S. M. Barr and S. Raby. Minimal SO(10) unification. *Phys. Rev. Lett.*, 79:4748–4751, 1997. doi: 10.1103/PhysRevLett.79.4748.

[193] D. Binosi and L. Theussl. JaxoDraw: A Graphical user interface for drawing Feynman diagrams. *Comput. Phys. Commun.*, 161:76–86, 2004. doi: 10.1016/j.cpc.2004.05.001.

[194] P. Nath and P. Fileviez Perez. Proton stability in grand unified theories, in strings and in branes. *Phys. Rept.*, 441:191–317, 2007. doi: 10.1016/j.physrep.2007.02.010.

[195] A. Bueno, Z. Dai, Y. Ge, M. Laffranchi, A. J. Melgarejo, A. Meregaglia, S. Navas, and A. Rubbia. Nucleon decay searches with large liquid argon TPC detectors at shallow depths: Atmospheric neutrinos and cosmogenic backgrounds. *JHEP*, 04: 041, 2007. doi: 10.1088/1126-6708/2007/04/041.

[196] H. Murayama and D. B. Kaplan. Family symmetries and proton decay. *Phys. Lett.*, B336:221–228, 1994. doi: 10.1016/0370-2693(94)90242-9.

[197] F. Björkeroth, F. J. de Anda, I. de Medeiros Varzielas, and S. F. King. Leptogenesis in a $\Delta(27)\times SO(10)$ SUSY GUT. *JHEP*, 01:077, 2017. doi: 10.1007/JHEP01(2017)077.

[198] G. G. Ross. Family symmetries. *J. Phys. Conf. Ser.*, 171:012006, 2009. doi: 10.1088/1742-6596/171/1/012006.

[199] S. Antusch and V. Maurer. Running quark and lepton parameters at various scales. *JHEP*, 11:115, 2013. doi: 10.1007/JHEP11(2013)115.

[200] I. Esteban, M. C. Gonzalez-Garcia, M. Maltoni, I. Martinez-Soler, and T. Schwetz. Updated fit to three neutrino mixing: exploring the accelerator-reactor complementarity. *JHEP*, 01:087, 2017. doi: 10.1007/JHEP01(2017)087.

[201] R. Andrae, T. Schulze-Hartung, and P. Melchior. Dos and don'ts of reduced chi-squared. 2010.

[202] S. Antusch, S. F. King, C. Luhn, and M. Spinrath. Trimaximal mixing with predicted θ_{13} from a new type of constrained sequential dominance. *Nucl. Phys.*, B856:328–341, 2012. doi: 10.1016/j.nuclphysb.2011.11.009.

[203] S. Antusch, J. Kersten, M. Lindner, M. Ratz, and M. A. Schmidt. Running neutrino mass parameters in see-saw scenarios. *JHEP*, 03:024, 2005. doi: 10.1088/1126-6708/2005/03/024.

[204] K. Abe et al. Combined Analysis of Neutrino and Antineutrino Oscillations at T2K. *Phys. Rev. Lett.*, 118(15):151801, 2017. doi: 10.1103/PhysRevLett.118.151801.

[205] S. Davidson. Parametrizations of the seesaw, or, can the seesaw be tested? In *Seesaw mechanism. Proceedings, International Conference, SEESAW25, Paris, France, June 10-11, 2004*, pages 249–260, 2004. doi: 10.1142/9789812702210_0018.

[206] P. Di Bari and M. Re Fiorentin. Supersymmetric $SO(10)$-inspired leptogenesis and a new N_2-dominated scenario. *JCAP*, 1603(03):039, 2016. doi: 10.1088/1475-7516/2016/03/039.

[207] A. Adulpravitchai and M. A. Schmidt. Flavored Orbifold GUT - an SO(10) x S4 model. *JHEP*, 01:106, 2011. doi: 10.1007/JHEP01(2011)106.

[208] F.J. de Anda and S. F. King. An $S_4 \times SU(5)$ SUSY GUT of flavour in 6d. *JHEP*, 07:057, 2018. doi: 10.1007/JHEP07(2018)057.

[209] F. J. de Anda and S. F. King. $SU(3) \times SO(10)$ in 6d. *JHEP*, 10:128, 2018. doi: 10.1007/JHEP10(2018)128.

[210] G. Altarelli and F. Feruglio. Tri-bimaximal neutrino mixing, A(4) and the modular symmetry. *Nucl. Phys.*, B741:215–235, 2006. doi: 10.1016/j.nuclphysb.2006.02.015.

[211] R. de Adelhart Toorop, F. Feruglio, and C. Hagedorn. Finite Modular Groups and Lepton Mixing. *Nucl. Phys.*, B858:437–467, 2012. doi: 10.1016/j.nuclphysb.2012.01.017.

[212] F. Feruglio. Are neutrino masses modular forms? In Aharon Levy, Stefano Forte, and Giovanni Ridolfi, editors, *From My Vast Repertoire ...: Guido Altarelli's Legacy*, pages 227–266. 2019. doi: 10.1142/9789813238053_0012.

[213] T. Kobayashi, K. Tanaka, and T. H. Tatsuishi. Neutrino mixing from finite modular groups. *Phys. Rev.*, D98(1):016004, 2018. doi: 10.1103/PhysRevD.98.016004.

[214] J. T. Penedo and S. T. Petcov. Lepton Masses and Mixing from Modular S_4 Symmetry. *Nucl. Phys.*, B939:292–307, 2019. doi: 10.1016/j.nuclphysb.2018.12.016.

[215] J. C. Criado and F. Feruglio. Modular Invariance Faces Precision Neutrino Data. *SciPost Phys.*, 5(5):042, 2018. doi: 10.21468/SciPostPhys.5.5.042.

[216] T. Kobayashi, N. Omoto, Y. Shimizu, K. Takagi, M. Tanimoto, and T. H. Tatsuishi. Modular A_4 invariance and neutrino mixing. *JHEP*, 11:196, 2018. doi: 10.1007/JHEP11(2018)196.

[217] P. P. Novichkov, J. T. Penedo, S. T. Petcov, and A. V. Titov. Modular S_4 models of lepton masses and mixing. *JHEP*, 04:005, 2019. doi: 10.1007/JHEP04(2019)005.

[218] P. P. Novichkov, J. T. Penedo, S. T. Petcov, and A. V. Titov. Modular A_5 symmetry for flavour model building. *JHEP*, 04:174, 2019. doi: 10.1007/JHEP04(2019)174.

[219] G.-J. Ding, S. F. King, and A. J. Stuart. Generalised CP and A_4 Family Symmetry. *JHEP*, 12:006, 2013. doi: 10.1007/JHEP12(2013)006.

[220] M. Holthausen, M. Lindner, and M. A. Schmidt. CP and Discrete Flavour Symmetries. *JHEP*, 04:122, 2013. doi: 10.1007/JHEP04(2013)122.

[221] L. E. Ibanez and G. G. Ross. SU(2)-L x U(1) Symmetry Breaking as a Radiative Effect of Supersymmetry Breaking in Guts. *Phys. Lett.*, 110B:215–220, 1982. doi: 10.1016/0370-2693(82)91239-4.

[222] L. E. Ibanez and G. G. Ross. Supersymmetric Higgs and radiative electroweak breaking. *Comptes Rendus Physique*, 8:1013–1028, 2007. doi: 10.1016/j.crhy.2007.02.004.

[223] B. R. Greene, K. H. Kirklin, P. J. Miron, and G. G. Ross. A Three Generation Superstring Model. 2. Symmetry Breaking and the Low-Energy Theory. *Nucl. Phys.*, B292:606–652, 1987. doi: 10.1016/0550-3213(87)90662-6.

[224] I. de Medeiros Varzielas. *Family symmetries and the origin of fermion masses and mixings*. PhD thesis, Oxford U., 2007.

[225] R. Howl and S. F. King. Solving the Flavour Problem in Supersymmetric Standard Models with Three Higgs Families. *Phys. Lett.*, B687:355–362, 2010. doi: 10.1016/j.physletb.2010.03.053.

[226] R. C. Gunning. Lectures on Modular Forms. *Princeton*, New Jersey USA:1962, Princeton University Press.

[227] Z.-Z. Xing and Z.-H. Zhao. A review of - flavor symmetry in neutrino physics. *Rept. Prog. Phys.*, 79(7):076201, 2016. doi: 10.1088/0034-4885/79/7/076201.

[228] Stephen F. King and Celso C. Nishi. Mu-tau symmetry and the Littlest Seesaw. *Phys. Lett.*, B785:391–398, 2018. doi: 10.1016/j.physletb.2018.08.056.

[229] P. F. Harrison and W. G. Scott. mu - tau reflection symmetry in lepton mixing and neutrino oscillations. *Phys. Lett.*, B547:219–228, 2002. doi: 10.1016/S0370-2693(02)02772-7.

[230] M. Tanabashi et al. Review of Particle Physics. *Phys. Rev.*, D98(3):030001, 2018. doi: 10.1103/PhysRevD.98.030001.

[231] S. Descotes-Genon, J. Matias, and J. Virto. Understanding the $B \to K^* \mu^+ \mu^-$ Anomaly. *Phys. Rev.*, D88:074002, 2013. doi: 10.1103/PhysRevD.88.074002.

[232] W. Altmannshofer and D. M. Straub. New Physics in $B \to K^* \mu\mu$? *Eur. Phys. J.*, C73:2646, 2013. doi: 10.1140/epjc/s10052-013-2646-9.

[233] D. Ghosh, M. Nardecchia, and S. A. Renner. Hint of Lepton Flavour Non-Universality in B Meson Decays. *JHEP*, 12:131, 2014. doi: 10.1007/JHEP12(2014)131.

[234] R. Aaij et al. Test of lepton universality using $B^+ \to K^+ \ell^+ \ell^-$ decays. *Phys. Rev. Lett.*, 113:151601, 2014. doi: 10.1103/PhysRevLett.113.151601.

[235] R. Aaij et al. Test of lepton universality with $B^0 \to K^{*0} \ell^+ \ell^-$ decays. *JHEP*, 08:055, 2017. doi: 10.1007/JHEP08(2017)055.

[236] B. Capdevila, A. Crivellin, S. Descotes-Genon, J. Matias, and J. Virto. Patterns of New Physics in $b \to s \ell^+ \ell^-$ transitions in the light of recent data. *JHEP*, 01:093, 2018. doi: 10.1007/JHEP01(2018)093.

[237] W. Altmannshofer, P. Stangl, and D. M. Straub. Interpreting Hints for Lepton Flavor Universality Violation. *Phys. Rev.*, D96(5):055008, 2017. doi: 10.1103/PhysRevD.96.055008.

[238] M. Ciuchini, A. M. Coutinho, M. Fedele, E. Franco, A. Paul, L. Silvestrini, and M. Valli. On Flavourful Easter eggs for New Physics hunger and Lepton Flavour Universality violation. *Eur. Phys. J.*, C77(10):688, 2017. doi: 10.1140/epjc/s10052-017-5270-2.

[239] G. Hiller and I. Nisandzic. R_K and R_{K^*} beyond the standard model. *Phys. Rev.*, D96(3):035003, 2017. doi: 10.1103/PhysRevD.96.035003.

[240] L.-S. Geng, B. Grinstein, S. Jger, J. Martin Camalich, X.-L. Ren, and R.-X. Shi. Towards the discovery of new physics with lepton-universality ratios of $b \to s\ell\ell$ decays. *Phys. Rev.*, D96(9):093006, 2017. doi: 10.1103/PhysRevD.96.093006.

[241] D. Ghosh. Explaining the R_K and R_{K^*} anomalies. *Eur. Phys. J.*, C77(10):694, 2017. doi: 10.1140/epjc/s10052-017-5282-y.

[242] D. Bardhan, P. Byakti, and D. Ghosh. Role of Tensor operators in R_K and R_{K^*}. *Phys. Lett.*, B773:505–512, 2017. doi: 10.1016/j.physletb.2017.08.062.

[243] G. D'Amico, M. Nardecchia, P. Panci, F. Sannino, A. Strumia, R. Torre, and A. Urbano. Flavour anomalies after the R_{K^*} measurement. *JHEP*, 09:010, 2017. doi: 10.1007/JHEP09(2017)010.

[244] A. K. Alok, B. Bhattacharya, A. Datta, D. Kumar, J. Kumar, and D. London. New Physics in $b \to s\mu^+\mu^-$ after the Measurement of R_{K^*}. *Phys. Rev.*, D96(9): 095009, 2017. doi: 10.1103/PhysRevD.96.095009.

[245] R. Gauld, F. Goertz, and U. Haisch. On minimal Z' explanations of the $B \to K^*\mu^+\mu^-$ anomaly. *Phys. Rev.*, D89:015005, 2014. doi: 10.1103/PhysRevD.89.015005.

[246] A. J. Buras and J. Girrbach. Left-handed Z' and Z FCNC quark couplings facing new $b \to s\mu^+\mu^-$ data. *JHEP*, 12:009, 2013. doi: 10.1007/JHEP12(2013)009.

[247] W. Altmannshofer, S. Gori, M. Pospelov, and I. Yavin. Quark flavor transitions in $L_\mu - L_\tau$ models. *Phys. Rev.*, D89:095033, 2014. doi: 10.1103/PhysRevD.89.095033.

[248] A. Crivellin, G. D'Ambrosio, and J. Heeck. Explaining $h \to \mu^\pm\tau^\mp$, $B \to K^*\mu^+\mu^-$ and $B \to K\mu^+\mu^-/B \to Ke^+e^-$ in a two-Higgs-doublet model with gauged $L_\mu - L_\tau$. *Phys. Rev. Lett.*, 114:151801, 2015. doi: 10.1103/PhysRevLett.114.151801.

[249] A. Crivellin, G. D'Ambrosio, and J. Heeck. Addressing the LHC flavor anomalies with horizontal gauge symmetries. *Phys. Rev.*, D91(7):075006, 2015. doi: 10.1103/PhysRevD.91.075006.

[250] C. Niehoff, P. Stangl, and D. M. Straub. Violation of lepton flavour universality in composite Higgs models. *Phys. Lett.*, B747:182–186, 2015. doi: 10.1016/j.physletb.2015.05.063.

[251] A. Celis, J. Fuentes-Martin, M. Jung, and H. Serodio. Family nonuniversal $Z\prime$ models with protected flavor-changing interactions. *Phys. Rev.*, D92(1):015007, 2015. doi: 10.1103/PhysRevD.92.015007.

[252] A. Greljo, G. Isidori, and D. Marzocca. On the breaking of Lepton Flavor Universality in B decays. *JHEP*, 07:142, 2015. doi: 10.1007/JHEP07(2015)142.

[253] C. Niehoff, P. Stangl, and D. M. Straub. Direct and indirect signals of natural composite Higgs models. *JHEP*, 01:119, 2016. doi: 10.1007/JHEP01(2016)119.

[254] W. Altmannshofer and I. Yavin. Predictions for lepton flavor universality violation in rare B decays in models with gauged $L_\mu - L_\tau$. *Phys. Rev.*, D92(7):075022, 2015. doi: 10.1103/PhysRevD.92.075022.

[255] A. Falkowski, M. Nardecchia, and R. Ziegler. Lepton Flavor Non-Universality in B-meson Decays from a U(2) Flavor Model. *JHEP*, 11:173, 2015. doi: 10.1007/JHEP11(2015)173.

[256] A. Carmona and F. Goertz. Lepton Flavor and Nonuniversality from Minimal Composite Higgs Setups. *Phys. Rev. Lett.*, 116(25):251801, 2016. doi: 10.1103/PhysRevLett.116.251801.

[257] I. Garcia Garcia. LHCb anomalies from a natural perspective. *JHEP*, 03:040, 2017. doi: 10.1007/JHEP03(2017)040.

[258] E. Megias, G. Panico, O. Pujolas, and M. Quiros. A Natural origin for the LHCb anomalies. *JHEP*, 09:118, 2016. doi: 10.1007/JHEP09(2016)118.

[259] C.-W. Chiang, X.-G. He, and G. Valencia. $Z\prime$ model for $b \to s\ell\overline{\ell}$ flavor anomalies. *Phys. Rev.*, D93(7):074003, 2016. doi: 10.1103/PhysRevD.93.074003.

[260] W. Altmannshofer, M. Carena, and A. Crivellin. $L_\mu - L_\tau$ theory of Higgs flavor violation and $(g-2)_\mu$. *Phys. Rev.*, D94(9):095026, 2016. doi: 10.1103/PhysRevD.94.095026.

[261] S. M. Boucenna, A. Celis, J. Fuentes-Martin, A. Vicente, and J. Virto. Phenomenology of an $SU(2) \times SU(2) \times U(1)$ model with lepton-flavour non-universality. *JHEP*, 12:059, 2016. doi: 10.1007/JHEP12(2016)059.

[262] P. Foldenauer and J. Jaeckel. Purely flavor-changing Z' bosons and where they might hide. *JHEP*, 05:010, 2017. doi: 10.1007/JHEP05(2017)010.

[263] J. F. Kamenik, Y. Soreq, and J. Zupan. Lepton flavor universality violation without new sources of quark flavor violation. *Phys. Rev.*, D97(3):035002, 2018. doi: 10.1103/PhysRevD.97.035002.

[264] R. S. Chivukula, J. Isaacson, K. A. Mohan, D. Sengupta, and E. H. Simmons. R_K anomalies and simplified limits on Z' models at the LHC. *Phys. Rev.*, D96(7): 075012, 2017. doi: 10.1103/PhysRevD.96.075012.

[265] G. Faisel and J. Tandean. Connecting $b \to s\ell\overline{\ell}$ anomalies to enhanced rare nonleptonic $\overline{B}_s^0$ decays in Z' model. *JHEP*, 02:074, 2018. doi: 10.1007/JHEP02(2018)074.

[266] J. Ellis, M. Fairbairn, and P. Tunney. Anomaly-Free Models for Flavour Anomalies. 2017.

[267] R. Alonso, P. Cox, C. Han, and T. T. Yanagida. Flavoured $B-L$ local symmetry and anomalous rare B decays. *Phys. Lett.*, B774:643–648, 2017. doi: 10.1016/j.physletb.2017.10.027.

[268] A. Carmona and F. Goertz. Recent $\boldsymbol{B}$ Physics Anomalies - a First Hint for Compositeness? 2017.

[269] M. Dalchenko, B. Dutta, R. Eusebi, P. Huang, T. Kamon, and D. Rathjens. Bottom-quark Fusion Processes at the LHC for Probing Z' Models and B-meson Decay Anomalies. 2017.

[270] S. Raby and A. Trautner. A "Vector-like chiral" fourth family to explain muon anomalies. 2017.

[271] L. Bian, S.-M. Choi, Y.-J. Kang, and H. M. Lee. A minimal flavored $U(1)'$ for B-meson anomalies. *Phys. Rev.*, D96(7):075038, 2017. doi: 10.1103/PhysRevD.96.075038.

[272] L. Bian, H. M. Lee, and C. B. Park. B-meson anomalies and Higgs physics in flavored $U(1)'$ model. 2017.

[273] A. K. Alok, B. Bhattacharya, D. Kumar, J. Kumar, D. London, and S. U. Sankar. New physics in $b \to s\mu^+\mu^-$: Distinguishing models through CP-violating effects. *Phys. Rev.*, D96(1):015034, 2017. doi: 10.1103/PhysRevD.96.015034.

[274] P. J. Fox, I. Low, and Y. Zhang. Top-philic Z' Forces at the LHC. 2018.

[275] M. Chala and M. Spannowsky. On the behaviour of composite resonances breaking lepton flavour universality. 2018.

[276] D. Aristizabal S., F. Staub, and A. Vicente. Shedding light on the $b \to s$ anomalies with a dark sector. *Phys. Rev.*, D92(1):015001, 2015. doi: 10.1103/PhysRevD.92.015001.

[277] G. Blanger, C. Delaunay, and S. Westhoff. A Dark Matter Relic From Muon Anomalies. *Phys. Rev.*, D92:055021, 2015. doi: 10.1103/PhysRevD.92.055021.

[278] A. Celis, W.-Z. Feng, and M. Vollmann. Dirac dark matter and $b \to s\ell^+\ell^-$ with U(1) gauge symmetry. *Phys. Rev.*, D95(3):035018, 2017. doi: 10.1103/PhysRevD.95.035018.

[279] W. Altmannshofer, S. Gori, S. Profumo, and F. S. Queiroz. Explaining dark matter and B decay anomalies with an $L_\mu - L_\tau$ model. *JHEP*, 12:106, 2016. doi: 10.1007/JHEP12(2016)106.

[280] S. Baek. Dark matter contribution to $b \to s\mu^+\mu^-$ anomaly in local $U(1)_{L_\mu - L_\tau}$ model. 2017.

[281] J. M. Cline and J. M. Cornell. $R(K^{(*)})$ from dark matter exchange. 2017.

[282] K. Fuyuto, H.-L. Li, and J.-H. Yu. Implications of hidden gauged $U(1)$ model for B anomalies. 2017.

[283] S. F. King. Flavourful Z$'$ models for $R_{K^{(*)}}$. *JHEP*, 08:019, 2017. doi: 10.1007/JHEP08(2017)019.

[284] M. C. Romao, S. F. King, and G. K. Leontaris. Non-universal Z' from Fluxed GUTs. 2017.

[285] S. Antusch, C. Hohl, S. F. King, and Vasja Susic. Non-universal Z' from SO(10) GUTs with vector-like family and the origin of neutrino masses. 2017.

[286] L. Di Luzio, M. Kirk, and A. Lenz. One constraint to kill them all? 2017.

[287] M. Artuso, G. Borissov, and A. Lenz. CP violation in the B_s^0 system. *Rev. Mod. Phys.*, 88(4):045002, 2016. doi: 10.1103/RevModPhys.88.045002.

[288] D. Geiregat et al. First observation of neutrino trident production. *Phys. Lett.*, B245:271–275, 1990. doi: 10.1016/0370-2693(90)90146-W.

[289] S. R. Mishra et al. Neutrino tridents and W Z interference. *Phys. Rev. Lett.*, 66: 3117–3120, 1991. doi: 10.1103/PhysRevLett.66.3117.

[290] W. Altmannshofer, S. Gori, M. Pospelov, and I. Yavin. Neutrino Trident Production: A Powerful Probe of New Physics with Neutrino Beams. *Phys. Rev. Lett.*, 113:091801, 2014. doi: 10.1103/PhysRevLett.113.091801.

[291] A. Falkowski, M. Gonzlez-Alonso, and K. Mimouni. Compilation of low-energy constraints on 4-fermion operators in the SMEFT. *JHEP*, 08:123, 2017. doi: 10.1007/JHEP08(2017)123.

[292] S. Chatrchyan et al. Observation of Z decays to four leptons with the CMS detector at the LHC. *JHEP*, 12:034, 2012. doi: 10.1007/JHEP12(2012)034.

[293] G. Aad et al. Measurements of Four-Lepton Production at the Z Resonance in pp Collisions at $\sqrt{s}$ =7 and 8 TeV with ATLAS. *Phys. Rev. Lett.*, 112(23):231806, 2014. doi: 10.1103/PhysRevLett.112.231806.

[294] D. A. Faroughy, A. Greljo, and J. F. Kamenik. Confronting lepton flavor universality violation in B decays with high-p_T tau lepton searches at LHC. *Phys. Lett.*, B764:126–134, 2017. doi: 10.1016/j.physletb.2016.11.011.

[295] J. Alwall, R. Frederix, S. Frixione, V. Hirschi, F. Maltoni, O. Mattelaer, H. S. Shao, T. Stelzer, P. Torrielli, and M. Zaro. The automated computation of tree-level and next-to-leading order differential cross sections, and their matching to parton shower simulations. *JHEP*, 07:079, 2014. doi: 10.1007/JHEP07(2014)079.

[296] M. Aaboud et al. Search for new high-mass phenomena in the dilepton final state using 36 fb^{-1} of proton-proton collision data at $\sqrt{s}$ = 13 TeV with the ATLAS detector. *JHEP*, 10:182, 2017. doi: 10.1007/JHEP10(2017)182.

[297] A. M. Baldini et al. Search for the lepton flavour violating decay $\mu^+ \to e^+\gamma$ with the full dataset of the MEG experiment. *Eur. Phys. J.*, C76(8):434, 2016. doi: 10.1140/epjc/s10052-016-4271-x.

[298] K. Hayasaka et al. Search for Lepton Flavor Violating Tau Decays into Three Leptons with 719 Million Produced Tau+Tau- Pairs. *Phys. Lett.*, B687:139–143, 2010. doi: 10.1016/j.physletb.2010.03.037.

[299] F. Jegerlehner and A. Nyffeler. The Muon g-2. *Phys. Rept.*, 477:1–110, 2009. doi: 10.1016/j.physrep.2009.04.003.

[300] D. Aloni, A. Efrati, Y. Grossman, and Y. Nir. Υ and ψ leptonic decays as probes of solutions to the $R_D^{(*)}$ puzzle. *JHEP*, 06:019, 2017. doi: 10.1007/JHEP06(2017)019.

[301] C. Patrignani et al. Review of Particle Physics. *Chin. Phys.*, C40(10):100001, 2016. doi: 10.1088/1674-1137/40/10/100001.

[302] C. Hagedorn, S. F. King, and C. Luhn. A SUSY GUT of Flavour with S4 x SU(5) to NLO. *JHEP*, 06:048, 2010. doi: 10.1007/JHEP06(2010)048.

[303] E. Ma and G. Rajasekaran. Softly broken A(4) symmetry for nearly degenerate neutrino masses. *Phys. Rev.*, D64:113012, 2001. doi: 10.1103/PhysRevD.64.113012.

[304] H. Ishimori, T. Kobayashi, H. Ohki, H. Okada, Y. Shimizu, and M. Tanimoto. An introduction to non-Abelian discrete symmetries for particle physicists. *Lect. Notes Phys.*, 858:1–227, 2012. doi: 10.1007/978-3-642-30805-5.

[305] H. Ishimori, T. Kobayashi, Y. Shimizu, H. Ohki, H. Okada, and M. Tanimoto. Non-Abelian discrete symmetry for flavors. *Fortsch. Phys.*, 61:441–465, 2013. doi: 10.1002/prop.201200124.

[306] W. Grimus and M. N. Rebelo. Automorphisms in gauge theories and the definition of CP and P. *Phys. Rept.*, 281:239–308, 1997. doi: 10.1016/S0370-1573(96)00030-0.

[307] F. Feruglio, C. Hagedorn, and R. Ziegler. Lepton Mixing Parameters from Discrete and CP Symmetries. *JHEP*, 07:027, 2013. doi: 10.1007/JHEP07(2013)027.

[308] L. J. Hall, R. Rattazzi, and U. Sarid. The Top quark mass in supersymmetric SO(10) unification. *Phys. Rev.*, D50:7048–7065, 1994. doi: 10.1103/PhysRevD.50.7048.